Modelling Down Syndrome leukaemia using transchromosomic ES cell lines.

De Vita, Serena

Modelling Down syndrome leukaemia using transchromosomic ES cell lines.

A Thesis submitted for the degree of Doctor of Philosophy at

Queen Mary University of London

Serena De Vita, MD

November 2009

The Blizard Institute of Cell and Molecular Science
Bart's & The London, Queen Mary's School of Medicine & Dentistry
Centre for Paediatrics
London, UK

Considerate la vostra semenza:
Fatti non foste a viver come bruti,
Ma per seguir virtute e conoscenza.

Consider well the seed that gave you birth:
You were not made to live your lives as
brutes,
But to be followers of worth and knowledge.

(Dante Alighieri, Inferno, Canto 26, vv. 110-116)

Abstract

AMKL (acute megakaryoblastic leukaemia) accounts for at least 50% of all cases of acute myeloid leukaemia (AML) associated with Down Syndrome (DS).

Every tenth neonate with DS develops Transient Myeloproliferative Disorder (TMD), a self-regressing neoplasia with features that closely resemble AMKL. Despite the vast majority of TMD cases self-regressing within a few weeks, approximately 30% of DS infants with TMD develop by the age of 2-4 years a more aggressive, full-blown AMKL. Both DS-TMD and DS-AMKL are associated with trisomy of human chromosome 21 (HSA21) and with acquired mutations of GATA-1 (a transcription factor essential for erythroid/megakaryocytic lineage specification) leading to the exclusive production of a short form of the protein known as GATA-1s. Additional molecular events involved in the progression from TMD to AMKL remain largely unknown.

The aim of this project was to shed new light on the critical events involved in the pathogenesis of DS-TMD and AMKL utilizing an innovative *in vitro* model that mimics Down syndrome, a murine embryonic stem cell line carrying an extra copy of human chromosome 21 (HSA21).

Using this transchromosomic ES cell system, I explored the effect of trisomy 21 (t21) on the generation of megakaryocytes *in vitro*, and showed that trisomic megakaryocyte precursors display increased levels of GATA-1 compared to euploid controls and exhibit the tendency of forming macroscopic colonies without overt GATA1 mutations. Furthermore, I genetically manipulated the transchromosomic ES cell system by retrovirally

overexpressing GATA1s and demonstrated that trisomy 21 is required for GATA-1s to exert its full hyperproliferative potential.

The influence of the supernumerary HSA21 on the ontogenesis of haematopoietic stem cells (HSCs) from mesodermal precursors was also studied in the transchromosomic system. In this thesis, I present evidence that mesodermal colonies derived from transchromosomic ES cells give rise to an increased number of immature haematopoietic progenitors compared to euploid controls. I demonstrate that at least two independent genes on HSA21 contribute to this effect, and that trisomy of RUNX-1 (a master regulator of primitive haematopoiesis encoded on chromosome 21) is required for an increased haematopoietic commitment from the mesodemal precursors.

This thesis shows that t21 influences haematopoiesis (in general) and the megakaryocytic lineage (in particular) at several levels and that it is responsible for an overall increase in levels of immature cells that are targets for acquisition of further leukaemogenic mutations.

Finally, in this study I clarify the role of JAK3, a gene whose mutations have been reported in AMKL, in the progression from TMD to AMKL.

Acknowledgments

I would like to thank my supervisor, Dean Nizetic, for his support and advice throughout this adventure; all the present and the past members of the Nizetic lab, mainly Claudia Canzonetta and Jurgen Groet, for their patience in dealing with my mood changes and their invaluable enthusiasm in the day-by day work in the lab, as well as for being really good friends; the people of the Haematology and Paediatrics department for making the last three years so pleasant; Sheela, Lauren, Rich, Mike and David for their persistent attempts to drag me out of the lab on a Friday night to discuss scientific and not so scientific matters in the pub; my friend Daniela for constantly being worried about the health of my cells (and about my mental sanity); my dad Nello, my mum Franca and my brother Antonio for their endless support, their love and their faith in me and in my choices; my grandmother, who always will be my role model and Aron, the amazing person who despite the physical distance, has always been at my side through the ups and downs of my PhD and constantly gave me advice and self-confidence. Finally, I would like to thank Leukaemia Research Fund for providing me with the financial support to bring this project to completion and the patients, the families, and the medical staff of the Haematology Department of the Catholic University in Rome. It was working there that I realized that only a better knowledge of the molecular mechanisms of leukaemia could help us fight this terrible disease.

Table of contents

List of figures and tables

FIGURES

TABLES

1. Introduction

1.1. Overview

Acute Leukaemias are clonal malignancies of the haematopoietic system. They are characterised by a block in the lineage specification from haematopoietic stem cells (HSCs) to mature blood cells, which can occur at different stages of the haematopoietic development causing the abnormal accumulation of immature progenitors or of more committed cells in the bone marrow and in the peripheral blood.

In human acute leukaemias, this block is very frequently caused by the abnormal function of transcription factors (TFs), which are vital players in the sophisticated regulation of physiological formation of blood cells. Abnormal function of TFs can be due to mutations or to chromosomal translocations leading to genetic rearrangements, which result in alternative, dysfunctional forms of TFs, alteration in TFs levels or complete loss of TFs production. According to the multi-step model of leukaemogenesis, cells bearing the first malignant lesion (dysplastic clone) acquire further hits (activating mutations) inducing abnormal activation of pro-survival or anti-apoptotic pathways, which ultimately lead to the uncontrolled proliferation of these cells and their selective advantage over "normal" cells in the bone marrow (Kelly and Gilliland, 2002; Gilliland and Tallman, 2002).

Leukaemias can be associated with predisposing conditions, such as bone marrow failure syndromes or congenital disorders. Even more than sporadic cases, these situations provide an ideal background to elucidate the onset and the progression of the malignant transformation. Leukaemia arising in Down syndrome (DS) provides one such example. Down syndrome is a genetic disorder caused by trisomy of human chromosome 21 (HSA21) that induces a

wide variety of clinical phenotypes. These include a peculiar type of paediatric leukaemia of the megakaryocytic lineage (acute megakaryoblastic leukaemia, AMKL) characterised by mutations of the transcription factor GATA-1 (encoded on the X chromosome) and by the presence of an extra copy of HSA21 in the malignant clone. Within the first weeks of life, as many as 10% of newborns with DS present with a transient myeloproliferative disorder (TMD), which is also associated with mutations of GATA-1. In the vast majority of children with DS, TMD spontaneously self-regresses. However, almost 30% of DS patients affected by this transient leukaemia (TL) will develop within 3 years a frank AMKL, which requires treatment.

Mechanisms by which trisomy 21 predisposes for development of leukaemia and how the increased gene dosage caused by the supernumerary chromosome cooperates with mutations of GATA-1 in the development of TMD and AMKL are unclear.

The high frequency of the predisposition to a myeloproliferative disorder among children with DS and the limited time frame when the malignant transformation occurs make DS leukaemia even more puzzling, and establish a unique paradigm to dissect the sequential steps of leukaemogenesis.

These reasons, and the availability of an exceptionally innovative mouse model of DS generated by introducing an extra copy of human chromosome 21 (HSA21) into a mouse euploid context, prompted us to investigate the generation of HSCs and the properties of the megakaryocytic lineage in Down syndrome. Utilizing the potential to explore early developmental phenomena offered by embryonic stem cells (ES cells) and the relevance of embryonic stages to the onset of leukaemia in DS, this thesis aims to address whether trisomy 21 perturbs HSCs formation from ES cells engineered to carry an extra copy of HSA21 (transchromosomic ES cells) and the extent to which

differentiation and proliferation of megakaryocytes derived from transchromosomic ES cells is impaired by trisomy 21.

Evidence of early disturbances in the generation of HSC from ES cells in DS are presented and genetic dissection of this *in vitro* phenotype is provided, harnessing the potential of the transchromosomic model to explore the contribution of individual genes to the phenotypes of DS.

Generation of megakaryocytes from the transchromosomic ES cells is also investigated in this thesis, leading to the conclusion that terminal differentiation of megakaryocytes is not impaired in this system. Further characterisation of the properties of the transchromosomic megakaryocytes is shown, with respect to their clonogenic property and their cooperation with GATA-1 mutations.

Finally, using primary clinical samples, this thesis attempts to clarify the role of JAK3, a gene whose mutations have been reported in DS leukaemia, in the progression of this disease.

1.2. Features of Down syndrome

1.2.1. Euploidy and aneuploidy

In humans the number of chromosomes is 46, including 22 pairs of autosomes and 2 sex chromosomes, X and Y. The presence of the entire set of chromosomes normal for a given species is a condition known as *euploidy*. Conversely, *aneuploidy* is defined by the presence of an abnormal number of chromosomes. The presence of an extra copy of a whole chromosome is called *trisomy,* whereas *monosomy* indicates the absence of one or more chromosomes from the number that is normal for the species. Both of these situations are classified as aneuploidies, and they result in an abnormal copy number of the genes residing on the chromosome that is acquired or lost. The

number of copies of a gene can also be affected by structural changes of a portion of it, such as deletions or duplications. These changes are said to result in *segmental aneusomy* when causing pathological conditions.

Approximately 12% of the genome, including several genes, varies in copy number within the human population without causing pathologic consequences (so called copy number variation, or CNV) (Redon et al., 2006; Shaikh et al., 2009).

Type of aneuploidy	Chromosome	Syndrome and phenotypes	Frequency
Trisomy	21	Down syndrome. Highly variable phenotypes, mental retardation and other abnormalities. Life expectancy of >55 years [1].	1/750
Trisomy	18	Edward syndrome. Severe developmental disorder. Children usually die within the first few months after birth.	1/7500
Trisomy	13	Patau syndrome. Rarely compatible with life, severe neurological and cardiac deficits usually leading to death within a few weeks after birth.	1/12000
Trisomy	X (XXX)	Normal sexual development, sometimes menstrual abnormalities.	1/975
Trisomy (Y disomy)	Y (XYY)	Increased risk of learning impairment and delayed language skills.	1/975
Trisomy	XXY	Klinefelter syndrome. Small testicles and reduced fertility.	1/5000
Monosomy	X	Turner syndrome. Variable features including short stature and ovarian dysgenesis.	1/8000

Table 1.1. Human aneuploidy syndromes and associated chromosomal abnormalities, with clinical features caused by the gene dosage imbalance and frequency in live birth (frequencies derived from Hassold et al., 2002 and Crider et al., 2008). [1] Life expectancy data for individuals with DS were taken from Glasson et al., 2002.

In the remaining cases, aneuploidy and segmental aneusomy are prominent causes of pregnancy loss, with approximately 30% of all spontaneous abortion and approximately 6% of all infant death resulting from aneuploidy (Hoffmann et al., 1986). When compatible with life, gene dosage imbalance is a well-known cause of human disease (Jacobs, 1992; Templado et al., 2005), resulting in a variety of phenotypes as summarized in table 1.1.

About 0.5-1% of live births have a numerical chromosomal abnormality (Aardema et al., 1997). The most common viable human aneuploidy, with a frequency of 1 in 750 live births (Antonarakis et al., 2004), is Down syndrome (DS) (Down, 1995), a congenital disorder caused by trisomy of chromosome 21 (HSA21) (Lejeune et al., 1959). According to the National Down Syndrome Cytogenetics Register (NDSCR), the diagnoses of DS in England and Wales in 2008 were 1843, 1112 of which were antenatal. Of the latter ones, 92.5% lead to termination of pregnancy, whereas 4.8% lead to the birth of a DS individual (Morris and Alberman, 2009).

1.2.2. Etiology of Down syndrome

Trisomy 21 (t21) can be full, involving the acquisition of a complete extra HSA21, or partial, involving three copies of specific HSA21 regions. Almost 95% of individuals with DS have full trisomy 21 (Thaline, 1982), which is caused by non-disjunction during maternal meiosis (Antonarakis, 1991; Brown et al., 2000), whereas only ~5% of trisomy 21 cases are attributable to errors occurring during spermatogenesis (Antonarakis, 1991; Savage et al., 1998). The predominant maternal meiotic errors that lead to full trisomy 21 mainly occur during meiosis I, when homologous chromosomes are supposed to separate from each other (Sherman et al., 1994). This intricate process has a few error prone stages, such as the maintenance of physical connections

16

between homologous chromosomes during prophase I and metaphase I, and the appropriate segregation of sister chromatids to the opposite poles of the meiotic spindle (Hassold and Hunt, 2001).

The significant bias towards maternal meiosis I errors in DS seems to be related to the delayed meiotic division that oocytes undergo. In fact, in females, meiosis is initiated in the foetal ovary but arrests before birth in meiotic prophase I and only resumes at puberty, many years after birth. Following completion of the first meiotic division, meiosis is arrested again, early in the second meiotic division and is completed only after fertilisation of the oocyte by a sperm cell. Male meiosis, instead, is initiated at puberty and it progresses continuously to its completion. Furthermore, unlike in females where there is a limited pool of oocytes that progressively depletes in successive menstrual cycles, sperm production does not cease during a male's lifetime (Hassold and Hunt, 2001).

The increased incidence of DS with increasing maternal age has been recognised for many years. Furthermore, an augmented risk of recurrence of DS in young women was observed a long time ago (Penrose, 1933); mechanisms underlying this increased risk are unexplained. While the segregation and recombination events that are required for the completion of meiosis I, and its delayed completion in the oocyte, are an extremely intricate process, the reasons for the positive correlation that exists between meiosis I errors and maternal age are not fully understood. An explanation for the increased incidence of maternal meiosis I errors is the possible association between reduced recombination and the non-disjunction of HSA21 that causes t21 (Brown et al., 2000; Lamb et al., 1996; Sherman et al., 1991). Recent studies have tried to define the mechanisms responsible for this effect and its relationship with maternal age. A widely accepted view postulates that multiple pathways lead to non-disjunction, some age-dependent, and others

age-independent. For young women, the greatest risk factor for meiosis I non-disjunction has been identified as the presence of a susceptible exchange pattern in the oocyte (Lamb et al., 2005). Over time, the proportion of non-disjunction due to normal exchange configurations increases as age-dependent risk factors exert their influence (Sherman et al., 2005).

Maternal meiosis II errors constitute 20–24% of all maternal meiosis errors, and 18– 23% of all cases of t21 (Antonarakis et al., 1992). Similar to meiosis I errors, meiosis II errors also have an associated maternal age effect (Hassold and Jacobs, 1984). The small numbers (about 5%) of paternally derived errors in meiosis leading to trisomy 21 (Antonarakis, 1991) are approximately equally distributed between the meiosis I and meiosis II. Unlike maternally derived errors, paternal errors do not have an age-associated effect. However, paternal non-disjunction in the first meiotic division is associated with a significant reduction in recombination similar to maternal meiosis I non-disjunction. There is no effect of recombination amongst paternally derived meiosis II errors (Savage et al., 1998).

Maj Hulten et al. have recently challenged the view that trisomy 21 is caused by non-disjunction of homologous chromosomes 21 during the first meiotic division by screening ovarian cells from eight phenotypically normal female foetuses. All foetuses analysed in this study were found by fluorescence in situ hybridization (FISH) to be mosaics, containing ovarian cells with an extra copy of HSA21. If every woman is a mosaic in her ovary, this could explain simultaneously the maternal age effect and the recurrence in younger women. In normal development, there is a dramatic reduction in the number of oocytes due to apoptosis, but trisomic oocytes lag behind in this process and they accumulate comprising a larger proportion of the ovarian reserve at later maternal ages. It is also logical to postulate that some women might have a high proportion of trisomic oocytes in their ovary, which might account for the

increased recurrence of DS pregnancies in young women (Hulten et al., 2008).

Only 3–5% of all cases of full trisomy 21 are attributable to errors in mitosis. These errors show no parental age effect and there is no preference for either the maternal or paternal HSA21 to be duplicated (Antonarakis et al., 1993).

In approximately 5% of full t21 cases, one copy of HSA21 is translocated to another HSA21 or to another acrocentric chromosome, usually chromosome 14 (Petersen et al., 1991; Shaffer et al., 1992). In most cases of a translocation involving two chromosomes 21, the t(21;21) is an isochromosome consisting of two long arms of HSA21 (Grasso et al., 1989). The distribution between maternally- and paternally-derived t(21;21) isochromosomes is approximately equal (Antonarakis et al., 1990). A minority of t(21;21) cases arise from Robertsonian translocations where exchanges between the proximal short arms of two chromosomes 21 produces a chromosome with two centromeres which function as one, thereby conferring stability to the resulting metacentric chromosome. In these cases the extra chromosome is maternally derived (Antonarakis et al., 1990; Shaffer et al., 1992). Trisomies caused by parental Robertsonian translocations involving chromosomes 14 and 21 (t(14;21)) also originate exclusively in maternal germ cells (Shaffer et al., 1992).

Approximately 3% of trisomy 21 cases occur as a result of post-zygotic mitosis, thereby producing t21 mosaicism (Mikkelsen, 1977). The final class of t21 individuals is comprised of partial trisomics, who have three copies of parts of HSA21 as a result of translocation events. These patients have been fundamental in mapping the phenotypic characteristics of t21 to specific HSA21 regions.

1.2.3. Phenotypes of Down syndrome

An English physician, John Langdon Down, first described Down syndrome in 1866 (Down, 1995). The mental and physical abnormalities Down described in his original report were resembling the facial characteristics of the Mongolian population, though he observed that these characteristics could appear at equal frequency in children of any race and ethnic group. The term "Mongolian idiocy" was therefore subsequently employed to describe Down syndrome, and "Mongoloids" was used to refer to people affected by this condition. It was not until 1961 that Langdon Down's original observations were officially credited to him. A late recognition came in the form of a letter to the scientific journal "The Lancet", signed by twenty prominent genetic experts (Allen et al., 1961) who suggested four alternative names for the condition. As a result, the editor of the Lancet ruled "Down's syndrome" as an appropriate term for the phenotypes described by Langdon Down, and a few years later (in 1965), the World Health Organisation officially designated "Down's syndrome" a the term for the phenotypes of trisomy 21 (Ward, 1999).

The causative link between trisomy 21 and DS came almost one century after Langdon Down's original observations (Jacobs et al., 1959; Lejeune et al., 1959) and since then there have been a variety of studies aiming to dissect the pathogenesis of DS and the mechanisms by which one extra copy of all, or a subset of HSA21 genes, leads to the broad spectrum of phenotypes collectively known as DS.

Phenotypes of DS can greatly vary within the affected population, however the characteristic combination of physical attributes that result from trisomy of HSA21 are collectively so indicative of the condition, that a diagnosis of DS

can often be preliminarily established based on the physical features alone (Rex and Preus, 1982). The physical characteristics of DS are summarized in Figure 1.1 with the average relative frequency and include: upslanting palpebral fissures, narrow palate, flat nasal bridge, a gap between the first and second toes and a protruding tongue (Rahmani et al., 1989; Delabar et al., 1993). As shown in table 1.2, phenotypes of DS are found in many different tissues. Approximately 40% of all DS individuals have some form of congenital heart defect. The ones that occur most commonly are endocardial cushion defects and an atrioventricular canal (Epstein, 2001). Congenital heart defects are one of the leading causes of death in the DS population, accounting for 30–35% of all deaths (Baird and Sadovnick, 1989).
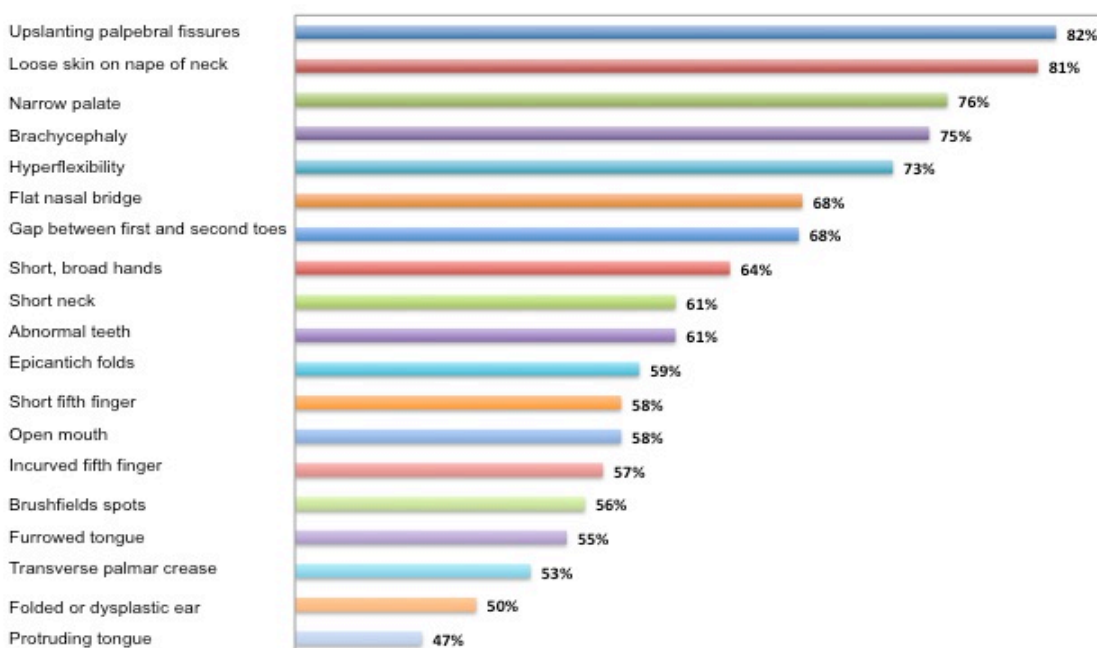
Fig. 1.1. Physical features of DS and average frequency of reported phenotypes. Data in this figure are derived from Epstein, C.J. in The Metabolic and Molecular Basis of inherited Diseases, 8th edition, 2001).

Duodenal stenosis is observed in 4-7% of Down syndrome patients. Approximately 90% of children with Down syndrome develop skin disorder such as hyperkeratosis, which may later in life lead to atopic dermatitis and

fungal infections of skin and nails (Roizen and Patterson, 2003). Between 38% and 78% of people with Down syndrome suffer from hearing loss which can be conductive, sensorineural or mixed (Balkany et al., 1979). Women with Down syndrome are able to conceive, whereas men have an impaired capacity to reproduce (Bovicelli et al., 1982).

The most significant and characteristic phenotypes of DS are those affecting the nervous system. Mental retardation and a histopathological signature indicative of Alzheimer's disease (AD) can be considered the hallmark manifestations of this class of phenotypes, occurring invariably in all DS individuals (Wisniewski et al., 1985; Williams and Matthysse, 1986).

Phenotypes	Average frequency (%)
Skeletal abnormalities	
Pelvic dysplasia	70
Atlantoaxial or atlantoccipital instability	15 to 20
Mental retardation	100
Hypothyroidism	7 to 17
Neurological features	
Hypotonia	100
Alzheimer like brain pathology	100
Delayed disappearance of early reflexes	80
Congenital abnormalities	
Congenital heart defects (CHD)	30 to 40
Atrioventricular canal (of total CHD)	40
Ventricular septal defect (of total CHD)	31
Atrial septal defect (of total CHD)	9
Fallot's tetralogy (of total CHD)	6
Patent ductus arteriosus (of total CHD)	9
Gastrointestinal abnormalities	
Duodenal atresia	2.5
Imperforated anus	1
Hirschsprung disease	0.6
Infertility in males	100
Leukaemia	
AMKL	200-400x normal
AML/ALL	10-20x normal

Table 1.2. Phenotypes of DS and frequency in percentage (data from Epstein, C.J. in The Metabolic and Molecular Basis of Inherited Diseases, 8th edition, 2001).

The trisomic status of one, or most likely several, HSA21 genes are likely to be a major predisposing factor for the neurological features of Down syndrome. Support for the direct or indirect role of HSA21 in the neurological defects of DS has been provided by the identification of several genes on HSA21 whose functions may be important in the development of the central nervous system (Agarwala et al., 2001; Hammerle et al., 2002; Sanchez-Font et al., 2003). Mental retardation in Down syndrome may be a result of a reduced number of neurons in all layers of the cerebral cortex. Furthermore, an impaired synapse formation and a synaptic plasticity defect were observed in individuals with Down syndrome (Ferrer and Gullotta, 1990). The post-mortem brains of DS adults aged 35 years or older display all the pathological and neurochemical hallmarks of the AD that occurs in euploids (Mann, 1988), including the deposition of neurofibrillary tangles and amyloid plaques in the brain (Teller et al., 1996). The order in which specific brain regions are affected as the disease progresses is equivalent in DS and euploid subjects (Epstein, 2001).

Immune system defects in DS individuals render them significantly more susceptible to infectious diseases, including pneumonia, meningitis and influenza, accounting for the greatest number of deaths amongst DS individuals (Scholl et al., 1982). Different classes of antibodies may be elevated or decreased in comparison to their serum levels in euploid individuals (Ugazio et al., 1990). A minor reduction in the number of peripheral blood (PB) lymphocytes is also observed, with the proportion of T-helper cells (CD4+) to suppressor cells (CD8+) being markedly reduced (Ugazio et al., 1990; Philip et al., 1986). These findings, together with observations of the altered expression profiles of T-cell receptors by PB T-cells (Murphy and Epstein, 1992), suggest that the ability of the DS thymus to generate functionally mature T-cells is impaired. Haematological abnormalities are

common in DS, especially in the first weeks of life. Apart from an increased risk of leukaemia compared to the euploid population (discussed extensively in 1.2.), DS newborns can present with thrombocytopenia, polycythemia and neutropenia. The frequency of these abnormalities is so high that it has been recommended to perform a routine blood cell count in all neonates with DS (Henry et al., 2007).

1.2.3. Gene dosage imbalance and its phenotypic effects in Down syndrome

Human chromosome 21 (HSA21) is one of the smallest human chromosomes, but contains almost 400 known genes; this number is estimated to increase integrating new information based on ESTs sequencing and comparative genome analysis (Antonarakis et al., 2004; Wiseman et al., 2009). A key goal of DS research (and in general of aneuploidy research) is to define how an increased dosage of normal genes can cause a clinical condition and a variety of associated phenotypes with different degrees of penetrance. Since the correlation between the presence of an extra copy of HSA21 and Down syndrome was discovered in 1959, it has been proposed that genes that are trisomic are expressed 1.5 fold more in DS individuals than in the euploid population. In spite of this assumption, it has been showed in human DS tissues (Ait Yahya-Graison et al., 2007; Prandini et al., 2007) and in mouse models of DS (Chrast et al., 2000; Sultan et al., 2007) that the increased expression of some of the genes caused by an extra copy of HSA21 does not significantly differ from the natural variation of gene expression in euploid controls, excluding these genes as candidate for the dosage-sensitive effect of trisomy in the tissues investigated. Based on a gene expression study, Prandini et al. proposed to classify genes on HSA21 in three groups: group A contains genes with minimal expression overlap between DS and control

samples, group B contains genes with partial overlap, and group C contains genes that show extensive overlap of expression values between DS and normal samples. This classification implies that genes of group A are candidates for involvement in DS phenotypes that are present in all affected individuals, such as mental retardation, muscle hypotonia, and Alzheimer disease; genes of group B are likely to be involved in the variable features of DS and if their level of expression reaches a given threshold (that must be above the highest value observed for unaffected individuals), then the probability of the manifestation of a given phenotype is very high; genes of group C are less likely to be involved in DS phenotypes, although some of them may still be responsible for DS phenotypes and change their expression through regulatory mechanisms that are specific to cell type or developmental stage (Prandini et al., 2007). In light of the latter consideration, it is arguable that a spatial and temporal map of the HSA21 gene expression is crucial to the understanding of the DS phenotypes.

Phenotypic variations in the DS population might also be caused by genomic variability, as suggested by a recent genome wide association-study (Lyle et al., 2009). The determination of SNPs involved in gene expression variation and in the predisposition to different variable phenotypes of DS is very likely to become a prominent avenue of investigation in the field in the near future.

Positional cloning and "candidate gene" approaches are another powerful strategy used to narrow down the contribution of genomic regions that harbour genes associated with a specific phenotype in DS. Once a physical map of a chromosome region is established, candidate genes for a particular phenotype can be identified by *in vitro* and *in vivo* assays. The study of rare patients with partial trisomy has been very important in this direction, and mouse models of DS provide an invaluable tool to dissect the contribution of candidate genes to a given phenotype. In studying DS phenotypes, genetic variations and gene

expression mechanisms should be integrated with the candidate gene approach, providing additional evidence for the contribution of a specific gene to one or more of the DS phenotypes.

Based on genotype-phenotype correlations, investigators have proposed the existence of a "DS critical region" (DSCR), which has been narrowed down to a region within 21q22 of about 4.3 Mb in length (Delabar et al., 1993; Korenberg et al., 1994; Arron et al., 2006; Ronan et al., 2007). The DSCR contains genes that contribute to mental retardation, heart defects and other common features of DS; however, the definition of such a region is controversial as patients with partial triplication outside of this region also manifest features of DS.

In conclusion, how the presence of a supernumerary copy of a normal allele results in the phenotypes associated with DS remains to be fully addressed. Elucidating the effect of gene dosage imbalance in DS will deepen our understanding not only of this condition, but also of the pathogenesis of other aneuploidy syndromes.

1.3. Down syndrome and cancer

1.3.1. Under-representation of solid tumours in DS

The incidence of solid tumours is strikingly reduced in DS individuals (Oster et al., 1975). A large American study of death certificates of millions of US citizens including 18.000 individuals with Down Syndrome showed that DS individuals have up to 100-fold lower likelihood of dying from many types of solid tissue cancer. Only testicular cancer was found slightly elevated in the Down syndrome population (Yang et al., 2002). Other studies have reported an increased incidence of some solid tumours such as gastro-intestinal tract cancers, lymphomas and retinoblastomas in DS compared to the euploid

population and a decrease incidence of all other solid tumours subtypes (Boker et al., 2001; Satge et al., 2003; Hill et al., 2003), or a reduction of the incidence of all solid tumours but GI tract cancers (Hermon et al., 2001; Goldacre et al., 2004).

The direct role of HSA21 in conferring protection from solid tumour formation has been demonstrated by observation of loss of HSA21 material in several solid cancers. Loss of heterozygosity (LOH) on HSA21 has been reported in breast cancer (Ohgaki et al., 1998), oral squamous cell carcinoma (Yamamoto et al., 2001), lung cancer (Groet et al., 2000; Kohno et al., 1998) and gastric cancer.

Judging by the variety of solid tumours that are suppressed in DS individuals and by the different regions of the chromosome that are deleted in different solid cancers, it is likely than one or more tumour suppressor genes exist on HSA21. A very exciting study has recently reported that crossing mouse models of DS with mice with an increased incidence of colon cancer (mice heterozygous for the APC^{min} mutation) reduced the formation of tumours of the colon, providing a role for ETS-2 (a gene present in three copies in the DS models which is known to be a powerful oncogene in other contexts) as a tumour suppressor gene (Sussan et al., 2008).

1.3.2. Down syndrome and leukaemia

DS children show an increased risk of developing leukaemia compared to their euploid counterpart. This is most prominent in early childhood, with the vast majority of cases of the disease occurring in children during the first four years of life (Hasle et al., 2000; Zipursky et al., 1992).

The most frequent form of leukaemia during childhood is B-cell precursor Acute Lymphoblastic Leukaemia ("common ALL") (Pui et al., 1993;

Ravindranath, 2005). The incidence of this type of leukaemia is approximately 20-fold higher in children with DS than in the euploid population. The peak age (about 5 years old) and the immunophenotype (blasts expressing the surface antigens CD10, CD19, and CD79a) of DS-ALL are indistinguishable from the ones of the sporadic childhood common ALL (Malinge et al., 2009). Because trisomy or tetrasomy of human chromosome 21 are the most common acquired somatic chromosomal abnormalities in sporadic common ALL, it is reasonable to speculate that constitutional and somatic trisomy 21 may facilitate leukaemogenesis with the same mechanisms. Therefore, studying DS-ALL may have direct implications for understanding sporadic childhood ALL as well. The most frequently observed cytogenetic abnormality in DS-ALL is the acquisition of an extra chromosome X (Forestier et al., 2008); other lesions include the t(8;14) translocation and the deletion of chromosome 9 (del(9p)). Mutations in PTPN11 and N-RAS have been described in DS-ALL samples (Yamamoto et al., 2006). An exciting breakthrough in the history of DS-ALL came from the finding that almost 20% of DS-ALL is associated with mutations in the tyrosine-kinase JAK2. The mutations described in DS-ALL occur in the JH2 pseudokinase domain affecting Arg683 and surrounding residues (Malinge et al., 2007; Bercovich et al., 2008; Kearney et al., 2009) and they are different from the V617F mutation associated with myeloproliferative disorders. Interestingly, these mutations were absent from the remission samples analysed, suggesting that they are a "second hit" acquired by trisomic progenitors and that they might constitute a promising therapeutic target in DS-ALL.

The form of leukaemia with the most remarkably increased incidence in DS children is AMKL (FAB-M7 subtype of Acute Myeloid Leukaemia) (Hitzler and Zipursky, 2005). The relative risk of developing AMKL is estimated to be 500 times higher in children with DS than in the general population (Zipursky et al.,

1992) and this type of leukaemia arises at a younger median age in DS children (2 years) than in euploid children (8 years) (Lange et al., 1998).

AMKL is characterised by the accumulation of megakaryoblasts, precursors of megakaryocytes, which are the cellular substrate of production of platelets. As in other types of leukaemia, the blasts in AMKL replace the normal bone marrow population causing a reduced production of erythrocytes, leukocytes and platelets. This leads to the main clinical aspects of the disease, which include anaemia, an impaired capacity to mount an immune response and a reduced capacity to fight infections as well as a decreased ability of the blood to clot after injuries. In young children and infants, FAB M7 leukaemia occurs as two separate entities. The first type is characterised by a very aggressive progression with bone marrow fibrosis and a poor prognosis and is associated with the translocation t(1;22)(p13;q13) (also known as *OTT-MAL*) (Ma et al., 2001). The second type of M7 occurs in DS (DS-AMKL) and is characterised by a good response to treatment and a better prognosis. In DS, a reversible form of megakaryoblastic leukaemia known as Transient Leukaemia (TL), or Transient Myeloid Disorder (TMD) usually precedes AMKL. At least 10% of infants with DS develop TMD, a disease in which immature megakaryoblasts accumulate in liver, bone marrow and peripheral blood. Even though this disorder undergoes spontaneous remission in most cases (Zipursky, 2003), approximately 30% of DS children with TMD develop AMKL within 3-4 years.

Megakaryoblasts of TMD are morphologically indistinguishable from the AMKL blasts. Immunophenotyping shows that both type of blasts express the myeloid markers CD33 and CD13, in addition to at least one platelet-associated antigen (CD41 or CD61) and frequently the haematopoietic stem cell marker CD34. As these blasts also express erythroid-specific mRNAs, such as globin and erythroid δ-aminolevulinate-synthase (Ito et al., 1995), it is

logical to postulate that TMD and AMKL arise from a disturbance in the maturation from a common erythroid-megakaryocytic progenitor (MEP).

The process resulting in TMD begins *in utero* and in most cases does not cause clinical symptoms in newborns, although the liver, the bone marrow and the blood are filled with a large number of blast cells. Only a small percentage (<5%) of TMD cases are severe and might be fatal as a result of liver damage or heart and lung complications.

1.4. Haematopoiesis, leukaemogenesis and trisomy 21

1.4.1 Developmental stages of haematopoiesis

Haematopoiesis is a complex process that starts from a multipotent stem cell capable of differentiation and self-renewal (haematopoietic stem cell, HSC), and leads to a hierarchy of progenitor cells with increasingly restricted potential of differentiation, ending with the fully differentiated blood cells (Weissman et al., 2001). During embryogenesis, the original pool of HSCs is formed in a developmentally regulated fashion that involves multiple anatomical sites (Mikkola and Orkin, 2006). The shift from one location to another is required as the embryo grows and supports the development of undifferentiated HSCs, which can replenish the "stemness" pool while giving rise to maturing blood cells that are exposed to different inductive signals from multiple locations with distinct microenvironments. In mice, where this process has been extensively characterised, embryonic haematopoiesis starts in the primitive streak, a specialized subset of mesodermal cells, and in the yolk sac. Yolk sac is the main site of embryonic red blood cells production (embryonic haematopoiesis) (Dzierzak and Speck, 2008; Lux et al., 2008). HSCs capable of forming all the haematopoietic lineages (definitive haematopoiesis) arise

subsequently in the aorta-gonad-mesonephros region (AGM) (de Bruijn et al., 2000; Jaffredo et al., 2005) and migrate to colonize the foetal liver. Seminal work from Ottersbach et al. and Rhodes et al. identified the placenta as a reservoir of HSC generation at the same developmental stage of the AGM region, and Rhodes et al. have also demonstrated that HSC development is initiated at this site independently from circulation (Ottersbach and Dzierzak, 2005; Rhodes et al., 2008). Finally, the bone marrow becomes the principal site of haematopoiesis after birth and it persists in this function through adulthood (Figure 1.2).
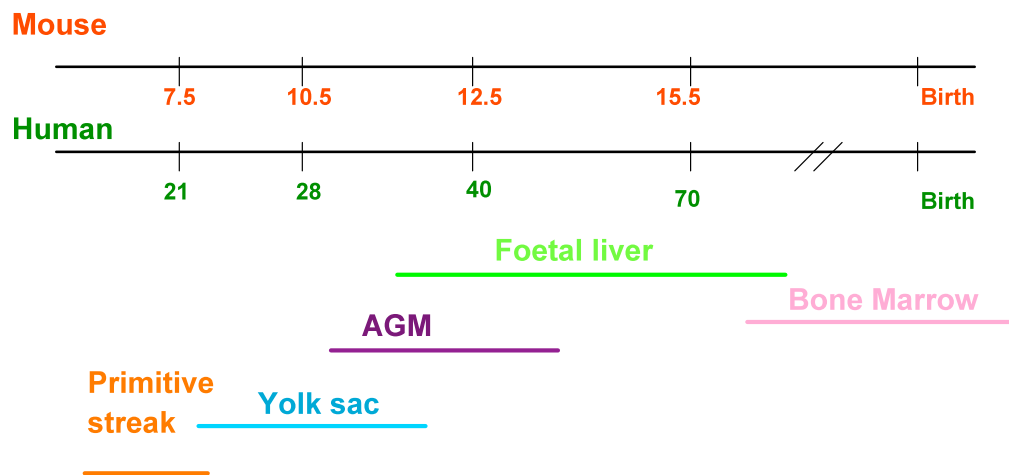
Fig. 1.2. Anatomical sites harbouring HSCs in mouse and human embryos. Data and figure modified from Mikkola et al, *Development*, 2006. Numbers indicate embryonic days. Figure shows the developmental migration of anatomical sites of haematopoiesis before birth. Primitive embryonic haematopoiesis starts in the primitive streak and in the yolk sac. Definitive haematopoiesis (with cells capable of giving rise to all haematopoietic lineages) first originates in the in the aorta-gonad-mesonephros region (AGM), then colonizes the foetal liver, and finally moves to the bone marrow, where it persists throughout adult life. Recent data suggest that definitive haematopoiesis arises simultaneously in the AGM and in the placenta.

Apart from the anatomical site of production, foetal HSCs differ from adult HSCs because they have to complete a maturation process that, whilst permitting their engraftment and survival in future haematopoietic niches,

allows the expansion of their number in order to provide an adequate supply of HSCs throughout adult life. Therefore, foetal HSCs are largely cycling and undergo symmetric cell division to expand the HSC pool (Lessard et al., 2004). In contrast, in homeostasis condition, adult HSCs are quiescent and only rarely divide to maintain an adequate supply of differentiated blood cells and to renew the HSCs pool.

Mechanisms underlying the complex task of producing blood cells and replenishing the stemness pool are not completely defined. Possible models include asymmetric cell divisions, in which every dividing stem cell forms one new stem cell and one differentiated cells, or environmental asymmetry, in which the daughter cell leaves the niche that sustain HSC self-renewal and through specific external environmental signals undergoes lineage differentiation (Wilson et al., 2004).

1.4.2. Transcription factors and lineage commitment

All the processes described above are widely controlled by cell-restricted transcription factors (TFs) (Weissman et al., 2001; Cantor and Orkin, 2002). TFs can directly regulate gene expression by their DNA binding properties but also influence lineage decisions by inhibition of competing TFs through direct protein-protein interactions. TFs are essential for haematopoietic cell development from the earliest stages, as illustrated in figure 1.3. TFs required for the initial specification and formation of HSCs include GATA-2, SCL/Tal1, c-MYB and RUNX-1 (Orkin and Zon, 2008).

The expression of lineage-specific TFs is required for the specification and the maturation of different lineages. The classical "hierarchical view" of haematopoiesis (based on prospective isolation of progenitors) is indeed based on the idea that the expression or the inhibition of specific TFs

32

corresponds to the progressive maturation of cells of each lineage, and that this process has a molecular correspondent in the expression of specific cellular surface markers.
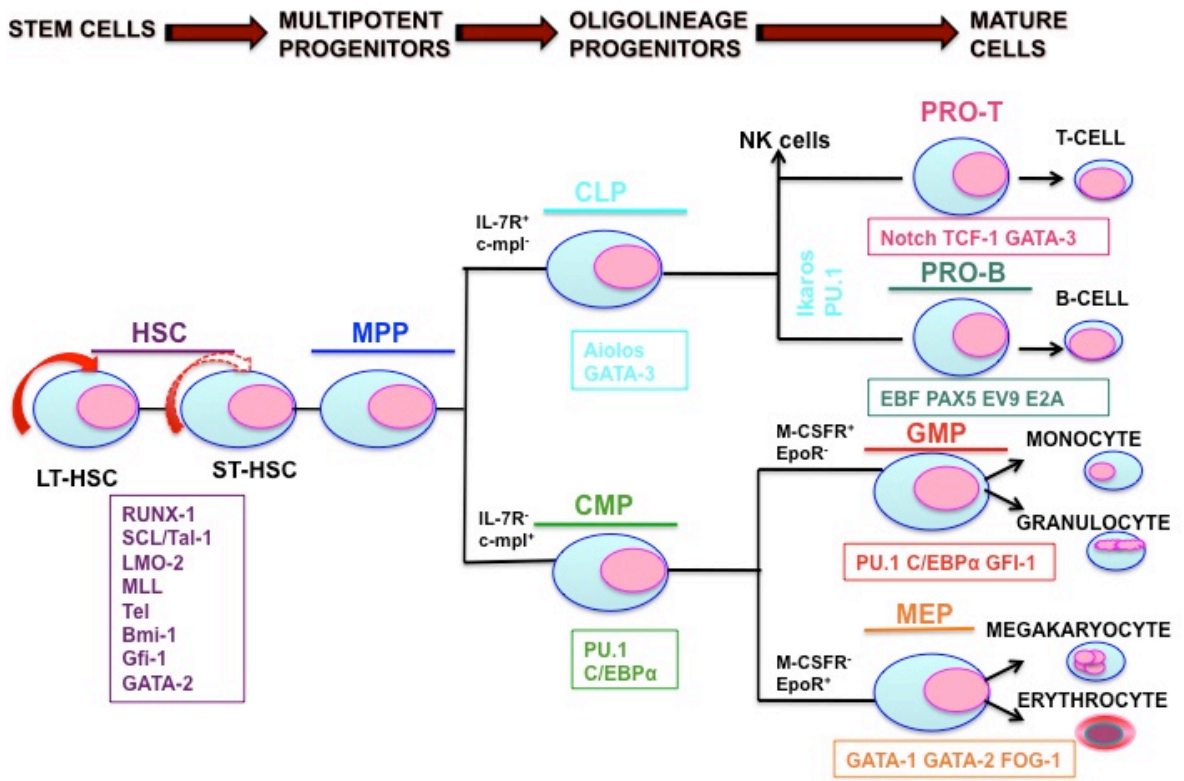
Fig. 1.3. A schematic view of haematopoiesis in the mouse, with the indication of some of the most well characterised transcription factors and their role in lineage specification (modified from Weissman *et al*, *Annu Rev Cell Dev Biol*, 2001)**.** HSCs can be divided into long-term HSCs (LT-HSCs), which are highly self-renewing, and short-term HSCs (ST-HSCs), which have a more limited self-renewal potential and differentiate into oligolineage-restricted progenitors that ultimately give rise to differentiated progeny. Common lymphoid progenitors (CLPs) give rise to T-lymphocytes, B-lymphocytes, and natural killer (NK) cells. Common myeloid progenitors (CMPs) give rise to granulocyte-macrophage progenitors (GMPs), which then differentiate into monocytes, macrophages and granulocytes, and to megakaryocytic-erythroid progenitors (MEP), which produce megakaryocytes, platelets and erythrocytes. All of these stem and progenitor populations are separable as pure populations by using cell surface markers. Each stage of the haematopoietic process is tightly regulated by the combined action of transcription factors (TFs). Main TFs playing a role at each haematopoietic stage are indicated in boxes.

For example, GATA-1 is highly expressed in the MEPs (megakaryocytic-erythroid progenitors) compartment, whereas C/EBPα expression specifies a commitment towards granulocyte-macrophage progenitors (GMPs).

The one-to-one correspondence of the expression of transcription factors and progenitors is a simplified view, which has been challenged by new models, such as the "lineage priming effect" (Fisher, 2002). This is a mechanism by which HSCs and early progenitors express markers of disparate lineages at a single cell level (albeit at low levels) (Orkin, 2003), and maintain the chromatin of genes involved in crucial haematopoietic programs in an open configuration that confers to these cells the plasticity to choose molecular fates rather than adhering to a single pre-established program. Furthermore, new techniques of progenitor separation and purification of TF complexes have rapidly progressed, deepening our understanding of the haematopoietic development. For example, the recent findings that short-term repopulating HSCs expressing GATA-1 or PU.1 may be committed to the myelo-erythroid or myelolymphoid lineage (Arinobu et al., 2007) has challenged the traditional view of HSCs and TF-restricted lineage commitment, suggesting that lineage specification decisions can be made at different branching points of the haematopoietic hierarchy.

Of the more than 20 haematopoietic TFs whose functions have been characterised, virtually all are associated with haematopoietic malignancy, and are often involved in chromosomal translocations present in leukaemia. Indeed, many were first studied for their pathogenic role in human disease. The aberrant expression of TFs, as well as their abnormal activation or inactivation caused by translocations or rearrangements have multiple downstream effects, including altered repression or derepression of target genes and inhibition of other critical factors, which all contribute to the execution of the malignancy program (Rosenbauer and Tenen, 2007).

In conclusion, TFs, epigenetic mechanisms and recently identified additional levels of control (such as that provided by micro-RNAs and other small RNAs) coordinate an extraordinary intricate and yet remarkably functional biological process, whose deregulation is directly associated with cancer and leukaemogenesis and whose understanding is the basis of crucial therapeutic implications.

1.4.3. GATA -1 mutations and Down syndrome leukaemia

GATA-1 is a transcription factor encoded on the X chromosome. It is physiologically expressed in erythroid and megakaryocytic cells, eosinophils and mast cells (Martin et al., 1990; Romeo et al., 1990; Zon et al., 1993). The GATA-1 protein has three functional domains (Figure 1.4). The C-terminal zinc finger domain is required for binding to specific DNA motifs. The N-terminal zinc finger domain increases the affinity of the protein for complex DNA binding motifs and interacts with the cofactor FOG1 (Muntean and Crispino, 2005).
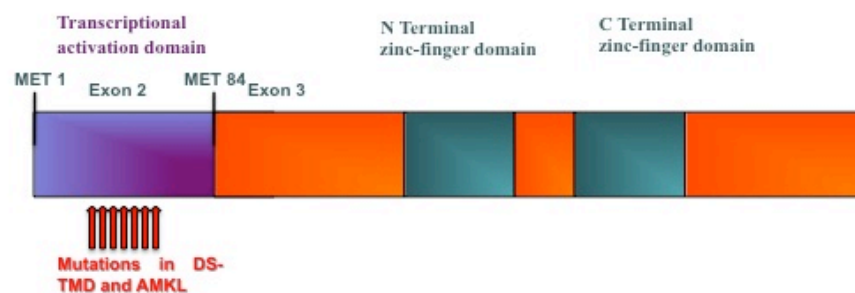
Fig.1.4. Structure of the GATA-1 protein. The diagram shows the three functional domains (in purple and dark green and the alternative translational start site (Met84) of the GATA-1 protein. Different mutations of GATA-1, which generally cluster within exon 2, have the same protein consequence, i.e. the production of a short form of GATA-1 (translated starting from Met84) that lacks the N-terminal "transactivation" domain.

Insights into the functions of the third domain of GATA-1 (the N-terminal transactivation domain) came from the finding that both DS-AMKL (Wechsler

et al., 2002) and DS-TMD (Groet et al., 2003; Hitzler et al., 2003) present acquired mutations in GATA-1.

The majority of the reported mutations in DS-TMD and AMKL involve point mutations, small deletions or insertions in the sequence encoding GATA-1 exon 2. Each of these alterations has been shown to result in a disruption of the normal reading frame of GATA-1, and an invariable introduction of a premature stop codon. As a consequence, full-length GATA-1 is not expressed in the leukaemic cells, but a short isoform of GATA-1, described as GATA-1s, remains the only form expressed in both DS-TMD and AMKL blasts. GATA-1s (that is physiologically expressed alongside full length GATA-1 in humans) arises by alternative translation from Met84, downstream of each of the patient mutations and lacks the N-terminal transactivation domain, but retains both zinc fingers and the entire C-terminus domain (Martin and Orkin, 1990; Calligaris et al., 1995).

1.4.4. GATA-1, GATA-1s and haematopoiesis

GATA-1 is essential for erythroid and megakaryocytic development and maturation (Ferreira et al., 2005). Both lineages arise from a common progenitor, the megakaryocytic-erythroid progenitor (MEP), which in turn is derived from a common myeloid progenitor (CMP). Similar to other TFs, the role of GATA-1 in haematopoietic development was determined through conventional gene knockouts. GATA-1$^-$ ES cells produce no mature erythroid cells *in vitro* (Simon et al., 1992) and *in vivo* (Fujiwara et al., 1996).

Using yeast, Crispino et al. demonstrated that this effect on the erythroid lineage is mediated by a critical interaction with the FOG factor that requires the presence of the GATA-1 N-terminus domain (Crispino et al., 1999).
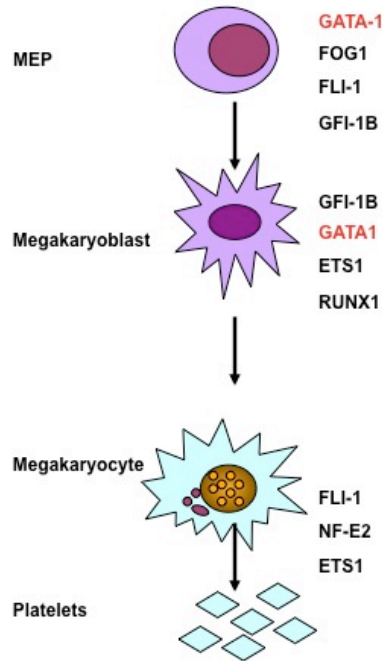
Fig.1.5. From MEP to megakaryocytes. Schematic view of the differentiation of the megakaryocytes from their precursors, with the indication of TFs essential for the specification of the lineage. GATA-1 is highlighted in red.

The role of GATA-1 in megakaryocytic development (Figure 1.5) was initially discovered through the creation and analysis of several lines of mutant mice expressing reduced level of GATA-1. One of these lines, the ΔneoHS GATA-1-targeted mouse, expresses normal levels of GATA-1 in erythroid cells but undetectable levels of GATA-1 in megakaryocytes (Shivdasani et al., 1997). ΔneoHS mice displayed marked, persistent thrombocytopenia, with platelets reduced to approximately 15% of normal counts, and a remarkable expansion of immature megakaryocytes in the bone marrow. GATA-1 deficient megakaryocytes are smaller than wild type cells and have multiple abnormalities, including a scant cytoplasm with paucity of granules, reduced proplatelet processes and an excess of rough endoplasmic reticulum (rER), as well as a reduced polyploidization. Platelets derived from these mice are also abnormal, containing few α-granules and an excess of rER. Loss of GATA-1 in the MK lineage leads to an abnormal proliferation of immature

37

megakaryocytes *in vitro* and *in vivo* (Vyas et al., 1999). Two other studies found that GATA-1s expression could not completely rescue megakaryocyte growth in foetal murine GATA-1-deficient progenitors compared with re-expression of full length GATA-1 (Muntean and Crispino, 2005; Kuhl et al., 2005). These two studies showed that the ability of GATA-1 to restrict megakaryocytic growth was not dependent on the critical interaction between GATA-1 and its cofactor FOG-1, because this interaction requires the N-terminal zinc finger that is also present in GATA-1s. In contrast, differentiation of megakaryocytes into proplatelets *in vitro* was critically dependent on this interaction and much less influenced by the N-terminal transactivational domain residues. These results further defined a requirement for different domains of GATA-1 in megakaryocytic development and suggested that the production of GATA-1s uncouples megakaryocytic growth from differentiation. During normal human haematopoiesis both GATA-1s and GATA-1 are translated, whereas in the leukaemic blasts of the DS-TMD and AMKL only the short form is produced because of the inactivating mutations, of the clonal nature of the malignant proliferation and of the X chromosome inactivation. The fact that GATA-1s can bind DNA and interact with FOG-1, but shows a less efficient transactivation potential than the full length protein, suggests it might act as a dominant negative protein in the context of the Down syndrome leukaemia. Further work is needed to fully address the function of GATA-1s in humans. An obvious limitation of mouse model studies is the possible species-specificity of GATA-1s function, since GATA-1s is physiologically expressed in humans, but not in the mouse. A recent report has described a family with a germline mutation in GATA-1 leading to the constitutive production of GATA-1s but not of GATA-1 full length. Strikingly, members of this family display postnatal anaemia, thrombocytopenia and neutropenia, but there was no record of haematological malignancies (Hollanda et al., 2006).

1.4.5. The role of trisomy 21

Several models have been proposed to explain the increased incidence of AMKL and TMD in DS. It is reasonable to hypothesize that trisomy 21 could result in increased levels of a leukaemia-predisposing gene (or genes) regulating haematopoiesis, encoded on chromosome 21 (Huret and Leonard, 1997). Alternatively, overexpression of a gene present on HSA21 may alter expression of genes on other chromosomes involved in haematopoiesis and megakaryopoiesis.

The following is a brief description of genes residing on HSA21 with known functions relevant to normal and/or malignant haematopoiesis.

RUNX-1

Probably the most interesting candidate leukaemia-predisposing gene on HSA21 is RUNX-1 (AML1). RUNX-1 is a transcription factor whose rearrangements are involved in some of the recurring translocations present in leukaemia, including t(8;21) in AML- M2, t(3;21) in CML blast crisis and t(12;21) in childhood ALL. Mutations of the DNA-binding Runt domain of RUNX-1 are present in approximately 10% of sporadic cases of de novo AML (Osato et al., 1999) and in myeloid malignancies with acquired trisomy (Preudhomme et al., 2000), but they were not detected in blast samples from patients with DS-AMKL (Bourquin et al., 2006). Even if RUNX-1 is most frequently inactivated in human leukaemias, an increased dose of this gene has also been suggested as a basis for several kinds of leukaemias of the lymphoid and of the myeloid lineage (Yanagida et al., 2005) and therefore may play a role in the mechanism underlying leukaemogenesis in Down syndrome. RUNX-1 is crucial for normal haematopoiesis. RUNX-1$^{-/-}$ embryos die at embryonic day 12-13 (E12-E13) with a complete lack of AGM and FL-based definitive haematopoiesis (Okuda et al., 1996; Wang et al., 1996).

Haploinsufficiency of RUNX-1 results in reduced adult repopulating ability and alters the temporal and spatial distribution of HSCs in mice (Cai et al., 2000). Until recently, two conflicting theories about the *in vivo* generation of HSC existed. The first postulated that endothelial cells and HSC developed from a common progenitor, the haemangioblast (Choi et al., 1998), whereas the second (Jaffredo et al., 1998) suggested that HSCs are directly derived from a specialized subset of endothelial cells (i.e. the "haemogenic endothelium"). Lancrin et al. have recently unified the two theories, proposing that the haemangioblast generates HSCs through the formation of an intermediate haemogenic endothelium. The authors also demonstrate that whereas the establishment of the haemogenic endothelium requires the TF SCL/Tal1, RUNX-1 has a crucial role for the emergence of HSCs from the haemogenic intermediate (Lancrin et al., 2009). Another study also reported that RUNX-1 function is essential for the formation of HSC and haematopoietic progenitors from the vasculature, but that the requirement for RUNX-1 in this process ends when VAV-1 (a pan-haematopoietic gene) is expressed (Chen et al., 2009).

RUNX-1 is a master regulator of the physiologic lymphoid and megakaryocytic development (Ichikawa et al., 2004a). RUNX-1 null mice show impaired maturation, morphological abnormalities and hypoploidy of megakaryocytes, and reduced platelet counts (Ichikawa et al., 2004b). Since RUNX-1 and GATA-1 are known to physically interact with each other and to promote megakaryocytic specific gene expression (Elagib et al., 2003), it is likely that an alteration of this network of transcription factors can be responsible for the observed lineage-specific phenotype. It is also noteworthy that haploinsufficiency of RUNX-1 caused by loss-of-function mutations results in an autosomal dominant congenital platelet defect (familial platelet disorder, FPD) characterised by qualitative and quantitative defects of the platelets and

by an increased propensity to develop AML (Dowton et al., 1985; Ho et al., 1996; Song et al., 1999). Song et al. analysed leukaemic blasts of two FPD/AML patients without finding evidence for mutations in the remaining RUNX-1 allele during the progression to AML, and concluded that additional mutations outside the RUNX-1 locus are required for the development of leukaemia in these patients. However, very recent data obtained by analyzing further patients with FPD with progression to AML suggest that, in addition to the germline RUNX1 mutation, a second RUNX1 alteration is often associated with progression to AML (Preudhomme et al., 2009). Of the 6 FPD/AML cases reported in this new study, 4 cases presented acquired point mutations in RUNX-1, and 2 cases displayed duplication of the altered RUNX1 allele associated with acquired trisomy 21.

ERG and ETS-2

ERG and ETS-2 are both members of the ETS family of transcription factors mapping to the Down Syndrome Critical Region on HSA21. Together with the closely related gene FLI-1 they share overlapping functions in megakaryocytic differentiation (Bouilloux et al., 2008; Ge et al., 2008). ERG is a potent proto-oncogene in cancer (prostate cancer, Ewing's sarcoma, acute leukaemias) and it constitutes a prominent candidate for a leukaemogenic effect in Down syndrome. Rainis et al suggested that the overexpression of ERG, in cooperation with other HSA21 genes such as RUNX-1 and ETS-2, facilitates the occurrence of megakaryoblastic leukaemia through a shift towards the megakaryoblastic lineage in haematopoietic progenitor cells (Rainis et al., 2005). Furthermore, a recent study has for the first time highlighted a physiological role for ERG in haematopoiesis (Loughran et al., 2008). Based on the results from an N-ethyl-N-nitrosourea (ENU) mutagenesis screening, the authors studied the effects on the haematopoietic system of an ERG mutation (Mdl2) inducing loss of its transactivation potential. The

consequences of this loss-of-function mutation were profound, including an impaired number and repopulation ability of HSCs, and a quantitative defect in the megakaryocytic lineage. Mdl2$^{-/-}$ mice showed a marked defect in the establishment of definitive haematopoiesis, which seemed to be independent from known ERG binding targets such as SCL/Tal1.

Similarly, a role in regulating the megakaryocytic gene expression has been suggested for ETS-2 (Lemarchandel et al., 1993). As for ERG, overexpression of ETS-2 in the leukaemic cell line K562 induced an erythroid to megakaryocytic switch, which was shown to be independent from GATA-1 levels (Ge et al., 2008). The authors of this study also demonstrated that GATA-1 and ETS-2 interplay to modulate sensitivity of leukaemic cells to anthracyclines. ERG and ETS-2 (together with FLI-1) have also been recently shown to facilitate the expansion of megakaryocytes from wild type and GATA-1s knock-in foetal liver progenitors (Stankiewicz and Crispino, 2009). In this study ETS-2 and ERG could only partially rescue the maturation block of the megakaryocytic lineage characteristic of the GATA-1 knockdown progenitors. Overexpression of ERG or FLI-1 (but not ETS-2) was also shown to immortalize GATA-1 knockdown and GATA-1s knock-in (but not wild-type) foetal liver progenitors, suggesting a synergistic effect between alterations in GATA-1 and increased levels of ETS proteins in malignant megakaryopoiesis.

DSCR1

DSCR1 is a member of the calcipressin family of calcineurin inhibitors and has been showed to be expressed 1.5 fold more in tissues from DS patients compared to euploid controls (Fuentes et al., 1995). A study from Arron et al. showed that increased dosage of DSCR1 and of the neighbouring kinase gene DYRK1A on HSA21 are responsible for the deregulation of NFAT (Nuclear Factor of Activated T cells) levels and activity in DS mouse models and in human trisomy 21 samples, with effects on the correct execution of

42

developmental programs (Arron et al., 2006). Furthermore, DSCR1 has been shown to be a calcium-induced NFAT target gene in megakaryocytes (Kyttala et al., 2009). This study suggests that the NFAT pathway activation might be controlled by DSCR1 with an auto feedback mechanism and through this mechanism DSCR1 might influence lineage specific gene expression in megakaryocytes.

TIAM1 and BACH1

TIAM1 (T-cell lymphoma invasion and metastasis-1) is a Rac specific guanine nucleotide exchange factor (GEF) that can mediate Ras activation of Rac. When simply amplified or overproduced, TIAM1 causes invasiveness of mouse lymphoma cells (Habets et al., 1994). A study from Ives et al. showed that TIAM1 is threefold more expressed in DS AML-M7 samples compared to the remission samples or samples from normal individuals (Ives et al., 1998).

BACH1, a transcriptional repressor expressed in the megakaryocytic lineage, was also shown to be overexpressed in DS-AMKL blasts compared to non DS-AMKL blasts (Bourquin et al., 2006). An interesting report has also elucidated a role for BACH1 in megakaryocyte development and platelet formation (Toki et al., 2005). BACH1 transgenic mice show thrombocytopenia associated with impaired maturation of megakaryocytes, and these effects seem to be linked to the function of BACH1 as a transcriptional repressor of megakaryocytic genes containing specific recognition motives.

Although the altered expression of TIAM1 and BACH1 is intriguing, their functional role in DS leukaemogenesis has not yet been investigated.

Other candidate genes

Other putative candidates for a leukaemogenic predisposition on HSA21 include the interferon α/β receptor (IFNAR), cytokine family 2-4 (CFR2-4), GART and SON (Legare et al., 1997).

In addition to protein-coding genes, there are at least 5 known microRNAs encoded by chromosome 21. Micro-RNAs are small non-coding RNAs, which can regulate gene expression through degradation of mRNA transcripts and inhibition of mRNA translation. Strong evidence suggests that some microRNAs, such as miR-181, miR-223, and miR-142 are differentially expressed in haematopoietic tissues, and their expression is regulated during haematopoiesis and lineage commitment in mice (Chen et al., 2004). A recent article (Garzon et al., 2006) has highlighted a role for microRNAs during human megakaryopoiesis. When comparing expression levels of several microRNAs between CD34$^+$ haematopoietic progenitors, AMKL cell lines and megakaryocytes differentiated *in vitro*, the authors observed that miR-99a, a microRNA residing on HSA21, was up-regulated in AMKL and down-regulated in CD34$^+$ progenitors and megakaryocytes. This inverse correlation could be an exciting starting point for the involvement of microRNAs in the pathogenesis of AMKL.

DS-AMKL shows a superior response to treatment with chemotherapy compared to AMKL in the general population. DS-AMKL blasts display an increased sensitivity to chemotherapeutic agents *in vitro* (Tchernia et al., 1996). The gene responsible for this feature is on HSA21 (in the region 21q22.3) and encodes for the enzyme cystathionine β-synthase (CBS), which is involved in cytosine arabinoside metabolism (Taub et al., 1999; Zwaan et al., 2000).

General remarks

Despite several attempts to dissect the contribution of individual genes to leukaemogenesis in Down syndrome, so far none of the genes on HSA21 has been unequivocally defined as critical for the predisposition to DS-TMD and AMKL. Recent findings have revealed that DS-ALL is characterised by acquired mutations of the tyrosine kinase JAK2, creating a situation that

mirrors the GATA-1 mutations in DS-TMD and AMKL. In view of this similarity, it is reasonable to postulate that the presence of the chromosome 21 as a whole (or part of it) might deregulate haematopoietic development through multiple mechanisms, and predispose different lineages to acquire mutations (GATA-1, JAK2) that cause abnormal proliferation and/or selective blocks in differentiation. The individual variations in the level of expression of the genes present in a third copy might explain why some of the DS individuals are more prone to get leukaemia than others. In spite of the tremendous progress made towards an understanding of the general mechanisms of leukaemogenesis in DS (derived from *in vitro* and *in vivo* models), a lot still needs to be done to explain the real biological relevance of some of the described (or suggested) phenotypes caused by genes on HSA21 to the pathogenesis of DS leukaemia.

1.4.6. Down syndrome Leukaemia: where does it arise from?

Both DS-TMD and AMKL occur within a limited time frame (neonatal and early childhood, respectively). This raises the question of whether a developmentally restricted cellular target mediates the GATA-1s oncogenic effect. The physiological down-regulation of this target during development would explain why older DS individuals do not get leukaemia with an increased incidence compared to the euploid population.

This fascinating hypothesis has been recently developed by Li et al., who have shown that knock-in mutations leading to the exclusive production of GATA-1s in place of full-length GATA-1 in the absence of trisomy 21, result in excessive proliferation and abnormal differentiation of an embryonic/foetal megakaryocytic progenitor population, suggesting a stage-specific requirement for the N-terminus of GATA-1 in haematopoietic progenitors (Li et al., 2005). If this foetal liver progenitor is the cellular origin of the

leukaemogenic program initiated by GATA-1s, then trisomy 21 might be providing a selective advantage for the proliferation of this mutated clone. Alternatively, trisomy 21 might be responsible for an abnormal accumulation of this precursor that predisposes it to acquire GATA-1 mutations (Izraeli, 2008). In other words, there could be an abnormal foetal haematopoietic programme in DS, which is responsible for a skewing of the haematopoietic lineages that promotes an abnormal number and/or function of the megakaryocytic precursors. Tunstall-Pedoe et al. and Chou et al. have both recently tested this hypothesis by comparing second trimester human foetal liver haematopoiesis in DS to gestational age matched euploid controls (Chou et al., 2008; Tunstall-Pedoe et al., 2008). In colony forming assays, both groups demonstrated that DS foetal livers have three times more megakaryocyte-erythroid progenitors than disomic controls, and that these progenitors have increased proliferation and self-renewal properties. The observed phenotype was independent of the presence of GATA-1 mutations and (at least in the observations from Tunstall-Pedoe et al.) was not present in bone marrow from DS foetuses. These reports further highlight the contributions of trisomy 21 to the development of leukaemia in DS and contribute to explaining why TMD often involves the liver but not the bone marrow. However, these studies also raise a question, about whether abnormal foetal haematopoiesis in DS is caused by specific properties of the foetal liver microenvironment or by cell intrinsic mechanisms deregulated by the trisomy. This is likely to be an intense area of investigation in the field in the near future.

1.4.7. A unique model of leukaemogenesis

GATA-1 mutations in DS leukaemia are acquired: they have been detected in both TMD and AMKL but are absent in the remission samples. Identical

mutations of GATA-1 have been reported in sequential samples from the same patients that progressed from TMD to AMKL (Hitzler et al., 2003). This suggests that AMKL arises after the initial TMD clone has acquired additional abnormalities (Ahmed et al., 2004). If different GATA-1 mutations, resulting in similar effects on GATA-1 protein, were restricted to a specific point of the differentiation process towards the megakaryocytic lineage, these mutations would be expected to arrest the affected clones at the same stage of differentiation. However, a report from Groet et al. demonstrates that independent clones with different mutations of GATA-1, each leading to the production of GATA-1s, can be arrested at different phases of the differentiation process in the same patient (Groet et al., 2005). An intriguing explanation of these results is that GATA-1 mutations do not arrest megakaryocytic differentiation completely, but trigger an abnormal proliferation of the mutant clone, as suggested in the murine GATA-1 knock-in model (Li et al., 2005). The transient and self regressive nature of TMD could be explained postulating that a transient myeloproliferation arises in the foetal liver and when the haematopoiesis migrates to the bone marrow the loss of a "permissive" environment causes the disappearance of the proliferating cells (Gamis and Hilden, 2002). Alternatively, the regression of the transient disorder might be due to the clearance of proliferating blasts by the immune system (Hitzler and Zipursky, 2005).
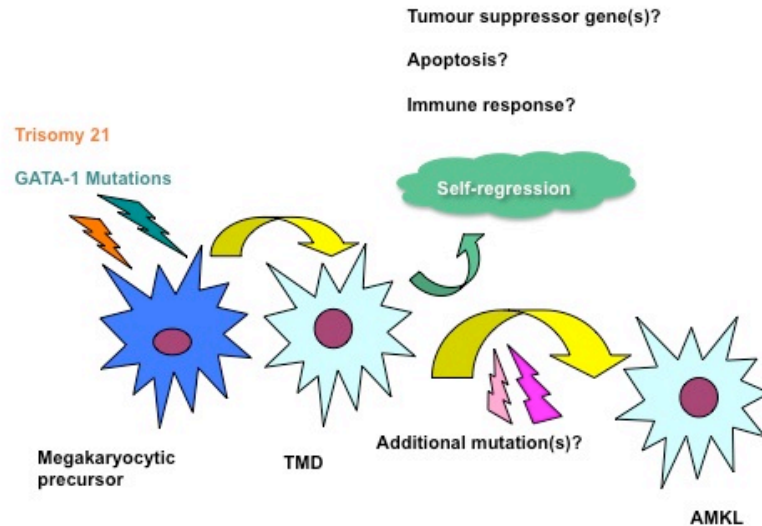
Fig. 1.6. A schematic view of leukaemogenesis in DS. Trisomy 21 might cause abnormal proliferation of megakaryocytic precursors. Mutations in GATA-1 uncouple differentiation and proliferation of these precursors and are responsible for the appearance of TMD. Additional events responsible for the self-regression of TMD or the recurrence of AMKL within 3-4 years are currently unknown.

It is clear that, besides the presence of the GATA-1 mutations and of the trisomy of chromosome 21, a **"**third hit" is necessary to trigger the progression of TMD to AMKL (Figure 1.6). For all the above reasons, TMD and AMKL in DS provide a unique paradigm for the study of different stages of leukaemogenesis in general.

1.4.8. Other mutations in DS Leukaemia

Several genes have been implicated as potential culprits of the evolution of TMD to AMKL. Analysis of the most common alterations found in acute myeloid leukaemia failed to confirm a role for FLT3, N-RAS and c-KIT mutations (Hirose et al., 2003). p53 mutations were found in a few cases of both AMKL and TMD, but these data were in contrast with a previous report (Malkin et al., 2000) suggesting the involvement of p53 mutations in the evolution from TMD to AMKL.

Mutations in JAK2 (Walters et al., 2006), which are reported in myeloproliferative disorders of adults, and of c-mpl, have also been screened in DS-TMD and DS-AMKL samples without any evidence of contribution to these malignancies (Norton et al., 2007).

A recent twist in the search for a "third hit" was the finding that mutations in the tyrosine kinase JAK3 are present in AMKL (Walters et al., 2006). Activating mutations of JAK3 were reported in AMKL from both Down syndrome and non Down syndrome patients. This finding prompted the proposal of using a JAK3 inhibitor, clinically approved in autoimmune diseases (Changelian et al., 2003), for the treatment of DS AMKL. A more detailed analysis is required to ascertain the role of mutations of JAK3 in the pathogenesis of DS leukaemia and in the progression of malignancy of the DS-TMD clone.

1.4.9. Molecular profile of DS Leukemia

To explore the molecular differences between TMD and AMKL blasts, which are immunophenotypically and morphologically indistinguishable, McElwaine et al. made use of comparative analysis of gene expression (McElwaine et al., 2004), which led to the identification of the tumor antigen PRAME (PReferentially expressed Antigen in MElanoma) as a specific marker for AMKL with no expression in TMD. The same type of analysis has revealed that CDKN2C (p18), the effector of GATA-1-mediated cell cycle arrest, was increased in AMKL but not TMD, whereas MYCN (neuroblastoma–derived oncogene) was expressed in TMD at a greater level than in AMKL, potentially contributing to the proliferative state and self-regressing features of TMD (Hitzler and Zipursky, 2005).

Another study has revealed a differential expression between the two diseases of other genes, such as Apolipoprotein C1, the MYL4 component of myosin and spermidine/spermine-N-acetyltransferase (Lightfoot et al., 2004).

To date, none of the differentially expressed genes has been proven to be responsible for the progression of leukaemia in DS. Nevertheless, the comparison between sequential stages of the leukaemic transformation is a very important approach likely to result in the definition of the specific genetic events that underlie the development of AMKL from the precursor lesion TMD (Hitzler, 2007).

Gene expression profiling has also been carried out comparing 24 DS and 39 non-DS AMKL samples (Bourquin et al., 2006). The main finding of this study is that there is a deregulation of a subset of genes in DS-AMKL, which is probably due to the absence of GATA-1 and to the exclusive presence of GATA-1s in the DS-AMKL blasts. However, this effect does not seem to depend on the presence of an extra copy of human chromosome 21. This conclusion further emphasizes the role of GATA-1s in the leukaemogenic process in DS, but needs to be evaluated taking into account the limited number of samples analysed.

1.5. Mouse models of Down syndrome

1.5.1. Partial trisomic models of Down syndrome

The human chromosome 21 is homologous to mouse chromosomal regions that map to three different mouse chromosomes (MMU): MMU16, MMU17 and MMU10. As approximately 23 Mb of the HSA21 are syntenic to MMU16, the vast majority of mouse models of Down syndrome generated in the past years are trisomic for variable regions of mouse chromosome 16.

The first mouse model of DS, Ts16, contains three copies of the entire MMU16. Trisomy of the entire mouse chromosome 16 is lethal, and Ts16 mice die *in utero* at E15, this being very likely due to the presence on MMU16 of a large extra set of genes non syntenic to genes of HSA21. Ts16 chimeric foetuses generated with a pre-implantation trisomic-diploid aggregation technique (Cox et al., 1984) exhibit immunological and cardiac abnormalities typical of DS (Epstein et al., 1985). Because of the significant limitations of this model, segmental trisomic models were generated later on.

To date, three segmental trisomy models of DS have been generated: Ts65Dn, Ts1Cje and Ms1Ts65. Each contains three copies of different regions of MMU16 (see Figure 1.7) and displays phenotypes of DS to various degrees.

The Ts65Dn mouse model is trisomic for a region of approximately 16 Mb of HSA21 encoding 104 conserved genes (Davisson et al., 1990). Because the triplicated region does not include genes that are not homologous to genes on HSA21, the Ts65Dn is a viable and effective model for some aspects of Down syndrome. Ts65Dn present craniofacial abnormalities (Richtsmeier et al., 2000), abnormal thymic functions (Paz-Miguel et al., 1999), male sterility and heart malformations (Moore, 2006), but their predominant phenotypes are confined to the nervous system. These mice exhibit profound defects in hippocampal-dependent spatial learning and memory (Reeves et al., 1995) and an age-dependent reduction of the number of cholinergic neurons in the basal forebrain (Granholm et al., 2000; Holtzman et al., 1996). Ts65Dn mice also have a significant reduction in cerebellar volume (Baxter et al., 2000) and a reduced number of granule cells. The postnatal viability of these mice, and the close resemblance of the spectrum of their phenotypes to the ones described in DS, make this model especially suitable for dissecting the role of candidate genes on HSA21 in the neuronal phenotypes of DS. This is

supported by the fact that after Ts65Dn were found to have a reduced number of cerebellar neurons, large cohorts of DS individuals were screened and found positive for this phenotype, which very likely accounts for the motor coordination disturbances in DS (Baxter et al., 2000).

The Ts1Cje mouse model is trisomic for a smaller region of MMU16 (~12 Mb) than that present in three copies in the Ts65Dn, and this region contains approximately two-thirds of the genes triplicated in the Ts65Dn. This mouse model resulted from translocation of the distal end of chromosome 16 to chromosome 12 (Sago et al., 1998) and was derived during a gene-targeting event for the gene SOD1. The smaller size of the triplicated region might be responsible for the slightly less severe spectrum of phenotypes observed in the Ts1Cje compared to the Ts65Dn. Like the Ts65Dn, these mice survive to adulthood. They do not show morphological abnormalities in the brain and they have less severely impaired learning abilities than the Ts65Dn. Ts1Cje mice also present abnormalities in their cerebellum (Olson et al., 2004), although to a smaller extent than the Ts65Dn.

In order to investigate the discrepancy in phenotypes between the Ts65Dn and the Ts1Cje models of DS, a third partial trisomy model for DS was generated. The Ms1Ts65 bears a third copy of the region that is triplicated in the Ts65Dn but is disomic in the Ts1Cje. These mice exhibit the least severe phenotypic defects of all the partial trisomic models (Sago et al., 2000). Their learning capacity is partially compromised and they have no changes in cerebellar volume, but present a slight reduction in the number of neurons of the cerebellar cortex (Olson et al., 2004).

Despite the penetrance of the phenotypes in the partial trisomic models, which reflects that of phenotypes observed in the DS population, none of the DS mouse models are fully imbred. Therefore, the variations in phenotypes might be a consequence of genotypic background differences.
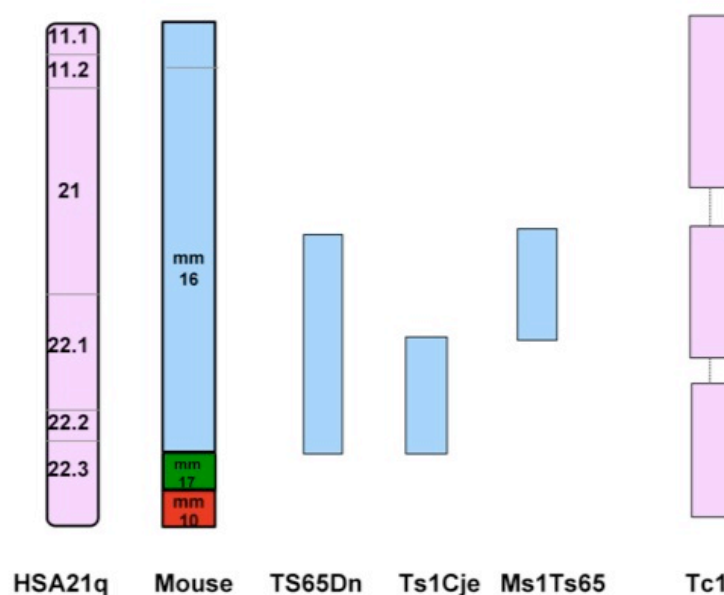
Fig. 1.7. Synteny between human chromosome 21 and mouse chromosomes 16, 17 and 10. MMU16 (depicted in blue) has the largest region of synteny with HSA21 (in pink) corresponding to 104 known genes on HSA21. MMU17 and MMU10 are syntenic with smaller distal portions of HSA21 (in green and red, respectively). Mouse models of trisomy 21 are shown on the right. The Ts65Dn, Ts1Cje and Ms1Ts65 mouse models are trisomic for different segmental regions of MMU16, with Ts65Dn being trisomic for the largest portion of MMU16. Tc1 carry an extra copy of freely segregating HSA21 into a mouse euploid background.

Nevertheless, these models have been extremely useful in studying nervous system and behavioural abnormalities and in validating the candidate region approach, whereby the gene dosage imbalance of a particular region of HSA21 is associated with a defined phenotype.

Several transgenic models overexpressing single genes orthologous to HSA21 genes have also been developed. Examples include the *TgSOD1* mice, which exhibit learning defects, or the *TgETS-2* and the *TgDYRK1A* (Dierssen et al., 2001) mice. It is arguable that despite a proven utility in elucidating the contribution of individual genes to the DS phenotypes, these models are less relevant to the biology of DS because they do not recapitulate the 1.5 fold overexpression observed in DS, and only in some cases the expression of the transgene is under the control of endogenous regulators.

An alternative approach would be to generate mice carrying yeast artificial chromosomes (YACs) containing fragments of genomic DNA encoding for different genes of interests under the control of their endogenous regulatory sequences. Such mice have already been generated for some regions of the HSA21 (Smith et al., 1997), although the obvious size limitation (up to 2 MB) of the inserts YACs can carry makes this approach less than ideal to model trisomy in the mouse.

1.5.2. Mice with a human chromosome 21: a novel model of Down syndrome

The most significant drawback of the partial trisomic models described is that none of them contain a third copy all of the genes that are triplicated in human DS. This crucial point has been addressed by a novel approach, consisting of the introduction of the human chromosome 21, in its entirety, into a mouse euploid background (Hernandez et al., 1999). This was achieved by creating mouse ES cells engineered to carry an entire human chromosome through a technique known as irradiation microcell-mediated chromosome transfer (XMMCT, illustrated in Figure 1.8). XMMCT is a unique technique with respect to the large amounts of genetic material that it can introduce into cells. Microcells are defined as cell-like structures with a small nucleus (micronucleus) that contains one or a few chromosomes (Fournier and Ruddle, 1977). They have been shown to be very efficient vehicles for the transfer of whole chromosomes to a wide range of cells, including ES cells (Cuthbert et al., 1995; Tomizuka et al., 1997).

The work from Hernandez et al. was initailly aimed to generate a human chromosome 21 targeted with a selectable marker (the neomycin resistant gene). This gene was inserted in the *D21S55* (part of the DSCR region) in a human donor cell line. The human donor cell line with the targeted

chromosome 21 was then treated with colcemid, an inhibitor of the mitotic spindle, to induce the formation of microcells. After colcemid treatment, the chromosomes became partitioned into discrete subnuclear compartments termed micronuclei. Micronuclei were then centrifuged in the presence of cytochalasin B to prevent formation of actin filaments. The centrifugation step resulted in the formation of a thin cytoplasm and outer plasma membrane around individual micronuclei. The microcell layer was collected after centrifugation and irradiated to kill any remaining donor human cells. Irradiated microcells were then fused to the parental ES cell line D3 using polyethylene glycol (PEG), and colonies were selected in G418. Subsequently, colonies were screened with FISH analysis using human Cot1 DNA as a probe, and the colonies showing presence of a single freely-segregating human chromosome were further characterised by PCR and Southern Blotting using markers spaced approximately 1-2 Mb apart on HSA21. After this procedure, selected transchromosomic cell lines were also karyotyped to determine mouse chromosome number, and only the euploid ones were used for further studies. It is known that the irradiation process can cause chromosomal rearrangements, but no radiation breakage "hot spots" or rearrangements were detected at that stage, and the radiation dose used in the experiments was carefully titrated to avoid these effects.

A panel of ES cells (Figure 1.9) carrying segments of HSA21 was generated, and one of them (named 47-1) appeared to contain the entire HSA21. Four different transchromosomic ES cell lines were then selected and injected into blastocysts to generate chimeric mice. Chimeric mice (as judged from the colour of the fur) were shown to contain human genomic DNA, but they exhibited deletions in the sequence of the human chromosome 21, most likely due to phenomena occurring during culture before the injection into blastocysts.
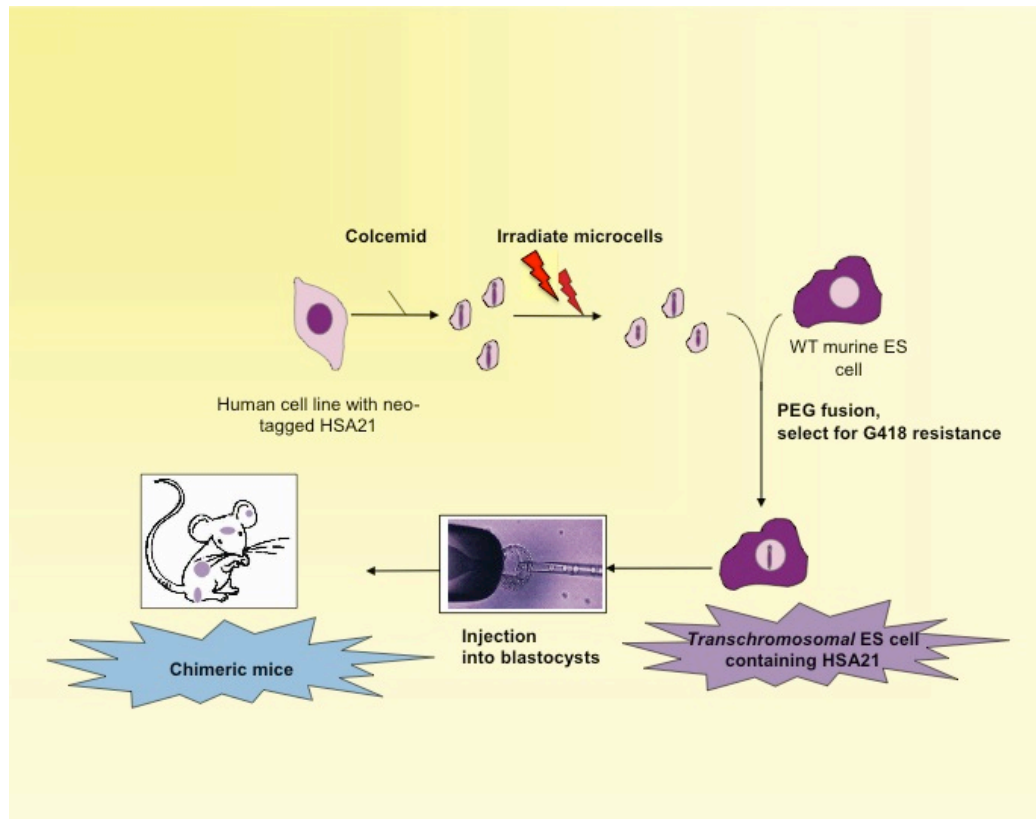
Fig. 1.8. A schematic view of the irradiation microcell-mediated chromosome transfer (XMMCT). Details of the procedure, which lead to the generation of chimeric mice, are described in the text.

RT-PCR analysis showed that gene expression driven from human specific sequences was conserved and tissue-specific, suggesting that gene regulation was maintained in the transchromosomic system. Unfortunately, the chimeric mice from these experiments failed to reach germline transmission, possibly due to sex and genetic background limitations of the transmitting animals. A second attempt was carried out by the same group, leading this time to the generation of a mouse strain (named Tc1) bearing a freely segregating copy of HSA21 (O'Doherty et al., 2005). The ES cells used to generate the strain were named 91-1, and were generated by XMMCT on the mouse background of the MPI-VI ES cells (a parental cell line different from the one used for the previous attempt). 91-1 contained at least 42 Mb (90%) of the 46.9 Mb of the HSA21 and approximately 92% of all known HSA21 genes.

Among the genes mapping in the deleted region in the 91-1 cells are RUNX-1 and DSCR-1; therefore these genes are not trisomic in the Tc1 model (F. Wiseman and E. Fisher, unpublished data).
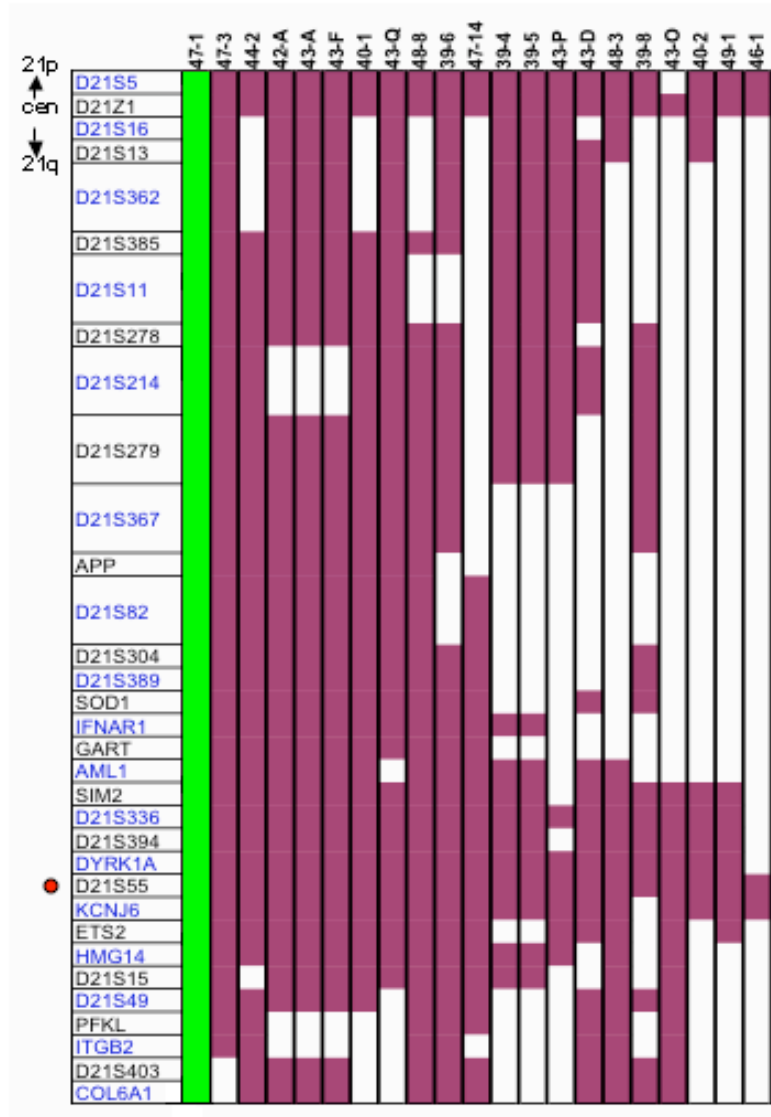
Fig. 1.9. Map of the panel of transchromosomic ES cells generated from Hernandez et al. The red dot indicates the insertion of the *neo*-resistance gene. Filled bars indicate that that region of HSA21 is expressed in the ES cell line; open bar indicates that that region is absent. **47-1 (in green) contains the HSA21 in its entirety.** (Reproduced from Hernandez et al, *HMG*, 1999).

91-1 ES cells were injected into blastocysts and the resulting chimeras were mated to mice from the C57BL/6J strain. The progeny from this mating contained a freely segregating HSA21 with the same profile as the 91-1 cell

line. Retention of the HSA21 in tissues from adult Tc1, measured by FISH and quantitative PCR, ranged from 66±7% in the brain to 49±5% in the spleen. Microarray, quantitative RT-PCR and western blot analysis all demonstrated specific expression of human genes in the transchromosomic mouse model.

Tc1 mice show the most complete range of phenotypes of human DS reproduced in a mouse model. Behavioural tests have revealed that they have impaired learning abilities and synaptic plasticity, exhibiting short-term memory defects but not long-term memory alterations (Morice et al., 2008). Other neurological phenotypes include a decreased density of cerebellar neurons and disturbed motor coordination (Galante et al., 2009). Tc1 mice display a high penetrance of congenital heart defects, mimicking the abnormalities in septum formation observed in newborns with DS. CT scans measurements also showed that these mice have a smaller mandible than that of their wild type littermate, a phenotype that has been described in DS humans as well.

The study of transchromosomic mice raises a series of issues. The first is that human genes may behave differently in a mouse context, possibly changing their pattern of spatial and temporal expression and their relative abundance. If a human protein works sub-optimally in the mouse, it will affect the gene dosage imbalance that these mice are trying to model.

Secondly, it is unclear how expression of human genes in a cross-species context is regulated. Genetic and epigenetic mechanisms of regulation of transcription might be different for human genes in a heterologous context. Wilson et al. have recently addressed this matter utilising hepatocytes from Tc1 mice. The authors demonstrated that transcriptional regulation is largely dependent on the DNA sequence of the genes in question, whereas interspecies differences in epigenetic machinery, cellular environment, and transcription factors themselves play secondary roles. This means that the

expression of human genes in a cross-species system is driven predominantly by human DNA regulatory sequences rather than by the mouse cellular context (Wilson et al., 2008).

The third issue concerns the stability of this system and the capacity of the animals to retain the human chromosome, which requires a thorough characterization and confirmation of the characteristics of the model itself before any experimental approach.

Despite the limitations arising from working with a trans-species system, this is currently the most comprehensive mouse model DS, and the possibility of expressing genes from an entire chromosome under the control of their own regulatory sequences provided by this approach offers an extraordinary powerful tool to model DS and other aneuploidies in the mouse.

1.5.3. Haematopoietic defects in mouse models of Down syndrome

Ts65Dn and Ts1CjE mouse models of DS have both been recently characterised with respect to their haematopoietic system.

Ts65Dn display macrocytic anaemia (humans with DS also display macrocytosis) and progressive thrombocytosis). Adult mice (14-15 months) develop a highly penetrant myeloproliferative-like disorder (MPD) with bone marrow fibrosis and hyperproliferation of the megakaryocytic lineage in the spleen and in the bone marrow. Megakaryocytes infiltrating the spleen and the bone marrow in Ts65Dn express CD41 (a marker of mature megakaryocytes) but their ploidy profile is distorted, suggesting an abnormal maturation of this lineage. Additionally, the bone marrow of the Ts65Dn contains an increased number of c-KIT positive cells compared to the WT littermates, indicating an expansion of immature progenitor cells. In vitro colony forming assays to assess the number of haematopoietic progenitors in

Ts65Dn bone marrow and spleen showed a shift towards erythroid and megakaryocytic lineages in the spleen, and analysis of compartments in the bone marrow revealed an expansion of the LSK (lineage$^-$Sca-1$^+$c-KIT$^+$) compartment, possibly reflecting deregulation of the haematopoietic stem cell pool. Long-term repopulating ability of Ts65Dn bone marrow cells was impaired and some of the characteristics of the adult MPD were also present in younger mice at the age of 4 months (Kirsammer et al., 2007). Interestingly, crossing the Ts65Dn with RUNX-1 heterozygous knockout mice to generate progeny trisomic for 103 genes of HSA21 but disomic for RUNX-1 did not attenuate the adult MPD phenotype, but somewhat influenced the megakaryocytic colony forming ability of the spleen derived cells. This result further highlights the complexity of mechanisms responsible for the phenotypic consequences of trisomy 21.

Ts1Cje mice (which are trisomic for approximately two thirds of the triplicated genes in the Ts65Dn) also display macrocytosis in the peripheral blood and anaemia, but unlike Ts65Dn mice, they do not present any histological abnormality in the spleen or in the bone marrow. Foetal livers (FL) from Ts1Cje at E12.5 do not present alterations in the number of LSK cells, but they appear unable to reconstitute the haematopoietic system of lethally irradiated mice. In addition, the ability of FL haematopoietic progenitors from Ts1Cje mice to form colonies *in vitro* is impaired. The number of bone marrow HSCs is decreased in Ts1Cje, but their engrafting ability is not affected. An increase in the granulocyte-macrophage progenitor (GMPs) number with a concomitant decrease in the common myeloid progenitor (CMPs) fraction was also observed in Ts1Cje bone marrow, but the megakaryocytic-erythroid (MEPs) compartment was not altered. Older mice did not develop any sign of MPD or acute leukaemia. These mice were then crossed to the GATA-1 [Plt13/+] mice, which carry a mutation in the exon 2 of GATA-1 leading to the loss of

translation of the full length GATA-1 protein but not to the production of its short form. The crossing did not lead to any exacerbation of the observed phenotype, or to the development of MPD (Carmichael et al., 2009). The difference between the phenotypes observed in Ts1Cje and Ts65Dn might be due to the genetic background of the strain used to breed the colonies, or maybe to the specific effects of the region of HSA21 that is not triplicated in the Ts1CjE.

Phenotype	Ts65Dn	Ts1Cje	Tc1
Macrocytosis and anaemia	Yes	Yes	Yes
Thrombocytosis	Yes	No	No
Foetal Liver- HPCs	Not studied	Fewer colonies in semisolid medium, altered reconstitution potential	NA
Bone marrow HSCs and HPCs	Expansion of HSCs in the bone marrow; fewer quiescent stem cells.	Skewing of CMPs to GMPs	NA
Bone marrow fibrosis	Yes	No	NA
MKs infiltrating the spleen	Yes	No	Yes
MPD-like disease in adult mice	Yes	No	Yes
Leukaemia	No	No	No

Table 1.3. A comparison between haematopoietic phenotypes in three mouse models of DS. Data for Ts65Dn and Ts1Cje are derived from Kirsammer et al. (*Blood,* 2009) and Carmichael et al. (*Blood,* 2009). At the moment K. Alford and V. Tybulewitcz are carrying out analysis of the haematopoietic system of the transchromosomic Tc1 mice.

It is also worth noting that the lack of any abnormal/malignant haematological proliferation in the progeny resulting from the breeding of the Ts1CjE with the

GATA-1 $^{Plt13/+}$ might have been influenced by the absence of the oncogenic effect of GATA-1s.

Analysis of the haematopoietic system in the Tc1 mouse model of DS is currently under way. Preliminary observations suggest that these mice also develop an MPD-like phenotype in adult age, without the occurrence of an overt acute leukaemia (K. Alford and V. Tybulewitcz, unpublished data).

Despite the relevance of some of the described phenotypes it is clear that there are peculiar differences between mouse models and humans with DS, which must be taken into account when trying to elucidate leukaemogenic mechanisms caused by the trisomy 21.

1.6. ES cells as a model to study developmental processes

The blastocyst stage of the mouse embryo is composed of three cell types: the trophectoderm, which gives rise to the placenta, the primitive endoderm, which leads to the visceral and parietal endoderm that lines the yolk sac cavity, and the inner cell mass (Evans and Kaufman, 1981; Martin, 1981).

Embryonic Stem cells (ES) are derived from the inner cell mass (ICM) and they can be propagated in culture in an undifferentiated state (self-renewal) while retaining the capacity to generate any cell type in the body (pluripotency). Self-renewal requires that the ES cell genome maintains a cellular memory that specifies its pluripotent capacity while existing in an undifferentiated state. Additionally, the genome in pluripotent ES cells must be highly plastic to be able to enter any distinct differentiation pathway. Once differentiation starts, lineage specification is accomplished by the execution of gene expression programs, which are specific for each cell type. The tight balance between pluripotency and differentiation in ES cells is regulated by

the coordinated action of various regulatory mechanisms (Chen and Daley, 2008).

A very well studied mechanism involves the action of a network of pluripotency transcription factors such as OCT4, SOX-2 and NANOG (Nichols et al., 1998; Mitsui et al., 2003). These factors primarily act to regulate the expression of targets that are vital for differentiation and development, and are transcriptionally inactive at the undifferentiated stage, or are actively involved in maintaining pluripotency of the ES cells. Apart from regulating the expression of target genes through their DNA binding properties, these pluripotency TFs are extensively interconnected via protein-protein interactions (Wang et al., 2006) and are very likely to interact with chromatin remodelling factors and histone-modifying enzymes to modulate chromatin conformation.

Given that the genome of ES cells is virtually identical to the one of somatic cells, it is likely that epigenetic regulation makes a major contribution to maintenance of pluripotency in ES cells. This is mainly achieved by silencing of genes whose up-regulation leads to differentiation through the action of repressive complexes known as Polycomb Group proteins (PcG) (Boyer et al., 2006; Lee et al., 2006), but also through activation of developmental regulators during differentiation. The latter process requires the presence of genes which are "poised" for activation, and recent work has demonstrated that these genes harbour a characteristic chromatin signature known as a "bivalent" histone code (Bernstein et al., 2006; Azuara et al., 2006), with histones bearing both active and repressive methylation markers. The methylation status of CpG islands in promoters or regulatory regions of specific genes, as well as specific features of chromatin conformation are also key contributors to the epigenetic control of pluripotency in ES cells.

Further players in the control of pluripotency in ES cells have been recently identified with specific sets of micro-RNAs that are down-regulated as ES cell differentiation progresses (Houbaviy et al., 2003; Suh et al., 2004).

Understanding the mechanisms underlying the molecular control of pluripotency is essential in order to direct ES cells differentiation into specific lineages and ultimately to exploit their full clinical potential for regenerative medicine.

1.6.1. ES cells as a system to study haematopoiesis

Haematopoietic stem cells (HSCs) are the best-characterised adult type of multipotent stem cells. Bone marrow transplantation has been the prototype of cellular therapy and is extensively employed for the treatment of a variety of bone marrow disorders. Unfortunately, it is very difficult to genetically manipulate HSCs and to expand them *in vitro.* ES cells offer an alternative, powerful source of HSCs. Haematopoietic differentiation of ES cells harbours therefore an implicit therapeutic potential, while it enables basic investigation into genetic and epigenetic mechanisms of HSC specification and fate (Daley, 2003). Mouse ES cells have been used as an invaluable tool for elucidating the mechanisms underlying normal and malignant haematopoiesis (Lensch and Daley, 2006). More than two decades of research into this field has provided researchers with a variety of protocols and experimental approaches to derive HSCs and blood cells of different lineages from mouse ES cells (Keller et al., 1993). The first demonstration that mouse ES cells can, under defined culture conditions, differentiate into at least four distinct haematopoietic lineages came in 1991 (Wiles and Keller, 1991). There are currently two *in vitro* approaches for the differentiation of the mES cells into the haematopoietic lineages.

The first one is known as the "two-step" *in vitro* assay (Keller et al., 1993) and requires the culture of ES cells in semisolid medium containing methylcellulose. This method promotes ES differentiation into haematopoietic cells through the formation of embryoid bodies (EBs). EBs can then be harvested and replated in secondary methylcellulose cultures containing specific growth factors (e.g. Erythropoietin (EPO), IL-1, IL-3, Thrombopoietin (TPO)) in order to obtain differentiated haematopoietic cells. The advantages of the two-step system are that the differentiation through the EBs formation resembles the process in the early embryo, and that haematopoietic colonies can be recovered and used for morphological and molecular analysis.

An alternative approach to obtain HSCs and blood cells from mES cells is a coculture system with stromal cells (Kitajima et al., 2003). Bone marrow stromal cells, foetal liver- and AGM-derived stromal cells have been successfully employed alone, or in combination with haematopoietic growth factors, to support HSC derivation from mouse and human ES cells (Weisel et al., 2006). This approach relies on the property of the supportive stromal population to reconstitute *in vitro* the haematopoietic niche that nurses HSCs during development. Unfortunately, the combination of cell surface associated molecules, soluble factors and extracellular matrix molecules expressed by the cells of the haematopoietic niche *in vivo* are not yet fully understood, making every attempt to recreate this situation *in vitro* less than optimal (Orlovskaya et al., 2008). Despite these limitations, this approach is currently very well established to generate megakaryocytes and lymphoid cells from mES cells *in vitro* (Moore et al., 2006).

1.6.3. Transchromosomic ES cell lines and their potential use as a tool to investigate and map DS phenotypes

Transchromosic ES cell lines have been successfully used to model *in vitro* phenotypic aspects of Down syndrome. Indeed, they provide a solid model to explore the contribution of gene dosage imbalance caused by trisomy 21 to early developmental stages. Furthermore, it is possible to combine information from different cell lines carrying non-overlapping segments of HSA21 to identify a candidate gene for a given phenotype. RNAi technology and genetic manipulation can also be used in this model to restore a euploid state for a particular gene. Some care needs to be taken when evaluating results generated using a cross-species system. The effect of some human genes might be masked in a different species context by a variety of factors, including genetic and epigenetic regulation, or altered formation of protein complexes. Nevertheless, at least two examples have validated the utility of this model to explore pathogenetic mechanisms of DS. First, subcutaneous injection of pluripotent transchromosomic ES cells containing an entire copy of HSA21 into syngeneic mice gave rise to teratomas containing a significantly decreased percentage of neuroectodermal tissues compared to tumours derived from the control ES cells (Mensah et al., 2007). A comparison between genes present on HSA21 at the undifferentiated ES cells stage (at the time of the injection) and in the teratomas derived from transchromosomic ES cells allowed to identify a region on human chromosome 21 potentially responsible for the inhibition of neuroectodermal differentiation of the ES cells. Second, transchromosomic ES cells showed a significant reduction in the neuron-restrictive silencer factor (NSRE/REST), a key regulator of pluripotency and differentiation, and this alteration was reproducible across several DS models. Using partial trisomic ES cells and eQTL analysis, altered

expression of REST was shown to be caused by trisomy of DYRK1A, a tyrosine kinase on HSA21. DYRK1A was also demonstrated to contribute to a very early developmental skewing of compartments during embryoid bodies formation from transchromosomic ES cells, prompting the idea that the effect of trisomy 21 might be crucial at early developmental stages (Canzonetta et al., 2008).

A further validation of the suitability of this model to explore pathological mechanisms of DS came from proteomic analysis of the transchromosomic ES cell lines. Mass spectrometry analysis identified approximately 50 proteins whose expression was significantly altered by the presence of an extra copy of HSA21 in comparison to the wild type ES cell control (Wang et al., 2009), suggesting that a perturbed dose of these proteins might contribute to DS phenotypes.

Taken together, these results prompted us to use the transchromosomic model to explore mechanisms underlying physiological haematopoiesis and development of leukaemia in DS.

1.7. Aims of this thesis

1) To derive megakaryocytes *in vitro* from the transchromosomic ES cells and to explore the effect of trisomy 21 on proliferation and differentiation of the megakaryocytic lineage.

2) To generate a model of ES cells trisomic for genes on HSA21 and expressing GATA-1s as a tool to investigate the cooperation between HSA21 and GATA-1 mutations during leukaemic transformation in DS.

3) To evaluate the effects of the gene dosage imbalance caused by the presence of an extra copy of HSA21 during the ontogenesis of haematopoietic stem cells from mesodermal precursors using transchromosomic ES cells.

4) To dissect the contribution of individual HSA21 genes/regions to the measurable cellular phenotypes established in the aims above.

5) To characterize the range and predict the consequences of acquired JAK3 mutations in DS-TMD and DS-AMKL cases.

2. Materials and methods

2.1. Cell culture

2.1.1. Mouse ES cell culture

The mouse embryonic stem (ES) cells D3 and 47-1 and mouse embryonic fibroblasts (MEFs) used for this study were provided by our collaborators (E. Fisher, Institute of Neurology, UCL, UK and V. Tybulewicz, NIMR, Mill Hill, UK). The wild type ES cell line D3 was originally established by Doetschman and colleagues from day 4 129/Sv blastocysts (Doetschman et al., 1985). The transchromosomic ES cell line 47-1 contains a freely segregating human chromosome 21 (HSA21) in the background of the diploid D3 mouse genome (Hernandez et al., 1999). Other transchromosomic ES cells used in this study contained fragments of HSA21 and were also generated from the parental cell line D3.

All ES cell lines were cultured using medium supplemented with 5×10^5 U/ml leukaemia inhibitory factor (LIF) in order to maintain them in an undifferentiated and pluripotent state. To optimally support their growth, ES cells were also cultured on a feeder layer of mouse embryonic fibroblasts (MEFs), mitotically inactivated by UV irradiation or treatment with mitomycin C. ES cell lines were grown on 25 cm^2 tissue culture (TC) flasks. A 0.1% weight/volume gelatin solution was prepared by dissolving gelatin from porcine skin (Sigma G1890) in distilled water and sterilized by autoclaving. For coating of dishes with gelatin, 4 ml of the 0.1% gelatin solution was evenly dispensed onto the surface of the flasks. Flasks were left at room temperature for an hour in a laminar flow hood and then excess gelatin solution was aspirated. 4 ml of ES cells medium (450 ml DMEM, Sigma, D5796; 75 ml ES batch-tested FCS, PAA, A15208; 5 ml 200 mM L-Glutamine, Sigma G3126; 5 ml 100x MEM Non-

Essential Amino Acids solution, Sigma, M71452; 5 ml 100x Penicillin/Streptomycin solution, Sigma, P4333; 3.5 µl β-mercaptoethanol, Sigma, M7522; 50 µl LIF-ESGRO®, Millipore, ESG1107) were subsequently added to gelatinised flasks to prevent the gelatin from drying out. Following this step, 2×10^6 MEFs were seeded onto each gelatinised flask. MEFs were left to attach from 1 hour to overnight at 37ºC in a humidified incubator with 5% CO_2. Medium was then changed and ES cells were seeded onto the feeder layer (MEFs). ES cells were passaged every two to three days by trypsinising and seeding onto fresh feeder or gelatin-coated flasks. Cells were typically split at ratios of 1:2 to 1:4 every two to three days, with the splitting ratio depending on their confluence. For splitting of cells, flasks were washed twice with sterile PBS, and then 1 ml of 0.25% trypsin-EDTA solution (Sigma T3924) was added and left on the cells for 1 – 2 minutes in a humidified, 37ºC, and 5% CO_2 incubator. 4 ml of ES cell medium were added to neutralize the trypsin and cells were further dissociated by vigorous pipetting before seeding onto fresh feeder plates. 47-1 and other transchromosomic ES cells were maintained in ES cell medium supplemented with 500 µg/ml G418 (Sigma, G5013) in order to select for cells containing the *neo* tagged HSA21. One passage before starting the differentiation experiment, 47-1 ES cells were grown in the absence of G418.

2.1.2. Adherent cell culture

The ecotropic packaging cell line PLAT-E was a kind gift from Prof. T. Kitamura (Tokio, Japan) (Morita et al., 2000). Cells were maintained on TC-treated 10 cm dishes in DMEM supplemented with 10% FCS, 5 ml 200 mM L-Glutamine, 100U/ml penicillin and 100 U/ml streptomycin, 1 µg/ml puromycin (Sigma, P7255), and 10 µg/ml blastidicin (Sigma, 15205). Cells were split

every 2-3 days, when they reached approximately 80% confluency. For splitting, cells were detached from the plate by gentle pipetting using fresh medium without addition of trypsin.

Puromycin-resistant primary mouse embryonic fibroblasts (used as feeder layers for culture of puromycin-resistant ES cells) were purchased from Stem Cell Technologies (Vancouver, Canada). Cells were grown on TC flasks in DMEM supplemented with 20% FCS, 5 ml 200 mM L-Glutamine, and 100 U/ml penicillin and 100 µg/ml streptomycin. To inhibit cell proliferation, mitomycin C treatment was carried out as follows. Confluent flasks of fibroblasts were treated with culture medium supplemented with 7.5 µg/ml of mitomycin-C (Melford) for 2 hours. Cells were then washed thoroughly three times with PBS to avoid any potential residue of mitomycin-C. Fresh culture medium was then added and cells were incubated for 3 hours to overnight before being trypsinised, harvested and frozen down at the concentration of 2 x 10^6 cells/vial. This amount of cells was enough to support ES cell growth in a small flask.

The mouse fibroblast NIH3T3 cell line was obtained from ATCC, and cultured in DMEM supplemented with 10% FCS, 5 ml 200 mM L-Glutamine, 100 U/ml penicillin and 100 µg/ml streptomycin, and split by trypsinization. Cells were typically split at ratios of 1:8 to 1:10 every three to four days, with the splitting ratio depending on their confluence.

2.2. Haematopoietic differentiation of the ES cells

Haematopoietic differentiation of the mouse ES cell line D3 and of the transchromosomic ES cells was performed using a coculture system based on the OP9 stromal cell line (Kitajima et al., 2003).

OP9 cells were obtained from ATCC (CRL-2749). They were grown on TC flasks and kept in a medium prepared as follows: 4,028 g of MEM powder, 6.4

mg Phenol Red, and 8 ml sodium bicarbonate were dissolved in 450 ml of distilled water; medium was then sterilized by filtration and foetal bovine serum (ATCC, 30-2021) and L-glutamine were added to achieve a final concentration of 20% and 2 mM, respectively. OP9 cells were routinely passaged every 3 days (at approximately 70–80% confluency) to avoid overgrowing. To passage OP9 cells, medium was removed, cells were washed once in PBS and incubated in 0.25% trypsin-EDTA at 37 °C in a humidified incubator with 5% CO_2 until they detached. Fresh medium was added, and after carefully pipetting to avoid clumps, one-third of the cells were dispensed into new flasks.

Haematopoietic differentiation of mouse ES cells was carried out in 6-well plates (Era et al., 2000). A confluent layer of OP9 cells ($2x10^5$ cells/well) was seeded in 6-well plates 16 hours before starting the differentiation protocol. At day 0, each well of a 6-well plate covered with a confluent layer of OP9 cells was seeded with $5x10^4$ ES cells using the OP9 medium. Half of the medium of each well was changed at day 3 of the differentiation protocol. At day 5, cells were trypsinised using 0.5 ml of trypsin-EDTA solution at 37 °C in a humidified incubator with 5% CO_2 until they detached. Fresh medium was added and cells from all the wells were harvested, pipetted vigorously to break clumps, and plated for 45 minutes into a T75 TC flask. This replating step was necessary to remove the stromal cells. The supernatant from this step contained the induced non-adherent fraction, which was used for further experiments.

2.2.1. Flow cytometry analysis

Day 5 HSCs/haematopoietic progenitors (HPs) derived from ES cells were washed once in PBS, centrifuged and resuspended in 100 µl of 10% FCS in

PBS containing anti-mouse CD41–FITC conjugated (BD Biosciences, 553848, clone MWReg30) and anti-mouse CD 117/c-KIT–APC conjugated (BD Biosciences, 553356, clone 2B8) at a dilution of 1:100, or the isotype controls rat IgG1 k-FITC conjugated (BD Biosciences, 553924) and rat IgG2b k-APC conjugated (BD Biosciences, 553991) at the same dilution. After 30 minutes of incubation at 4 ºC, cells were brought to the FACS facility for analysis. Data were collected on a LSRII instrument from BD Biosciences and analysed with the FlowJo software version 8.7.1. A minimum of 30,000 events was recorded per sample. A main gate was placed to exclude dead cells. Compensation for each fluorophore was performed using Becton Dickinson compensation beads with the FACSDiva software. The frequency of positive cells and the mean fluorescence intensity for FITC and APC within this subpopulation were then calculated. The same statistical analysis was applied to all the samples analysed, including the isotype controls.

2.2.2. Assay for counting haematopoietic colonies derived from mesodermal precursors

Induction of differentiation was carried out as in 2.2, and the cells were harvested by treatment with trypsin at day 5. Cells were then counted and replated onto a fresh OP9 feeder layer at a density of 5 x 10^2 cells/plate in a 96-well plate. At day 12, wells were scored under a light microscope for the presence of haematopoietic colonies composed of round-shape cells loosely attached to the stromal cell layer.

2.2.3. Colony forming assay

At day 5 of the haematopoietic differentiation protocol, cells were harvested by treatment with trypsin, resuspended vigorously to a single cell suspension and

replated onto a fresh OP9 feeder layer. Three days later (day 8), cells were trypsinised again, pipetted up and down several times to break clumps, counted and plated into semisolid medium supplemented with cytokines (Methocult®, M3434, Stem Cell Technologies, France) at a density of 1x 10^5/dish in 35 mm dishes. Medium used for these experiments contained recombinant mouse IL-3, recombinant human IL-6 and recombinant human erythropoietin (EPO). Each culture was seeded in duplicate and left in a humidified incubator with 5% CO_2 for 14 days. Scoring of the colonies was performed using a light microscope according to the manufacturer's instructions.

2.3. Megakaryocytic differentiation of the murine ES cell lines

2.3.1. Megakaryocytic differentiation protocol

Megakaryocytic differentiation (Figure 2.1) of mouse ES cell was induced using a coculture system based on the OP9 stromal cell line as described in 2.2. At day 5 after the original seeding, induced cells (non-adherent fraction) were harvested and plated onto a fresh layer of OP9 in a 6-well plate at a concentration of $1x10^5$ cells/well. 20 ng/mL of mouse recombinant thrombopoietin (TPO) was added to the medium. At day 8, cells were harvested again after a preplating step of 45 minutes and resuspended in fresh OP9 medium supplemented with TPO at a concentration of 10 ng/mL, recombinant murine IL-6 at a concentration of 10 ng/mL and recombinant human IL-11 at a concentration of 10 ng/mL. All cytokines were purchased from Peprotech, UK. Cells were kept in culture up to day 13.

2.3.2. Cytospin and AchE staining

Day 13 megakaryocytes/megakaryocyte precursors were washed once in PBS and resuspended at a concentration of 1 x10^6 cells/ml. 100 µl were then spun onto poly-D-Lysine treated slides (VWR) in a Shandon Cytospin 3 centrifuge at 800 rpm for 5 minutes. Acetylcholinesterase (AchE) staining was performed on unfixed cells as described in 2.4.5.
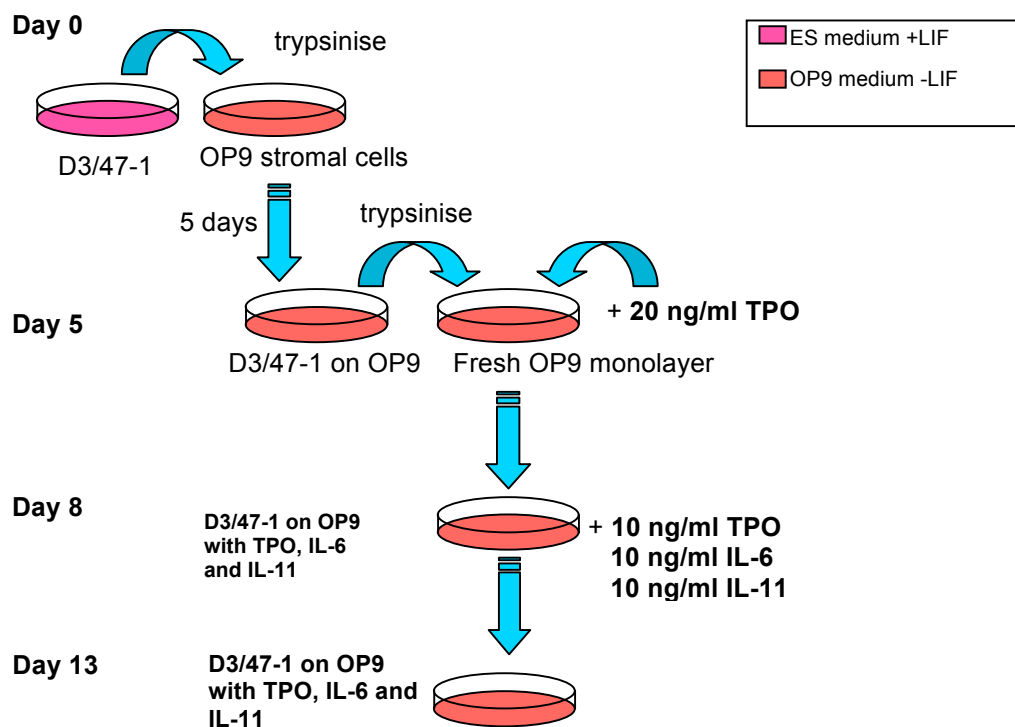
Fig. 2.1. **Schematic view of the differentiation protocol used in this study to differentiate mES cells into megakaryocytes.** The protocol is based on the presence of a stromal cell line (OP9) and the addition of cytokines with a known role in megakaryopoiesis.

2.3.3. Surface antigen labelling and ploidy assay

Day 13 ES-derived megakaryocytes were harvested and depleted of OP9 by a 45 minutes preplating step (see 2.2). Cells were washed once in PBS,

centrifuged and resuspended in 200 µl of 10% FCS in PBS containing anti-mouse CD41–FITC conjugated (BD Biosciences, 553848, clone MWReg30) at a dilution of 1:100 or the isotype control Rat IgG1 k-FITC conjugated (BD Biosciences, 553924) at the same dilution. After 30 minutes of incubation on ice in the dark, cells were brought to the FACS facility for analysis. Data were collected on a LSRII (BD Biosciences) instrument and analysed with the FlowJo software version 8.7.1. The same number of events (30,000) was acquired for each sample, and the same acquisition parameters were applied to test tubes and isotype controls. A main gate was designed to exclude dead cells and applied to all samples. A positive subpopulation was then gated, and data obtained from this population were presented as histogram plots with overlay of curves of the isotype controls and test tube. Mean fluorescence intensity of the sample was plotted on the x-axis, and the number of events was plotted on the y-axis.

Antibody labeling was performed as described above to perform sorting of CD41$^+$ cells. Sorting was performed on a FACSAria platform (BD Biosciences). Cells were sorted in 10% FCS in PBS, washed once in PBS, then fixed in 70% ice-cold ethanol for 30 minutes on ice. After this step, cells were centrifuged at 1200 rpm for 5 minutes, washed once in PBS and centrifuged again. Cells were then incubated with 50 µL of RNase (100 mg/ml Sigma) for 15 minutes at 37 ºC. Before analyzing them on the FACS platform LSRII, 200 µL of propidium iodide (PI) solution (Sigma P4170, 50 mg/ml) were added to the cells. Data were acquired on the LSRII using the FACSDiva Software. The linear voltage on the 610/20 nm channel was adjusted so that a doublet discrimination gate was placed on the "Area versus Width" parameter. 25,000 events were acquired per sample, and 2N, 4N, 8N and 16N classes were displayed on a linear scale.

2.3.4 TPO dependent colonies formation

CFU-MK assay was performed using the MegaCult®-C kit (Stem Cell Technologies, 0496). At day 13 of the differentiation protocol, one tube of MegaCult®-C medium without cytokines was defrosted overnight at 4ºC and supplemented with 50 ng/mL of TPO, 100 U/ml penicillin and 100 µg/ml streptomycin. $1x10^5$ cells for each slide were counted for each cell population using a Neubauer counting chamber and resuspended in 0.1 ml of Iscove's MDM medium. Cells were then added to the MegaCult®-C medium and the tubes were vortexed. 1.2 ml of bovine collagen solution (StemCell Technologies, Europe), kept on ice, was then added to the tube containing cells and semisolid medium and vortexed again. 0.75 ml of the final culture was then dispensed into each of the two wells of a double chamber slide (StemCell Technologies, Europe) avoiding air bubbles formation. Slides were then placed in a covered 100 mm Petri dish containing 1 uncovered 35 mm dish with 3 ml of sterile water to ensure appropriate humidity, and transferred to a 37 ºC humidified incubator with 5% CO_2.

Slides were removed from the incubator after 10 days. At that point, the plastic walls and the rubber seal of the chamber slides were removed. A pre-cut spacer and a filter card were then placed onto the chamber slides and the liquid was allowed to soak the card. Slides were then fixed in ice-cold acetone for 5 minutes on ice, and then left to air dry. After that, a staining solution composed of 10 mg of acetylthiocholiniodide (Sigma, UK) in 15 ml of 0.1 M sodium phosphate buffer with the addition of 1 ml of 0.1 M sodium citrate, 2 ml of 30 mM copper sulfate and 2 ml of potassium ferricyanide was added to the slides, which were incubated in a humid chamber for 4 hours at room temperature in the dark. The staining solution was then removed and slides were fixed in 95% ethanol for 10 minutes and rinsed in water, counterstained

with Harris' hematoxylin solution (Sigma) for 30 seconds, rinsed again and allowed to air dry. Scoring of the colonies was carried out by light microscopy using a 20x objective. Mouse megakaryocytes and early megakaryocytic progenitors appeared brown due to the copper ferricyanide in the cytoplasm resulting from the enzymatic reaction catalyzed by acetylcholinesterase. Colonies containing at least 3 brown cells were considered positive. Images from sequential fields of every slide were taken on a Leica Q5501W microscope. The Leica Qwin v3.2 software was used to determine the area of the colonies, in square pixels (pp^2), by manually tracing the 20x magnification images, captured at a resolution of 37.79 pixels/cm. Colony size was classified in 3 categories (small: 2000-15,000 pp^2, medium: 15,000-50,000 pp^2 and large: > 50,000 pp^2) and compared using the Pearson X-square test.

CFU-MK assay was performed in slightly different conditions to address the effect of GATA-1s on the megakaryocytic lineage. MKs/MK progenitors were obtained by in vitro differentiation of D3 and 47-1 ES cells transduced with GATA-1s or the MSCV-PURO vector as described in 2.3.1. At day 13 of the differentiation protocol, $1x10^5$ cells were counted and resuspended in Methocult® semisolid medium (Stem Cell Technologies, M3231) supplemented with TPO at a concentration of 20 ng/mL, and recombinant murine IL-6, IL-3, and human IL-11 all at a concentration of 10 ng/mL. Medium was supplemented with puromycin at the concentration of 1 µg/mL to select for the growth of transduced cells only. Cytokines were purchased from Peprotech, UK. Each culture was seeded in two 35 mm dishes and left in a humidified incubator with 5% CO_2 for 8 days. Scoring of the colonies was performed using a light microscope.

2.4. ES cells manipulation

2.4.1 Human specific RNAi

Human-specific, RNAi-mediated knockdown of RUNX-1 was achieved in 47-1 ES cells by utilizing siRNA oligos targeting four different portions of the human RUNX-1 sequence. A pool of 4 different duplexes was purchased from Dharmacon (siGenome SMARTPool, M-003926-02-0005) and specificity of the targeted sequences was verified using the NCBI Basic Local Alignment Search Tool (BLAST). Target sequences are listed in Appendix 6.1. 100 picomoles (pmol) of the oligo mixture were transfected into the mouse transchromosomic ES cell line 47-1 using 4 μg of the Lipofectamine 2000® reagent (Invitrogen, 11668019) and the Opti-MEM® medium (Invitrogen, 1058-021), according to standard manufacturer's instructions for transfection of cells in suspension. Transfection was carried out in a 12-well plate; 5×10^5 cells/well were transfected in suspension in a gelatinised plate without a feeder layer. Identical conditions were applied in parallel to the transfection of a control RNAi (targeting an irrelevant sequence of the mouse genome, see appendix 1.6). Opti-MEM® medium was replaced with fresh ES cell medium 5 hours after transfection.

2.4.2 Retroviral transduction

To generate retroviral supernatant, 20 μg of the retroviral vectors MSCV-PURO-GATA-1s and MSCV-PURO (details of the constructs are shown in Appendix I) were transfected into the ecotropic packaging cell line PLAT-E (stably expressing the viral components gag, pol and env) in a 10 cm dish format using the Lipofectamine 2000® reagent. Medium was replaced 24 hours after the transfection and the retroviral supernatant was used at 48 and

72 hours. The retroviral supernatant was carefully collected from the plate, filtered through a 0.45 acetate cellulose filter and supplemented with 8 μg/ml Polybrene (Sigma, H9268). Medium containing the retroviral supernatant from 8 plates per construct was pooled together and concentrated by centrifugation at 11,200 rpm for 2 hours at 4 ºC. The resulting viral pellet was resuspended in fresh ES medium (1/10 of the original volume) and used for the transduction procedure, derived with minor modifications from (Cherry et al., 2000). ES cells were washed, trypsinised and resuspended in retroviral containing medium; cells were then plated at the density of 8 x 10^5/well in a gelatinized 6-well plate and centrifuged for 45 min at 2500 rpm at room temperature. The retroviral supernatant was then removed and replaced with fresh medium. 24 hs after the "spinfection" procedure, ES medium was aspirated and replaced with freshly collected retroviral supernatant prepared as the day before. Cells were then incubated overnight with the retroviral supernatant, and the morning after medium was replaced by fresh medium. 48 hours after the infection, cells were trypsinised, plated on puromycin-resistant feeder cells, and puromycin at the concentration of 1 μg/mL was added. Selection was carried out for at least 10 days before sampling the cells for verification of the integration and expression of the retroviral construct by PCR on genomic and complementary DNA.

For optimizing the protocol of infection, production of retroviruses was also carried out by triple transfection of 293T cells with the retroviral vector MSCV-IRES-GFP (MIG) and plasmids encoding the viral components gag, pol and env. Details of these plasmids are provided in Appendix 6.1. The efficiency of the transduction protocol was tested by infecting NIH3T3 with retroviral supernatant produced by transfection of the PLAT-E packaging cell line or by triple transfection of the 293T cell line using the MIG vector. The level of GFP

expression was monitored by FACS analysis. The MIG vector was also utilized to test the transduction protocol on ES cells.

2.5. Immunohistochemical analysis

2.5.1. Immunohistochemistry protocol on paraffin-embedded tissues

Archived material was obtained from the autopsy collection of specimens at the Department of Pathology, University of Split Medical School. All archived material was consented for use in research, and the project was covered by ethical approval from the North East London Health Authority.

To dissolve the paraffin, 5 μm thick sections were incubated twice in fresh xylene (Fluka, 95673) for 5 minutes. Slides were then incubated twice for 5 minutes in 100% ethanol, once for 5 minutes in 95% and 70% ethanol solutions, and then subjected to two rehydration steps of 5 minutes each in distilled water. Antigen retrieval was performed by incubating the sections for 20 minutes in citrate buffer (10 mM Na-citrate, 0.05% Tween20, pH6.0) pre-heated to 95°C in a boiling water bath. For staining with the anti-CD34 antibody, the citrate buffer was replaced by an EDTA Buffer (1 mM EDTA, 0.05% Tween 20, pH 8.0). Endogenous peroxidase activity was blocked incubating slides for 10 minutes with a 3% H_2O_2 solution in methanol. After this step, blocking solution (10% donkey or horse serum in PBS) was added to the sections, which were then incubated for an hour at room temperature in a humidified chamber. After a wash with agitation in PBS for 5 minutes, slides were incubated with the primary antibody solution (antibody in 2% serum in PBS) from an hour to overnight. A list of primary antibodies used for staining and their dilutions is provided in table 2.1.

Antibody	Species	Dilution	Manufacturer
Anti CD41	Goat Polyclonal	1:500	Santa Cruz
Anti CD34	Mouse Monoclonal	1:50	Dako
Anti von Willebrand	Rabbit Polyclonal	1:400	Dako

Table 2.1. Antibodies used for immunohistochemical analysis. List of primary antibodies, species they were derived from, and manufacturers. Working dilution in 2% serum in PBS is also indicated.

The incubation with primary antibody was followed by 3 x 10 minute washes in 0.05% Tween-20 in PBS. Slides were then incubated with the secondary antibody solution (antibody in 1% serum in PBS) for 1 hour at room temperature. Secondary antibodies used were: biotinylated horse anti-goat IgG; biotinylated donkey anti-mouse IgG; biotinylated goat anti-rabbit IgG. All secondary antibodies were used at a dilution of 1:1000. Immunoreactivity was developed with the Vectastain Elite ABC Kit (VectorLabs, UK). Following incubation with secondary antibodies, sections were washed twice in 0.05% Tween-20 in PBS for 10 minutes; in the meantime, two drops of solution A and B from the kit were mixed in 5 ml PBS (ABC-HRP solution) and incubated at room temperature for 30 minutes before use. The ABC-HRP solution was then added to the slides and left to act for 30 minutes. After extensive washes in 0.05% Tween-20 in PBS, diaminobenzidine (DAB) liquid substrate solution (Sigma, D6815) prepared according to the manufacturer instructions was added to the sections for 30 seconds-5 minutes. Slides were washed in distilled water twice for 5 minutes, stained for 10 minutes at RT with Harris Haematoxylin solution (Sigma, H3136), flooded for 15 seconds in a 1% acid alcohol solution (1 ml of concentrated HCl in 100 ml of 70% Ethanol) and washed again twice in distilled water for 5 minutes. Tissues were finally dehydrated through sequential steps in 70%, 95%, 100% Ethanol, equilibrated for 10 minutes in xylene and sealed with a few drops of DPX mounting medium (Sigma) and a coverslip. Slides not incubated with the primary

antibody served as negative controls. Sections were analysed with the Leica Application Suite software on a Leica Q5501W Microscope.

2.6. Western Blotting

2.6.1 Nuclear extracts preparation

Nuclear extracts from cells transfected with hRUNX-1 RNAi oligos and control RNAi oligos were prepared by Dr. Frederic Delom with the Qproteome Nuclear Protein Kit (Qiagen) according to the manufacturer's instructions.

2.6.2. Western Blotting

Proteins were separated by SDS-PAGE. The separating and stacking gels for two minigels (BioRad system) were prepared as described below:

Separating gel (12%)**:**

H_2O	1.78 ml
Buffer A (0.75 M Tris pH 8.8, 0.2% SDS)	6.75 ml
Acrylamide/Bisacrilamyde (30%)	5.4 ml
TEMED	37.5 µl
APS 10%	95 µl

Table 2.2. Components of the separating gel for SDS page. 7 ml of this solution were poured into each Bio-Rad MiniPROTEAN® casting frame and used as a separating gel.

Stacking gel:

H2O	1.64 ml
Buffer A (0.25 M Tris pH 6.8, 0.2% SDS)	2.5 ml
Acrylamide/Bisacrilamyde (30%)	660 µl
TEMED	10 µl
APS 10%	25 µl

Table 2.3. Components of the stacking gel. 3 ml of a 4% gel were used as stacking gel.

The SDS-PAGE running buffer was composed of Tris-glycine (30 g Tris-HCl, 144 g glycine in deionized water up to 1 L) plus 0.1% SDS. The stacking gel was electrophorised at 20 mA until the dye front reached the separating gel, then the current was increased to 40 mA. Proteins were then transferred to nitrocellulose membranes by wet blotting in transfer buffer (1.8 L Tris-glycine plus 0.2 L methanol) with a Bio-Rad mini Trans-Blot apparatus. The transfer was allowed to proceed for one hour at a current of 160 mA. The blotting sandwich was disassembled and the membrane was rinsed in TBST buffer (20 mM Tris, 150 mM NaCl, 0.1% Tween 20), and then blocked for 1 h at room temperature in 5% dry milk in TBST buffer. After blocking, the membrane was cut into strips to separate proteins with different molecular weight, and the strips were probed with individual primary antibodies at 4°C overnight. Primary antibodies used in this study are reported in table 2.4. The membrane was then rinsed 3 times, washed 5 times x 5 minutes with TBST and then incubated for 1 hr at room temperature with the secondary antibody (anti mouse or rabbit IgG HRP-conjugated at a concentration of 1:5000 in 5% dry milk in TBST). Finally, membranes were washed 3 x 5 minutes in TBST and proteins were visualized using the ECL (enhanced chemiluminescence) detection system (Amersham).

Antibody	Species	Dilution	Manufacturer
Anti RUNX-1	Mouse Monoclonal	1:500	Abcam
Anti-EXH2	Rabbit Polyclonal	1:1000	Abcam

Table 2.4. Primary antibodies used for western blot analysis in this study.

2.7. gDNA analysis

2.7.1. gDNA extraction from formalin archived material

Formalin fixed tissue was extensively washed overnight at 4°C in PBS, then washed three times for 30 minutes each in TE buffer (10 mM TRIS, 1 mM

EDTA, pH 8.0). After removal of excess liquid, the sample was snap frozen in liquid nitrogen and ground into a fine powder. The powder was then resuspended in 500 µL of genomic DNA lysis buffer (10 mM Tris (pH 8); 100 mM NaCl; 100 mM EDTA and 0.5% SDS). 5 µl of Proteinase K (20 mg/mL, Qiagen, 19131) were added and the sample was incubated overnight at 55 ºC. After the incubation, 500 µl of phenol were added to the samples, and after vigorous shaking for 3 minutes to mix phases completely, the tube was centrifuged at maximum speed for 3 minutes to separate the phases. The aqueous phase was then transferred to a new microfuge tube, 500 µl of phenol/chloroform (1:1) were added, and the sample was shaken vigorously for 2 minutes and centrifuged again at maximum speed for 2 minutes. The aqueous phase was removed and transferred to a clean microfuge tube. After adding 50 µl of 3 M sodium acetate (NaOAc pH 6) and 500 µl of 100% ethanol (EtOH) at room temperature (RT) to the tube, the DNA precipitate was pelleted, and the ethanol supernatant was removed. The DNA pellet was washed in 1 ml of 70% Ethanol at RT, and then air-dried and resuspended in 30-50 µl of TE buffer. Details of alternative methods to extract gDNA from archived material are provided in chapter III.1. The heat/alkaline lysis antigen-retrieval method was derived from Shi et al (Shi et al., 2004).

2.7.2. gDNA extraction from fixed TPO-dependent colonies

After fixation and Ache staining of megakaryocytic colonies, gDNA was extracted from selected large colonies with the following procedure. Selected colonies were scratched with a G18 needle from double chamber slides and resuspended in 50 µL of 1x Amplitaq Gold PCR buffer (Applied Biosystems). The buffer containing the fixed cells was then transferred to a well of a 96-well plate and supplemented with 1 µl of Proteinase K (20 mg/mL, Qiagen). The

96-well plate was then wrapped in cling film and incubated in a hybridisation oven at 55 ºC overnight. The plate was then placed on a heating block at 100 ºC for 10 mins to avoid carryover of the proteinase K in the PCR reaction. 5 µl of this solution were used as a template in the PCR reaction to amplify and sequence GATA-1 exon 2.

2.7.3. PCR and sequencing analysis of mouse and human GATA-1

PCR amplification was performed in a thermal cycler with the following conditions: 7.5 mins at 95 ºC; 35 cycles of 30 seconds at 95 ºC, 30 seconds at 56 ºC and 1 min at 72 ºC; followed by 10 mins at 72 ºC. Reaction components were as follows:

PCR component	Volume (µl)	Final Concentration
10x Gold Buffer	2.5	1X
10 mM dNTPs	1	0.4 mM
25 mM MgCl2	2.5	2.5 mM
5 mM FWD/REV primer	0.5 of each	500 nM of each
Amplitaq Gold (5 U/**µl**)	0.2	1 U
gDNA	1-2	-
H_2O	Up to 25	-

Table 2.5. Reaction components for PCR analysis of genomic DNA. PCR reactions were performed in a final volume of 25 μl.

Human GATA-1 I1 Forward	GGATTTCTGTGTCTGAGGAC
Human GATA-1 I2 Reverse	CCAACAGCACTCAGCCAATG
Mouse GATA-1 I1 Forward	CACAACCCTTTCTGTTCCTC
Mouse GATA-1 I2 Reverse	CGGTACACCTATCCACAGAG

Table 2.6. Primers used for amplification of human and mouse GATA-1. Primers were designed in intron 1 (forward primer) and intron 2 (reverse primer) to amplify the entire exon 2 of both mouse and human GATA-1.

Primers used in PCR amplifications of gDNA extracted from mouse colonies or archived material are listed in table 2.6. They were designed to span GATA-1 exon 2 in both species. Primers were 18-22 bases in length, melting

temperatures were between 55 ºC and 62 ºC and CG content was between 35% and 60%. Agarose gel electrophoresis was performed using 1.2% agarose gels in 0.5% TAE (Tris-Acetate-EDTA) buffer. Amplified fragments were run next to a 100 bp DNA ladder (Promega). After the run, agarose gels were stained with ethidium bromide. Stained gels were analysed under a UV analyser (Alpha Innotech Corporation). Amplified DNA products were purified for sequencing analysis using ExoSap-IT, (USB, GE Amersham). 2 μl of Exosap-IT were added to 5 μl of PCR product and incubated in a thermal cycler at 37 ºC for 45 mins, then 80 ºC for 15 mins to inactivate the enzyme.

Cycle sequencing was performed with an ABI BigDye terminator V3.1 using an ABI3130XL automated sequencer (Applied Biosystems). Components of the sequencing reaction were as follows:

Sequencing reaction component	Volume (μl)
PCR purified product	1-4
Primer (Forward or Reverse 0.8 nM each)	2
BigDye Buffer 5x	2
BigDye terminator V3. 1	2
H_2O	Up to 10

Table 2.7. Sequencing reaction components. Sequencing reaction was carried out in a final volume of 10 μL.

Sequencing reactions were performed in a thermal cycler with the following conditions: 25 cycles of 10 seconds at 96 ºC; 5 seconds at 50 ºC, 4 minutes at 60 ºC. After sequencing cycles, 1 μl of NaOAc 3M (pH 5.2) and 25 μl of ice-cold ethanol were added; samples were incubated for 10 minutes on ice and centrifuged for 20 minutes at maximum speed. The ethanol supernatant was then removed, and after a wash in 1 ml of 70% Ethanol at RT, DNA pellets were dried carefully and resuspended in 10 μl of formamide. Samples were then subjected to capillary electrophoresis in the ABI3130XL automated

sequencer and sequences were analysed using the Chromaslite201 software, Technelysium Pty.

2.7.4. Verification of integration of retroviral constructs in ES cells

gDNA was extracted from undifferentiated ES cells grown under puromycin selection for at least 10 days. Cells were trypsinised, washed once in PBS and centrifuged to obtain a compact pellet. After removal of the supernatant, the cell pellet was resuspended in 250 μl of genomic lysis buffer and 5 μl of Proteinase K, and then incubated at 55 ºC for 2 hours. Samples were then subjected to a standard phenol/chloroform extraction and the gDNA was precipitated with EtOH (see 2.7.1). gDNA was resuspended in 20 μl of TE buffer, and 2 μl were used as a template for PCR analysis. PCR was performed using the same conditions and the same reagents described in 2.7.2, but with primers listed below.

Mouse GATA-1 EXON 5 Forward	ATGAGGAAAGATGGAATCCAGAC
FLAG Reverse	ATCGTCGTCATCCTTGTAATC

Table 2.8. Primers used for verification and expression of the GATA-1s-MSCV-PURO vector in transduced ES cells.

Primers were designed to amplify a fragment of 374 bp. Because the forward primer was designed in the GATA-1s insert and the reverse in the FLAG-tag, a PCR product would result only from gDNA where the GATA-1s construct is integrated.

2.8. RNA analysis

2.8.1. Total RNA extraction from frozen tissues

Total RNA was extracted from frozen tissues using the Trizol® reagent (Invitrogen, 15596-026), a solution containing phenol and guanidine

thiocyanate. RNaseZap® wipes (Ambion) were used to remove RNases from work surfaces and equipment. Individual frozen tissues were ground into powder using a DEPC-treated pestle and mortar (a different pestle and mortar was used for each sample). Liquid nitrogen was added to samples during grinding to maintain a low temperature. Ground material was then added to a 2 ml RNase-free Eppendorf tube containing 1 ml of Trizol® reagent. RNA was then chloroform extracted, isopropanol precipitated and washed with 75% ethanol in accordance with the manufacturer's instructions. For RNA solubilisation, each air-dried RNA pellet was dissolved in DEPC-treated H_2O. To ensure full dissolution of RNA, RNA solutions were pipetted several times and then incubated in a 55 ºC heat-block for 10 minutes. The volume of DEPC H_2O used for dissolving RNA ranged from 50 μl to 200 μl, depending on the amount of tissue from which the RNA was extracted. If not being used immediately, RNA solutions were stored at -80 ºC.

For determining the purity and concentration of RNA solutions, spectrophotometric analysis of diluted RNA solutions was carried out in a Biophotometer (Eppendorf). For assessing RNA purity, 1 μl of each RNA solution was diluted 1:60 in 10 mM Tris-HCl solution, pH 7.5. The A_{260}/A_{280} ratio of the diluted RNA sample was used to determine its purity. A_{260}/A_{280} ratios of 1.8 and above were considered to indicate adequate RNA purity. For the determination of RNA concentration, 1 μl of each RNA solution was diluted 1:60 in DEPC-treated H_2O before being spectrophotometrically analysed. The following formula was used to calculate the concentration of each RNA sample: A_{260} of diluted RNA x 60 (dilution factor) x 40 (extinction coefficient of absorbance of RNA, μg/ml).

All RNA samples were DNase treated before being used in RT-PCR reactions. For DNase treatment of RNA, up to 5 μg of RNA solution was added to a

reaction mixture containing a final concentration of 1X DNase buffer and 1 U/μg of RNase free DNase (Promega). Samples were incubated for 30 minutes at 37 ºC. Each reaction was terminated by adding 1 μl of RQ1 DNase Stop Solution and further incubated at 65°C for 10 minutes to inactivate the DNase.

2.8.2. RNA extraction from cells

RNA from cell lines was extracted using RNeasy mini kit (Qiagen) with the gDNA eliminator columns step, according to the manufacturer's instructions. The volume of RNase-free H_2O used for eluting RNA ranged from 30 μl to 50 μl, depending on the amount of cells from which the RNA was extracted. Purity and concentration of RNA solutions were determined as in 2.8.1.

2.8.3. cDNA synthesis

Up to 5 μg of RNA were reverse-transcribed using 200 U of the Superscript II enzyme (Invitrogen) in a total volume of 20 μl, with 10 μM DTT, 100 ng random hexamers, 0.5 mM dNTPs and 40 U RNase OUT (all from Invitrogen, Paisley, UK). Details of the reaction are shown below:

Reaction component	Volume (μl)
100 ng random hexamers	1
5 μg RNA	(max 10 μl)
10 mM dNTP mix	1
RNase-free water	up to 12 μl

Table 2.9. Components of the reverse-transcription reaction (1).

Initially, all reaction components listed in table 2.8 were incubated at 65 ºC for 5 minutes. Reaction tubes were then cooled on ice before the addition of the following components to the reaction:

Reaction component	Volume (µl)
5x buffer (First Strand Buffer for Invitrogen Superscript II RT)	4
RNaseOUT (40 U/µl)	1
Superscript II RT	1
DTT 0.1 M	1

Table 2.10. Components of the reverse-transcription reaction (2). Final volume of the reverse transcription reaction was 20 µL.

This final reaction mixture was incubated in a thermal cycler at 25 ºC for 10 minutes, at 42 °C for 50 minutes, at 70 °C for 15 minutes and then cooled down to 4 °C. A reaction without reverse transcriptase served as a negative control (RT- control). The final volume was adjusted to 50 µl with DEPC-treated water. Reverse transcription products were used immediately in PCR reactions or stored at –20ºC until required.

2.8.4. RT-PCR analysis

Human-specific RT-PCR was performed on cDNA derived from the 47-1 ES cells using human-specific primers. Primers were designed to flank a large intron in the sequence of the gene analysed to minimize amplification of contaminant gDNA. The sequence of the primers was aligned to the mouse genome using the NCBI BLAST tool to avoid interspecies amplification. Primers used for RT-PCR experiments are shown in table 2.11. PCR conditions and components of the reaction mix were as indicated in 2.7.2; the number of PCR cycles was between 32 and 37 for all of the amplicons.

Mutational analysis of GATA-1 exon 2 was carried out on cDNA derived from human foetal liver tissues amplified with the primers GATA-1 exon 2 Forward (TAATCCCCAGAGGCTCCATG) and GATA-1 exon 2 Reverse (CTGGGGAGTGTCTGTAGGCC). Sequencing analysis of GATA-1 exon 2 was performed as in 2.7.2.

Human DYRK1A Forward	ATGACCTTGCCATTGATATGTG
Human DYRK1A Reverse	GAATACCCAGAACTTCCACTAT
Human RUNX-1 Forward	GATGGCACTCTGGTCACTGT
Human RUNX-1 Reverse	CTTTTCCCTCTTCCACTTCG
Mouse RUNX-1 Forward	GGTGGAGGTACTAGCTGACCA
Mouse RUNX-1 Reverse	AGTGCCACCACCTTGAAAGC
Mouse GAPDH Forward	TCACCACCATGGAGAAGGC
Mouse GAPDH Reverse	GCTAAGCAGTTGGTGGTGCA

Table 2.11. Primers used for human-specific RT-PCR analysis.

2.8.5. Verification of expression of retroviral constructs in ES cells and MKs

RNA was extracted from undifferentiated ES cells grown under puromycin selection for at least 10 days and from megakaryocytes derived from *in vitro* differentiation of the ES cells. Cells were harvested, washed once in PBS and centrifuged to obtain a compact pellet. RNA was extracted using the RNeasy mini kit from Qiagen and eluted in 30 μl of RNAse-free water. 2 μg of RNA was reverse transcribed as in 2.8.3 and 1 μl was used as a template for RT-PCR analysis. PCR was performed using the same conditions, reagents and primers described in 2.7.2. An RT- control was included for samples transduced with the MSCV-PURO-GATA-1s vector to exclude that the presence of a specific product was due to amplification of residues of contaminant gDNA. A positive control PCR was performed on the same amount of cDNA with β-actin primers (FWD-CTAAGGCCAACCGTGAAAAGTGAT; REV-CACAGCCTGGATGGCTACGT).

2.9. Gene expression analysis by qRT-PCR

Quantitative RT-PCR (qRT-PCR) experiments were carried out in the ABI PRISM 7500 Sequence Detection System (Applied Biosystems).

2.9.1. qRT-PCR reaction conditions

Experiments described in this study were performed using both the Taqman® and the SYBR® Green detection systems from Applied Biosystems, UK.

The Taqman® probe-based chemistry employs a probe with a reporter fluorescent dye bound at the 5' end and a quencher dye at the 3' end. When bound to the target sequence, the probe (which anneals between primer sites) gets cleaved by the Taq polymerase present in the Master Mix, and the fluorescent signal from the reporter dye (previously reduced by the proximity with the quencher dye) greatly increases. Because an increased number of dyes are cleaved with each cycle, there is an increase in fluorescence intensity, which is proportional to the amount of amplicons produced during the PCR. This detection strategy is highly specific, and quick, because primers and probes are pre-designed. Assays chosen for the work described in this thesis produced amplicons of a size ranging between 60 and 150 nucleotides. Assay-on-demand® primers and probes used in this study are listed in table 2.11.

Gene	Assay ID
Mouse GATA-1	Mm00484678_m1
Mouse ETS-1	Mm01175817_m1
Mouse Integrin alpha2b (CD41)	Mm00439768_m1
Mouse Pouf51 (Oct4)	Mm00658129_gH
Mouse GAPDH	4352932E
Human GATA-1	At02279226_g1
Human CD41	Hs00166246_m1
Human GAPDH	Hs99999905_m1

Table 2.12. Taqman Assay-on-Demand® primers and probes used in this study.

Details of the qRT-PCR reaction performed with Assays-on-Demand® kits are provided in the table below:

Reaction component	Volume (µl)	Final concentration
2X TaqMan PCR Mix[1]	12.5	1X
20X Assays-on-Demand Mix[2]	1.25	1X
cDNA in sterile H_2O	Up to 25	-

Table 2.13. Components of the Taqman qRT-PCR reactions. [1]TaqMan PCR mix contains Amplitaq Gold polymerase, Gold Buffer, $MgCl_2$ and dNTPs. [2]Assays-on-Demand mix contains primers and a FAM-labelled probe at optimised concentrations.

Thermal cycling conditions for qPCRs were: 95 ºC for 10 minutes, followed by 40 cycles of 95 ºC for 15 seconds and 60 ºC for 1 min.

The SYBR® Green dye binds to all double-stranded DNA; hence the fluorescent signal increases proportionally to the amount of double-stranded PCR products. Even if SYBR Green based detection is a cost effective approach, its major limitation is the presence of non-specific binding to unwanted PCR products, i.e. primer dimers or residual genomic DNA, when performing gene expression analysis. When using this platform, non-specific product formation needs to be checked to avoid false positives. Primers for experiments performed using the SYBR green detection system in this thesis were designed spanning large introns to avoid amplification of genomic DNA contamination. CG content of the primers was between 50 and 60%; sequences were chosen to avoid secondary structure formation. Melting temperature of the primers ranged between 58 °C and 63 °C and amplicon size was between 100 and 150 nucleotides. A list of the primers used in this study is given in table 2.15. Before being used in qRT-PCR reactions, primers were tested for their ability to amplify specific target sequences on control cDNA. Reaction setup and cycling conditions for RT-PCRs to test primers were as described in section 2.8.4.

Reaction components of the SYBR Green based qRT- PCRs were as follows:

Component	Volume (µl)	Final concentration
2X SYBR Green PCR Mix[1]	10	1X
5 mM FWD/REV primers	1.2	300 nM/300 nM
2.5 mM FWD/REV primers	1.2	150 nM/150 nM
cDNA in sterile H$_2$O	Up to 20 µl	-

Table 2.14. Components of SYBR Green qRT-PCR reactions. [1]SYBR Green PCR mix contains Amplitaq Gold polymerase, Gold Buffer, MgCl$_2$, dNTPs and SYBR Green dye.

Mouse GATA2 Forward	ACCACACTTGTTGCACAGC
Mouse GATA2 Reverse	GGGTGCTCCAGCAGCTGAG
Mouse c-KIT Forward	CTCACATAGCAGGGAGCACA
Mouse c-KIT Reverse	ACAACTCACCCACACGCATA
Mouse FLK-1 Forward	CTGAATGGCACCATGTTTTC
Mouse FLK-1 Reverse	CTGTTTGACCAGGCAATGTC
Mouse SCL Forward	CAGCCTGATGCTAAGGCAAG
Mouse SCL Reverse	AGCCAACCTACCATGCACAC
Mouse TIE-2 Forward	GAAGTCGAGAGGCGATCCC
Mouse TIE-2 Reverse	GTTGACTCTAGCTCGGACTGT
Mouse PECAM Forward	AGAGACGGTCTTGTCGCAGT
Mouse PECAM Reverse	TACTGGGCTTCGAGAGCATT
Mouse VEGF Forward	CATAGAGAGAATGAGCTTCCTACAGC
Mouse VEGF Reverse	TGCTTTCTCCGCTCTGAACAAGG
Mouse RUNX-1 Forward	GGTGGAGGTACTAGCTGACCA
Mouse RUNX-1 Reverse	AGTGCCACCACCTTGAAAGC
Mouse GAPDH Forward	TCACCACCATGGAGAAGGC
Mouse GAPDH Reverse	GCTAAGCAGTTGGTGGTGCA
Human GATA2 Forward	CTGGCTCCCACCTTTTCG
Human GATA2 Reverse	CGTCCTTGTCCTCTCCTCG
Human RUNX-1 Forward	GATGGCACTCTGGTCACTGT
Human RUNX-1 Reverse	CTTTTCCCTCTTCCACTTCG
Human c-KIT Forward	TGACTTACGACAGGCTCGTG
Human c-KIT Reverse	AAATGCTTTCAGGTGCCATC
Human GAPDH Forward	GGTCATCCATGACAACTTTG
Human GAPDH Reverse	GCCATCACGCCACAGTTTC

Table 2.15. Primers used for SYBR Green qRT-PCRs.

Thermal cycling conditions for SYBR Green qPCRs were: 95 ºC for 10 mins, followed by 40 cycles of 95 ºC for 15 secs and 60 ºC for 1 min. A dissociation stage was performed at the end of each run. Conditions used were: 95 °C for 15 s, 60 °C for 30 s, then temperature was ramped up from 60 °C to 95 °C (at

the rate of 0.03 °C/s), and fluorescence intensity data were collected continuously over the ramping stage for 20 min.

For all qRT-PCRs carried out, cDNA templates were diluted 1:5 in sterile H_2O. 10-fold serially diluted cDNA expressing the gene of interest were used as standards. 5 standards ranging in concentration from 100 (neat cDNA) to 0.1 arbitrary units were set up for each primer pair. A non-template control (NTC) was always added and both standards and unknown samples were run in duplicates. The level of every gene of interest was normalized to an endogenous housekeeping control (usually GAPDH). An RT- control was added to each GAPDH run. An absence of amplification in the RT- control indicated absence of contaminant genomic DNA in the cDNA synthesized for that particular experiment.

2.9.2. qRT-PCR data analysis

Gene expression data were obtained in this thesis using the method of the absolute quantification with a standard curve. Data were analysed with the Software SDS version 2.1 (Applied Biosystems).

A typical amplification plot of fluorescence signal versus cycle number obtained from a run is represented in Figure 2.2.

In this plot, the threshold cycle (Ct) is the PCR cycle at which the fluorescence generated in a reaction exceeds the threshold. Therefore, it reflects a statistically significant accumulation of amplicons above the baseline, in a particular reaction well. Two manual adjustments were required in the amplification plot before analysis. These were an adjustment of the baseline fluorescence level (the background signal generated during the initial cycles of PCR before significant accumulation of the target amplicon has occurred) and

a manual positioning of the threshold bar at the beginning of the exponential

region of PCR amplification.
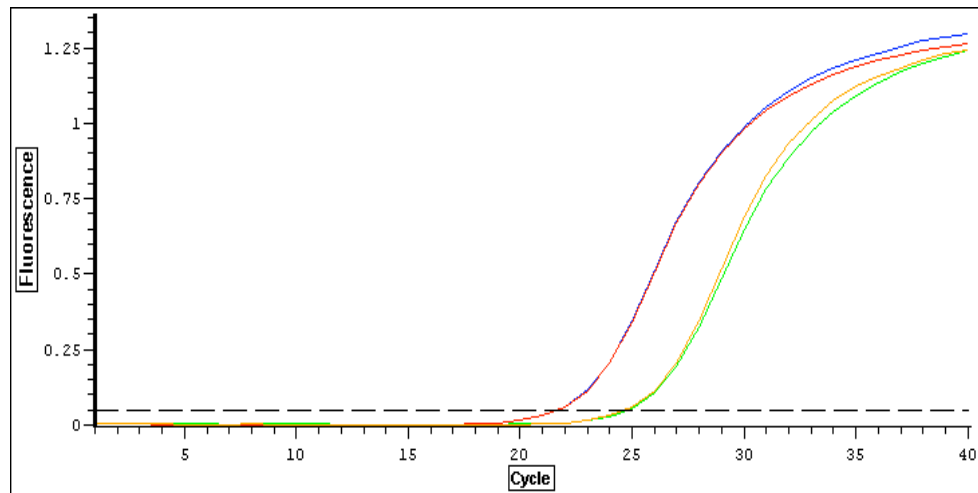
Fig. 2.2. A typical output obtained by the ABI PRISM 7500 Sequence Detection System (Applied Biosystems). Amplification plot shows number of cycles on the x-axis and fluorescence intensity on the y-axis. Ct (cycle threshold) value is defined as the number of cycles required for the fluorescent signal to cross the threshold (or background fluorescence level). Using the Ct value for each unknown and parameters deduced by the equation of the standard curve, the SDS software calculates the amount of target mRNA/cDNA present in each 'unknown' sample.

The standard curve plot was then visualized to ensure that all of the Ct values

for "unknowns" fell within the boundaries of the standard curve. The equation

for the standard curve was: $y = mx + b$, where b denotes the y intercept of

the standard curve line, and m represents the slope of the standard curve. b

and m were then used by the software to calculate the amount of target

mRNA/cDNA present in each 'unknown' sample as follows:

1. [Ct value of 'unknown' – b] / m = log input amount of the target mRNA/cDNA

2. $10^{[log input amount]}$ = input amount of the target mRNA/cDNA

3. Sum of input amounts for *'unknown A'*/ number of replicates for *'unknown A'*

    = average input amount of target mRNA/cDNA in *'unknown A'*

The average input amount of the mRNA/cDNA of interest for each '*unknown'* was then divided by the average input amount of the endogenous control (GAPDH) for that '*unknown'* sample. This gave the normalised amount of the mRNA/cDNA of interest present in each '*unknown'* sample.

Melting curve analysis was performed according to the dissociation stage data and only reactions with a single peak at expected melting temperature (Tm) were considered for further analysis. This allowed to determine the specificity of an amplification product and to distinguish specific PCR products from primer dimer products (which have a comparatively lower Tm than the amplicons).

2.10. JAK3 mutational analysis on primary samples

2.10.1. Patient samples

The sequencing project on DS-AMKL and DS-TMD patients was approved by the North East London Health Authority's Ethical Committee. Samples were surplus clinical or archived material collected by the tissue bank of the Italian National Association for Pediatric Haematology-Oncology and the Italian National Down's Syndrome Association (samples kept by the team of Galliera Genetic Bank, http://ggb.galliera.it/). The tissue banks obtained informed written consent for all subjects included in this study. Details about the patients are presented in Chapter IV.2. Every patient included in the study had constitutional trisomy 21, and all had acquired mutations in GATA-1.

2.10.2. JAK3 mutational analysis

RT-PCR was performed with 1 µl of random primed cDNA using 5 pairs of overlapping primers, spanning the JAK3 coding sequence (table 2.16).

cDNA Forward Primer	cDNA Reverse Primer
C1F-CGCCCTTCGAAAGTCCAGG	C1R-CCAGGTCCATGATGTACTTG
C2F-TGATCCAGGGCCTGAGCTTC	C2R-CAGGAAGTGAGGGTCACTGC
C3F-CCACAGGAACCTTCCTTCTG	C3R-CCCACTTGTCAGCTTCCAAG
C4F-CTGTGTTAAGCCTGGAGATG	C4R-CGAGGAATAGAGAAGGAGGC
C5F-GTCATGGAGTACCTGCCCAG	C5R-GTAGAGGACCCTCATAAGGC

Table 2.16. Primers used for JAK3 cDNA sequencing. Primers were designed to span the entire coding sequence of JAK3.

Amplification of the 24 exons of JAK3 was performed by PCR with 5-10 ng of gDNA using 15 pairs of primers as indicated in the following table:

Exon	Forward Primer	Reverse Primer
1	ACTTTCGGTAAATGACAGTGG	AGCCTTTGCCCTGGCAGCAC
2 and 3	CCCTGCTCAGAAGTCCAATC	TGGGCACCTCGAAATGCAAG
4 and 5	ATAATGTCACTCCTACTGAGG	GAAAGCTTGCAGGAGAACTC
6	CAGCTAAAAGGCCTGTGGG	CCCACTTCCCCAAGTCTTTC
7 and 8	CCACTTCGGTACTCCCCCTC	AGGGCTCCTGGAAGGTGAG
9	GAGGTACCTGAATTTGAGCC	CAGGAACCAAATGCTGACTG
10	TGTCTGTCGCTCAGTCCCAC	ACTTGCCACCCACACAGGAG
11 and 12	CTCAAACTAAGGCATGAGTTAG	ATTTCTCTGCATCCACGACC
13	GGGCCAAAGGTGACCTGTG	TATAGCGGCTCAGAACAGAG
14	CAGGGTGTTGGCAGAACCTC	CTCCTATGCATACTACAGAGC
15, 16 and 17	GATGCTGGAGCATGTCTGAG	GCTGCAAACCACGCTCCTTC
18 and 19	TGCACAGCAAGTCAACTCAG	TTCCCAGCCTACCTAAAGTG
20 and 21	TCGAGAGGGACACAAGGTCC	GCTAAGGCTGGGGAGCAAAG
22 and 23	GACCAGTTCCCCATTCCAAG	TCAGTACAGAGACTCAGGCG
24	CGCTGAATGGGAGTTGTGTC	CTACATGAATGTCCCCATTG

Table 2.17. Primers used for JAK3 genomic sequencing. Primers were designed to cover the 24 exons of the human JAK3 gene. 23 of these exons are coding.

PCR conditions were: 7.5 mins at 95 ºC; 35 cycles of 30 seconds at 95 ºC, 30 seconds at 58 ºC, and 1 min at 72 ºC; followed by 10 min at 72 ºC. DNA preparation before sequencing and sequencing analysis were performed as in 2.7.2. Sequences were analysed using the Chromaslite201 software, Technelysium Pty, LTD.

Selected PCR products were cloned into the pCR-TOPO 2.1 vector using the TOPO-TA® cloning kit (Invitrogen, K2000-01). Ligation reaction and tranformation of the One Shot® competent cells were performed according to the manufacturer's instructions. Ten light blue colonies per plate were screened by PCR to check for the presence of the insert. PCR products of the right size were then sequenced to identify the nature of the mutation cloned.

2.11. Statistical analysis

Statistical analysis on parametric data was performed in this thesis using the Student's t-test function of Excel, Microsoft. T-tests carried out were unpaired tests, with a two-tailed distribution.

Differences in the level of expression of haematopoietic genes in primary samples were assessed using the two-sided Wilcoxon's signed ranks test. For determining the correlation between certain measured variables (see Chapter III.2), Pearson correlation coefficients (r values) were calculated using the StatsDirect software. Directional and non-directional probability values for the statistical significance of r were given by the analysis tool. The non-directional probability was used in this thesis as it allows for the significance of either a positive or a negative correlation to be assessed, and is more stringent than the directional probability.

Fisher's exact test was used to assess statistical significance of categorical data. A 2x2 contingency table was built and a Fisher two-sided test was performed using the StatsDirect (StatsDirect, Ltd) software.

For every type of statistical analysis, probability values (p values) of 0.05 or less (<0.05) were considered to be statistically significant. In graphs of this thesis, p values between 0.05 and 0.01 are denoted with *, p values between 0.01 and 0.001 with **, p values = or < 0.001 with ***.

2.12. Declaration of individual contribution and authenticity of the work presented in this thesis

The work presented in this thesis was entirely carried out by the author at the ICMS, Queen Mary University of London, England, with the following exceptions. Flow-cytometry experiments and analysis of data were performed under the supervision of Dr. Gary Warnes at the Flow Cytometry Facility of the ICMS, QMUL, London. Dr. Gary Warnes and Miss Sandra Martin performed cell sorting for experiments presented in 3.I.3 at the FACS facility of the ICMS, using a FACSAria (BD Biosciences) instrument. Dr. Frederic Delom performed nuclear extracts preparation for the western blot experiment presented in Figure II.9C. Constructs used for retroviral transduction of ES cells were cloned by Dr. Jurgen Groet. Strategy for the cloning and information about the vectors are included in Appendix I. Dr. Groet also analysed CGH array data for the panel of transchromosomic ES cells included in the experiments showed in II.4.

3. Results

I. Effects of trisomy 21 on megakaryocytic differentiation of ES cells

In vitro production of blood cells of different lineages from both mouse and human ES cells has been successfully achieved using the EBs formation system, as well as employing a coculture approach with stromal cell lines (Olsen et al., 2006).

Differentiation of mouse ES cells with either of these two approaches leads to the production of a relatively homogenous population of blood cells of different lineages upon addition of lineage-specific cytokines.

The data shown in this chapter were generated adopting an established system to obtain a population of megakaryocytes/megakaryocytic precursors from mouse ES cells (Era et al., 2000; Eto et al., 2003). The experimental approach I used has been previously employed to study the formation of platelets and the biology of megakaryocytes (Eto et al., 2002), and is based on the coculture of ES cells with the mouse stromal cell line OP9. OP9 cells are derived from the op⁻/op⁻ mice. Due to a mutation in the coding region of the macrophage colony-stimulating factor (M-CSF) gene, these mice are defective in osteoclast formation, resulting in bones that lack the bone marrow cavity. When stromal cell lines other than the OP9 are used, differentiation of mouse ES cells is drastically shifted toward macrophages, with an inhibition of other haematopoietic lineages (Borzillo et al., 1990). In contrast, OP9 stromal cells support efficient production of blood cells of all different lineages.

Previous studies have demonstrated that upon withdrawal of LIF, mouse ES cells seeded onto OP9 stromal cells form mesodermal colonies containing HSCs/immature haematopoietic precursors within five days (Nakano et al., 1994). If left on the same stromal layer, differentiating ES cells tend to get buried underneath the feeder layer. After a trypinization step and replating onto fresh OP9, cells within the mesodermal colonies become less firmly attached to the stromal layer and more circularly shaped. At this stage, without the addition of any cytokines, the colonies almost exclusively consist of HSCs. Upon addition of lineage-specific recombinant cytokines, generation of blood cells of specific lineages is greatly enhanced. Differentiated cells of the desired lineage appear to detach from the feeder layer and can be collected and used for further analysis.

The established cocktail of cytokines to obtain megakaryocytes from mouse ES cells seeded onto OP9 cells include mouse recombinant thrombopoietin (TPO), which acts through the Mpl receptor and stimulates late differentiation of megakaryocytes and production of platelets, and mouse IL-6 and human IL-11, which both have pro-survival effect on the differentiating cells (the use of a human cytokine is based on the high inter-species homology of these glycoproteins and on previous studies testing its effects on differentiating mouse ES cells). The addition of the IL-6 and IL-11 has been shown to be dispensable for obtaining a good *in vitro* differentiation of the mouse ES cells, but it promotes the survival of the cells and was included in all of my differentiation experiments (Eto et al., 2003).

Because of the megakaryoblastic nature of DS-TMD and AMKL, I decided to investigate developmental phenomena associated with megakaryocytic differentiation of mouse ES cells containing an extra copy of HSA21. Several genes present on HSA21 (most notably RUNX-1, but also ERG and ETS-2) have a specific effect on proliferation/differentiation of megakaryocytes (as

discussed in 1.4.5). I therefore aimed to investigate whether trisomy 21 would cause abnormalities in the megakaryocytic compartment using the transchromosomic model. The working hypothesis was that an extra copy of HSA21 causes an abnormal proliferation of the megakaryocytic lineage, which underlies the differentiation arrest caused by GATA-1 mutations in DS-leukaemia. To test this hypothesis, I compared megakaryocytic differentiation of the transchromosomic ES cells 47-1 (which previous data have shown to contain virtually the entire chromosome 21, see (Hernandez et al., 1999; Mensah et al., 2007; Canzonetta et al., 2008)) to the parental ES cell line D3 from which the 47-1 were derived.

Taking into account the peculiar cooperation between trisomy 21 and GATA-1s in the malignant transformation of DS-leukaemia, I also wanted to establish an *in vitro* model to study this interplay. Experimental evidence to address these points is presented in this chapter.

I.1. Terminal megakaryocytic differentiation is not impaired by the presence of an extra copy of HSA21

Several factors can influence mouse ES cells behaviour in culture, such as the type of reagents employed, the use of a supportive feeder layer, and the maintenance of the ES cells at an ideal, constant confluence.

All of the experiments described in this thesis were performed using serum that was batch-tested for ES cells. Batches of foetal calf serum were routinely screened in our laboratory for their capacity to maintain ES cells in a pluripotent state, as judged by morphological appearance of the cells and by transcriptional levels of at least one pluripotency factor (routinely OCT-4). Several batches of serum were also tested for their capacity to support optimal growth of OP9 stromal cells and to induce ES cell differentiation into mesodermal colonies.

A preliminary assessment of the efficiency of the differentiation protocol used for the set of experiments described in this chapter was obtained by performing acetylcholinesterase (AchE) staining on the cells. Figure I.1 represents morphology of the undifferentiated ES cells under standard culture conditions and AchE staining performed on megakaryocytic precursors/megakaryocytes derived from ES cells after 13 days of culture on the OP9 cells with the addition of recombinant TPO and other cytokines. Mouse megakaryocytes or precursors that express AchE have brown granular deposits of copper ferricyanide in the cytoplasm resulting from the enzymatic reaction, and they appear brown.

A Undifferentiated ES cells **B** AchE staining **C** MK derived from ES cells
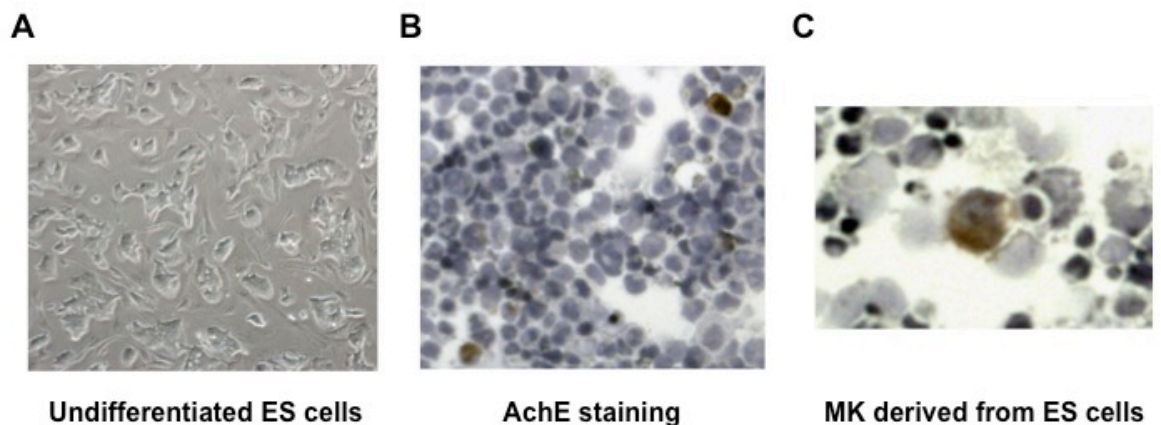
Fig. I.1. Morphology of undifferentiated ES cells (A) and megakaryocytes (B, C) obtained from *in vitro* differentiation of mouse ES cells stained with Acetylcholinesterase staining. Pictures were taken at 20x magnification. **C** shows a large megakaryocyte (stained brown) with multiple lobules in the nucleus and ferrous deposits in the cytoplasm. Picture was taken at 40x magnification.

I.1.1. CD41 expression and ploidy of MKs are not altered by the presence of an extra copy of HSA21

In order to quantify the efficiency of the differentiation protocol, a fluorescence-activated cell sorting (FACS) staining for the megakaryocyte-specific surface marker CD41 was performed on MKs at day 13 of the protocol. The number of CD41 positive cells in three independent differentiation experiments did not show a significant difference between D3 and 47-1.
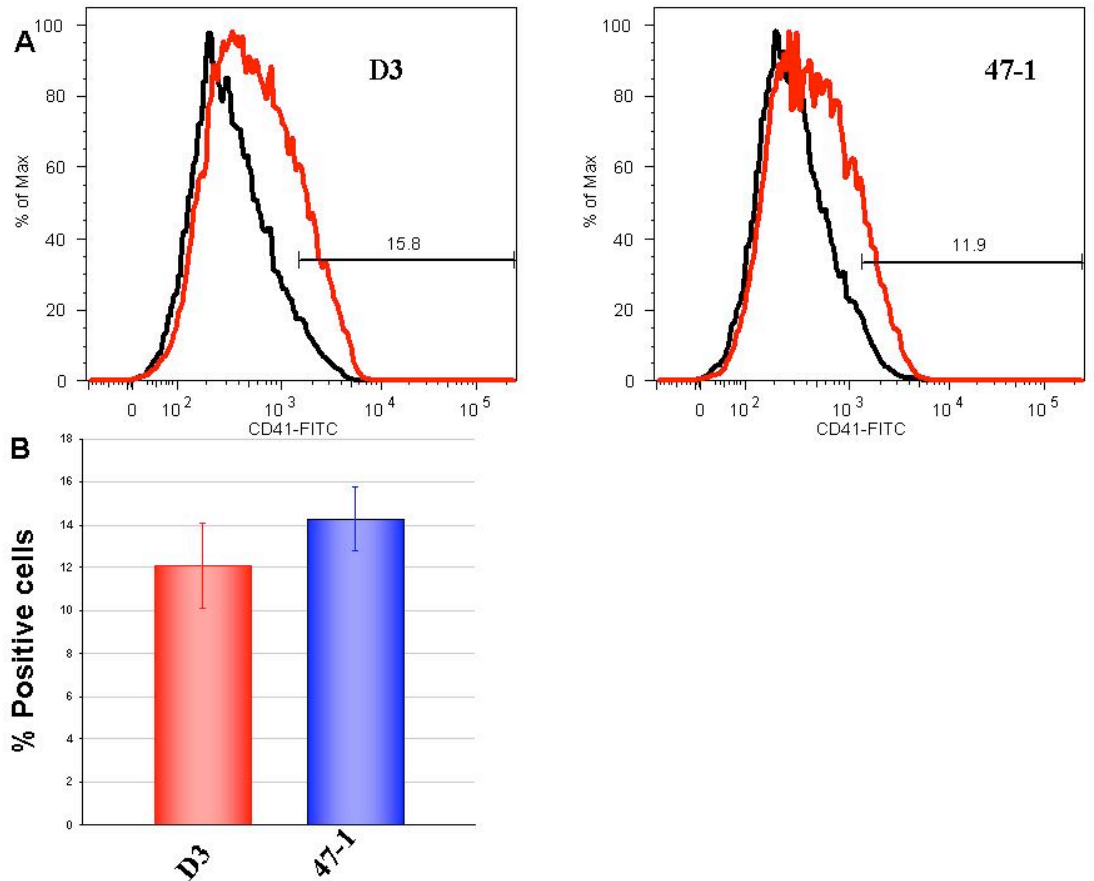
Fig. I.2. CD41 expression in MKs/MK progenitors derived from D3 and 47-1. A. Histogram plots of the FACS measurement of CD41-FITC in MKs/MK progenitors derived from D3 and 47-1 at day 13 of the differentiation protocol. Black lines indicate the isotype control, red lines the FITC-CD41 expression. Data were collected on a LSRII FACS instrument (BD Biosciences); results were analysed with the FlowJo software version 8.1. One representative experiment is shown for each cell line. **B.** Average percentage of cells expressing CD41-FITC within the gated population (main gate was placed to exclude death cells) in three independent experiments. Error bars indicate s.e.m.

An example of the FACS staining for each cell line and a bar graph showing the mean percentage of CD41 positive cells are showed in Figure I.2

In addition to the expression of specific surface markers (such as CD41, CD42 and CD61), before releasing platelets MKs become increasingly bigger and undergo several rounds of DNA replication without cell division. This phenomenon, called endomitosis, is responsible for the increased DNA content (ploidy) of these cells (Ravid et al., 2002). To investigate the nature of the cells derived from the differentiation protocol, I performed an analysis of the DNA content of the in vitro derived CD41 positive MKs. CD41$^+$ sorted cells

were fixed and stained with a nuclear dye (propidium iodide) to determine their DNA content. The average percentage of endomitotic cells, as judged by the number of cells with a DNA content of 8n and 16n, was comparable between the populations derived from the D3 and the 47-1 cells, as shown in Figure I.3. MKs isolated from mouse or human bone marrow usually display even higher classes of ploidy (32n, 64n and sometimes even up to 128n), however in this set of experiments the population analysed contained cells at non-synchronous stages of maturation and OP9 stromal cells derived from previous steps of the protocol, making it difficult to detect the low number of cells with higher classes of ploidy. Maintaining the differentiating cells in culture for longer might have been a way to address if more immature progenitors would have eventually reached higher classes of ploidy, but the viability of the cultures tends to decrease after 13 days.

The conclusion from these experiments is that *in vitro* generation of MKs is generally unaffected by the presence of an extra copy of human chromosome 21, and proceeds at the same rate in transchromosomic and WT cells.
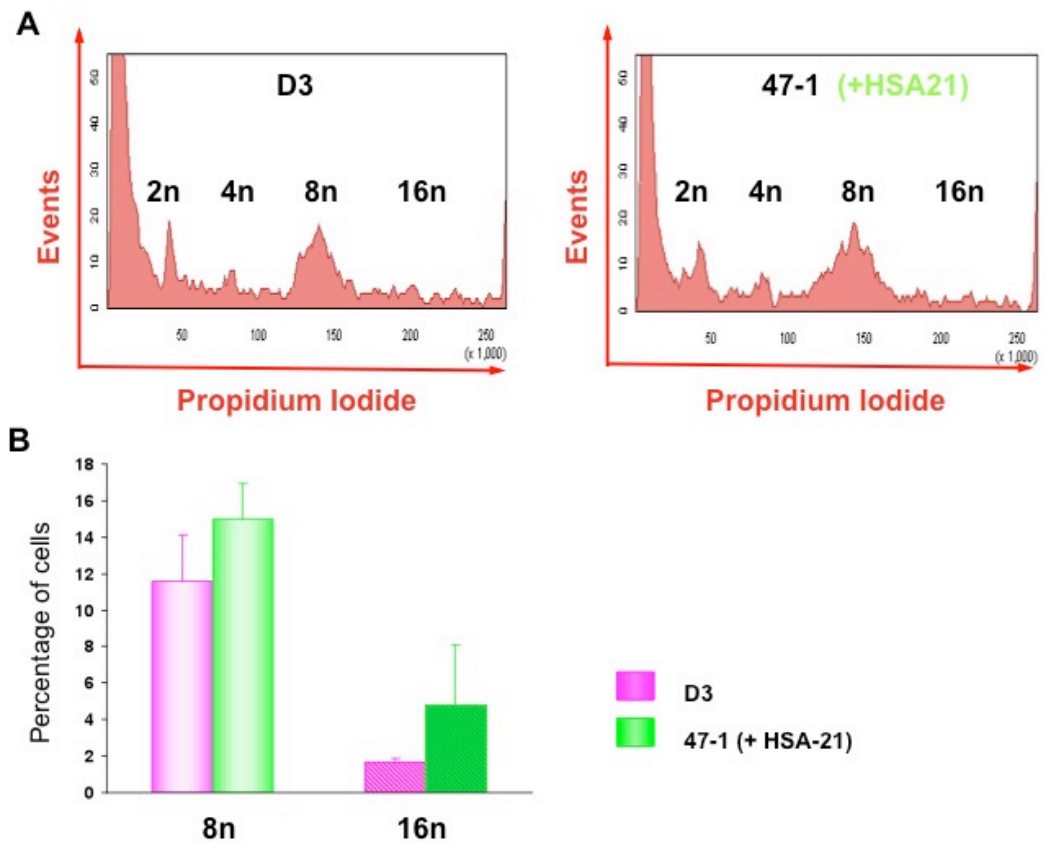
Fig. I.3. DNA content analysis in CD41 positive cells derived from D3 (pink bars) and 47-1 (green bars). A, Histogram plots of the DNA content in the two populations. Propidium iodide staining intensity is represented on the *x*-axis; number of events acquired is plotted on the *y*-axis. The bar graph in **B** represents the mean percentage frequency of cells with a DNA content of 8n or 16n in three independent experiments. Error bars indicate s.e.m. No significant differences were detected in the distribution of ploidy of MKs/MK progenitors derived from D3 and 47-1 at day 13 of the differentiation protocol.

I.1.2. Effect of trisomy 21 on the molecular signature of megakaryocytic differentiation of ES cells

To identify the molecular differences, if any, between the 47-1 transchromosomic cells and the D3 parental cells during megakaryocytic differentiation, I took advantage of the differentiation protocol based on the OP9 stromal cell line, which allows for the harvesting of cells at different stages of megakaryocyte development. I then analysed the expression levels of various markers to uncover any differences between 47-1 and D3 cells at specific time points along the megakaryocytic differentiation program.
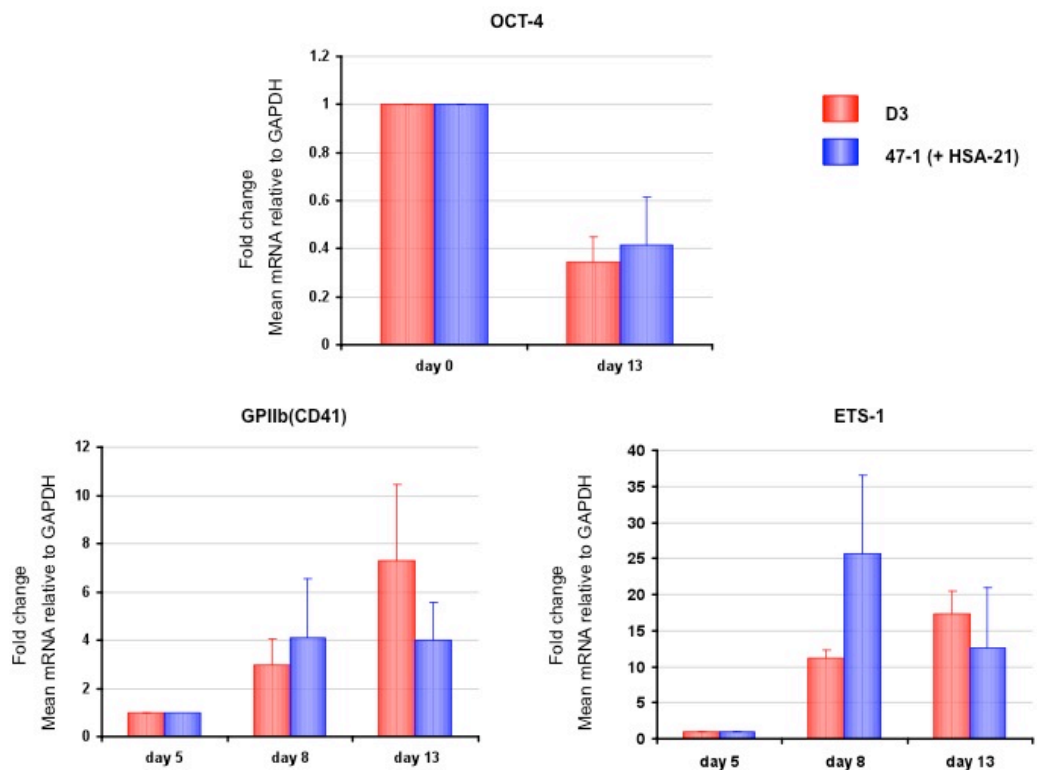
Fig. I.4. A molecular signature of megakaryocytic differentiation in D3 and 47-1. Mean mRNA levels of OCT4, CD41 and ETS-1 relative to GAPDH are indicated in this figure. No significant differences were detected between levels of the analysed markers during megakaryocytic differentiation (at day 5, day 8, and day 13 after initial seeding of the ES cells on the OP9 stromal cells) in D3 (red) and 47-1 (blue) derived populations. Levels of OCT4 (a pluripotency marker) are expressed as fold change of levels at day 0 (undifferentiated ES cells), whereas other markers are normalized to day 5, when their expression becomes detectable. Bar graphs show the average fold change of mRNA levels divided by GAPDH in 4 independent experiments. Error bars indicate s.e.m.

Markers analysed in this set of experiments included: ETS-1, a transcription factor known to activate megakaryocyte-specific gene expression programs (Jackers et al., 2004; Pang et al., 2006), CD41, a megakaryocyte and platelet-specific surface antigen, and OCT4, a pluripotency transcription factor whose expression declines upon *in vitro* differentiation of mouse ES cells. Gene expression analysis was performed using the Taqman® chemistry and primers and probes from Applied Biosystems. Expression levels of mOCT4,

mETS-1, and mGPIIB (CD41) in the 47-1 transchromosomic ES cell line and in the D3 parental line are shown in Figure I.4. Details of qRT-PCR analysis performed with the SDS software version 2.1 by Applied Biosystems are discussed in 2.9. The average quantity of mRNA for each gene of interest in duplicate samples was divided by the level of mRNA of the housekeeping gene GAPDH for each time point. Results in the bar graphs are expressed as fold change of the average level of these values above a baseline (day of differentiation in which the expression of the gene of interest becomes detectable) set as 1. For OCT-4, data are presented as fold change relative to day 0, where the expression of this pluripotency marker is the highest. Graphs report the results from four independent experiments. Error bars indicate standard error of the mean (s.e.m). Data presented here indicate that by day 13 of the differentiation protocol, both D3 and 47-1 (transchromosomic ES cells) derived populations lost pluripotency (as indicated by the reduction in mRNA levels of OCT4), and achieved an efficient megakaryocytic differentiation (as indicated by the progressive expression of ETS1 and CD41). No significant differences were observed between the two populations in the levels of the MK specific genes CD41 and ETS-1, confirming that, at a molecular level, programs specifying megakaryocytic differentiation are not perturbed by the presence of an extra copy of HSA21.

I.1.3. Human specific gene expression during megakaryocytic differentiation of the transchromosomic ES cells

Retention of the human chromosome in the mouse ES cell system was confirmed in the 47-1 ES cells used in this study by FISH analysis and human specific PCRs on genomic DNA or cDNA performed by Hernandez et al. (Hernandez et al., 1999). Unpublished data from Jurgen Groet et al. have also

provided a fine map of the content of these ES cells based on high resolution CGH array analysis. In the experiments described in this thesis, undifferentiated 47-1 ES cells were cultured under continuous selection with G418 to ensure retention of human chromosome 21. Furthermore, cells were defrosted right before starting an experiment, avoiding prolonged maintenance in culture. Previous data have showed that chromosome 21 is maintained in the undifferentiated mouse ES cell lines for up to 6 passages, even without selection (Afua Mensah, PhD Thesis, University of London).

To investigate if human specific genes were expressed in the transchromosomic model during megakaryocytic differentiation, I performed an RT-PCR analysis using human-specific primers. Primers were chosen in non-conserved regions to specifically amplify the human mRNA for RUNX-1 and DYRK1A. Both genes are expressed during megakaryocyte differentiation (Kyttala et al., 2009; Huang et al., 2009a), therefore I postulated that (if the chromosome was properly retained) their expression was likely to be driven from the human chromosome during megakaryocytic differentiation of the transchromosomic system.

Figure I.5 shows that the primers used for this analysis were human specific, and that both hRUNX-1 and hDYRK1A mRNA were transcribed from the human chromosome throughout megakaryocytic differentiation. The presence of at least two human-specific mRNAs during megakaryocytic differentiation of the transchromosomic system is indicative of a good retention of the chromosome despite the absence of selection during the differentiation protocol. It is also a proof of principle that human genes are expressed in the mouse background and might exert their influence as supernumerary copies during the megakaryocytic differentiation process, mimicking the presence of the third copy of genes on HSA21 seen in Down syndrome.
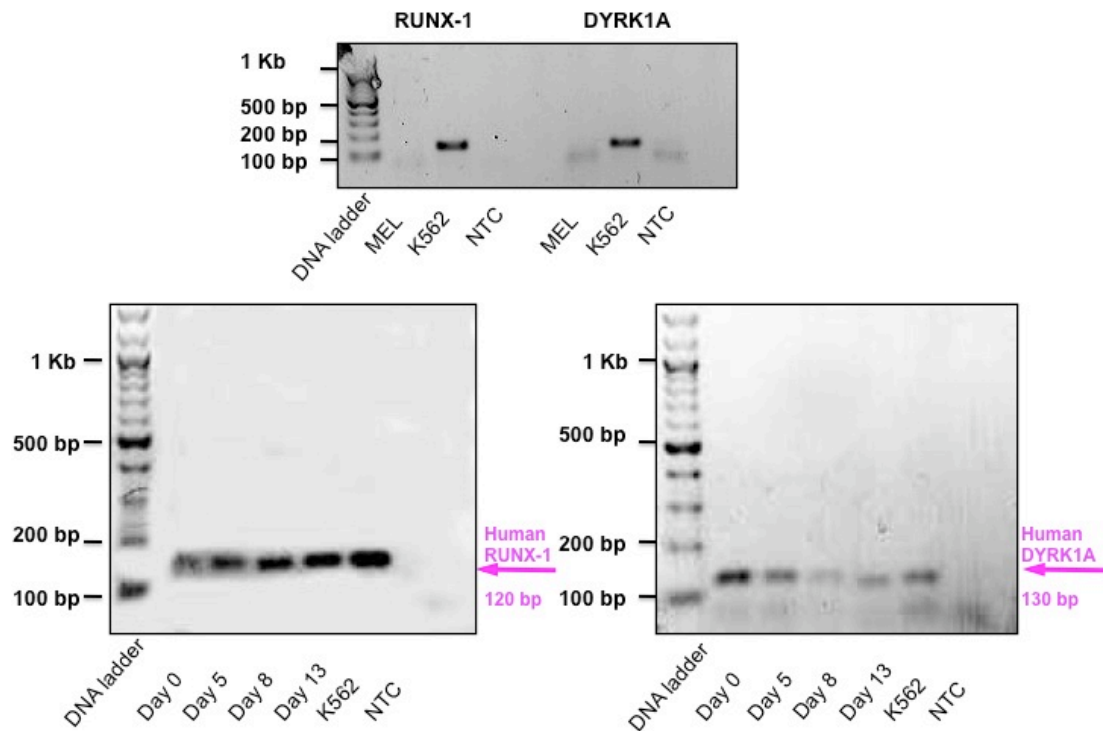
Fig.I.5. Human-specific gene expression during megakaryocytic differentiation of the transchromosomic system. Human-specific primers do not show cross-amplification with cDNA from the mouse erythroleukaemia cell line MEL, but specifically amplify the human RUNX-1 in cDNA derived from the human cell line K562 (upper panel), Lower panels show human RUNX-1 and human DYRK1A expression during megakaryocytic differentiation of the transchromosomic ES cells. NTC indicates non-template control Human-specific primers were designed to span two exons to minimize risk of amplifying contaminant gDNA. PCR products were run on a 2% agarose gel and visualized by ethidium bromide staining.

I.1.4. GATA-1 mRNA levels are increased in transchromosomic ES cells compared to the euploid control during megakaryocytic differentiation

Because GATA-1 is a master regulator of megakaryocytic differentiation, and mutations of this gene leading to the exclusive production of GATA-1s are associated with the development of TMD/AMKL in DS, I sought to analyse GATA-1 levels during megakaryocytic differentiation of the 47-1 ES cells. Levels of GATA-1 mRNA were quantified using the Taqman® chemistry and

primers and probes from Applied Biosystems®. Results are presented as in I.1.2. Figure I.6A shows that levels of GATA-1 are increased during megakaryocytic differentiation in the transchromosomic system compared to the parental cell lines. This increase is statistically significant at day 8 (unpaired t-test, p-value = 0 .007); a near significant trend is also observed at day 13 (unpaired t-test, p-value = 0.06). Next, I asked whether the increase in GATA-1 mRNA levels in 47-1 was due to the presence of a shorter transcript (GATA-1s) or to the exclusive presence of the GATA-1 full-length transcript. Panel B of Figure I.6 shows that in both D3 and 47-1 cells GATA-1 mRNA is only present as a full-length transcript during megakaryocytic differentiation. These data suggest that the presence of one (or more than one) gene on HSA21 might trigger an abnormal expression of GATA-1 during megakaryocytic differentiation of the transchromosomic system.
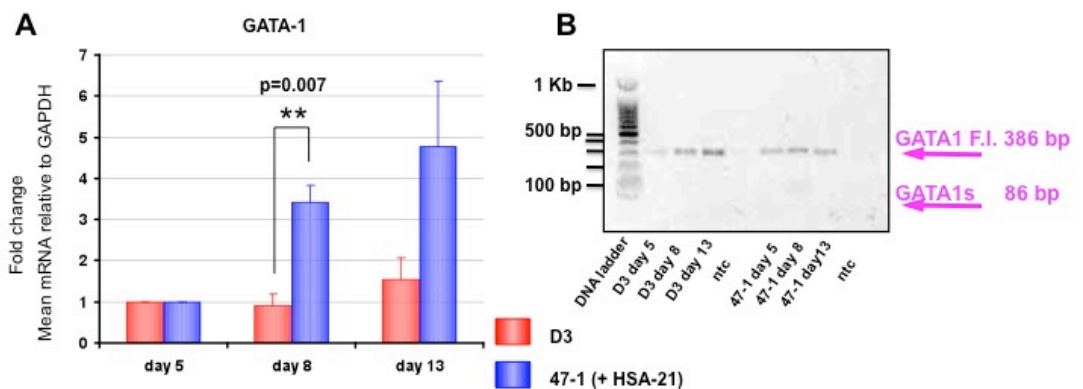
Fig. I.6. GATA-1 mRNA levels during megakaryocytic differentiation of D3 and 47-1 cells. Panel **A** represents fold change of mean GATA-1 mRNA normalized to the housekeeping gene GAPDH, relative to day 5, as detected by qRT-PCR on D3 (red) and 47-1 (blue) cells during megakaryocytic differentiation. Graph bar represent average fold change of mRNAs levels divided by GAPDH in 3 independent experiments. Error bars indicate s.e.m. Panel **B** shows RT-PCR products on a 1.2% agarose gel visualized by ethidium bromide staining. Primers used for RT-PCR analysis flank GATA-1 exon 2, therefore they would detect the presence of the short transcript (GATA-1s) arising as a consequence of splicing events affecting exon 2, which are a frequent finding in human DS-TMD and AMKL samples. Insertions or deletions in the genomic sequence of GATA-1 exon 2 would result in an altered size of the amplicon generated by these primers.

GATA-1 specifies megakaryocyte identity, but the increased levels of GATA-1 mRNA did not translate into an increased number of MKs (CD41$^+$ cells in Figure I.2) derived from the trisomic cells, suggesting that the observed phenotype might reflect cell-intrinsic mechanisms, rather then being the consequence of an increased number of cells expressing GATA-1.

I.2. MKs and MK progenitors derived from transchromosomic ES cells generate a bigger number of large TPO-dependent colonies than parental ES cells

The clonogenic potential of MK progenitors/megakaryocytes derived from 47-1 transchromosomic ES cells and the D3 parental cell line was assessed using a collagen-based colony-forming assay (colony forming unit megakaryocytes, CFU-MK). An equal number of progenitors/MKs was seeded into semisolid medium supplemented with recombinant TPO (50 ng/ml) and collagen and colonies were scored after 10 days. Addition of collagen to the semisolid medium allows for the fixing of cells and staining with AchE (a megakaryocyte-specific staining), making morphology of the colonies and of individual cells within colonies more easily recognisable. A positive colony was judged by the presence of at least 3 cells stained for AchE (brown). The number of positive colonies formed by an equal number of progenitors (1×10^5 cells) derived from 47-1 transchromosomic cells and the D3 parental cells was not significantly different in four independent experiments, each performed in duplicate slides (Figure I.7A). Despite the fact that the size of the colonies was extremely variable, even within a single chamber, there was a clear tendency of the colonies derived from 47-1 cells to be larger and to contain fewer AchE-positive cells than D3-derived colonies. Figure I.7B shows representative pictures of colonies derived from D3 and 47-1.
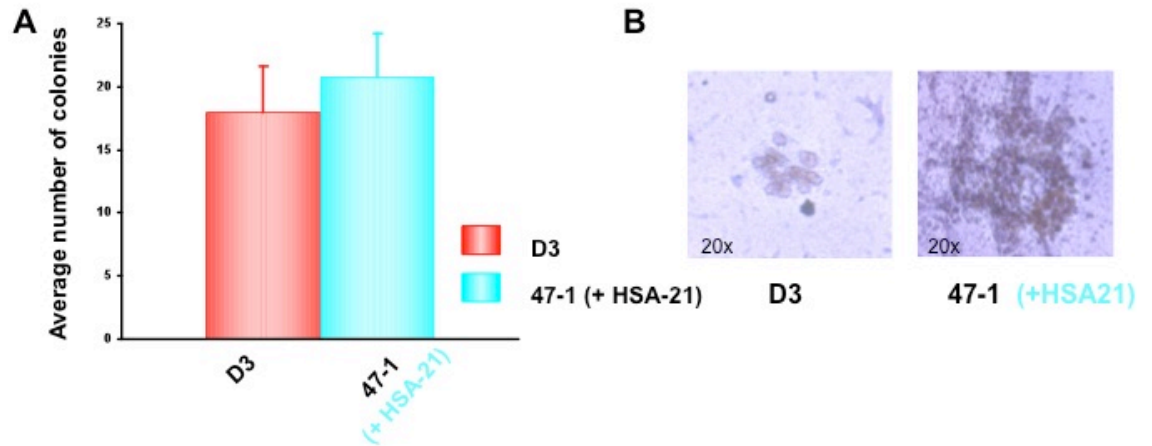
Fig. I.7. CFU-MK assay for D3 and 47-1 derived progenitors. A. Average number of AchE positive colonies/100,000 cells in 4 independent experiments. Error bars indicate s.e.m. Colonies were scored 10 days after initial seeding. **B.** Representative images of colonies derived from D3 and 47-1. Pictures were taken at 20x magnification.

To quantify the observed phenotype, colony size was calculated using images of sequential fields spanning the entire slide captured at 20x magnification, and examined using the Leica QWin Software. Manual tracing of the perimeter of each positive colony was performed, and the area of individual colonies was automatically calculated by the software in square pixels (pp^2). The average area of the colonies is shown in Figure I.8A. To examine the distribution of the size of the colonies, data were organized into three arbitrary categories: **small** colonies (2000-15,000 pp^2), **medium** colonies (15,000-50,000 pp^2) and **large** colonies (>50,000 pp^2).

The probability of forming large rather than small colonies was significantly higher for the MKs derived from 47-1 than for the D3 derived ones (Pearson X-square test, p value = 0.002487). Figure I.8.C shows a dot plot of the size of the large colonies derived from D3 and 47-1 cells in four independent experiments each performed in duplicate. The average number of large colonies derived from each of the two populations in 4 independent experiments is indicated in bar graph I.8B. Error bars represent s.e.m. of 4 experiments.
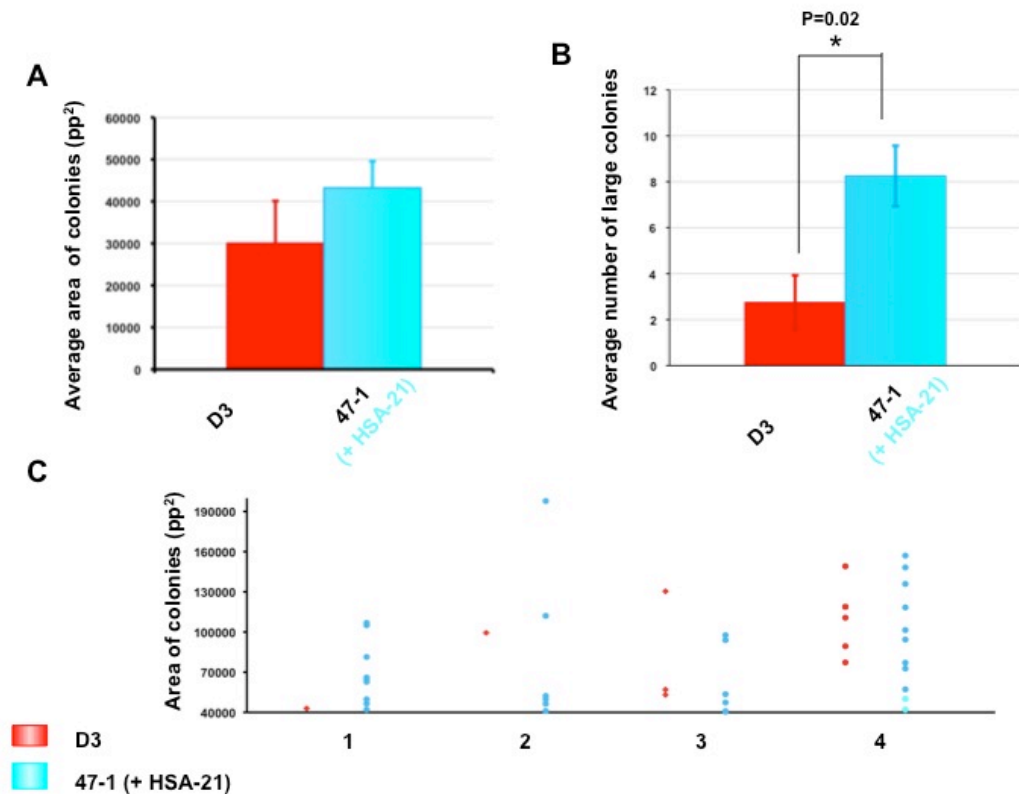
Fig. I.8. CFU-MK assay for D3 and 47-1 derived progenitors. Panel **A** indicates the average size of all of the colonies formed from D3 and 47-1 derived MK progenitors/MKs in 4 independent experiments, each performed in duplicate. Area of the colonies was quantified using the Leica QWin software and is indicated in pp^2. Error bars indicate s.e.m. Panel **B** shows the average number of large colonies in 4 independent experiments. Error bars indicate s.e.m. The average number of large colonies was significantly higher in 47-1 compared to D3 (unpaired t-test, p-value=0.02). Panel **C** is a dot plot showing the number and the size of the large colonies (size > 50,000 pp^2) in 4 independent experiments.

These results indicate that the presence of an additional copy of HSA21 in megakaryocytes derived from mES cells confers the potential to form larger colonies upon TPO-dependent growth conditions.

I.2.1. Large colonies derived from transchromosomic ES cells do not harbour GATA-1 mutations

Transchromosomic-derived MKs or MK progenitors form bigger colonies containing fewer AchE-positive cells than the control colonies. This phenomenon is suggestive of an abnormal tendency of the MKs and MK

116

progenitors derived from 47-1 to proliferate rather than to differentiate after day 13 of the differentiation protocol. Li et al. (Li et al., 2005) described a similar phenotype in a knock-in mouse model bearing a GATA-1$^{\Delta e2}$ allele, which exclusively expresses the GATA-1s protein. Foetal liver progenitors and differentiating ES cells from this model cultured with TPO produced hyperproliferative MK colonies compared to the wild type GATA-1 expressing controls. To exclude that the phenotype observed in the 47-1 derived colonies was caused by acquired mutations of GATA-1, leading to the expression of GATA-1s, gDNA extraction and sequencing analysis of GATA-1 exon 2 was performed on 10 large ("hyperproliferative") colonies derived from 47-1 cells and 10 colonies derived from the D3 parental cells (as a control).

Due to the limited amount of material available for gDNA extraction, and the nature of the material itself (colonies had been fixed and stained with AchE), this procedure required a few optimisation steps. Several gDNA extraction methods were tested, including phenol-chloroform based methods and commercially available kits, but none of them yielded amplifiable gDNA. Ultimately, a mechanical lysis of the colonies scraped off the slide directly in PCR buffer, followed by treatment with proteinase K, gave an amplifiable product. Once an extraction method was established on test samples, PCR and sequencing analysis were performed on 10 large colonies from 47-1 cells and on 10 control colonies derived from D3 cells using primers spanning GATA-1 exon 2 (Figure I.9A, 1.9B). None of the colonies showed mutations in the GATA-1 exon 2, suggesting that the phenotype observed in the large colonies derived from 47-1 cells was entirely independent from the production of GATA-1s, and most likely caused by a gene dosage imbalance due to the presence of an extra copy of HSA21 in the transchromosomic system.
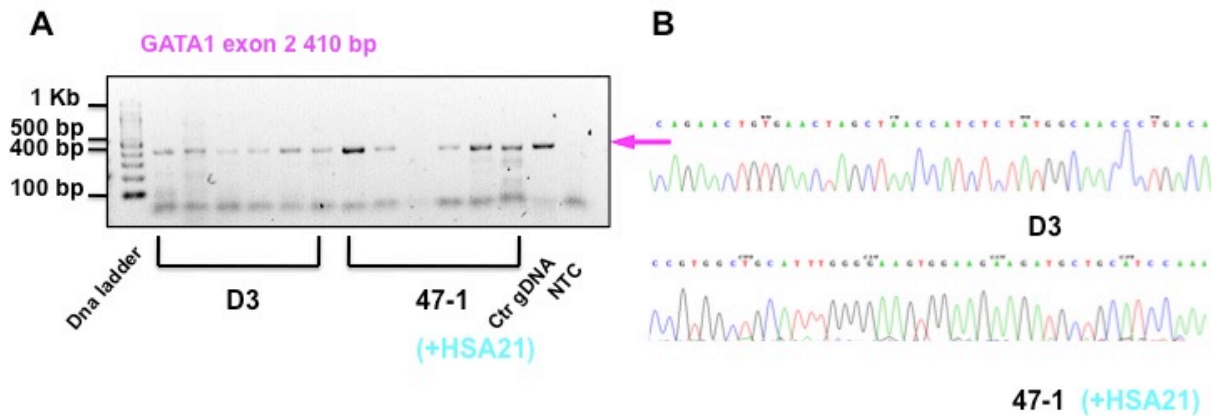
Fig. I.9. gDNA extraction and GATA-1 sequencing analysis from hyperproliferative colonies. gDNA was extracted (after fixing and staining with AchE) from hyperproliferative colonies using a direct lysis in PCR buffer. Panel **A** shows efficient amplification obtained from colonies of 50-100 cells using GATA-1 exon 2 primers. PCR products were run on an on a 1.2% agarose gel and visualized by ethidium bromide staining. Panel **B** shows an example of electropherogram obtained from GATA-1 exon 2 sequencing of D3 and 47-1 colonies. No mutations were detected in GATA-1 exon 2 in either the 47-1 transchromosomic derived colonies or the D3 derived controls.

I.3. Investigating the effect of GATA-1s on megakaryocytes derived from the transchromosomic system

After having established that 1) transchromosomic ES cells can differentiate into megakaryocytes *in vitro*, 2) terminal megakaryocytic differentiation is not impaired by the presence of an extra copy of human chromosome 21, and 3) transchromosomic ES cells form "hyperproliferative" megakaryocytic colonies independently of overt GATA-1 mutations, I sought a way to investigate the oncogenic cooperation between GATA-1s and trisomy 21.

I therefore decided to genetically manipulate the transchromosomic ES cells and the parental control to force the expression of GATA-1s. The purpose of the experiments described in this subchapter was to investigate whether the

known hyperproliferative effect of GATA-1s overexpression during megakaryocytic differentiation (Li et al., 2005) was exacerbated by the presence of an extra copy of chromosome 21 in the transchromosomic model. Due to the nature and the length of the differentiation protocol, I needed to generate a stable system capable of ensuring expression of GATA-1s from the undifferentiated stage throughout the entire process of generation of MKs/MK precursors. To achieve this, I chose to adopt a well-established system of gene transfer, retroviral transduction. Retroviruses are a powerful vehicle of gene delivery into dividing mammalian cells, and they can achieve high levels of expression through the stable integration of their genome into the one of the target cell (Yang et al., 1999). Efficiency of the transduction, which is mediated by an interaction of the viruses with specific receptors on the cell surface, is essential to achieve stable integration and subsequent expression. Despite the advantage of using this system, certain cell types are notoriously less susceptible to infection with retroviruses. ES cells, in particular, are quite difficult to infect. Furthermore, even after integration, ES cells tend to transcriptionally silence integrated viral DNAs (Wolf and Goff, 2009). Therefore, the choice of a retroviral vector that contains a promoter that will not be repressed after integration is crucial for achieving an efficient expression of the gene of interest. This is the reason why (for this set of experiments) I utilised the retroviral vector MSCV, which contains a 5' LTR (Long Terminal Repeat) promoter that enhances transcriptional activation and prevents transcriptional repression in ES cells. GATA-1s-FLAG tagged cDNA was cloned into the MSCV-PURO backbone (Clontech), and the MSCV-PURO was used as a control. Full details of the vectors used in this chapter can be found in Appendix 6.1.

Retroviral particles to be used for transduction of target cells not only need the viral genome, but also the viral-specific proteins (gag, pol and env) to ensure

the appropriate infection, reverse transcription and integration of the viral genome into the DNA of the host cell. The most common way of producing retroviruses is by transient transfection of a retroviral vector and of the viral components gag, pol and env into the 293T cell line. This cell line is very easy to transfect by standard lipid-based methods and can produce high virus titers after transfection. To optimise the efficiency of infection of the ES cells, I tested different conditions to produce retroviruses to transduce readily infectable target cells (NIH3T3, a mouse fibroblast cell line). All the optimisation experiments (see Figure I.10 for a schematic view of the conditions tried) were carried out using a retroviral vector (MIG) containing no insert, but carrying a green fluorescent protein (GFP) tag.

The first approach I used was based on a triple transfection of the viral components (gag-pol and env vectors) and the MSCV-IRES-GFP (MIG) retroviral vector into 293T cells. Details of the constructs are provided in Appendix 6.1. Infection was carried out by overnight incubation of the retroviral supernatant, generated by transfection of a confluent 10 cm dish of 293T cells, with adherent NIH3T3 in exponential growth phase. Polybrene at the concentration of 4 μg/ml was added to enhance infection. Fortyeight hours after the infection, cells were analysed by FACS for GFP expression. Only 15% of the NIH3T3 analysed were positive (Figure I.11A). I therefore decided to employ an alternative approach, based on the use of a "packaging" cell line. The vast majority of packaging cell lines has been generated by stable transfection of plasmids containing viral elements (gag-pol and env) into 293T cells.

The packaging cell line ("PLAT-E") I used in this study was a kind gift from T. Kitamura (Morita et al., 2000). Compared to other packaging cell lines, PLAT-E express viral structural proteins at high levels because of the substitution in the viral packaging constructs of the MMuLV-LTR promoter with EF1α, which

is almost 10 fold stronger than MMuLV-LTR in 293T cells. Furthermore, I chose to utilize the PLAT-E for safety reasons, as they produce ecotropic viruses capable of infecting mouse cells only. Upon transient transfection of the MIG vector into a confluent 10 cm dish of PLAT-E cells, and infection performed in the same conditions as described above, the percentage of GFP-positive cells was still 18% (Figure I.11B). Because of the equivalent results given by the two described methods, I decided to use the packaging cell line PLAT-E, and to further optimise the conditions of infection.

The conditions that gave the highest percentage of infection for the NIH3T3 cells utilised virus-containing supernatant from a 10 cm dish collected 48 hours after the transfection of the MIG vector into PLAT-E cells. Supernatant containing viral particles was centrifuged at room temperature for 45 minutes, together with NIH3T3 cells in a six-well plate ("spinfection"). Twenty-four hours later, fresh supernatant collected from PLAT-E cells (i.e., at 72 hours after the original transfection) was added to the NIH3T3 that had been "spinfected" the day before. This procedure gave a percentage of 98% GFP-positive NIH3T3 (Figure I.11C). The same conditions were therefore applied to the infection of ES cells. The preparation of retroviral particles and infection procedure (spinfection plus an extra round of infection) were repeated as for NIH3T3 cells but reducing the number of target cells from 1×10^6 to 8×10^5. Under these conditions, 30.4% of D3 ES cells were GFP positive (Figure I.11D).

I then used the optimised infection protocol to transduce both D3 and 47-1 (transchromosomic ES cells) with a retroviral vector expressing GATA-1s (MSCV-PURO-GATA-1s) or with the empty vector control (MSCV-PURO) for further experiments.

1) TRIPLE TRANSFECTION (A) *vs.* **PACKAGING CELL LINE (B).**

A

ENV

MIG GAG-POL

LIPID-BASED TRANSFECTION

PRODUCING CELLS (293T)

B

MIG

LIPID-BASED TRANSFECTION

PACKAGING CELL LINE (PLAT-E)

VIRAL PARTICLES

2) INFECTION PROCEDURE.

C

Overnight incubation with medium containing viral particles, with the addition of Polybrene.

D

Overnight incubation with medium containing viral particles, with the addition of Polybrene.

SPINFECTION

Fig. I.10. Schematic view of the optimisation steps for the retroviral transduction protocol of ES cells. Two ways of producing viruses were tested: the triple transfection method, based on the simultaneous transfection of viral components (gag-pol and env plasmids) and retroviral construct (MIG) into the 293T cells **(A),** and the transfection of the retroviral construct into a packaging cell line (PLAT-E) stably expressing the viral components (gag-pol and env) **(B).** The packaging cell line method was selected because of simplicity and safety reasons. Conditions tested for optimal transduction included the overnight incubation of target cells with viral-containing supernatant with the addition of polybrene **(C),** and a combination of spinfection (centrifugation of viruses and cells in the presence of polybrene) and overnight incubation with fresh virus-containing medium after 24 hours **(D).**
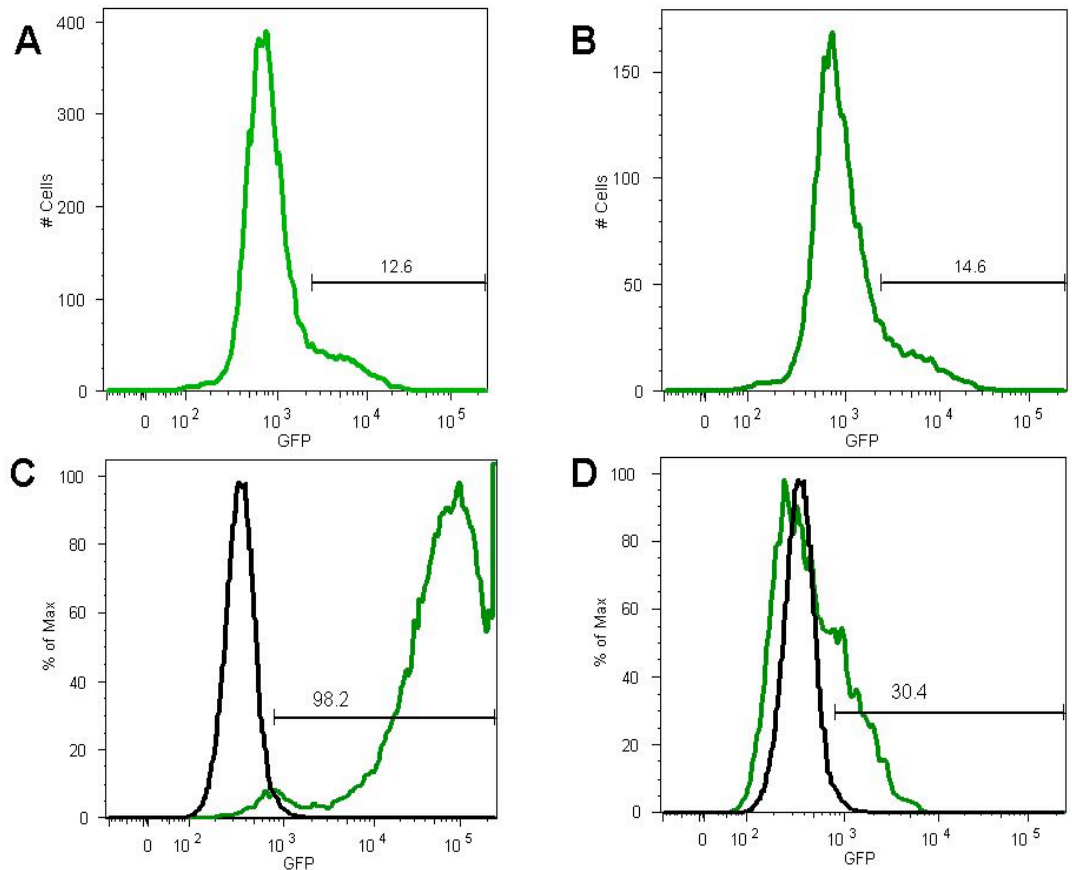
Fig. I.11. GFP expression in cells infected with the MIG retroviral vector. Panels **A** and **B** show the percentage of NIH3T3 cells expressing GFP 48 hours after infection. Retroviruses were prepared by **(A)** transient transfection of 293T with the packaging plasmids gag-pol and env and the retroviral vector MIG or **(B)** transfecting the MIG vector into the packaging cell line PLAT-E. Infection in **A** and **B** was performed by overnight incubation of target cells with virus-containing medium. Infection in **B-D** was performed with a combination of spinfection and subsequent overnight incubation with fresh retroviral containing supernatant. Panel **C** shows the efficiency of transduction of NIH3T3 cells, and panel **D** shows the efficiency of transduction of D3 ES cells. In all histogram plots, GFP fluorescence intensity on a logarithmic scale is plotted on the x-axis, number of cells is plotted on the y-axis. Numbers indicate the percentage of positive cells. Black line in panels **C** and **D** indicate basal background fluorescence of the untransduced cells.

For further studies, PURO-MSCV retroviral vector was preferred to the MIG used for the optimisation of the protocol because the expression of the puromycin resistance cassette in this vector allows for antibiotic selection of the infected cells.

I.3.1. Generation of ES cell lines overexpressing GATA-1s

After transduction of the D3 and 47-1 ES cells with the MSCV-PURO-GATA-1s or the MSCV-PURO vector, infected cells were grown under puromycin selection for at least 10 days. By day 10, untransduced cells treated with puromycin at the same concentration of the transduced ones had all been killed by the antibiotic. Once a puromycin-resistant population was obtained, verification of the integration and expression of the viral constructs was carried out by PCR analysis on gDNA and RT-PCR on cDNA extracted from the transduced ES cells, respectively (Figure I.12). PCR was performed on gDNA using a forward primer in the GATA-1 insert and a reverse primer in the FLAG tag (cloned in frame with the GATA-1s cDNA in the retroviral vector). No amplification was detected in the D3 and 47-1 cells infected with the MSCV-PURO vector, whereas a specific product of 374 bp was detected in the gDNA extracted from the cells transduced with the MSCV-PURO-GATA-1s vector. Likewise, a specific band of the same size was detected in RT-PCR using the same pairs of primers as for the PCR on gDNA, but there was no amplification in the MSCV-PURO controls or in the samples without reverse transcriptase (RT- controls).
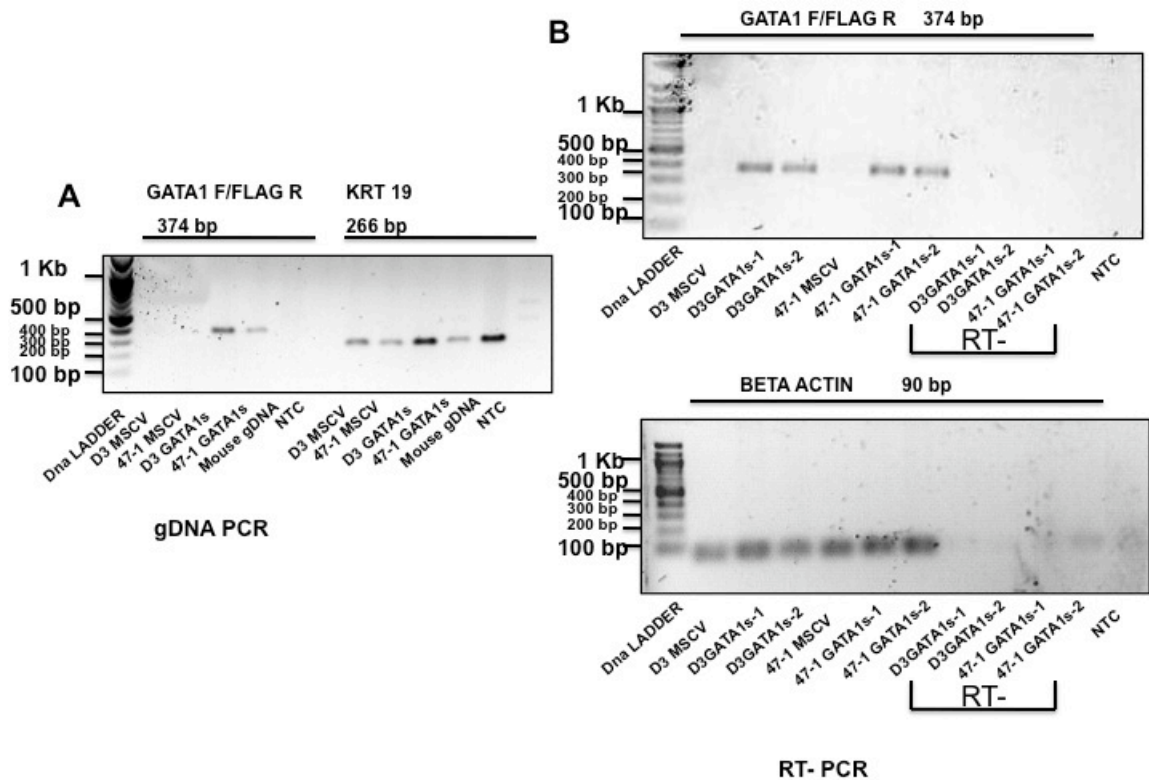
Fig. I.12. Integration and expression of GATA-1s-FLAG in D3 and 47-1 undifferentiated ES cells. Panel **A** shows agarose gel electrophoresis of DNA fragments obtained by PCR amplification of gDNA extracted from D3 and 47-1 transduced with GATA-1s and MSCV control. PCR was performed with a GATA-1 exon 5 forward primer and a FLAG-tag reverse primer. Amplicon size was 374 bp. A mouse genomic DNA was included in the PCR as a negative control. Positive control PCR was performed with Keratin 19 primers (amplicon size 266bp). PCR products were visualized on a 1.2% agarose gel stained with Ethidium bromide. Panel **B** shows RT-PCR analysis performed on cDNA synthesized from RNA extracted from undifferentiated D3 and 47-1 transduced with GATA-1s or MSCV control. RT- controls were included in the PCR to ensure that amplification was driven by mRNA in the samples, rather than from contaminant gDNA. Bottom panel in **B** shows a positive control RT-PCR performed with β-actin primers on the same samples used for PCR in upper panel. Amplicon size for β-actin PCR was 90 bp.

3.3.2 Clonogenic potential of the GATA-1s expressing cells

Once a system to overexpress GATA-1s in the transchromosomic ES cells and in the parental control was established, I aimed to assess the effect of GATA-1s expression on the megakaryocytic lineage in the trisomic context.

125

The first point to address was whether GATA-1s was still expressed throughout MK differentiation of both D3 and 47-1 (even in absence of selection). To examine this, RT-PCR analysis was performed on MKs/MK progenitors derived *in vitro* from D3 and 47-1 infected with GATA-1s and the control vector. (Figure I.13).
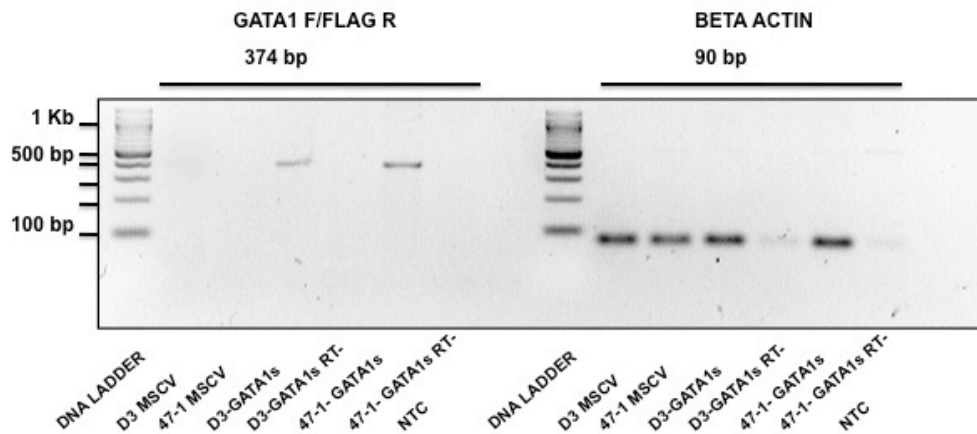
Fig. I.13. Expression of GATA-1s-FLAG in D3 and 47-1 derived MKs/MK progenitors. RT-PCR analysis was performed on MKs/MK progenitors derived from D3 and 47-1 transduced with GATA-1s and MSCV control. An RT- control was included for the GATA-1s transduced samples to ensure that amplification was driven by the presence of cDNA in samples, not from contaminant gDNA. RT-PCR analysis was performed with the GATA-1 forward primer and the FLAG reverse primer used in I.12. Amplicon size was 374 bp. A control RT-PCR was performed with primers for β-actin using the same amount of template cDNA used for the GATA-1s PCR. Amplicon size of the β-actin PCR was 90 bp.

.

At day 13, both D3 and 47-1 cells transduced with MSCV-PURO-GATA-1s expressed GATA-1s, as shown by amplification of a specific product of 374 bp. No product was detected in the MSCV-PURO controls or in the controls without reverse transcriptase. Absence of amplification from contaminant gDNA in the RT- control proved that the construct was not only integrated, but also expressed in the transduced cells.

Once continuous expression of GATA-1s was verified during megakaryocytic differentiation, I assessed the clonogenic potential of the D3 and 47-1 derived

MKs/MK progenitors expressing this truncated "oncogenic" form of GATA-1 protein. A CFU-MK assay was performed, comparing D3 and 47-1 cells transduced with GATA-1s or the empty retroviral vector. Because AchE staining was not performed to identify these colonies, a selective cocktail of cytokines was used to supplement the semisolid medium employed in these experiments.
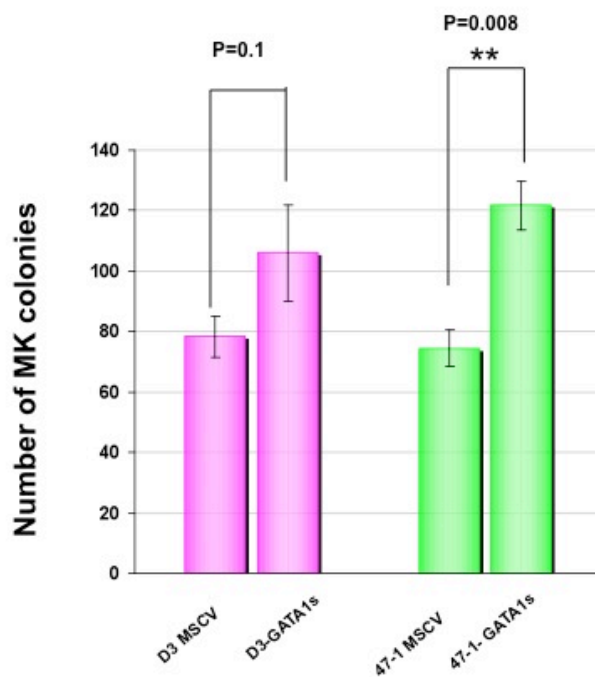
Murine recombinant interleukin 3 was added to TPO, IL-6 and IL-11 to create stringent megakaryocytic growth conditions. Under the same culture conditions, Salek-Ardakani et al. recently demonstrated the cooperating effect of overexpression of ERG (a candidate megakaryocytic oncogene on HSA21) with GATA-1s in foetal liver progenitors {Salek-Ardakani, 2009 #293}.

Fig. I.14. Number of megakaryocytic colonies derived from D3 and 47-1 infected with GATA-1s and MSCV control. Colonies derived from MK/MK progenitors infected with GATA-1 or MSCV control were scored 8 days after the initial seeding (the number of progenitor cells was $1x \ 10^5$/dish; every culture was seeded in duplicate dishes). Colonies were grown in a selective semisolid medium supplemented with IL-3, IL-6, IL-11 and TPO. Puromycin (1 μg/ ml) was also added to maintain selection pressure. The number of colonies in GATA-1s-transduced D3 and 47-1 cultures was higher than MSCV-transduced cultures. This difference was statistically significant when comparing 47-1 infected with MSCV to 47-1 infected with GATA-1s (unpaired t-test, p value = 0.008). D3-GATA-1s derived colonies were also increased in number compared to colonies derived from D3 transduced with the control vector, but the difference was not statistically significant between these two groups (unpaired t-test, p value = 0.1). The difference between D3-GATA-1s and 47-1-GATA-1s was also not statistically significant (unpaired t-test, p value = 0.2).

Eight days after the initial seeding of an equal number of MK/MK progenitors transduced with the GATA-1s or the control vector, the number of colonies generated under puromycin selection was assessed. The average number of colonies in three independent experiments - each performed in duplicate - was increased in both D3 and 47-1 derived MKs transduced with GATA-1s compared to the MSCV control.

The fold increase in the number of megakaryocytic colonies relative to the control caused by the ectopic expression of GATA-1s was about 1.15 for D3 cells and 1.8 for 47-1 cells. The difference between colonies derived from cells transduced with MSCV-PURO-GATA-1s versus control vector reached a statistical significance using an unpaired t-test only in the 47-1 transchromosomic cells (p-value = 0.008), suggesting that the effect of the ectopic expression of GATA-1s, although present in the D3 cells as well, is further exacerbated by the trisomy 21. Data are represented in Figure I.14.

I.4. Final remarks

AMKL and TMD arise in DS through pathological perturbation of the balance between proliferation and differentiation of the megakaryocytic lineage. New evidence suggests that abnormalities of the MEP compartments are present in DS human foetal livers and are caused by the dosage imbalance of one (or possibly more) gene(s) on HSA21, which have yet to be identified (Chou et al., 2008; Tunstall-Pedoe et al., 2008).

In this chapter, I have presented a comprehensive analysis, with respect to megakaryocytic differentiation, of an innovative model of Down syndrome generated by introducing an extra copy of a freely segregating HSA21 on a mouse euploid background. The transchromosomic system is a powerful tool to dissect the contribution of trisomy 21 to the development of

megakaryoblastic leukaemia in DS because it provides the most comprehensive model of DS generated so far. All of the genes trisomic in DS are present in a third, human copy in the cell line (47-1) used in this study. Furthermore, their level of expression mimics closely the situation of DS, avoiding the artificial overexpression observed in other transgenic models.

Despite the presence of an extra copy of HSA21, transchromosomic ES cells (47-1) can efficiently generate MKs/MK progenitors *in vitro*. The population of MKs/MK progenitors derived from the *in vitro* differentiation of the transchromosomic ES cells does not exhibit any abnormalities in quantity (as demonstrated by the percentage of CD41 positive cells) or quality (as shown by the ploidy assay) when compared to the ones derived from the wild type. However, on the molecular level, MKs derived from 47-1 cells express higher levels of GATA-1 mRNA. It is known that GATA-1 levels tightly regulate the balance between proliferation and terminal differentiation of erythroid cells through a direct effect on the cell cycle machinery (Whyatt et al., 1997; Whyatt et al., 2000; Kadri et al., 2009), and it is intriguing to speculate that this effect might apply to the megakaryocytic lineage as well. Muntean et al. have recently demonstrated that GATA-1 directly regulates proliferation of megakaryocytes by controlling their entry in the cell cycle through mechanisms that are specific for this lineage and not shared with erythroid cells (Muntean et al., 2007). The increased levels of GATA-1 during the megakaryocytic differentiation of the transchromosomic cells might therefore account for an imbalance between proliferation and differentiation at late stages of the *in vitro* generation of megakaryocytes (day 8 and 13 of the OP9 protocol). Megakaryocytes generated by the ES cells containing an extra copy of HSA21 form the same number of colonies as the ones derived from the control, parental ES cells (D3). The colonies generated by the 47-1 transchromosomic cells show remarkable morphological differences compared

to the controls; they are larger (i.e., contain more cells) and contain fewer cells positively staining for AchE (compared to the total number of cells forming an individual colony). This phenotype suggests a reduction in the number of terminally differentiated MKs per colony and an increased tendency of the more immature progenitors derived from the 47-1 ES cells to proliferate. The data presented in this chapter supports the hypothesis that this effect is independent from the presence of overt GATA-1 mutations, and is induced by the set of extra genes present in a third copy in the 47-1 cells. Whether this phenotype is linked to the imbalance in GATA-1 levels observed at day 8 and 13 of the differentiation protocol needs to be determined.

Ectopic expression of GATA-1s in the transchromosomic system gives rise to a higher number of colonies compared to the empty vector. Despite the fact that the short form of GATA-1 exerts a positive effect on the clonogenic potential of the megakaryocytic lineage even in the wild type (D3) context (which is in agreement with previously published data (Li et al., 2005)), this effect is more pronounced in the trisomic (47-1) model. Of note, the "oncogenic" effect of GATA-1s might be attenuated in the 47-1 experimental system by the presence of full length GATA-1, as opposed to the human situation of DS-AMKL where only GATA-1s is produced in the megakaryoblasts.

Taken together, the data presented in this chapter suggest that trisomy 21 shifts the balance between proliferation and differentiation during megakaryocyte development. Ectopic expression of GATA-1s, as shown by the increase in the clonogenic potential of the transchromosomic-derived colonies, exacerbates this phenomenon. In the future, it will be important to expand these observations by testing the contribution of individual genes to the described phenotypes by human-specific RNAi silencing. This approach, combined with data obtained by ES cell lines carrying partial fragments of the

HSA21, is likely to define a more specific role for trisomy in the observed phenotypes and to provide further support for the observations carried out so far.

II. Effects of trisomy 21 on the ontogenesis of HSCs from mesodermal precursors cells

II.1. Identifying developmental stages of haematopoietic differentiation in the OP9 based system

Canzonetta et al. recently described a disturbance of all embryonic lineages in the transchromosomic model used in this study (Canzonetta et al., 2008). The authors of this paper have shown that trisomy for the kinase DYRK1A (which is encoded on HSA21) causes a disturbance in the levels of some pluripotency regulators, which results in the premature expression of transcription factors that drive early endodermal and mesodermal differentiation. Given that this disturbance is present in the undifferentiated ES cells, I wanted to investigate whether trisomy 21 would cause any further effects during the mesodermal commitment and the generation of HSCs from the transchromosomic ES cells.

After the removal of LIF and seeding on a confluent layer of OP9 cells, the first step of haematopoietic differentiation of ES cells is the formation of colonies containing the precursors of the major derivatives of mesodermal tissues, including haematopoietic progenitors (Figure II.1).
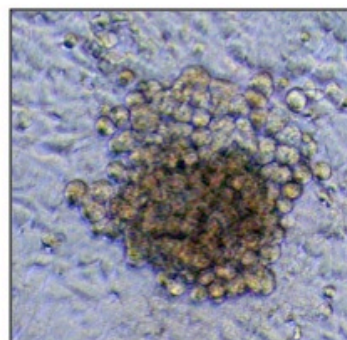
Fig. II.1. A mesodermal colony generated from D3 ES cells upon removal of LIF and 5 days of culture on the OP9 stromal cell line. Picture was taken at a 20x magnification.

Initially, I aimed to dissect the early stages of the haematopoietic differentiation and to define the composition of mesodermal colonies at day 5. Although mesodermal colonies arise from ES cells within 2.5-3 days, day 5 was chosen as a time point of analysis because the commitment of differentiation towards the haematopoietic lineage requires a longer exposure to the OP9 feeder cells (Zhang et al., 2005). In the first set of experiments that I performed, a molecular signature for the day 5 colonies was established by qRT-PCR analysis.

Gene	Marker of:	Expression
SCL	HSC, CMP	++
GATA-2	HSC, CMP	+++
C-MYB	HSC, CMP	+++
C-MPL	MEP	-
NF-E2	CMP, MEP	-
GATA-1	MEP	+/-
EPO-R	MEP	+/-
PU.1	CMP, GMP	+/-
C/EBPα	GMP	+/-

Table 3.1. Definition of the composition of mesodermal colonies generated from ES cells after 5 days on OP9 cells. Differentiating ES cells (both D3 and 47-1) were harvested at day 5 after a preplating step of 45 minutes. Total RNA was extracted, cDNA synthesised and expression of indicated markers was assessed by qRT-PCR analysis. +++ indicates that the target was abundant (Ct values between 18 and 25); ++ denotes that the target was present at moderate quantities (Ct values between 26 and 30); +/- indicates low to very low expression (Ct values between 30 and 38), whereas - indicates that the marker was undetectable. HSC stands for haematopoietic stem cells, CMP for common myeloid progenitors, GMP for granulocyte-macrophage progenitors, MEP for megakaryocyte-erythroid progenitors.

Day 5 colonies were analysed for the expression of several markers of the haematopoietic stem cell compartment (HSCs) and of the lineage progenitors, such as the common myeloid progenitors (CMP), the granulocyte-macrophage progenitors (GMP) and the megakaryocyte-erythroid progenitors (MEP). A seminal paper in the field from Akashi et al. guided the choice of markers analysed (Akashi et al., 2000). Results from this analysis are summarized in table 3.1. Assessment of the transcriptional profile of the mesodermal colonies at day 5 suggested that the predominant haematopoietic population within the colonies was comprised of HSCs and lineage non-restricted cells. A detailed analysis and characterization of the effect of trisomy 21 on these initial steps of haematopoietic commitment is presented in this chapter.

II.2. Transcriptional levels of markers of the haemogenic endothelium and HSCs compartments are increased during differentiation of trisomic ES cells

Generation of HSCs from ES cells *in vitro* proceeds through a mesodermal commitment (characterised by the onset of an FLK-1 positive population of cells), followed by the appearance of a transient common precursor of the endothelial cells and haematopoietic cells. This precursor, named the *haemangioblast*, has been identified *in vivo* and during the embryoid bodies stage of the *in vitro* differentiation of both mouse and human ES cells (Jaffredo et al., 2005; Park et al., 2005; Jezierski et al., 2007). The haemangioblast is a bipotent cell, capable of generating both endothelial and haematopoietic cells *in vivo*. *In vitro*, this transitory precursor gives rise to blast colonies with both endothelial and haematopoietic components. Using ES *in vitro* differentiation, a recent paper has proposed that HSCs derive from early mesodermal progenitors through the formation of an intermediate specialised haemogenic

endothelium, which expresses high levels of TIE-2 and c-KIT and is CD41 negative (Lancrin et al., 2009). I reasoned that, besides HSCs and immature haematopoietic progenitors, the *in vitro* colonies should contain populations of cells at different stages of mesodermal development, and decided to test a variety of markers associated with each stage (see Figure II.2). GATA-2, c-KIT and SCL were chosen as markers of HSCs. Levels of FLK-1 (a marker of early mesodermal precursors), TIE-2 (also known as TEK), and the endothelial markers PECAM and VEGF were compared between the colonies formed by the 47-1 transchromosomic cells and the D3 parental cells.
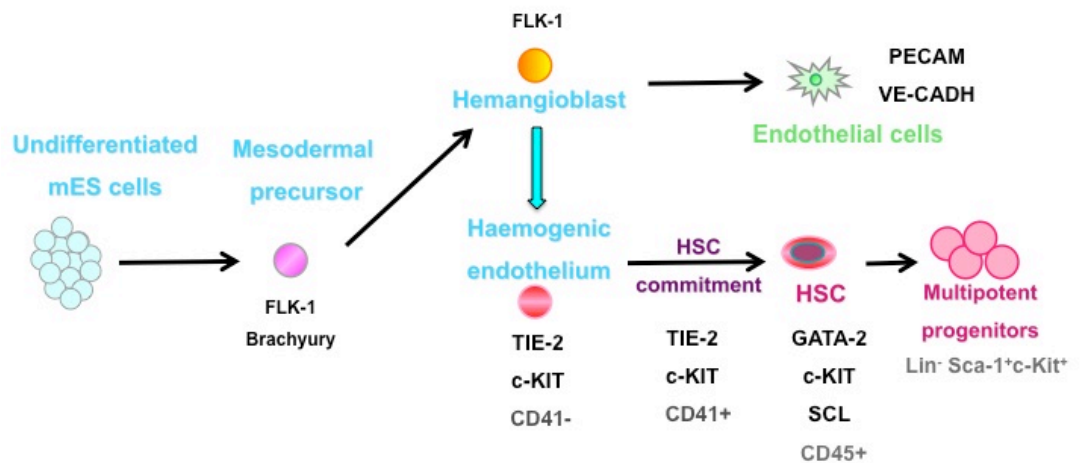
Fig. II.2. From ES cells to HSCs. Schematic diagram showing the development of HSCs from mouse ES cells. *In vitro* generation of HSCs proceeds through the formation of a mesodermal precursor (marked by the expression of the receptor FLK-1, known in humans as KDR) followed by the generation of the haemangioblast, a common precursor for endothelial cells and HSCs. Recent findings indicate that HSCs derive from a transitory intermediate (haemogenic endothelium), which is a specialized subset of cells of endothelial nature with haematopoietic potential. The haemogenic endothelium expresses high levels of TIE-2 and c-KIT and is CD41 negative. Markers of HSCs and immature haematopoietic progenitors include GATA-2, c-KIT and SCL. Markers of endothelial cells include PECAM, VEGF and VE-cadherin.

Figure II.2 summarizes the development of haematopoietic stem cells and endothelial cells from mouse ES cells, and the markers associated with each stage of this process. No morphological or numerical differences were detected between the mesodermal colonies derived from D3 and 47-1 starting

at day 0 from the same number of pluripotent undifferentiated ES cells. Figure II.3 shows a comparison of mRNA levels for FLK-1, TIE-2, VEGF and PECAM in transchromosomic 47-1 cells and the parental D3 cells.
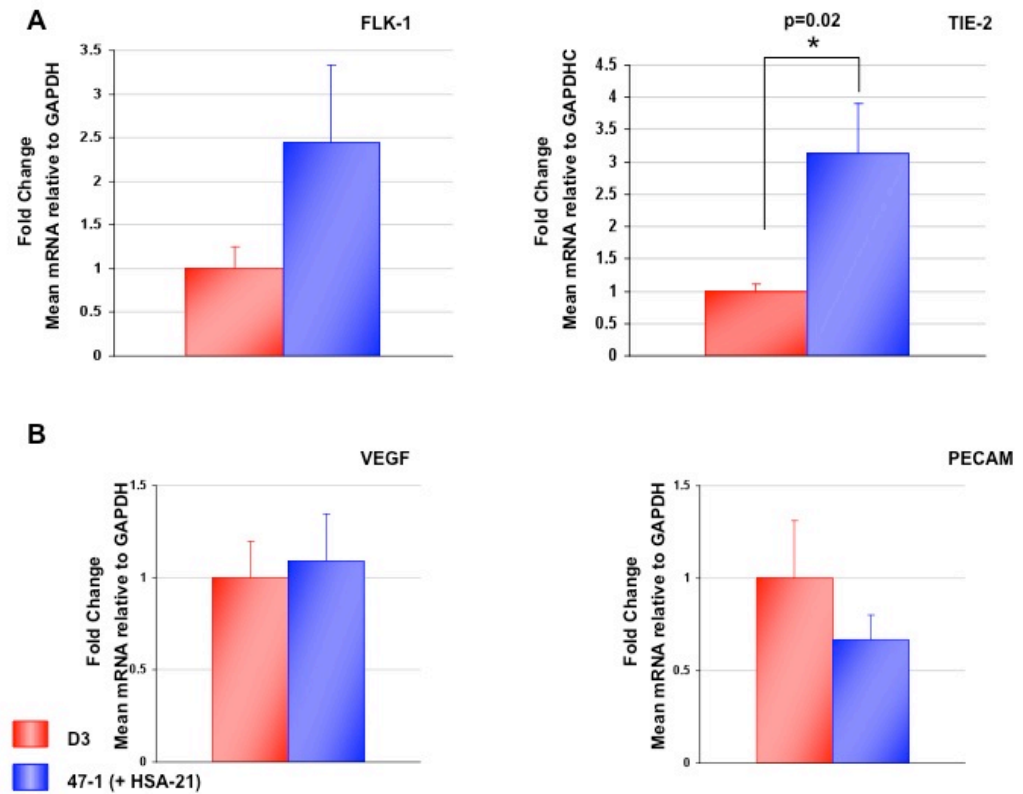
Fig. II.3. A comparison between D3 and 47-1 of mRNA levels of markers of the haemangioblast and the haemogenic endothelium. Total RNA was extracted from D3 and 47-1 at day 5 of the haematopoietic differentiation protocol, cDNA synthesised and qRT-PCR analysis performed. Mean mRNA levels of the gene of interest relative to the housekeeping gene GAPDH are expressed as fold changes of levels in D3 cells. There was no significant difference in the levels of FLK-1 (marker of mesodermal specification), or PECAM and VEGF (endothelial markers) between D3 and 47-1. mRNA levels of TIE-2 were significantly increased (unpaired t-test; p-value = 0.02) in the 47-1 (transchromosomic ES cells) compared with D3 (parental ES cells). Data from three to six independent experiments are shown. Error bars indicate the standard error of the mean (s.e.m.).

The expression level of each marker was analysed by qRT-PCR using cDNA synthesised from day 5 mesodermal colonies after a preplating step of 45 minutes necessary to eliminate the OP9 stromal cells. Results in the bar graphs are expressed as fold change of the average mRNA level in the

parental D3 cells. The data used for the graphs in Figure II.3 are from three to six independent experiments. Error bars indicate standard error of the mean (s.e.m.). No significant difference was observed in the levels of mRNA of FLK-1, PECAM and VEGF between mesodermal colonies derived from D3 and 47-1. However, a statistically significant increase was observed in the mRNA levels of TIE-2 in the 47-1 colonies compared to D3 (unpaired t-test; p-value = 0.02). Absolute levels of FLK-1 were quite low in this set of samples (Ct values = 28-30), suggesting that the mesodermal precursors had already evolved to further stages of development by day 5.
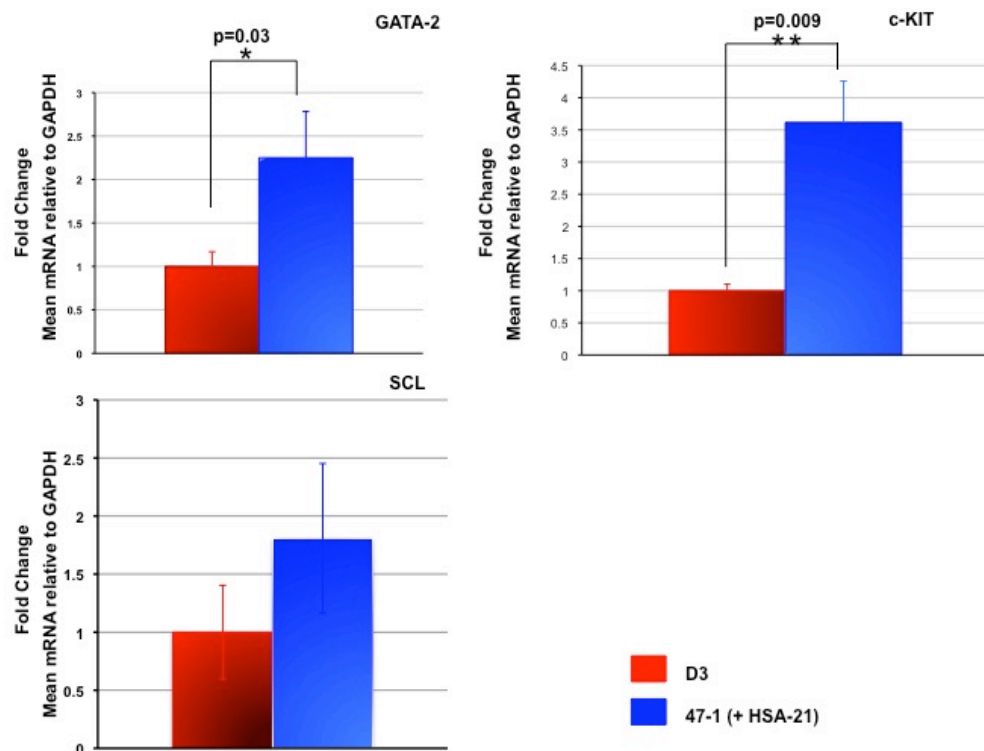
Fig. II.4. A comparison between D3 and 47-1 of mRNA levels of markers of the haematopoietic stem cell compartment/immature haematopoietic precursors. Total RNA was extracted from D3 and 47-1 at day 5 of the haematopoietic differentiation protocol, cDNA synthesised and qRT-PCR analysis performed. Mean mRNA levels of the gene of interest relative to the housekeeping gene GAPDH are expressed as fold change of levels in D3. There was no significant difference in the levels of SCL between D3 and 47-1. mRNA levels of GATA-2 and c-KIT were significantly increased in the 47-1 (transchromosomic ES cells) compared to D3 cells (unpaired t-test; p-value = 0.03 and 0.009, respectively). Data shown are from six independent experiments. Error bars indicate standard error of the mean (s.e.m.).

Expression analysis of markers of the haematopoietic stem cell compartment/immature haematopoietic precursors is shown in Figure II.4. No significant differences were detected when comparing SCL mRNA levels between D3 and 47-1. However, levels of mRNA for GATA-2 were significantly increased in the 47-1 compared to D3 (unpaired t-test; p-value = 0.03). Levels of mRNA for c-KIT also showed a significant increase in the DS model (unpaired t-test; p-value = 0.009). Results in the Figure II.4 are expressed as fold change of the average D3 mRNA levels. Error bars indicate standard error of the mean (s.e.m.) of six independent experiments.

II.2.1. Trisomic ES cells produce an increased number of haemogenic endothelial cells

To define whether the increase observed in the mRNA levels of haematopoietic markers in trisomic cells reflected an increase in a specific population of cells, I performed a FACS analysis of CD41 and c-KIT expression.

In addition to being used as a marker for mature megakaryocytes and platelets, CD41 has recently been associated with the early onset of haematopoiesis in the mouse (Ferkowicz et al., 2003; Mikkola et al., 2003). c-KIT is a marker of HSCs and immature haematopoietic progenitors. High levels of c-KIT, in combination with the absence of CD41 and the expression of TIE-2, define a specific subset of cells within the mesodermal colonies capable of giving rise to the haematopoietic stem cells (i.e., the haemogenic endothelium) (Lancrin et al., 2009).

Double staining for c-KIT and CD41 revealed an increase in the percentage of c-KIT$^+$CD41$^-$ cells in 47-1 compared to D3 (unpaired t-test; p value = 0.04).

There was no significant difference in the percentage of c-KIT⁺CD41⁺ cells in the two populations analysed (Figure II.5).
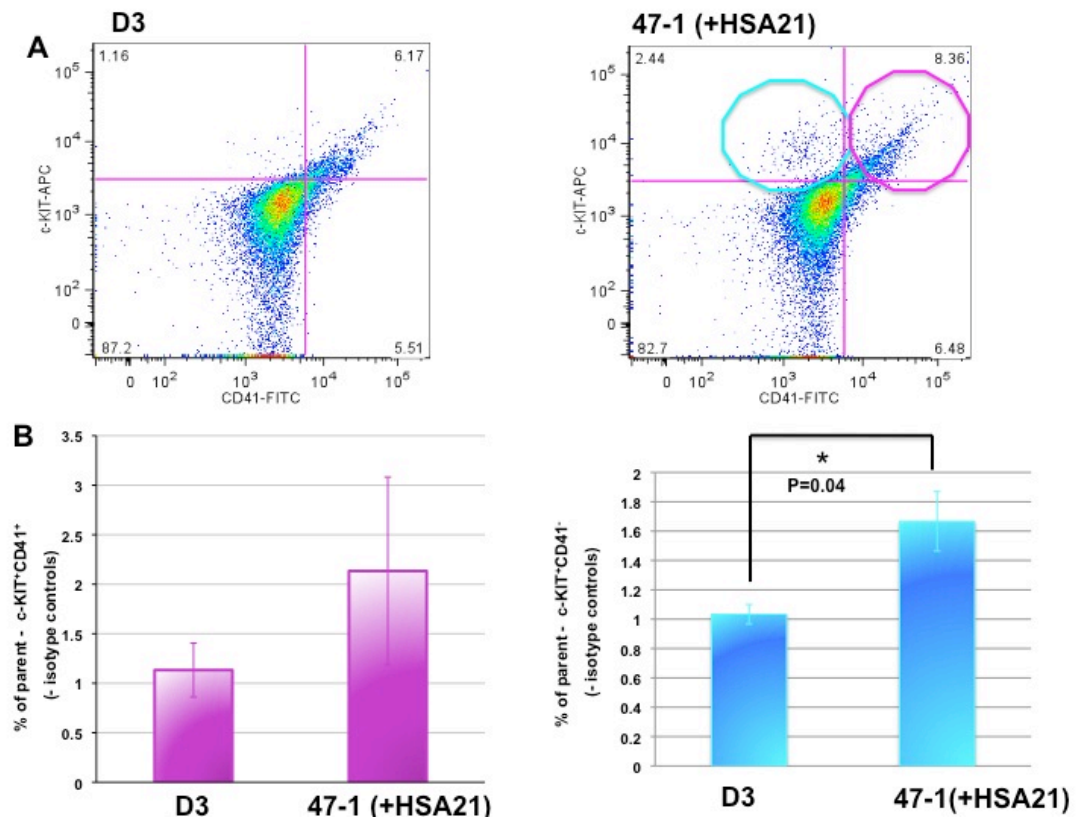
Fig. II.5. FACS analysis of the expression of CD41 and c-KIT in mesodermal colonies at day 5 of the differentiation protocol. Cells differentiated for 5 days on OP9 stromal cells were subjected to FACS staining with an anti CD41-FITC antibody at a 1:100 dilution and anti-c-KIT-APC at the same dilution. Data were collected on a LSRII instrument and analysed with FlowJo software version 8.1. Panel **A** shows two-colour fluorescence dot plots for D3 and 47-1. Quadrant circled in blue contains the CD41⁻c-kit⁺ population; quadrant circled in purple contains the CD41⁺c-kit⁺ population. Panel **B** shows the quantification of the two different populations highlighted in **A**. Chart in purple indicates the percentage of cells positive for CD41 and c-KIT in both D3 and 47-1 (minus the isotype control); chart in blue shows the percentage of c-KIT positive CD41 negative cells (minus the isotype control). Data shown in both charts represents the average percentage of three independent experiments. Error bars indicate s.e.m. The percentage of cells positive for c-KIT and negative for CD41 was significantly higher in the trisomic cells than in the control (unpaired t-test, p value = 0.04).

The data presented in this sub-chapter indicate that mesodermal colonies derived from 47-1 transchromosomic ES cells contain a higher percentage of CD41⁻c-KIT⁺ cells and express higher levels of TIE-2 and GATA-2 than

colonies derived from D3 parental ES cells. Assuming that the observed increase in TIE-2 expression in 47-1 is associated with the increase in the number of CD41⁻c-KIT⁺ cells, it is logical to postulate that the mesodermal colonies derived from 47-1 cells contain more intermediate precursors with haematopoietic potential than the control colonies.

GATA-2 is a master regulator of haematopoiesis. GATA-2 null ES cells and chimeric mice generated from GATA-2$^{-/-}$ ES cells display a profound deficit in haematopoietic stem cells or progenitor cells (Tsai et al., 1994). Accordingly, conditional expression of GATA-2 from a tetracycline-inducible promoter enhances the production of hematopoietic progenitors from murine embryonic stem cells (Kitajima et al., 2002). Given that GATA-2 mRNA levels are increased in 47-1 cells compared with D3 cells, I next asked whether haematopoietic specification from the intermediate progenitors is boosted in trisomic cells compared to the control.

II.3. Functional analysis of haematopoietic progenitors derived from the transchromosomic ES cells

II.3.1. Quantifying the number of haematopoietic progenitors derived from ES cells

To assess whether the increased expression of GATA-2 translates into the generation of more haematopoietic progenitors from the mesodermal colonies derived from trisomic ES cells on OP9 stromal cells, a limited dilution assay was performed. Mesodermal colonies at day 5 of the differentiation protocol were trypsinised and cells were dissociated and replated at a density of 500 cells/well in a 96-well plate containing a fresh layer of OP9 cells. The prolonged contact with stromal cells allows for the generation of colonies containing haematopoietic precursors that are capable of generating colonies of all haematopoietic lineages in semisolid medium (see II.3.2). The low

density of cells seeded allows for easy scoring of the positive wells. The number of haematopoietic colonies generated from D3 cells and 47-1 cells under these conditions was assessed after 7 days; the experiment was performed starting from five independent cultures for each cell line, each seeded in duplicate for a total of ten 96-well plates for each ES cell line (Figure II.6).
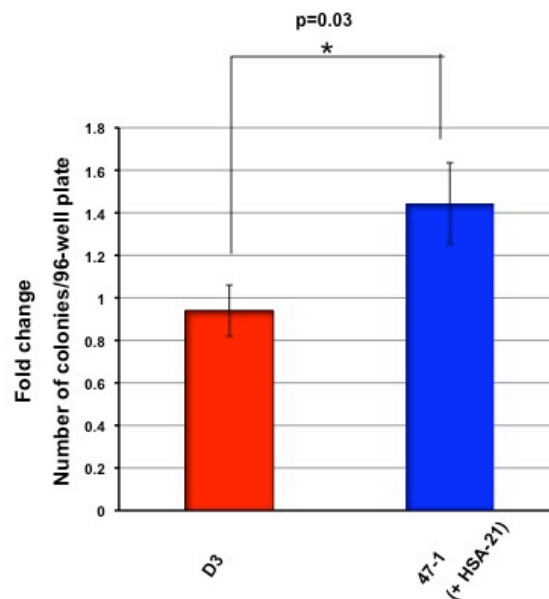
Fig. II.6. Assay for counting cells producing haematopoietic colonies. Mesodermal colonies at day 5 of the differentiation protocol were trypsinised and cells were dissociated, counted and replated at a density of 500 cells/ plate in a 96-well plate containing a fresh layer of OP9 cells. Number of haematopoietic colonies generated from D3 cells and 47-1 cells under these conditions was assessed at day 12. The bar graph represents the average number of 47-1 colonies relative to the average number of D3 colonies in ten 96-well plates (5 independent cultures each seeded in duplicate). Error bars indicate s.e.m. The number of haematopoietic colonies formed by transchromosomic cells (47-1) was higher than the euploid control (D3) (unpaired t-test p value = 0.03).

Data in Figure II.6 are presented as fold change of the average number of 47-1-derived colonies relative to D3-derived colonies. Error bars indicate s.e.m. The number of colonies varied broadly between plates, however despite this variation, the number of haematopoietic colonies formed by transchromosomic

cells (47-1) was significantly higher than the control (D3) (unpaired t-test, p value = 0.03).

II.3.2. Clonal analysis of haematopoietic progenitors derived from ES cells

A well-established *in vitro* assay to test the identity and the functional properties of HSCs and haematopoietic progenitors from the bone marrow is the colony-forming cell (CFC) assay. In this assay, under appropriate culture conditions (a selected cocktail of cytokines and a supporting matrix of methylcellulose), HSCs/haematopoietic progenitors can give rise to a variety of colonies of all blood lineages. Despite the utility of the CFC assay, the most stringent assays to measure HSC number and their functional potential are: 1) the long-term *in vivo* competitive repopulation assay, which tests the capacity of a particular set of HSCs to repopulate the bone marrow of irradiated host mice compared to a set number of HSCs (usually derived from bone marrow of congenic wild-type mice), and 2) serial transplantation assays, which assess the ability of HSCs to sustain haematopoiesis by presumptive self-renewing divisions (Purton and Scadden, 2007). To date, it has not been possible to generate from ES cells HSCs that are capable of reconstitution of the bone marrow of an irradiated host mouse, with the well-known exceptions of murine ES cells transduced with HOXB4 (Helgason et al., 1996; Kyba et al., 2002), BCR/ABL (Peters et al., 2001) or STAT-5 (Schuringa et al., 2004). It is therefore necessary to utilise surrogate *in vitro* assays (i.e., CFC assay) to test the ability of the immature precursors derived *in vitro* from ES cells to give rise to all blood lineages.

A colony-forming cell assay was performed with haematopoietic progenitors derived from 47-1 trisomic ES cells and the D3 parental cell line to compare

their ability to form colonies of different blood lineages. The system utilised for this set of experiments is commercially available from Stem Cell Technologies and it does not assess the potential of haematopoietic progenitors to form B and T lymphocytes. However, it allows for the scoring of colonies of three different types: erythroid (BFU-E), granulocyte-macrophages (CFU-GM), and mixed (CFU-GEMM), which are composed of at least two different lineages and reflect the number of immature progenitors.

D3 and 47-1 cells were differentiated for 5 days on a layer of OP9 cells without LIF, and then trypsinised and replated onto a fresh layer of OP9 cells for three more days. At day 8, cells were counted and seeded at the density of $1 \times 10^5/35$ mm dish and grown in a humidified incubator with 5% CO_2 for 14 days. Colonies were then evaluated using a light microscope with a 20x objective and classified based on morphology according to the manufacturer's instructions.

Myeloid   **Erythroid**   **Mixed**
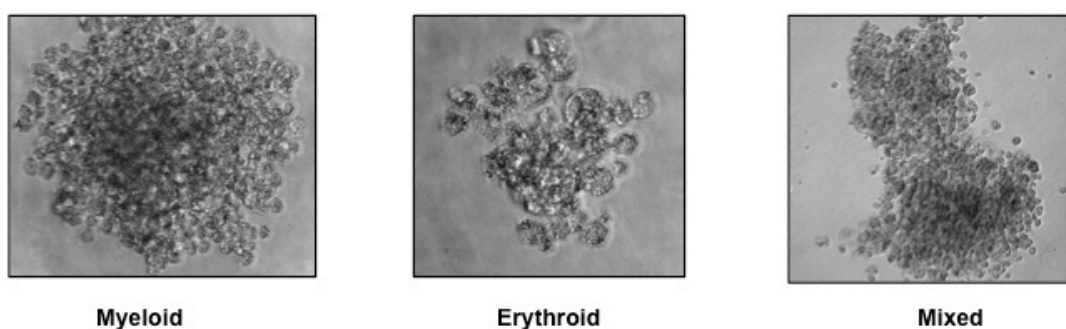
Fig. II.7. Morphology of colonies generated from haematopoietic progenitors in semisolid medium supplemented with IL-3, IL-6 and EPO. Figure shows the three types of colonies scored at day 14 after seeding in semisolid medium. CFU-GM (myeloid) colonies have a dense core surrounded by cells and are composed of at least 30 cells. Individual cells of a CFU-GM colony are easily distinguishable, especially at the periphery of the colony. BFU-E (erythroid) colonies are composed of a minimum of 30 cells; they do not usually have a dense core and the clusters are relatively scattered. CFU-GEMM (mixed) colonies are generally large and contain cells of different lineages. Pictures were taken on a light microscope using a 20x objective.

Results from these experiments are shown in Figure II.8. Bar charts represent the average number of total colonies, as well as the average number of

myeloid, erythroid and mixed colonies in three independent experiments, each performed in duplicate. Error bars indicate the s.e.m.
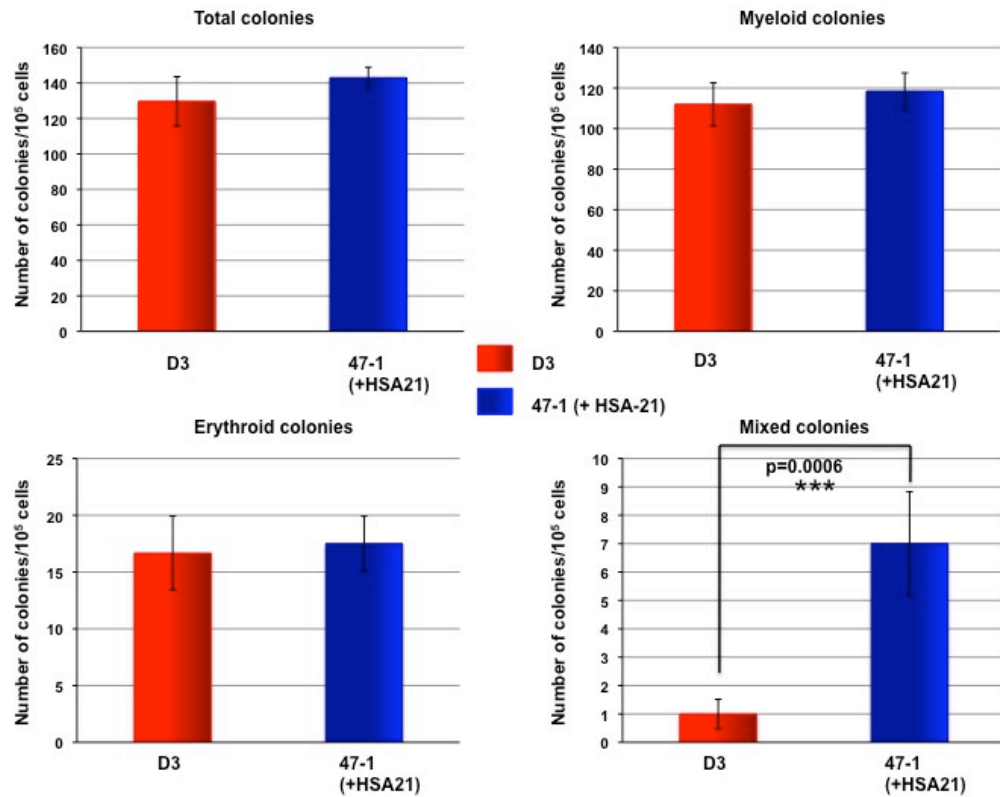
Fig. II.8. Quantification of colonies derived from haematopoietic progenitors in semisolid medium supplemented with IL-3, IL-6 and EPO. ES cells were seeded onto a confluent layer of OP9 cells. On day 5, differentiated ES cells were harvested and seeded onto a new OP9 layer. On day 8, haematopoietic cells developing on the OP9 layers were harvested and plated in methylcellulose-based medium supplemented with IL-3, IL-6 and EPO. Fourteen days later, colonies were counted and classified according to morphology. Shown are bar charts indicating the average number of total colonies, myeloid colonies, erythroid colonies and mixed colonies in three independent experiments, each performed in duplicate. Error bars indicate s.e.m. No significant differences were detected between control cells and trisomic cells in the total number of colonies or in the number of erythroid and myeloid colonies. However, a highly significant (unpaired t-test, p value<0.001) increase was detected in the number of mixed colonies (a measure of the number of more immature progenitors) derived from 47-1 cells compared to the control.

The ability of the trisomic haematopoietic progenitors to form erythroid and myeloid colonies did not significantly differ from the control D3 progenitors. However the number of mixed colonies, which reflects the most immature (multipotent) progenitors (Broxmeyer et al., 2003) was dramatically increased

in 47-1 compared to the control (unpaired t-test, p value < 0.001). Together with the increase observed in 47-1 cells in the limited dilution experiment (see Figure II.6), these findings strongly argue that trisomy 21 increases the number of immature haematopoietic precursors generated *in vitro* from ES cells.

II.4. Alteration of HSC ontogenesis in transchromosomic ES cells is caused by trisomy of specific HSA21 genes/regions

Transchromosomic ES cells generate a higher number of specialized cells with haematopoietic potential (i.e., haemogenic endothelium) and a higher number of immature haematopoietic progenitors than the wild type ES cells.

One of the major players in the generation of the haematopoietic cells from the mesoderm and the haemangioblast is a gene on HSA-21, RUNX-1.

A recent study has provided evidence for the role of RUNX-1 in this developmental process (Lancrin et al., 2009). Authors of this study demonstrated that the TIE-2$^+$c-KIT$^+$CD41$^-$ haemogenic endothelial cell population is generated in absence of RUNX-1, but that RUNX-1 is indispensable for the generation of definitive haematopoietic cells from this population.

Using conditional gene expression in ES cells, Sakai et al. have also recently suggested that RUNX-1 increases the number of haematopoietic progenitors and suppresses endothelial gene expression during *in vitro* ES differentiation, without affecting number of haemogenic cells (Sakai et al., 2009). The involvement of RUNX-1 in the phenotypes described during *in vitro* differentiation of trisomic ES cells was therefore tested. In order to do so, I undertook two separate approaches, which are described in II.4.1 and 2.

II.4.1. Silencing the third copy of RUNX-1 by human-specific RNAi

The first approach I employed took advantage of a peculiar feature of the transchromosomic system, which is the possibility of restoring the diploid dose of a gene on HSA21 by specifically silencing its third human copy.

Low levels of the mouse RUNX-1 mRNA transcript were detected in undifferentiated ES cells, as previously reported in the literature (Fujita et al., 2001). Human RUNX-1 was also found to be expressed in the undifferentiated transchromosomic ES cells (see I.1.3, Figure I.5). Human-specific knockdown of RUNX-1 was accomplished by transient transfection of the undifferentiated ES cells with a pool of human-specific oligos (designed and produced by Dharmacon, Belgium). Species-specificity of the human RNAi was screened by aligning the target sequences of the oligos with both mouse and human mRNA sequences of RUNX-1 using the BLAST feature of the NCBI website (http://blast.ncbi.nlm.nih.gov/Blast.cgi). Sequences targeted by the oligos were found to be human-specific. To test the efficiency of the knockdown of the human RUNX-1, and its specificity against the human form of the gene, RT-PCR and western blot analysis were performed.

In all RNAi experiments, a transfection with oligos targeting an irrelevant sequence of the genome was performed as a control. Figure II.9 shows that the human-specific RNAi was efficient in knocking down the human RUNX-1 gene (panel A; primers used for this RT-PCR were the same as the primers used for RT-PCR shown in Figure I.5, and they were previously shown to be human-specific) and did not affect the mouse gene, as demonstrated by RT-PCR analysis with mouse specific primers shown in panel B.

Panel C shows that human RUNX-1 protein was efficiently reduced by 72 hours after siRNA transfection. No effects on human RUNX-1 were observed in the control RNAi samples both at the mRNA and at the protein level.
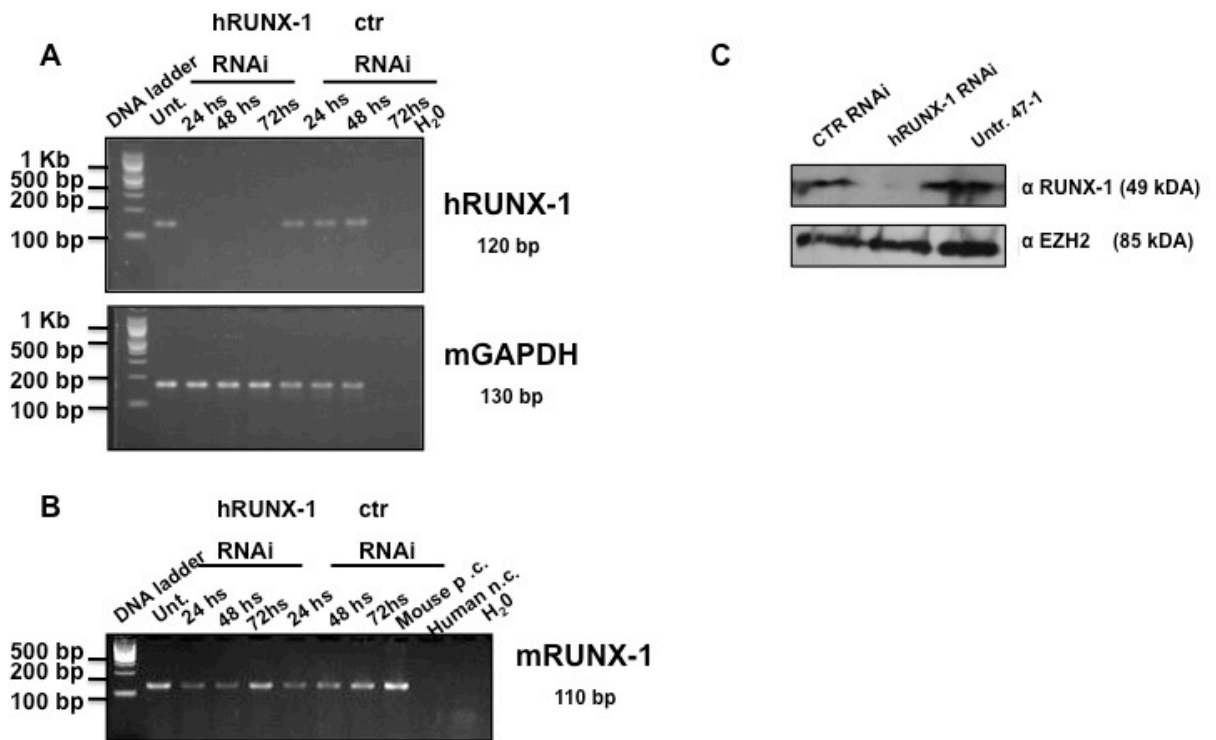
After having established that the knockdown for RUNX-1 was efficient and human-specific, I used this experimental tool to investigate the molecular changes caused by an increased dosage of RUNX-1 during the early stages of the haematopoietic differentiation of the transchromosomic system. In order to do so, undifferentiated ES cells were transfected with human specific oligos targeting RUNX-1 or with non-targeting oligos and seeded onto a confluent layer of OP9 cells twelve hours after transfection.
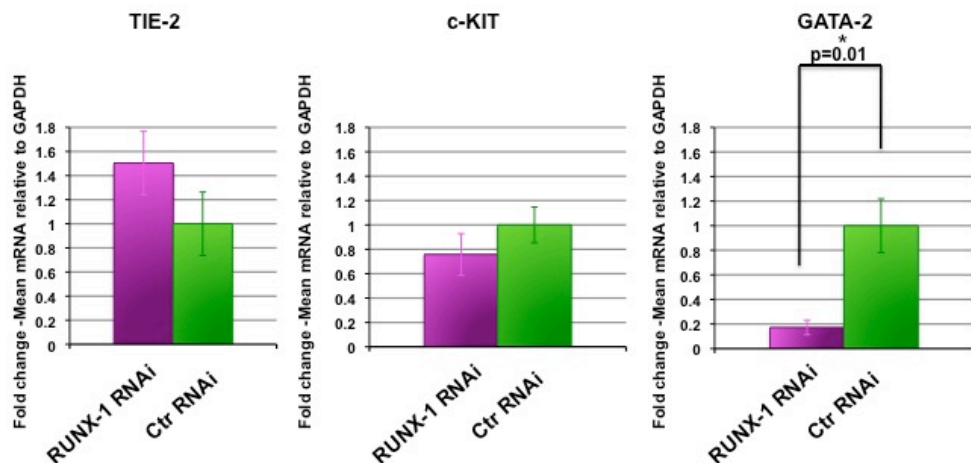
Fig. II.10. Effect of hRUNX-1 RNAi on the expression of haematopoietic markers during differentiation of transchromosomic ES cells. Twelve hours after transfection with oligos targeting human RUNX-1 or non-targeting oligos, transchromosomic ES cells were seeded onto a confluent layer of OP9 cells. After 5 days, mesodermal colonies were harvested, total RNA extracted and cDNA synthesised. qRT-PCR analysis was performed to quantify the levels of mRNA for TIE-2, GATA-2 and c-KIT. Bar charts represent the mean mRNA levels divided by GAPDH of 5 independent experiments. Error bars indicate s.e.m. There was a significant reduction (unpaired t-test, p value = 0.01) of the levels of GATA-2 in the hRUNX-1 RNAi compared to the control, suggesting that GATA-2 levels are sensitive to the gene dosage of RUNX-1.

Haematopoietic differentiation was carried out for 5 days, at which time the cells were harvested, total RNA extracted and cDNA synthesised. Quantitative RT-PCR analysis was performed to assess levels of markers that previously showed an alteration in the transchromosomic system. As shown in Figure II.9, no significant difference was observed in levels of mRNA for TIE-2 and c-KIT between the hRUNX-1 RNAi and the control RNAi, indicating that RUNX-1 is not required for the increased formation of the haemogenic endothelium during *in vitro* differentiation of the ES cells. In contrast, a significant reduction of the levels of mRNA for GATA-2 was detected in the hRUNX-1 RNAi compared to control RNAi (unpaired t-test, p value = 0.01), suggesting that haematopoietic specification from the haemogenic endothelium was sensitive to the gene dosage of RUNX-1.

These results support a recent study, which demonstrated that conditional overexpression of RUNX-1 in ES cells promotes an increase in immature haematopoietic cells without affecting the number of haemogenic cells (Sakai et al., 2009). These data also reinforce the crucial findings from the study of Lancrin et al. that the haemogenic endothelium is generated in the absence of RUNX-1, but that RUNX-1 is necessary for the generation of definitive haematopoietic cells from this population (Lancrin et al., 2009). For the first time, these data suggest that the described effect might be accomplished by RUNX-1 through up-regulation of GATA-2.

II.4.2. Reproducing the observed phenotypes in partial trisomic ES cells

During the experimental procedure required to generate a murine ES cell line carrying a freely segregating copy of HSA21, Hernandez et al. generated a panel of at least 21 ES cell lines containing partial fragments of HSA21 (Hernandez et al., 1999). These cell lines have morphological characteristics of the parental D3 cell line from which they were derived, and they all carry partial stretches of HSA21 extending proximally or distally from the D21S55 locus, where the G418 selection marker is inserted.

Hernandez et al. grossly characterised the panel of partial trisomic ES cells. A more detailed analysis of the genomic content of these cells is being carried out by Jurgen Groet et al. using high-resolution comparative genomic hybridization (CGH) array (HG-18-CHR21 tiling oligo arrays from NimbleGen at 70 bp resolution). Preliminary unpublished data from this analysis, together with more conventional mapping data, were integrated to choose partial trisomic ES cell lines with a defined content to address the following points: 1) the molecular changes observed in 47-1 are not an artefact of this particular cell line, but are reproducible across a range of trisomic ES cells; 2) it is

possible to combine information derived from different transchromosomic ES cells in order to pinpoint a role for a candidate gene on HSA21 (in this case RUNX-1) in DS-related phenotypes.

Data from the RUNX-1 RNAi experiment suggest that RUNX-1 gene dosage does not affect the formation of the intermediate haemogenic endothelium, but has an effect on the generation of immature haematopoietic progenitors during *in vitro* differentiation of transchromosomic ES cells through regulation of GATA-2 levels. To provide further evidence in support of these data, I performed a molecular analysis of markers related to haematopoietic differentiation in partial trisomic ES cells, chosen according to RUNX-1 presence and expression. Figure II.11 shows RT-PCR analysis performed on a variety of ES cell lines from the panel of transchromosomic ES cells with primers specific for human RUNX-1.
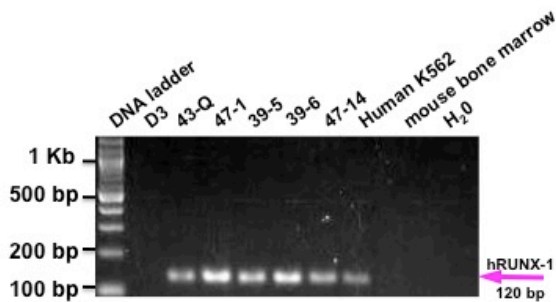
Fig. II.11. RT-PCR analysis performed with human-specific RUNX-1 primers on a variety of transchromosomic ES cell lines.

Total RNA was extracted from undifferentiated transchromosomic ES cells cultured under G418 selection. cDNA was synthetized and RT-PCR performed with human-specific RUNX-1 perimers. ES cells included in this experiment were chosen according to their availability in the lab and their growth properties.

I included in this PCR the parental cell line D3 from which the transchromosomic cells were derived, a positive (human leukaemic cell line K562) and a negative (mouse bone marrow) control. Data from this experiment were then compared to the original mapping data published from Hernandez et al.
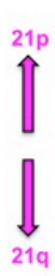
Surprisingly, 43-Q ES cells, which were shown by Hernandez et al. to carry a deletion encompassing the RUNX-1 gene, expressed hRUNX-1 at the undifferentiated stage (see Figure II.12). This might be due to rearrangements or amplification of portions of the human chromosome carried by the murine

ES cells, or to contamination from clones derived from a different panel of ES cells due to extensive handling in tissue culture. The presence of the human RUNX-1 gene was also confirmed at the gDNA level. Due to this discrepancy with Hernandez et al., 43-Q cells were excluded from further analysis. These data show the necessity of verifying expression of individual candidate genes in the panel of ES cells and to use the most comprehensive approach possible in determining genomic content of cells carrying distinct fragments of HSA21 when performing experiments aimed to pinpoint genes causing phenotypes associated to DS in this system.

Figure II.13 shows mRNA levels of TIE-2, c-KIT and GATA-2 in partial trisomic ES cells. In agreement with the hRUNX-1RNAi data, results from the partial trisomic ES cell lines highlight different requirements for distinct fragments of HSA21 in the regulation of mRNA levels of genes regulating the formation of the haemogenic endothelium and the generation of HSCs during *in vitro* differentiation of ES cells.

47-14 ES cells contain a large proportion of the genes on HSA21, including RUNX-1, but they harbour at least two deletions, one of which affects a region of at least 11.65 Mbs (from D21516 to APP). 47-14 cells show a molecular signature that is nearly indistinguishable from 47-1 cells, with levels of mRNA for TIE-2, c-KIT and GATA-2 significantly increased compared to the parental D3 control (unpaired t-test p values = 0.006, 0.006 and 0.03, respectively). These data demonstrate that alteration of the levels of mRNA for the markers analysed is not an artefact of the 47-1 cell line and is reproducible in at least another ES cell line with a defined HSA21 content (47-14).

in Mbp	Symbol	39-5	47-14	43-Q	47-1
	D21Z1			grey	grey
14.8	D21S16			grey	grey
14.8	SAMSN1			grey	grey
15.4	D21S13			grey	grey
18.1	D21S362			grey	grey
18.1	D21S385			grey	grey
19.5	D21S11			grey	grey
21.6	D21S214			grey	grey
22.6	D21S278			grey	grey
22.6	D21S279			grey	grey
24.5	D21S367			grey	grey
260	GABPA			grey	grey
26.2	APP			grey	grey
29.1	D21S82		grey	grey	grey
29.6	BACH1		grey	grey	grey
31.3	D21S304		grey	grey	grey
31.4	TIAM1		grey	grey	grey
31.9	D21S389		grey	grey	grey
32	SOD1		grey	grey	grey
33.6	IFNAR1	grey	grey	grey	grey
33.8	GART	grey	grey	grey	grey
34.8	RCAN1	grey	grey		grey
35.1	RUNX1	grey	grey		grey
37	SIM2	grey	grey	grey	grey
37.6	D21S336	grey	grey	grey	grey
37.7	D21S394	grey	grey	grey	grey
37.7	DYRK1A	grey	grey	grey	grey
37.9	KCNJ6	grey	grey	grey	grey
38	D21S55 ●	grey	grey	grey	grey
38.7	ERG	grey	grey	grey	grey
39.1	ETS2		grey	grey	grey
39.6	HMGN1		grey	grey	grey
40.6	D21S15		grey	grey	grey
42.7	D21S49		grey	grey	grey
44.5	PFKL		grey	grey	grey
45.1	ITGB2		grey	grey	grey
46.2	D21S403		grey	grey	grey
46.2	COL6A1		grey	grey	grey

Fig. II.12. Characterisation of HSA21 content of transchromosomic ES cell lines used for experiments described in this chapter. Figure summarises the original data published from Hernandez et al. (*Hum Mol Gen*, 1999) integrated with available results from HR-CGH array (from J. Groet). D21S55 (where the neomycin resistance marker is integrated) is indicated by a red dot, and is present in every transchromosomic ES cell line. Light grey bars indicate that a given gene on HSA21 is present in the ES cell line; white bars indicate that that gene is absen**t.** According to data from Hernandez et al., 43-Q cells have a deletion encompassing RUNX-1. However, RT-PCR analysis revealed expression of hRUNX-1 in the undifferentiated 43-Q ES cells; hence these cells were excluded from further analysis. Although RUNX-1 was present in both 39-5 and 47-14 ES cell lines, HSA21 genomic content of these two cell lines was not overlapping. Of the HSA21 genes with a potential role in haematopoiesis/leukaemogenesis, ERG and DSCR-1 were present in both 39-5 and 47-14, and so was DYRK1A, whereas ETS-2 and BACH-1 were absent in 39-5 but present in 47-14. 47-1 ES cells contain the entire HSA21.

In this set of experiments I also included an additional trisomic cell line (39-5), with a HSA21 genomic content different from both 47-1 and 47-14. In 39-5, mRNA for GATA-2 was up-regulated compared to D3 parental cells, as seen to a similar extent in 47-1 and 47-14. However mRNA levels for TIE-2 and c-KIT did not show a significant difference when compared to the parental cell line D3. These data, in agreement with the RNAi results shown in II.4.1

suggest that whereas RUNX-1 might be responsible for regulation of expression of GATA-2, its presence does not influence levels of TIE-2 and c-KIT.
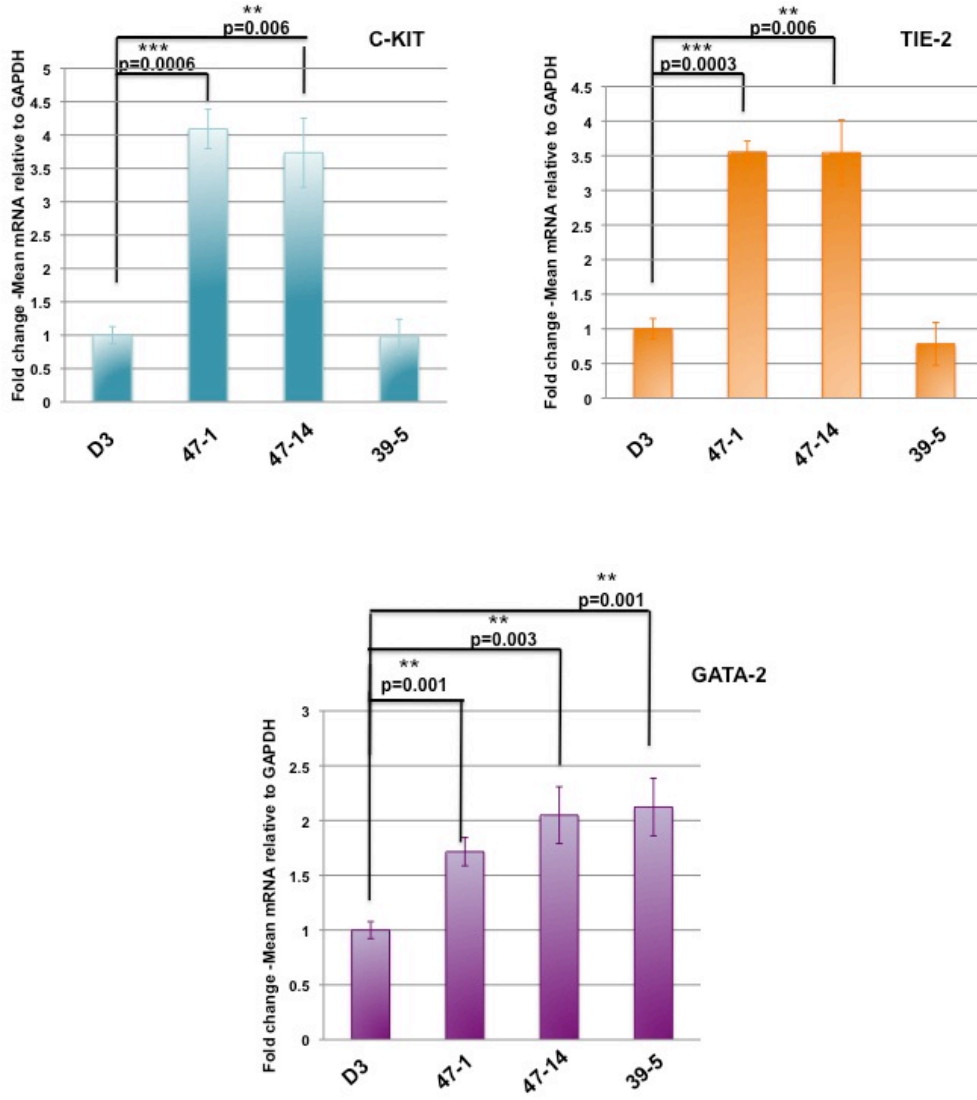
Fig. II.13. Comparison of the molecular changes observed in 47-1 across a panel of partially trisomic ES cells. TIE-2, c-KIT and GATA-2 mRNA levels were tested in two additional transchromosomic ES cell lines, 47-14 and 39-5, and compared with 47-1 cells and D3 parental cells. Bar charts show the average mRNA levels of 3 independent experiments. Error bars indicate s.e.m. All p values were calculated using the unpaired two-tailed t-test. Levels of GATA-2 mRNA were significantly increased in both 47-14 and 39-5 compared to the D3 euploid control (unpaired t-test, p value = 0.003 and 0.001, respectively). Levels of TIE-2 and c-KIT were significantly up-regulated in 47-14 compared to the D3 control (p value = 0.006), but not in 39-5. Data are represented as fold change relative to levels in D3 parental cells.

These data also indicate that one or more genes, which are present in 47-1 and 47-14 but absent in 39-5, are required for regulating levels of TIE-2 and c-KIT. Interestingly, among the genes that fit this genetic criterion are the transcription factors ETS-2, which has a known role in haematopoiesis, and BACH1. Finer mapping of the HSA21 content for 39-5 is ongoing and will very likely guide the identification of potential candidates responsible for the regulation of TIE-2 and c-KIT mRNA levels.

Very recently, a study from Korbel et al. has attempted to identify the regions on HSA21 involved in several DS phenotypes by high-resolution analysis of samples from patients with segmental trisomies (Korbel et al., 2009). Three of the 30 patients included in this study had TMD (2) or AMKL (1). Based on this approach, the authors found a critical leukaemia-predisposing region on HSA21 of 8.35 Mb (35-43.35). Despite the limited number of patients analysed, it is striking that the region identified in this study includes RUNX-1, ERG and ETS-2, but not BACH-1 or TIAM-1. The authors also suggested that a deletion in the short arm of HSA21 common to all three of the patients analysed might contribute to the phenotype. Besides leading to the same direction as my study, results from Korbel et al. also prompt a deeper investigation on the genomic content of the short arm of HSA21.

II.5. Final remarks

In this chapter, analyses of the early stages of haematopoietic differentiation in the transchromosomic system are described.

It is quite difficult to unequivocally define separate stages of the developmental process that leads to the *in vitro* generation of haematopoietic cells from mesodermal precursors. One reason for this is the appearance of transient populations at intermediate developmental stages, which often share

expression of surface markers and TFs with previous or subsequent stages. Furthermore, new findings often challenge previous theories in the field, and there is a lot of open debate regarding the nature of this developmental process. The aim of the experiments described in this chapter was to apply the most recent knowledge in the field to characterise the effect of trisomy 21 on early haematopoietic development from embryonic stem cells.

A combination of FACS staining and gene expression analysis revealed that trisomic ES cells generate a larger number of CD41⁻c-KIT⁺ cells, and express higher levels of mRNA for TIE-2, GATA-2 and c-KIT than the parental D3 control during haematopoietic development. These data indicate that direct precursors of the haematopoietic stem cells (haemogenic endothelial cells, CD41⁻c-KIT⁺TIE-2⁺) are generated at a higher rate in the transchromosomic system.

GATA-2 is crucial for the maintenance, proliferation, and/or survival of immature hematopoietic progenitors (Tsai and Orkin, 1997). *In vivo* data support the hypothesis that GATA-2 plays a role in haemogenic precursor formation in the AGM region. Transgenic embryos with a GFP marker under the control of GATA-2 transcriptional regulatory sequences show high levels of GATA-2 expression in CD45⁻ AGM cells with haemogenic potential, and there is a significant decrease in the percentage of CD45⁺ cells (HSCs) in AGM regions from GATA-2⁺/⁻ mice (Minegishi et al., 2003). Moreover, GATA-2 is expressed in the endothelial cells lining the dorsal aorta and some underlying mesenchymal cells at the time of the first induction of HSCs, during midgestation. Hence, high GATA-2 expression in haemogenic cells of the AGM suggests that GATA-2 is acting on the cells just prior to the induction of HSCs (Ling et al., 2004). Recent data from Lugus et al. suggest that GATA-2 might play multiple roles in haemangioblast development and differentiation, including acting as a proliferative signal to primitive erythroid progenitors

(Lugus et al., 2007). In my analysis, GATA-2 expression was used as a marker of haematopoietic commitment during the differentiation of ES cells. Because mRNA levels were higher in the transchromosomic ES cells compared to the D3, I set out to test whether there was an increased production of haematopoietic progenitors in the transchromosomic system. An assay designed to count the number of haematopoietic progenitors showed that the number of haematopoietic colonies derived from the transchromosomic ES cells was higher than the ones formed by the D3 control, and I also observed a significant increase in the number of immature haematopoietic colonies derived from the trisomic cells in a colony formation assay.

Reducing RUNX-1 to the disomic stage using human-specific RNAi decreased mRNA levels for GATA-2 in transchromosomic ES cells, without affecting levels of mRNA for TIE-2 and c-KIT. The data obtained from the RNAi studies showed that the copy number of RUNX-1 does not influence the formation of the haemogenic endothelium, but might affect generation of haematopoietic stem cells through up-regulation of GATA-2. Data generated from a panel of ES cells containing different fragments of HSA21 support this conclusion, underlining a requirement for RUNX-1 in the regulation of mRNA levels of GATA-2 but not of TIE-2 and c-KIT. A previous study has demonstrated that during HSCs ontogenesis, GATA-2 transcriptionally regulates RUNX-1 by binding to the haematopoietic-specific +23 enhancer element (Nottingham et al., 2007). Furthermore, Pimanda et al. have demonstrated that key stages of mouse HSC specification in the AGM region and in the midgestation foetal liver are regulated by the three specific haematopoietic enhancers GATA-2 -3, FLI-1 +12 and SCL +19, each bound by the TFs GATA-2, FLI-1 and SCL to form a fully connected kernel operating during mammalian development (Pimanda et al., 2007). These types of regulatory circuits are emerging as key

controllers of HSC development, and it is possible that a regulatory network controlling the development of HSCs includes the reciprocal regulation of RUNX-1 and GATA-2. In silico analysis that I performed with the TFSEARCH software (Yutaka Akiyama: "TFSEARCH: Searching Transcription Factor Binding Sites", http://www.rwcp.or.jp/papia) has revealed that the 1 kb region upstream the TSS of the murine GATA-2 contains at least 2 consensus binding sites for RUNX-1, giving rise to the possibility that GATA-2 might be a direct target of RUNX-1. Further studies are therefore required to establish the mechanisms by which RUNX-1 can control GATA-2 levels, contributing to HSC formation *in vitro* and *in vivo*.

A model for the effect of trisomy 21 during early stages of haematopoietic development based on the data presented in this chapter is shown in Figure II.14.
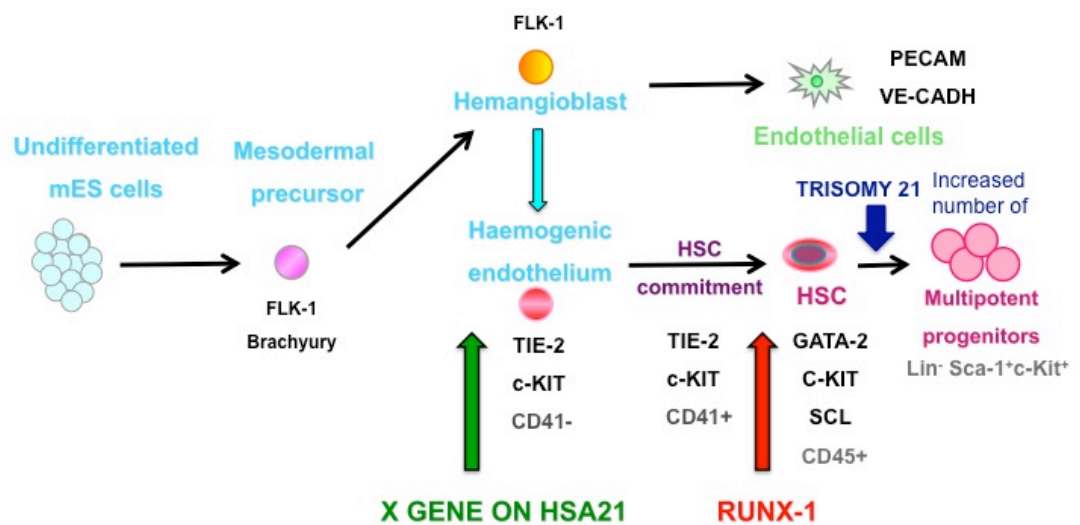
Fig. II.14. Effect of trisomy 21 on *in vitro* haematopoietic development from transchromosomic ES cells. ES cells containing an extra copy of HSA21 express higher levels of markers associated with the transient haemogenic endothelium compared to normal euploid mouse ES cells. This effect is not dependent on an increased dosage of RUNX-1, but it is very likely caused by trisomy of another gene (or genes) on HSA21. However, copy number of RUNX-1 affects the specification of a haematopoietic programme during development, very likely by regulating levels of GATA-2. The combined effect of these two phenomena is that the number of immature haematopoietic progenitors generated by the transchromosomic ES cells is higher than the control.

According to this model, one or more unidentified gene(s) on HSA21 are responsible for an increased formation of specialised haemogenic endothelial cells, but RUNX-1 is not required for this phenomenon. However, an increased gene dosage for RUNX-1 is associated with increased mRNA levels of GATA-2, a key regulator of HSC ontogenesis and specification. The overall consequence of trisomy 21 on the haematopoietic differentiation of ES cells is the formation of an increased number of immature haematopoietic precursors. It is intriguing to speculate that this larger pool of progenitors might be dysfunctionally regulated *in vivo*, constituting the substrate allowing for the acquisition of mutations such as GATA-1 or JAK-2, and ultimately accounting for the increased incidence of acute leukaemias of both lymphoid and myeloid lineages in DS.

III. Haematopoietic defects in DS: insights from primary samples

Megakaryocytic leukaemia in DS is characterized by the presence of acquired mutations of the erythroid-megakaryocytic transcription factor GATA-1, and by the presence of a supernumerary chromosome 21 in the blast cells. Factors that predispose 10% of DS children to develop megakaryocytic leukaemia, and additional events that are necessary for progression from TMD to AMKL, are largely unknown (Hitzler and Zipursky, 2005). GATA-1 mutations leading to the exclusive production of GATA-1s (a truncated, "oncogenic" form of the protein) are acquired *in utero* (Ahmed et al., 2004) and can be detected in genomic DNA from foetal livers at 18–23 weeks of gestational age (Taub et al., 2004). To date, acquired GATA-1 mutations have never been reported in blast cells that did not also carry a trisomy 21 (either as constitutional DS, or in individuals mosaic for trisomy 21). The role of trisomy 21 in the pathogenesis of DS leukaemia remains to be fully clarified. In chapter I, I have presented experimental evidence supporting the hypothesis that trisomy 21 provides a proliferative advantage to the megakaryocytic lineage, creating conditions favorable to the block of differentiation caused by GATA-1s. The possible contribution of trisomy 21 (through one or more genes on HSA21) to the increased risk of occurrence of GATA-1 mutations is an additional possible mechanism to explain the laeukaemogenic process in DS.

In the first part of this chapter, I describe an intriguing case of a perinatal hydrops foetalis (HF) in DS, with hyperproliferation of megakaryocytes in both foetal liver and spleen, without a detectable GATA1 mutation. This case gives further substance to the theory that abnormalities of the megakaryocytic compartment might occur in DS independently from mutations of GATA-1. The second part of this chapter describes a gene expression analysis performed

on matched DS and euploid human foetal liver samples.

III.1. Hyperproliferation of the megakaryocytic lineage in the liver of a DS foetus

III.1.1. Immunohistochemical analysis on archived tissues

Clinical records of the Pathology Department of the University of Split Medical School showed that a preterm female was delivered at 29 gestational weeks with slight dysmorphic facial features resembling DS, and lived for less than one hour before dying with severe hydrops foetalis (HF). Standard karyotype analysis revealed trisomy 21 (47, XX+21). Histopathological analysis of liver and spleen biopsies showed numerous clusters of large, polyploid cells with megakaryocytic morphology in the parenchyma of the two organs. Deposits of haemosiderin and a mild degree of fibrosis were also observed in liver and spleen of the foetus.

Paraffin-embedded archived tissue from the liver and spleen biopsy specimens were obtained from the Pathology Department of the University of Split to perform a characterisation of the nature of the cells infiltrating the organs.

Haematoxylin/Eosin staining performed on 5 μm thick sections from the liver and the spleen of the case confirmed an evident infiltration of polyploid cells, resembling mature megakaryocytes (Figure III.1 and III.3). Figure III.1 shows a comparison between a section of the liver of the HF case and a control archived foetal liver biopsy of a therapeutically terminated DS matched for sex and gestational age. Both liver and spleen sections from the case revealed numerous and widespread islands of apparent hyperproliferation of large cells, containing multiple nuclei. In contrast, no such islands were visible in the gestational age-matched DS foetal liver.

Analysis of phenotypic markers associated with the megakaryocytic markers CD41 and von Willebrand factor (vWF) was then performed on sections from the liver of the case, and the infiltrating cells showed strong positive staining for both markers (Figure III.1 and III.2). Approximately 93% of DS-TMD and 50% of DS-AMKL cases express the surface antigen CD34 on their blasts (Langebrake et al., 2005), so this marker was also tested on the liver sections from the case. Cells infiltrating liver and spleen were negative for CD34 expression, revealing their mature megakaryocytic nature.
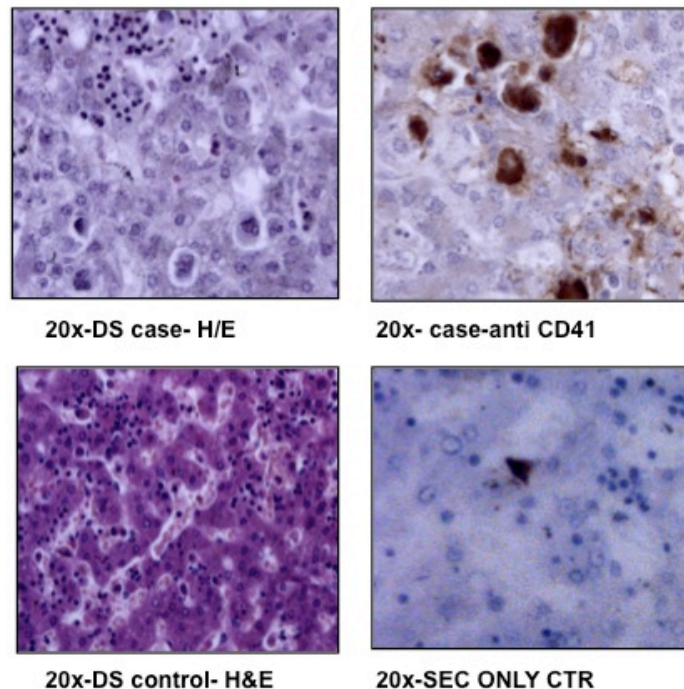
Fig. III.1 Morphological features of the megakaryocytic hyperproliferation in the liver of a Down syndrome case prematurely born with hydrops foetalis (1). Panels on the left show H/E staining of the DS case and of a DS control matched for sex and gestational age. Upper panel on the right shows cells infiltrating the parenchyma stained with a goat polyclonal anti-CD41. Lower right panel display a control slide incubated with secondary antibody only. Pictures were taken on a Leica Q5501W microscope at 20x magnification.

20x- case- anti CD34   20x- case- anti VW

20x-SEC. ONLY CTR   20x-SEC. ONLY CTR
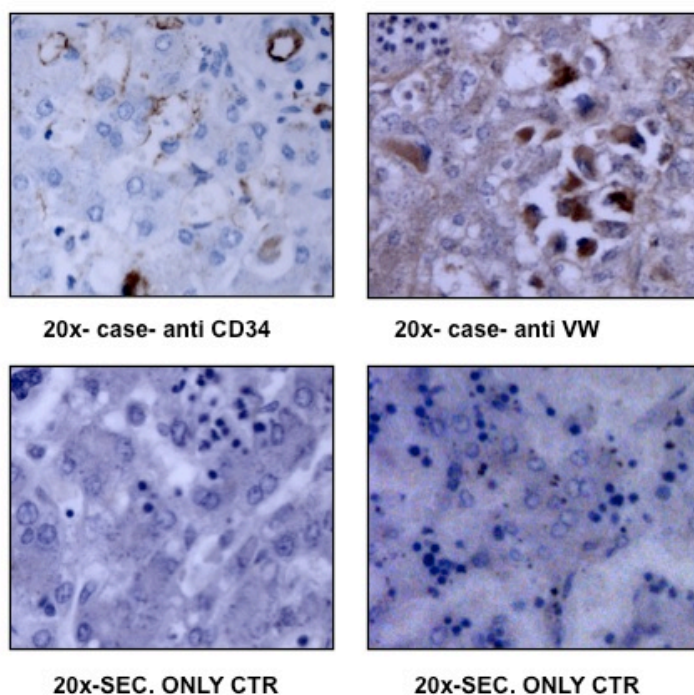
Fig. III.2 Morphological features of the megakaryocytic hyperproliferation in the liver of at Down syndrome case prematurely born with hydrops foetalis (2). Upper panel on the left shows cells infiltrating the liver parenchyma stained with a mouse monoclonal anti-CD34. Upper panel on the right shows staining with a rabbit polyclonal anti-von Willebrand antibody. Lower panel display control slides incubated with secondary antibody only. Pictures were taken on a Leica Q5501W microscope at 20x magnification.

Figure III.3 shows staining results for the sections taken from the spleen of the case. Infiltrating cells were less numerous in this tissue, but had the same features (CD41 positive, vWF positive, CD34 negative) of the cells infiltrating the liver. Taken together, data from histochemical analysis distinguished this case from the majority of DS-TMD cases, which typically show a proliferation of immature megakaryoblasts, rarely multinucleated, usually vWF$^-$ and CD34$^+$.

| 20x-case-Spleen H/E | 20x- case-Spleen- anti CD41 | 20x- case-Spleen- anti vW |
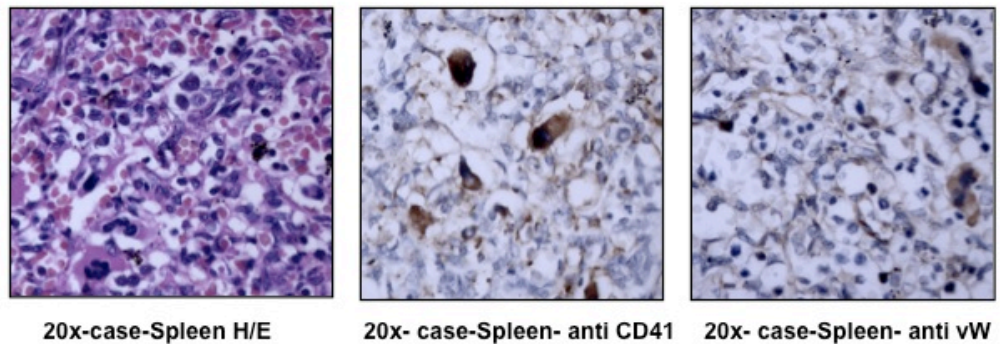
Fig. III.3 Morphological features of the megakaryocytic hyperproliferation in the spleen of a Down syndrome case prematurely born with hydrops foetalis. Figure shows that cells infiltrating the spleen, although less numerous, displayed the same features of the ones infiltrating the liver, as they were strongly positive for both CD41 and vWF expression. Pictures were taken on a Leica Q5501W microscope at 20x magnification.

III.1.2. GATA-1 sequencing analysis on archived material

After having established that the cells infiltrating the liver and the spleen of the patient were mature megakaryocytes, I wanted to assess whether this abnormal proliferation was associated with the mutations in the GATA-1 gene pathognomonic of DS-TMD and AMKL. Therefore, GATA-1 mutational analysis was performed on formalin-fixed, paraffin-embedded tissues from the liver and spleen of the patient.

The challenge of this approach is that treatment with formalin induces chemical modification of DNA, making it difficult to extract gDNA of PCR-amplifiable grade from fixed archived tissues (Shi et al., 2004). A summary of different protocols tested is provided in Figure III.4.

1) Deparaffinisation with Xylene, followed by overnight digestion with standard genomic lysis buffer and proteinase K; then phenol/chloroform extraction.

2) High temperature denaturation, followed by automated gDNA extraction with EZ1 BioRobot from Qiagen.

3) High temperature denaturation in alkaline lysis solution followed by extraction with phenol/cloroform and DNA precipitation with addition of tRNA (method from Shan-Rong Shi et al.).

On a piece of tissue cut from the paraffin block:

4) Deparaffinisation with Xylene, followed by overnight digestion with standard genomic lysis buffer and proteinase K; then phenol/chloroform extraction.

5) Deparaffinisation with Xylene followed by extraction with the Gentra Puregene Tissue Kit (Qiagen).

On formalin fixed (not embedded) tissue:

6) Overnight wash in a large volumes of PBS, followed by 3 washes in Tris-EDTA and overnight digestion with standard genomic lysis buffer and proteinase K; then phenol/chloroform extraction.

7) Overnight wash in a large volumes of PBS, followed by 3 washes in Tris-EDTA, then extraction with the Gentra Puregene Tissue Kit (Qiagen).

8) Three washes in PBS, followed by overnight digestion with standard genomic lysis buffer and proteinase K; then phenol/chloroform extraction.

Fig. III.4. Experimental conditions tried to extract gDNA of PCR-amplifiable quality from archived material. Several extraction methods were performed, starting from sections cut from the paraffin block or from bigger pieces of tissue from both the paraffin block and the formalin-fixed tissue.

To facilitate amplification, PCR was performed on gDNA extracted with each of the experimental conditions listed in Figure III.4 using a very short amplicon. Figure III.5 shows an agarose gel electrophoresis analysis of fragments amplified with test primers from gDNA extracted from archived tissue using conditions 4 to 8 of Figure III.4.

Only conditions 6 and 7, listed in red in Figure III.4, gave an amplifiable product in the test PCRs.
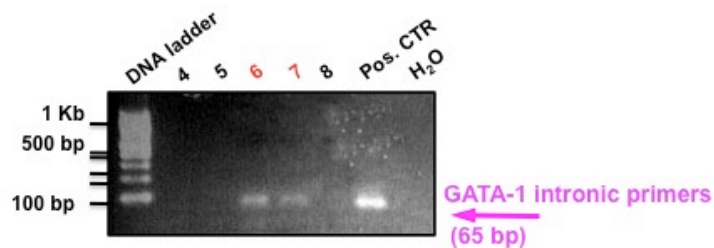
Fig. III.5. PCR analysis performed on gDNA extracted from archived material using test primers. gDNA extracted according to methods from 4 to 8 listed in Figure III.4 was tested by PCR with primers spanning an intron of GATA-1. Amplicon size was very short (65 bp) to facilitate amplification. Figure shows agarose gel electrophoresis of DNA fragments performed on a 1.8% gel stained with ethidium bromide. The only two conditions of extraction that gave amplifiable products were the ones performed with a piece of tissue cut out of the formalin-fixed tissue (not paraffin embedded) regardless of the extraction method. However, the number and length of washes performed before starting the extraction influenced the quality of extracted gDNA (compare lanes 6-8).

Both of the amplifiable gDNA samples were extracted from formalin-fixed tissue. Both a kit-based and a standard phenol/chloroform extraction procedure gave an amplifiable product. However, the number and length of the washes performed before starting the extraction, to eliminate the fixative, highly influenced quality of gDNA extracted.

Once the quality of extracted gDNA was tested, the same material was used as a template in a GATA-1 specific PCR. Primers used in this PCR allowed amplification of the entire exon 2 of GATA-1, which was then sequenced to screen for mutations that would lead to the production of GATA-1s.

Figure III.6 shows an agarose gel electrophoresis analysis of the DNA fragment amplified from the formalin-fixed liver tissue of the HF case and a positive control (human genomic DNA from unfixed tissue) using primers specific for GATA-1 exon 2. Panel B of Figure III.6 shows a portion of the electropherogram obtained by sequencing GATA-1 exon 2 in the DS case. The amplified product of GATA1 exon 2 was the correct length, with a wild type sequence that showed no signs of mutation.
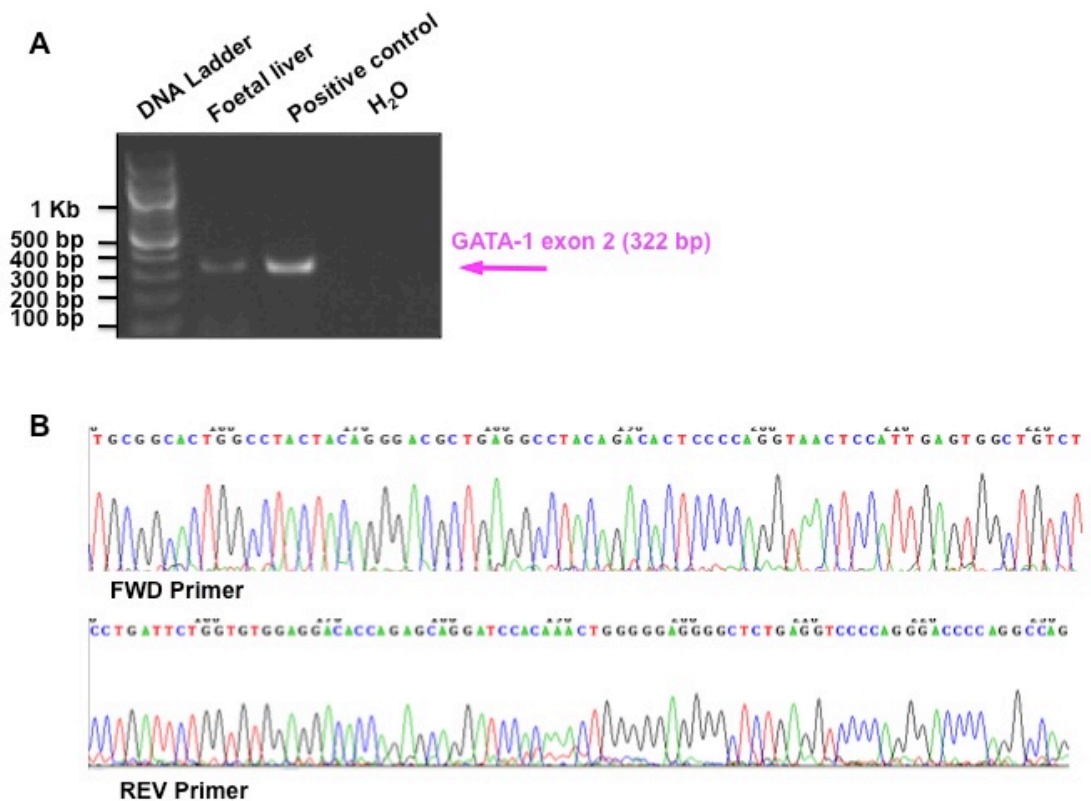
Fig. III.6. GATA-1 sequencing analysis performed on gDNA extracted from foetal liver archived material. Panel **A** shows agarose gel electrophoresis of DNA fragments amplified with primers for GATA-1 exon 2. PCR was performed on fixed tissue from the foetal liver of a DS preterm with severe hydrops foetalis and on a human genomic DNA control. Panel **B** shows electropherogram of the sequencing analysis performed on the gDNA from the case with both the forward and the reverse primer used for the ampification of GATA-1 exon 2. No mutations in GATA-1 were detected in gDNA from the DS foetal liver.

These data suggest that hyperproliferation of megakaryocytic cells can occur in DS foetal liver in the absence of GATA-1 mutations. The hyperproliferation described in this case is distinct from a typical TMD, because it is not associated with GATA-1 mutations and the proliferative cells appear to have a more mature phenotype. Nevertheless, it is an intriguing possibility that unknown events different from GATA-1 mutations (likely related to the gene dosage imbalance caused by trisomy 21) may initiate an abnormal megakaryocytic hyperproliferation. This shift toward megakaryopoiesis in a fraction of DS foetuses may increase the risk of acquisition of GATA1

mutations, subsequently providing the mutated clone with a proliferative advantage, which ultimately causes TMD.

III.2. Gene expression study in foetal liver samples

The foetal liver (FL) is the major haematopoietic organ during embryonic development, while in adults haematopoiesis occurs exclusively in the bone marrow. A study from Li et al. has hypothesized that the foetal liver represents the *milieu* where a transient megakaryocytic progenitor that expresses GATA-1s hyperproliferates, explaining why DS-TMD and AMKL (both characterized by the exclusive presence of GATA-1s) occur in a restricted time frame (Li et al., 2005).

Two articles from independent groups have also recently compared foetal liver haematopoiesis in DS material with euploid controls matched for gestational age and sex. Both groups observed an increased frequency of megakaryocyte-erythroid progenitors in second trimester samples, leading to the hypothesis that trisomy 21, independently from GATA-1 mutations, profoundly disturbs FL haematopoiesis creating an imbalance in lineage commitment that predisposes DS foetal liver cells for the acquisition of GATA-1 mutations (Chou et al., 2008; Tunstall-Pedoe et al., 2008).

In previous chapters, using a transchromosomic model of DS, I have presented evidence that: 1) the presence of an extra copy of trisomy 21 allows GATA-1s to exert a hyperproliferative effect on the megakaryocytic lineage (chapter I); 2) embryonic haematopoiesis is influenced by trisomy 21 in DS, and RUNX-1, which is encoded on HSA21, plays a role in this phenotype (chapter II).

To gain insights into the molecular changes caused by trisomy 21 during foetal liver haematopoiesis, I performed a qRT-PCR study to quantify the level of

expression of a panel of genes associated with haematopoiesis in DS primary samples. Six DS livers were compared to euploid controls matched for sex and gestational age. Samples were part of two separate collections of frozen tissues from therapeutically terminated DS or euploid pregnancies, and they were all from the second trimester. Table 3.2 shows characteristics of the samples used in this analysis.

DS sample		Matched euploid control	
R-595300M	M, 18 Wks	MRC 11253	M, 20.4 Wks
M-B59593M	M, N.A.	MRC 1113	M, 21.4 Wks
I-P9437M	M, 20 Wks	MRC 1114	M, 21.1 Wks
C-9599F	F, 20 Wks	MRC 11097	F, 20 Wks
P-696400M	M, 20 Wks	MRC 11252	M, 20.4 Wks
N-P0047 M	M, 18 Wks	MRC 11259	M, 20.4 Wks

Table 3.2. Characteristics of primary samples used in this study. Table indicates patient identification number, sex and gestational age. Matched samples are reported on the same line. N.A. indicates that data for that sample is not available. M stands for male, F for female, Wks for weeks.

Initially, all samples were screened for the presence of mutations in GATA-1 (data not shown). All DS-foetal livers were wild type for GATA-1, which allowed for the investigation of the effect of trisomy 21 (without overt mutations) on foetal haematopoiesis. Markers analysed in this study included CD41 and GATA-1, RUNX-1, GATA-2 and c-KIT. Besides being a master player directing the onset and function of haematopoietic stem cells, GATA-2 is a key regulator of the mekagaryocyte lineage (Huang et al., 2009b) and is up-regulated in blast cells from DS-AMKL (Bourquin et al., 2006). GATA-1 and CD41 were analysed for their specific role in megakaryopoiesis.
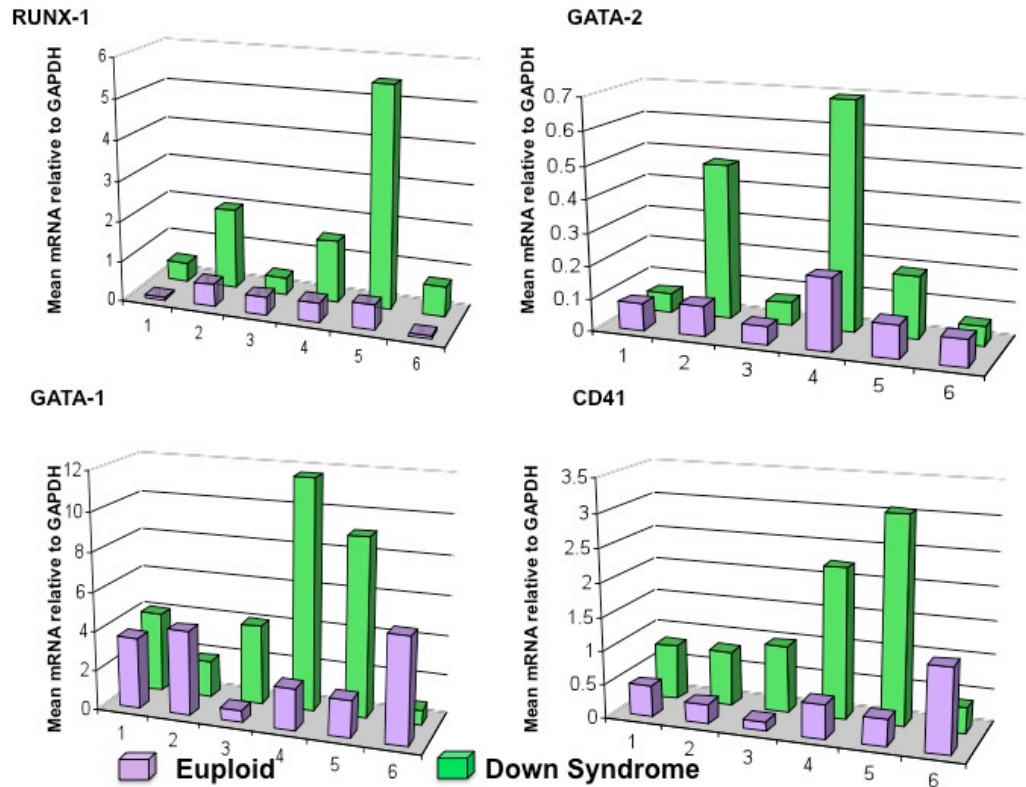
Fig. III.7. Analysis of mRNA levels of haematopoietic markers in foetal livers from DS and euploid controls. Figure shows expression levels of markers associated with megakaryopoiesis in foetal livers from DS and matched euploid controls, as detected by qRT-PCR analysis. Data are presented as average levels of mRNA normalised to GAPDH in duplicate samples.

RUNX-1 levels were assessed because of its function in establishment of definitive haematopoiesis and in megakaryopoiesis, but also because of its presence on HSA21, whereas c-KIT was studied as an indicator of early haematopoietic progenitors in FL (Ogawa et al., 1993; Teyssier-Le Discorde et al., 1999). Figure III.7 and III.8 show the results of the analysis. Data are presented as mean mRNA values of duplicate samples, normalised to the housekeeping gene GAPDH. Each DS sample is shown with its matched euploid control.
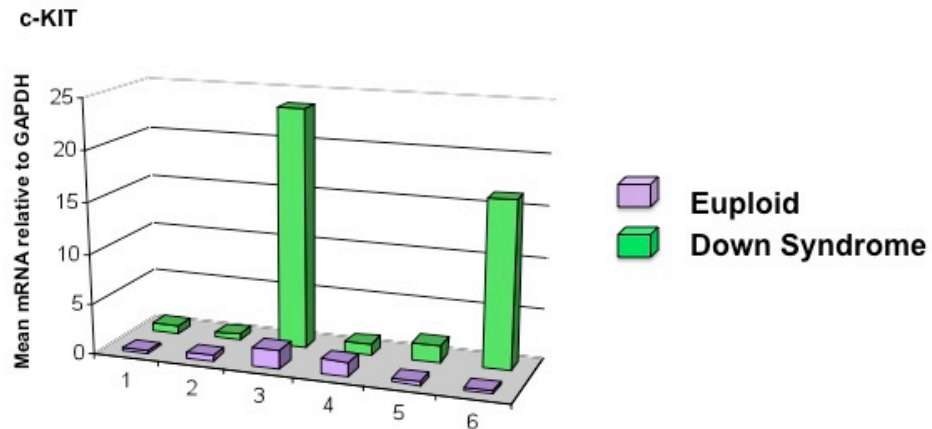
Fig. III.8. Analysis of mRNA levels of c-KIT in foetal livers from DS and euploid controls. Figure shows expression levels of c-KIT in foetal livers from DS and matched euploid controls. Data are presented as average levels of mRNA normalised to GAPDH in duplicate samples.

Differences between DS and normal foetal liver samples with respect to RUNX-1, GATA-1, GATA-2, CD41 and c-KIT expression were analysed with the Wilcoxon signed-rank test. The correlation between markers was tested by the linear regression test (Pearson correlation coefficient) performed on ratios of levels of mRNA for a given gene in DS to normal controls. All p values were two-tailed.

Tunstall Pedoe et al. and Chou et al. reported contradictory results regarding levels of expression of RUNX-1 in total RNA extracted from DS foetal livers (Tunstall-Pedoe et al., 2008; Chou et al., 2008). Bourquin et al. observed that RUNX-1 levels are not augmented in DS-AMKL blasts compared to non-DS AMKL leukaemic cells (Bourquin et al., 2006). Given the presence of a third copy of this gene on the supernumerary HSA21, I predicted an increased level of RUNX-1 mRNA in specific DS tissues, such as the foetal liver. Wilcoxon signed-rank tests performed on the six matched pairs of foetal livers included in this analysis showed that RUNX-1 mRNA levels are higher in the DS foetal livers than in the euploid controls (p value = 0.01). There was no statistically

significant difference in the levels of GATA-1, GATA-2 and CD41 between the two sets of samples. However, a significant increase in levels of mRNA for c-KIT was observed in DS samples compared to the controls (p value = 0.04).

Analysis of the correlation between levels of the markers revealed a positive correlation (linear relation) between GATA-1 levels and CD41 levels (r=0.8; p value=0.02). Indeed, GATA-1 has been previously shown to regulate the expression of CD41 through direct binding to its promoter (Gaines et al., 2000). No significant correlations were observed among the other markers. It is worth noting that levels of the markers analysed were heterogeneous, making it difficult to reach statistical significance even when a trend was apparent comparing matched data (see levels of RUNX-1 and GATA-2, which were increased in at least the same three DS samples compared to matched euploid controls). This might be due to individual characteristics of the samples (e.g., age, sex of the samples), but could also be due to differences in the integrity of the samples and quality of archived material.

Several conclusions can be drawn from these data. First, RUNX-1 is overexpressed in foetal liver of DS, supporting the hypothesis that early haematopoietic development in DS is influenced by the increased gene dosage of RUNX-1. Furthermore, because of the concomitant increase of CD41 and GATA-1 in some of the samples, it is possible that (at least in some DS foetuses) an increased number of megakaryocytes might present in trisomic foetal livers. The increased levels of c-KIT would suggest that immature haematopoietic precursors are more numerous in DS foetal livers than in euploid controls. This is further supported by the data from Tunstall-Pedoe et al., who, apart from describing a skewing of oligolineage progenitor numbers towards an increased number of MEPs, demonstrated that overall clonogenic ability of FL CD34^{+} from DS foetal liver is increased compared to

euploid controls, and that the replating ability of CFU-GEMM (the more immature type of colonies) is augmented in DS samples.

III.3. Final remarks

Results presented in this chapter highlight the importance of utilising primary samples to validate data obtained from *in vitro* models of DS. Despite the fact that valuable insights could be drawn from the transchromosomic model, there are conspicuous differences between mouse models of DS and the human disease. Being able to integrate information from two complementary approaches provides a more detailed view for some of the phenotypes associated with DS, and gives the possibility to define a more specific role for genes on HSA21 in causing these phenotypes.

Despite the limited conclusions that can be drawn from just one case, the first part of this chapter shows that there can be an abnormal proliferation of trisomic megakaryocytes in absence of GATA-1 mutations. A more extensive analysis of similar cases may reveal that this event is more frequent in DS foetal livers than previously appreciated, supporting the hypothesis that trisomy 21 creates the condition for GATA-1s to exert its oncogenic potential on the megakaryocytic lineage selectively in the *milieu* of the foetal liver.

Gene expression data revealed that RUNX-1 is overexpressed in DS foetal livers compared with matched euploid controls. The limited size of the samples analysed and the variability associated with primary samples are a caveat for this approach. However, given the role of RUNX-1 in both the generation of HSCs and the megakaryocytic lineage, it is intriguing to postulate that this gene might play a role in determining the haematopoietic phenotypes seen in DS. Integrating data presented here with results obtained

from other primary sample collections is likely to more specifically define a role

for RUNX-1 and other candidate genes on HSA21 in these phenotypes.

IV. Elucidating a role for JAK3 in the pathogenesis of DS-Leukaemia

IV.1. Janus Kinases (JAKs) and haematological malignancies

The four mammalian Janus kinase (JAK) family members JAK1, JAK2, JAK3 and TYK2 are non-receptor protein tyrosine kinases that are crucial for cytokine receptor signaling in blood formation and immune response. Members of this family share a highly conserved structure; JAKs have seven defined regions of homology, called JAK homology (JH) domains (JH1-7). The carboxyl terminus contains the kinase and pseudokinase domains, termed JH1 and JH2, respectively. The JH1 domain contains all the typical features of a catalytic tyrosine kinase. In contrast, the JH2 pseudokinase domain, also called kinase-like domain, is highly homologous to the kinase domain but lacks characteristic residues of active tyrosine kinases, and it is therefore catalytically inactive. JH3 and JH4 domains share homology with Src-homology-2 (SH2) domains. Functional studies have demonstrated that the SH2 domain in JAKs have scaffolding rather than signaling roles. The JH5-JH7 (N-terminal region) domains contain a predicted FERM (band 4.1, ezrin, radixin and moesin)-like motif, which is supposed to play a role in mediating the interaction between JAKs and their cytokine receptors (Vainchenker et al., 2008).

A single recurrent mutation in the JAK2 tyrosine kinase (JAK2V617F) has been identified in >90% of patients with polycythemia vera (PV) and in a significant proportion of patients with essential thrombocythemia (ET) and primary myelofibrosis (PMF) (Levine et al., 2005; Baxter et al., 2005). Subsequent studies of JAK2V617F-negative myeloproliferative disorders have identified mutations in JAK2 exon 12, also resulting in constitutive activation of

JAK2 (Scott et al., 2007). Recently, somatically acquired mutations clustering around the R683 residue in the pseudokinase domain of JAK2 have been described in approximately 20% of patients with Down's syndrome-associated acute lymphoblastic leukaemia, revealing a specific association between constitutional trisomy 21 and JAK2 mutations, which is similar to that of GATA-1 mutations with DS-AMKL (Bercovich et al., 2008).

Several somatic gain-of-function mutations in JAK1 have been reported in as much as 18% of patients with adult T-ALL (Flex et al., 2008). Three of the reported mutations induced IL-3 independence in Ba/F3 cells and IL-9 independent resistance to dexamethasone-induced apoptosis in T-cell lymphoma cell lines. Of these mutations, the one with the strongest activating potential is the A634D mutation in the pseudokinase domain of JAK1, at a position predicted to affect the inhibition exerted by the pseudokinase domain on the kinase domain.

JAK3 is the only JAK kinase that binds to γ_c, the common signaling subunit of IL-2, IL-4, IL-7, IL-9, IL-15 and IL-21 receptor complexes. Most cases of human severe combined immunodeficiency (SCID) are caused by inherited loss-of-function mutations in γ_c (X-SCID), JAK3 or the IL-7-receptor genes (Candotti et al., 1997).

Patients with JAK3 or γ_c mutations typically display the same phenotype, which is the absence of T and NK cells and impaired function of B cells. Mutations located in each of the domains of JAK3 have been identified. No hot spots have been reported; however, the majority of JAK-3 loss-of-function mutations associated with SCID are located in the JH2 pseudokinase domain (O'Shea et al., 2004).

In 2006, Walters et al. reported three acquired mutations in JAK3 in samples from both DS and non-DS AMKL (Walters et al., 2006). Each of the described

mutations constitutively activates JAK3 and confers cytokine-independent growth properties to the Ba/F3 cells, and causes a disease resembling human AMKL once transplanted into recipient mice. These data suggest that activating mutations of JAK3 are an important event in the pathogenesis of AMKL. Selective chemical inhibitors of JAK3, already in clinical use as immunosuppressives (Changelian et al., 2003) have therefore been proposed as a therapeutic concept for AMKL (Walters et al., 2006).

IV.2. Performing a screen for JAK3 mutations in DS-TMD and AMKL samples

Trisomy 21 and acquired mutations in GATA-1, an erythroid-megakaryocyte transcription factor encoded on chromosome X, have been reported to coexist in blast cells in both DS-TMD and AMKL (Wechsler et al., 2002; Groet et al., 2003). Despite the presence of these two genetic lesions, which are common to both forms of DS-leukaemia, factors that predispose one-third of the TMD patients to subsequently develop AMKL, and additional molecular events that are necessary for progression from TMD to AMKL, remain largely unknown (Hitzler and Zipursky, 2005; Muntean et al., 2006).

In order to explore whether mutations of JAK3 can be considered a pathogenic event in the progression from TMD to AMKL, I performed a mutational analysis of JAK3 on a collection of samples from DS-AMKL and DS-TMD with a known GATA-1 mutational status. Results from this analysis are presented in this chapter.

III.1.1. Describing novel JAK3 mutations in DS-TMD and AMKL

JAK-3 mutational analysis was performed on surplus clinical materials from DS-TMD and AMKL received from specialized centers in Europe. For the vast

majority of samples, gDNA and RNA had been previously extracted for assessment of mutational status of GATA-1. Table 3.3 indicates characteristics of patients included in this study (last column lists the type of GATA-1 mutation observed in clinical samples) and nature of the material (gDNA or CDNA) used for the analysis.

Patient	Material	Blasts percentage	GATA-1 mutations
DS-TL (TMD1)	cDNA	85	270-271ins7bp
DS-TL (TMD1)	gDNA	85	270-271ins7bp
DS-TL (TMD2)	gDNA	50	259dup34bp,305dup4bp, 307ins8bp
DS-TL (TMD3)	cDNA	60	161C>T, STOP
DS-TL (TMD6)	cDNA	ND	Splice Δ-exon2
DS-TL (TMD8)	cDNA	50	344-345ins2bp
DS-TL (TMD10)	cDNA	98	245-266del22bp
DS-TL (TMD11)	cDNA	78	263delG
DS-TL (TMD15)	gDNA	ND	259dup34bp
DS-AML-M7 (AMKL1)	cDNA	50	270-271ins7bp
DS-AML-M7 (AMKL4)	cDNA	40	Splice Δ-exon2
DS-AML-M7 (AMKL5)	cDNA	95	251delT
DS-AML-M7 (AMKL7)	cDNA	60	Splice -Δexon2
DS-AML-M7 (AMKL8)	cDNA	>50	197G>T, STOP
DS-AML-M7 (AMKL11)	cDNA	50	262-263ins7bp
DS-AML-M7 (AMKL12)	gDNA	20	285-286ins19bp
DS-AML-M7 (AMKL13)	gDNA	ND	298-299ins5bp
DS-AML-M7 (AMKL14)	gDNA	ND	WT

Table 3.3. Patients table modified from De Vita et al. *(BJH, 2007).* Table lists the clinical samples used in this study. Materials used for JAK3 mutational analysis were total cDNA or genomic DNA (gDNA). GATA-1 mutation status of the samples included in the study is shown. Splice Δ-exon 2 indicates that only a shorter product of GATA-1 was detected by RT-PCR, resulting from a splicing event skipping the entire exon 2. ND indicates not determined; WT, wild type; ins, insertion; dup, duplication; del, deletion.

The sequence of JAK3 in samples from 8 DS-TMD and 8 DS-AMKL patients was analysed. For 3 TMD patients and 2 AMKL patients, genomic DNA was available. In these samples all 24 exons of JAK3 were sequenced, and no mutations were detected. The remaining patient samples (11) were available as cDNA.

In these samples, the entire coding sequence of JAK3 was studied by using 5 pairs of overlapping primers. Seven out of eleven samples in this subset

presented mutations in the JAK3 transcript. Figure IV.1 shows different JAK3 mutations detected in this study and their consequences on the JAK3 protein structure. Interestingly, 3 patients (TMD3, TMD11 and AMKL4) showed a large (592 bp) deletion eliminating the C-terminal 192 amino acids (exons 20-24). This region includes the JH1 kinase domain, which is essential for the kinase function of JAK3. Mutations resulting in a premature stop codon in exon 21 were shown to completely abolish JAK3 kinase activity in a patient with SCID (Mella et al., 2001); even smaller deletions in the JH1 domain have been reported to abolish the kinase activity of the JAK3 protein (Lai et al., 1995).

Two of the patients (TMD8 and AMKL1) showed alternatively spliced forms of JAK3, eliminating a large portion of the FERM region from the protein. The predicted start codon for the alternatively spliced cDNAs in these patients is at amino acid (aa) position 235 in exon 6 of JAK3. The alternatively spliced product was absent from the remission sample from patient AMKL-1, indicating that this change was specific for the leukaemic clone. The large deletion and the splicing variants were confirmed by cloning and sequencing of the RT-PCR products (the chromatogram in Figure IV.1 is derived from the cloned RT-PCR products for patients TMD8 and TMD11). One out of one clone from patient TMD8 showed the alternative splicing, and one out of four clones from patient TMD11 showed the large deletion. In chromatograms from sequences of cDNA synthesized from uncloned samples, the peaks of the alternatively spliced and of the deleted product were approximately half the height of the wild-type sequence, reflecting the proportion of blasts in the total population.
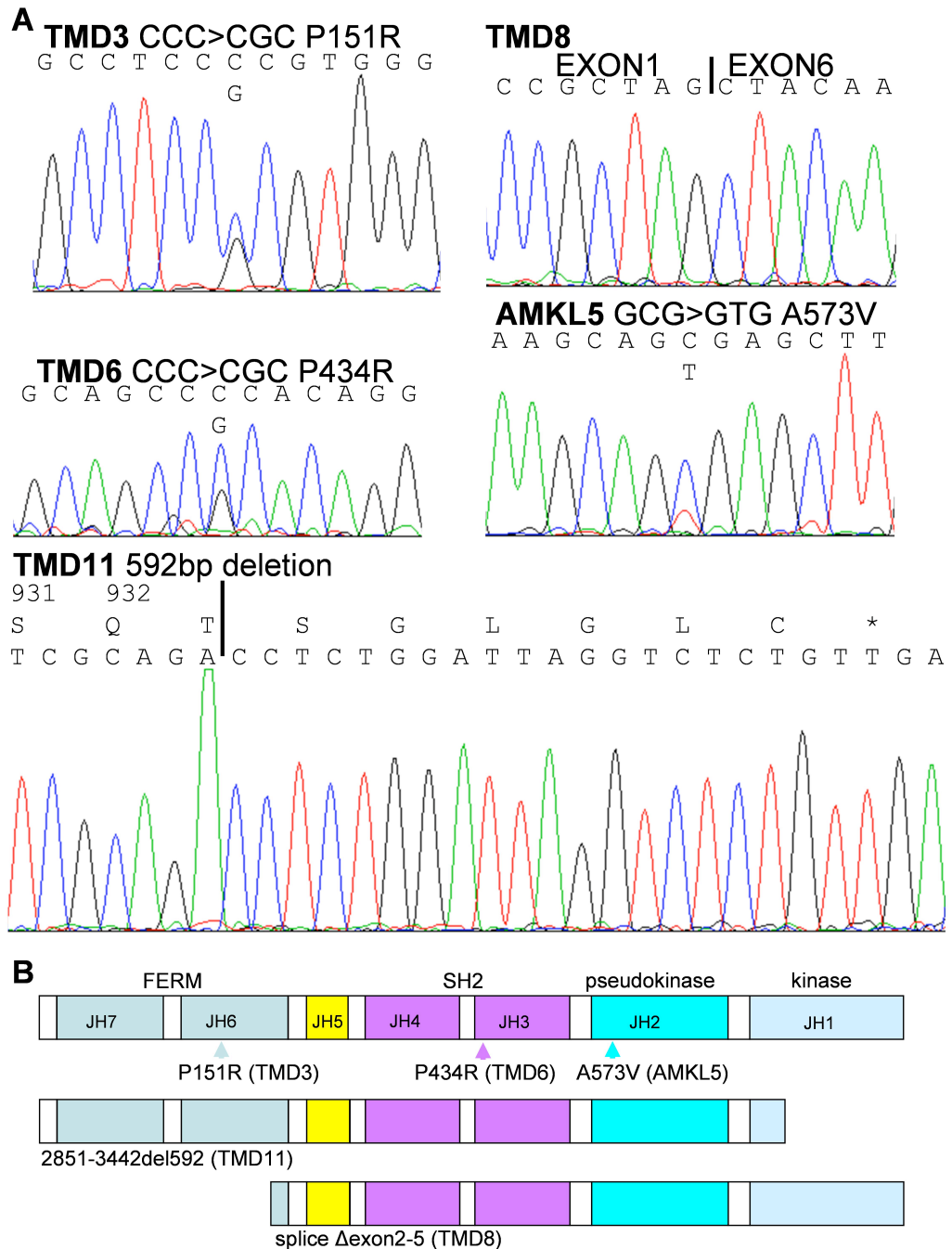
Fig. IV.1. JAK3 mutations in DS-TMD and DS-AMKL samples. Panel **A** shows electropherograms revealing JAK3 mutations in Down syndrome patients with transient myeloproliferative disorder (TMD) and acute megakaryoblastic leukaemia (AMKL). Patients TMD3, TMD6 and AMKL5 showed single nucleotide substitutions in presentation sample cDNA. In TMD8, alternative splicing removes exons 2-5 from the transcript, possibly removing the 234 N-terminal amino acids. In TMD11 a 592 bp deletion removes the C-terminal 192 amino acids. Chromatograms of sequences from patients TMD8 and TMD11 are derived from cloned RT-PCR products (sequencing analysis on cDNA from presentation samples shows wild-type JAK3 sequence in addition to the mutation). Panel **B** shows predicted consequences of the mutations on the structural organization of the JAK3 protein. Boxes represent the 7 domains (JH1-JH7) of the JAK3 protein, arrowheads point to single nucleotide substitutions, whereas middle and lower diagrams show the consequences on the protein structure of the C-terminus 592 aa deletion and of the alternative splicing of exon 2-5.

Apart from containing a 592 amino acid deletion in the C-terminus, patient TMD3 had a single nucleotide substitution (P151R) in the FERM domain that had been previously reported among the loss-of-function inherited mutations in patients with SCID (O'Shea et al., 2004). It was impossible to establish whether this patient was a compound heterozygote for the two mutations or had two independent mutations on the same chromosome.

Patient	Material	JAK3 mutations	Outcome
TMD1	cDNA	WT	CR (>5 yrs)
TMD1	gDNA	WT	CR (>5 yrs)
TMD2	gDNA	WT	CR (>10 yrs)
TMD3	cDNA	P151R, 2851-3442del592	CR (>10 yrs)
TMD6	cDNA	P434R	CR (>10 yrs)
TMD8	cDNA	Splice exon2-5	NA
TMD10	cDNA	WT	Died with TMD
TMD11	cDNA	2851-3442del592	CR (>4 yrs)
TMD15	gDNA	WT	NA
AMKL-1	cDNA	Splice exon2-5	CR (>7 yrs)
AMKL-4	cDNA	2851-3442del592	Died during therapy
AMKL-5	cDNA	A573V	Died during therapy
AMKL-7	cDNA	WT	Died during therapy
AMKL-8	cDNA	WT	NA
AMKL-11	cDNA	WT	NA
AMKL-12	gDNA	WT	NA
AMKL-13	gDNA	WT	NA
AMKL-14	gDNA	WT	NA

Table 3.4. Table indicating JAK3 mutations and clinical outcome of patients included in this study. Table indicates patients, nature of the material used for JAK3 mutational analysis and clinical outcome of analysed patients. NA indicates not available; CR, complete remission (in brackets number of years); WT, wild type; del, deletion.

Patient TMD6 contained a P434R substitution in the SH2 domain. The function of this domain is not completely understood, and binding partners have not yet been identified. Patient AMKL5 showed an A573V substitution, directly adjacent to A572V, one of the mutations described from Walters et al., as an activating (gain-of-function) mutation (Walters et al., 2006).

Table 3.4 summarizes the mutations in JAK3 detected in this study and the

clinical outcome of patients analysed.

IV.3. Final remarks

IV.3.1. A revised role for JAK3 mutations in the pathogenesis of DS-TMD and AMKL

According to the "multistep" view of leukaemogenesis, acute leukaemias arise from the cooperation between one class of mutations that interferes with differentiation, such as loss-of-function mutations in haematopoietic transcription factors, and a second class of mutations that confers a proliferative advantage to cells, such as activating mutations in tyrosine kinases (Gilliland and Tallman, 2002).

Walters et al. described gain-of-function JAK3 mutations in AMKL and demonstrated that these mutations have oncogenic potential both *in vitro* and *in vivo.* These findings would argue in favour of a cooperating effect of JAK3 activating mutations with GATA-1 mutations in the context of DS-leukaemogenesis. Walters et al. also suggested the use of a recently developed selective small molecule inhibitor of JAK3 as a therapeutic option for AMKL (Walters et al., 2006).

Data presented in this chapter reveal a more complex spectrum of JAK3 mutations (gain-of-function as well as loss-of-function) associated with both DS-TMD and AMKL.

The following conclusions can be drawn from experimental evidence here presented. First, because mutations of JAK3 are present in both DS-TMD and DS-AMKL, they are unlikely to constitute the "third hit" responsible for progression of DS-TMD to DS-AMKL.

Functional consequences of the described mutations have not been assessed. However, the nature of some of them (big deletions or alternative splicing events altering the architecture of the JAK3 protein) suggests that they would

result in a loss-of-function phenotype, which doesn't support their role as cooperating events promoting proliferation of a clone, which has already acquired mutations causing a block in differentiation. These considerations argue against a therapeutic role for JAK3 inhibition in DS leukaemia.

Finally, since 3/3 DS-TMD patients for whom relevant data were available (TMD3, TMD6 and TMD11) are all in spontaneous complete remission (for >10, >10 and >4 years, respectively), past the age typical for progression to AMKL, JAK3 mutations do not seem to constitute a predictive factor for the progression from TMD to AMKL.

IV.3.2. Further studies on the role of activating mutations of tyrosine kinases in DS-leukaemia

After or at the same time as data presented in this chapter were published, further studies reported contradictory evidence for a role for JAK3 in the pathogenesis of DS-TMD and AMKL. Kiyoi et al. described two additional AMKL patients (one with DS and one without DS) with mutations in the same domain of JAK3 (JH2 pseudokinase domain) shown to harbour activating mutations. They also reported a single DS-TMD patient with a mutation in a different JAK3 domain, without examining the functional consequences of this mutation.

Norton et al. screened a collection of 16 DS-AMKL and TMD samples and could not detect any mutation in JAK3. However, these results might be due to technical differences in the way this study was conducted (the authors screened only genomic DNA using a denaturing high-performance liquid chromatography platform for their study) (Norton et al., 2007). JAK2 and c-mpl were also analysed in the same set of samples, with no additional mutations found.

Sato et al. described two additional JAK3 point mutations in the DS-AMKL cell line MGS. One mutation was in the pseudokinase domain and the other in the SH2 domain of JAK3. The authors showed that both mutations were on the same allele in MGS and tested the transforming potential of these mutations individually and in combination using the Ba/F3 assay, concluding that both mutations were gain-of-function and that their transforming potential was higher when they were both present (Sato et al., 2008). The authors of this study also identified a novel point mutation in a TMD patient. This mutation was in the FERM domain of JAK3 and was shown to have a weaker transforming potential than the two novel mutations identified in the AMKL cell line. In addition, the authors tested the effect of two novel JAK3 inhibitors (less toxic than the one proposed in (Changelian et al., 2003)) and reinforced the idea of a therapeutic inhibition of JAK3 in DS-TMD and AMKL patients. Based on these findings, the authors suggested a role for JAK3 mutations in the progression from TMD to AMKL; however they could not give substance to this hypothesis by analysing sequential samples from individual TMD and AMKL patients.

Lastly, Malinge et al. investigated the mutational status of the tyrosine kinases JAK2, JAK3, KIT, FLT-3 and MPL in DS and non-DS AMKL and in two TMD samples (Malinge et al., 2008). The authors reported a JAK-3 activating mutation in one DS-AMKL sample and the presence of the V617F JAK2 mutation in another DS-AMKL, concluding that (despite the small size of samples analysed) mutations in tyrosine kinases might contribute to DS-leukaemogenesis. Interestingly, examination of a unique non-DS AMKL patient with a FLT3 mutation showed that he harboured an additional chromosome 21 and a mutated GATA-1 gene, further strengthening the idea of an oncogenic cooperation between tyrosine kinases signaling and GATA1s in the trisomic context. Authors of this study also identified a novel mutation of

the MPL cytokine receptor (MPLT487A) in a non–DS-AMKL patient, and proposed that it might be specific for megakaryoblastic diseases, since it was not present in 30 other AML samples. Study of the MPLT487A mutant showed that this mutation was able to induce a myeloproliferative-like disease (MPD) in mice, underscoring a link between MPD and AMKL outside of the trisomic context.

4. General discussion

DS is a complex condition with variable degrees of penetrance of different phenotypes. This broad spectrum of phenotypes is caused by the presence of a third copy of the entire human chromosome 21. Not all of the more than 400 genes on HSA21 contribute to phenotypes of DS, therefore a definition of the trisomic increase compared to natural variation in expression levels in the euploid population, as well as a spatial and temporal map of expression of these genes are crucial in determining their role in specific pathogenic process associated with trisomy 21.

Although the incidence of solid tumours is strikingly reduced at every age in DS, the risk of developing all types of leukaemia is highly increased in the DS population compared to the euploid counterpart. This increase is most prominent in early childhood and is contributed by both lymphoid and myeloid leukaemias, but the mechanisms underlying this increased risk, or the HSA21 genes causing them, remain unknown. The incidence of ALL is approximately 20-fold higher in children with DS than in the euploid population. As for AML, the relative risk of developing a particular subtype, the FAB-M7 AML or acute megakaryoblastic leukaemia (AMKL), is estimated to be 500 times higher in children with DS than in the general population (Zipursky et al., 1992). Approximately 1/10 of DS newborns present in the first few weeks of life a transient form of megakaryocytic leukaemia (TMD), which in the vast majority of cases self-regresses. However, as many as 30% of the patients with TMD will develop within 4 years a full-blown AMKL, characterised by megakaryocytic blasts with the same morphological and immunophenotypical features of TMD. Both TMD and AMKL present with a constitutional trisomy 21 and acquired mutations of GATA-1 leading to the elimination of its full-length

form and to the exclusive production of GATA-1s, a partially functional form of this crucial megakaryocytic-erythroid transcription factor encoded on the X chromosome. It is clear that both these events are needed for the leukaemogenic transformation, but the contribution of individual genes on HSA21 to the development of leukaemia in DS has not yet been defined.

In this study, an ES cell line generated by introducing an extra copy of a freely segregating HSA21 in the mouse euploid backgound was employed to assess developmental effects of trisomy 21 on the megakaryocytic lineage. The transchromosomic ES cells used in this study, namely 47-1, contain virtually all the genes on HSA21 and therefore represent the most comprehensive cellular model of DS so far generated. This system has been previously employed to model *in vitro* some of the other phenotypes associated with DS (Canzonetta et al., 2008; Mensah et al., 2007), however no data on the haematopoietic and megakaryocytic differentiation of trisomic ES cells are available to date.

The results presented in this thesis show that an efficient generation of MKs from ES cells could be carried out on both the euploid and trisomic cells. Megakaryocytes generated *in vitro* from trisomic cells did not show morphological or numerical abnormalities compared to the ones derived from the euploid control (Figure I.2 and I.3). On a molecular level, megakaryocytes derived from the two populations of ES cells expressed mRNA of appropriate genes associated with megakaryopoiesis and down-regulated the levels of at least one pluripotency factor (OCT-4) in a similar fashion (Figure I.4). Canzonetta et al. have recently demonstrated that trisomy 21 causes an unbalance in the regulatory network maintaining pluripotency in undifferentiated ES cells by the effect of DYRK1A (a gene on HSA21) on NRSF/REST (a TF which is a master regulator of neurogenesis and has recently been implicated in the circuitry of pluripotency/differentiation of ES

cells). Levels of NANOG and SOX-2 are sensitive to the gene dose effect of DYRK1A in transchromosomic ES cells, however levels of OCT-4 are unaffected. Therefore OCT-4 down-regulation was chosen as a further parameter to measure the efficiency of the megakaryocyte differentiation protocol utilized in my experiments.

An interesting finding of my study was that during megakaryocytic differentiation, transchromosomic ES cells showed a 3 fold higher transcript level of GATA-1 than the euploid (D3) control (Figure I.6). In yeast, it has been demonstrated that high level of transcription of a gene can trigger the acquisition of spontaneous mutations (Datta and Jinks-Robertson, 1995). It is intriguing to speculate that the presence of one or more genes on HSA21 might drive an abnormal transcription of GATA-1 that increases the chance of acquiring mutations in GATA-1. Alternatively, augmented levels of GATA-1 might be responsible for, or a reflection of, an increased commitment of haematopoietic precursors towards the megakaryocytic lineage. Either one of these possible explanation for this phenotype (increased GATA-1 mRNA levels per cell, or higher number of GATA-1s expressing cells) could be a predisposing condition for a significantly increased chance of occurrence of GATA-1 mutations in DS.

When I tested the clonogenic potential of trisomic megakaryocytes, I did not observe any numerical difference compared to the euploid cells, although I noticed a striking tendence of these cells to form macroscopic colonies (larger than 50,000 pp^2) containing more undifferentiated cells (Figure I.7 and I.8).

Macroscopic colonies formed by foetal liver progenitors, or ES cells, expressing GATA-1s have been previously reported as a proof of the hyperproliferative potential of the truncated form of GATA-1 (Li et al., 2005). In my study, the hyperproliferative tendency of megakaryocytes derived from transchromosomic ES cells at late stages of the differentiation process was

not due to acquired mutations of GATA-1 (Figure 1.9), but was instead attributable to the trisomy 21. It might be argued that this phenotype would be more robust if the number, rather than the morphology, of the megakaryocytic colonies formed by an equal number of progenitors was augmented by the presence of a supernumerary chromosome 21. In a similar type of assay (Figure I.14), ectopic expression of GATA-1s in trisomic cells indeed significantly augmented the number of megakaryocytic colonies compared to the empty vector, whereas this difference was not significant when comparing euploid cells transfected with GATA-1s and with the control vector.

Taken together, these data suggest that trisomy 21 is a condition, which can *per se* influence the properties of the megakaryocytic lineage, and exacerbates the hyperproliferative effect of GATA-1s on the megakaryocytic lineage. In order to confer a significant growth advantage to megakaryocytes, GATA-1s, which also influences to less extent the euploid cells, requires the presence of a preexisting predisposing background, which is provided by trisomy 21.

Data presented in this thesis support a paradigm shift in thinking about DS-TMD and AMKL. The "classical view" by Li et al. postulated that GATA-1 mutation occurs randomly at a constant rate even in disomy, conferring little or no proliferative advantage to euploid foetal liver progenitors. In the presence of trisomy 21, however, the pre-malignant clone carrying a mutation in GATA-1 would acquire a profound growth advantage, ultimately leading to TMD. In this thesis, I support the alternative hypothesis that trisomy 21 is a leukaemia-predisposing condition and suggest that abnormalities of the megakaryocytic compartment might precede and favour the acquisition of GATA-1 mutations necessary for the development of leukaemia in DS.

The case of hydrops foetalis with abnormal proliferation of the megakaryocytic lineage reported in chapter III provides a further *in vivo*-correlate for this view,

as a demonstration that trisomy 21 alone can cause hyperproliferation of the megakaryocytic lineage in DS. Furthermore, at least two independent studies published last year (Chou et al., 2008; Tunstall-Pedoe et al., 2008) suggested that trisomy 21 increases the number of MEPs in DS foetal livers. Moreover, at the time of writing this thesis, a report by Cabelof et al. reinforced the idea that trisomy is a condition that predisposes cells to acquire mutations in GATA-1 by postulating that increased oxidative stress and defective DNA repair are two independent mechanisms contributing to the acquisition of GATA-1 mutations in DS. Through analysis of foetal livers from DS aborted materials, the authors suggested that increased dosage of some genes on HSA21 (such as SOD1 and CBS) might cause increased DNA damage and a decrease in DNA repair ultimately leading to GATA-1 mutations (Cabelof et al., 2009).

On a more general note, results presented in the first part of this thesis also demonstrate that haematopoietic differentiation *in vitro* of transchromosomic ES cells is a viable approach to identify phenotypes caused by the presence of trisomy 21. Despite the trans-species nature of the system, this study confirms that human genes on HSA21 are expressed and exert an effect on appropriate cellular target in the transchromosomic model (Figure I.5), as suggested by the recent systematic study on regulation of human gene expression in a mouse context by (Wilson et al., 2008).

One of the major advantages of the tranchromosomic approach is that once *in vitro* phenotypes are described, they can be mapped to a candidate region, or even a single gene, on HSA21 combining the use of segmentally trisomic ES cells and human-specific RNAi silencing (Canzonetta et al., 2008). For the increased transcriptional levels of GATA-1 and the formation of macroscopic TPO-dependent colonies, these combined approaches are likely to identify a region responsible for these phenotypes. For the cooperation between GATA-1s and trisomy 21 during megakaryocytic differentation, a more appropriate

approach would be to retrovirally silence human genes on HSA21 by shRNA, overcoming the fact that the megakaryocytic differentiation protocol used for this set of experiments lasts longer than the effective time range of the siRNA silencing by oligonucleotide transfection.

Given its proven utility in addressing developmental disturbances caused by a supernumerary chromosome 21, the transchromosomic system was also employed in this study to test whether trisomy 21 would affect early mesodermal commitment and haematopoietic differentiation of the ES cells. One of the consequences of the perturbance of REST levels caused by the action of DYRK1A in transchromosomic ES cells is the premature and aberrant expression of differentiation-driving TFs of the mesoderm and the endoderm embryonic lineages (Canzonetta et al., 2008). Considering that haematopoietic cells originate from mesoderm during embryogenesis, it is intriguing to speculate that this early skewing of embryonic choices might be responsible for aberrant differentiation programs during mesodermal and haematopoietic commitment of trisomic ES cells. My study shows that although FLK-1 mRNA levels (indicative of the number of mesodermal progenitors during early stages of haematopoietic commitment) of the DS ES cells are not significantly different from the levels in the euploid control (Figure II.3), subsequent stages of the haematopoietic differentiation are profoundly affected by the presence of trisomy 21.

Transchromosomic ES cells displayed higher transcriptional levels of TIE-2, c-KIT and GATA-2 (Figure II.4). According to the most recent publications in the field, expression of these genes reflects two separate stages of the haematopoietic differentiation of ES cells, both present in the mesodermal colonies at day 5. According to recently published data, the co-expression of TIE-2 and c-KIT and absence of CD41 identifies the haemogenic endothelium stage, which corresponds to the formation of a specialized set of precursors of

endothelial origin capable of giving rise to HSCs (Lancrin et al., 2009), whereas GATA-2 influences the haematopoietic commitment of differentiating ES cells and is required for proliferation and survival of early HSCs (Lugus et al., 2007; Tsai and Orkin, 1997). One of the limitations of this study was that the transcriptional signature deregulated in trisomic ES cells was only partially confirmed by the identification of a population of individual cells expressing the above-mentioned markers. A CD41$^-$c-KIT$^+$ population was proven to be numerically bigger in the transchromosomic ES cells after five days of haematopoietic differentiation than in the euploid control (Figure II.5), however a simultaneous FACS staining for the other markers analyzed could not be performed for technical and logistical reasons. On the other hand, because the working hypothesis was to compare two different ES cell lines and to evaluate the effect of trisomy 21 on early stages of the development of the haematopoietic lineage, data presented in this study are sufficient to draw some valid conclusions.

If a supernumerary HSA21 affects molecular profiling of markers crucial to the ontogenesis of HSC, this should have some consequences on the number or functional ability of HSCs/immature haematopoietic progenitors. Using a limited dilution assay, I could demonstrate that the number of haematopoietic colonies derived from the DS ES cells was higher than from the control euploid cells (Figure II.6). Remarkably, adult Ts65Dn mice (a partially trisomic model of DS) display an increased LSK (lineage$^-$ Sca-1$^+$c-KIT$^+$) compartment in the bone marrow compared to the wild type littermates, indicating a deregulation of the haematopoietic stem cell pool (Kirsammer et al., 2007). When I assessed the functional capability of the trisomic haematopoietic progenitors using a colony forming assay, I didn't detect any abormalities in the ability of haematopoietic progenitors to form erythroid or myeloid colonies, showing that differentiation potential along different haematopoietic lineages

was preserved in the transchromosomic system. However the number of mixed colonies, indicative of the number of immature progenitors, was significanty augmented in the trisomic cells, possibly reflecting a deceleration in the speed of lineage commitment caused by trisomy 21 in multipotent haematopoietic progenitors (Figure II.8).

Next, harnessing the potential of the transchromosomic system, I aimed to identify which gene or region on HSA21 was responsible for the observed perturbance in the expression of markers driving haematopoietic ontogenesis from trisomic ES cells. Between all the genes on HSA21, RUNX-1 appeared one of the most appealing candidates because of its fundamental role in the establishment of definitive haematopoiesis (Okuda et al., 1996). Growing lines of evidence suggest that RUNX-1 is not required for the formation of the haemogenic endothelium, but is necessary for the haematopoietic specification from this specialized set of cells (Sakai et al., 2009; Lancrin et al., 2009). In agreement with these reports, my results exclude a role for an increased gene dosage of RUNX-1 in the augmented generation of haemogenic endothelial cells, but show that the presence of a third copy of RUNX-1 is necessary to influence GATA-2 levels, possibly exerting an overall effect on the number of haematopoietic progenitors generated by trisomic ES cells. These conclusions were based on the reduction to disomy of the gene in transchromosomic ES cells by means of the human-specific RNAi silencing and are corroborated by transcriptional data obtained in segmentally trisomic ES cells. The fact that the panel of transchromosomic ES cells used to map the transcriptional phenotype might contain other complex rearrangements cannot be ruled out at this stage, and leaves open the possibility that RUNX-1 might not be sufficient, or might not be the only contributor to this phenotype. Furthermore, it is possible to conclude that the tyrosine kinase DYRK1A (on HSA21) responsible for the original skewing of embryonic lineages through

regulation of levels of NRSF/REST (Canzonetta et al., 2008), does not affect the increased generation of the haemogenic endothelium in the transchromosomic system, as this phenomenon cannot be observed in the cell line 39-5, a segmental ES cell line which contains a third copy of this gene but harbours deletions affecting several other regions.

The overall effect of trisomy 21 on haematopoietic development is that there is an increased generation of multipotent haematopoietic progenitors. It could be argued that this unbalanced pool of precursors might constitute a "sensitized" target for acquisition of mutations (JAK-2, JAK-3, GATA-1 or other) responsible for leukaemic transformation of both lymphoid and myeloid lineages. Alternatively and/or additionally, abnormal expression of lineage-specific transcription factors driven by trisomy 21 further down the way (as shown for GATA-1) might influence lineage choices of this augmented pool of progenitors, with the consequence of a numerical increase of specific compartments that therefore become more prone to acquire further leukaemogenic hits.

Data generated in the transchromosomic system point towards the definition of a complex complement of *in vitro* phenotypes (attributable to the presence of an extra copy of HSA21), which might be independent or interrelated and synergistically cooperating. Individual phenotypes within this complex complement might be caused by the same or different genes/regions on HSA21. This thesis provides mapping data for at least two of these phenotypes, identifying at least two genes independently responsible for these two phenotypes.

Figure 4.1 emphasizes the novel phenotypes identified during haematopoietic differentiation of the transchromosomic ES cells and outlines the multi-faceted effects of trisomy 21 during this process. The novel phenotypes warrant a validation of their relevance *in vivo*, keeping in mind that their occurrence

might be variable and influenced by HSA21 genomic content and regulation of gene expression. For example, using primary foetal liver samples, I could confirm that RUNX-1 is overexpressed in DS tissues (that is compatible with its potential role as a player in determining the early haematopoietic stages-phenotype), but I could not demonstrate a significant increase in the mRNA levels of GATA-1 in these samples. This might be due to the limited size of samples analyzed, but also to discrepancies between the mouse and human situations. The top part of the Figure 4.1 shows that a combined effect of at least 3 trisomic genes from HSA21 could contribute to the stochastic process ultimately resulting in an increased cell number of the haematopoietic stem cell compartment. This increase has an *in vivo* correlate in an observation of the increased LSK (lineage$^-$Sca-1$^+$c-KIT$^+$) compartment in the bone marrow of Ts65Dn (partial DS model mice) compared to the wild type littermates (Kirsammer et al., 2007). The initial disturbance caused by trisomy of DYRK1A, via NRSF/REST pathway, increases the endodermal and mesodermal progenitor pools at the expense of neuroectodermal progenitor lineages (Canzonetta et al., 2008). This skewing is likely to cause an increase in the mesodermal lineage progenitors *in vivo*. My experiments, starting from the same number of mesodermal colonies, demonstrate a further effect that leads to the increase of cells with a molecular signature of haemogenic endothelium. My analysis of partially trisomic ES cells shows that this phenomenon cannot be attributed to either DYRK1A or RUNX1, and therefore must be caused by another (unknown) HSA21 gene present in a third copy. Synergistically with this, an increased commitment of haemogenic endothelial cells to functional HSCs is also shown in my experiments, demonstrating that trisomy of RUNX1 is necessary for this cellular phenotype.
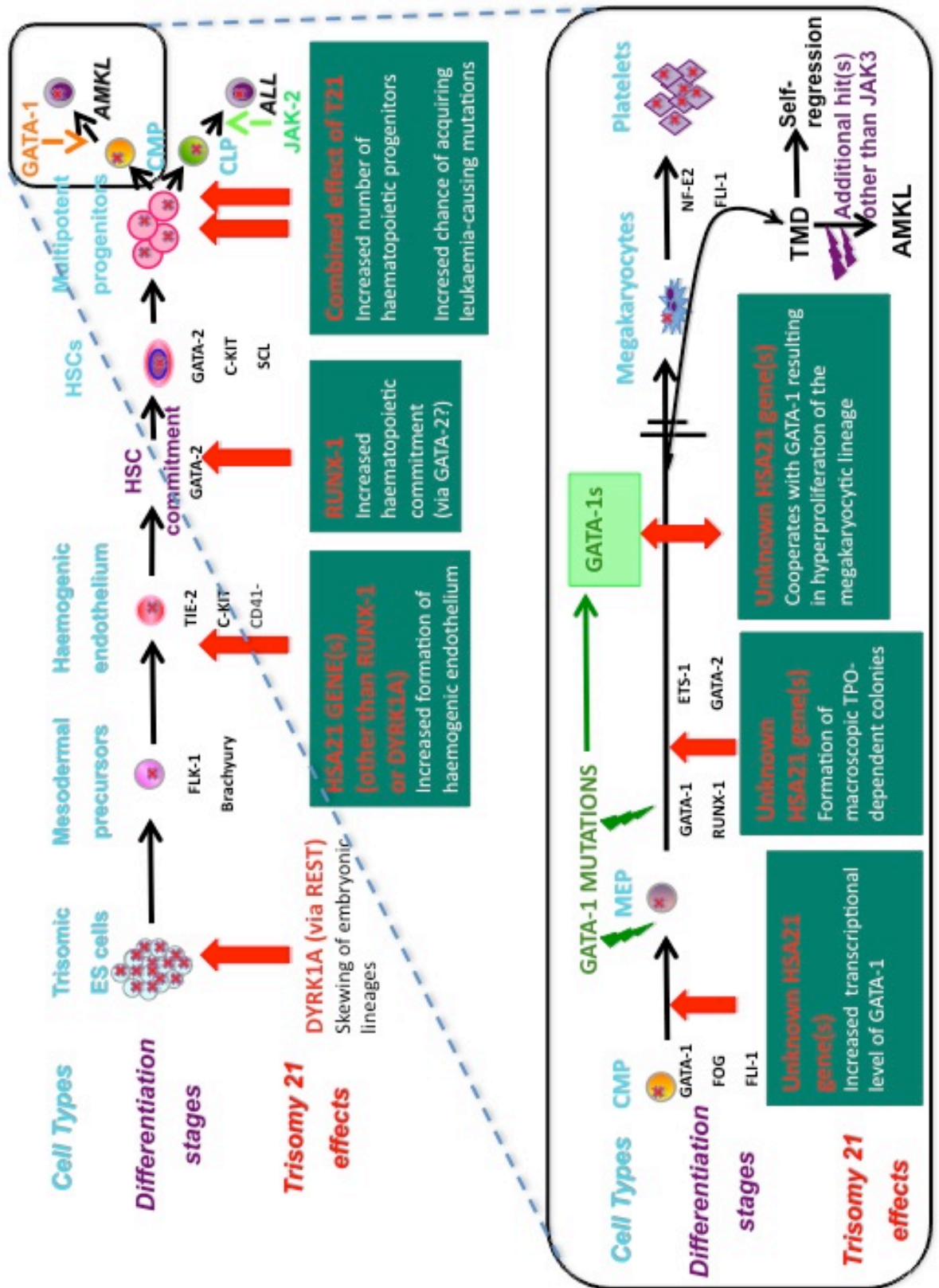
Fig. 4.1. Multiple effects of trisomy 21 on HSCs ontogenesis and on the megakaryocytic lineage

The combined action of all of these cellular phenotypes, not ruling out potential additional trisomy 21 effects, leads to an increased number of HSCs, that have an increased propensity to generate more immature multipotent precursors of haematopoietic lineages, as demonstrated by my limited dilution assay. I propose that all of these factors combined create an increased chance for the occurrence of additional leukaemogenic mutations, which could explain the increased risk of childhood leukaemias of all types in DS.

The bottom part of the figure IV.1 focuses on the megakaryocytic lineage, the cellular substrate of the DS-associated TMD and AMKL. At this level, my experiments uncover three separate additional cellular phenotypes that may be caused by the same or different HSA21 genes. I propose that these effects additionally create conditions of a high risk of acquisitions of the GATA1 mutations. When the nature of acquired mutations generates GATA1s, such cells acquire a further proliferative boost provided by yet another (unknown) trisomic HSA21 gene.

This last phenotype may be caused by the trisomy of the HSA21 gene ERG, as recently published data show (Salek-Ardakani et al., 2009). In the absence of GATA1 mutations, these combined effects on the megakaryocytic lineage lead to a hyperproliferative state, perhaps depending on the variant of the overall level of expression of the culprit HSA21 genes, and/or their interactors. The clinical outcome of such a hyperproliferative state can, in extreme cases, be very similar to the full-blown TMD, even in the absence of GATA1 mutations, as the case of the hydrops foetalis described in this thesis, and recently published data on DS foetal liver progenitors (Tunstall-Pedoe et al., 2008; Chou et al., 2008) would suggest.

Lastly, the final part of this work aimed to address a role for JAK-3 in the pathogenesis of DS megakaryocytic leukaemia. A puzzling aspect of this

disease is that, although in the vast majority of DS newborns with TMD the abnormal megakaryoblastic proliferation self-regresses, as many as 30% of these patients will develop a more aggressive acute leukaemia within a few years. It is clear that further unidentified hits are required for the progression of malignancy of the TMD clone that harbours an extra HSA21 and mutations in GATA-1. Previous data had suggested a role for JAK-3 in this progression (Walters et al., 2006), however analysis of primary samples reported in chapter IV and results from independent groups (Kiyoi et al., 2007) (Sato et al., 2008) generated simultaneously, or after this study, allow to exclude that the evolution of TMD to AMKL might be ascribable to activating mutations of this gene, because they are present in both DS-TMD and AMKL primary samples. Furthermore, this study identifies for the first time loss-of-function mutations of JAK3, demonstrating that the proposed therapeutic inhibition of this tyrosine kinase is not an effective approach for DS leukaemia.

In conclusion, this thesis provides a comprehensive analysis of the effects of trisomy 21 on haematopoietic development with a special focus on the megakaryocytic lineage, and identifies novel phenotypes that might be relevant to the occurrence of leukaemia while providing a viable approach to dissect the contribution of individual gene/regions of HSA21 in determining these phenotypes.

4.1. Summary of conclusions

- Megakaryocytes can be derived *in vitro* from transchromosomic ES cells at the same rate and with the same morphological properties as from the euploid control. However, during megakaryocytic differentiation, trisomy 21 drives an increased expression of the transcription factor GATA-1, which might predispose these cells to acquire mutations of the gene. Trisomy 21 alone, independently of mutations in GATA-1, is also responsible for the formation of macroscopic megakaryocytic colonies with a hyperproliferative tendency.

- Overexpression of GATA-1s exacerbates the hyperproliferative effect seen in megakaryocytic colonies derived from trisomic progenitors. Number of megakaryocytic colonies generated by transchromosomic progenitors expressing GATA-1s is significantly higher than the number generated from trisomic cells transduced with a control vector. Although this increase is also induced by GATA-1s in euploid progenitors, the difference between disomic cells transfected with GATA-1s or an empty vector is not significant.

- Ontogenesis of HSCs from mesodermal precursors is profoundly affected by trisomy 21. The presence of a supernumerary copy of HSA21 causes an increased formation of haemogenic endothelial cells and an increased commitment towards the haematopoietic lineage, with the overall consequence of the formation of more trisomic immature haematopoietic progenitors.

- A third copy of at least two independent genes on HSA21 is required for the increased generation of trisomic haematopoietic progenitors from mesodermal precursors. Trisomy of a gene other than RUNX-1 or DYRK1A is required for the increased formation of haemogenic endothelial cells, whereas trisomy of RUNX-1 is necessary for the regulation of the mRNA levels of GATA-2 (controlling the haematopoietic commitment), which ultimately results in the increased formation of trisomic immature haematopoietic progenitors.

- Mutations in JAK3 can occur in both DS-TMD and AMKL; therefore they are not required for the progression of malignancy of DS leukaemia. Furthermore, both gain- as well as loss-of-function mutations of JAK3 are present in primary DS samples, undermining a role for a therapeutic inhibition of JAK3 in this disease.

- A new paradigm for leukaemogenesis in DS is established in this thesis. Trisomy 21 influences haematopoiesis (in general) and the megakaryocytic lineage (in particular) at several levels. Three copies of more than one gene on HSA21 are required for these effects and the overall consequence of these independent or inter-related events is compatible with an increased predisposition to acquire further leukaemogenic mutations in all haematopoietic lineages.

5. References

Aardema, M.J., Crosby, L.L., Gibson, D.P., Kerckaert, G.A., and LeBoeuf, R.A. (1997). Aneuploidy and consistent structural chromosome changes associated with transformation of Syrian hamster embryo cells. Cancer Genet Cytogenet *96*, 140-150.

Agarwala, K.L., Ganesh, S., Suzuki, T., Akagi, T., Kaneko, K., Amano, K., Tsutsumi, Y., Yamaguchi, K., Hashikawa, T., and Yamakawa, K. (2001). Dscam is associated with axonal and dendritic features of neuronal cells. J Neurosci Res *66*, 337-346.

Ahmed, M., Sternberg, A., Hall, G., Thomas, A., Smith, O., O'Marcaigh, A., Wynn, R., Stevens, R., Addison, M., King, D.*, et al.* (2004). Natural history of GATA1 mutations in Down syndrome. Blood *103*, 2480-2489.

Ait Yahya-Graison, E., Aubert, J., Dauphinot, L., Rivals, I., Prieur, M., Golfier, G., Rossier, J., Personnaz, L., Creau, N., Blehaut, H.*, et al.* (2007). Classification of human chromosome 21 gene-expression variations in Down syndrome: impact on disease phenotypes. Am J Hum Genet *81*, 475-491.

Akashi, K., Traver, D., Miyamoto, T., and Weissman, I.L. (2000). A clonogenic common myeloid progenitor that gives rise to all myeloid lineages. Nature *404*, 193-197.

Allen, G., Benda, C.E., Book, J.A., Carter, C.O., Ford, C.E., Chu, E.H., Hanhart, E., Jervis, G., Langdon-Down, W., Lejeune, J.*, et al.* (1961). Mongolism. Am J Hum Genet *13*, 426.

Antonarakis, S.E. (1991). Parental origin of the extra chromosome in trisomy 21 as indicated by analysis of DNA polymorphisms. Down Syndrome Collaborative Group. N Engl J Med *324*, 872-876.

Antonarakis, S.E., Adelsberger, P.A., Petersen, M.B., Binkert, F., and Schinzel, A.A. (1990). Analysis of DNA polymorphisms suggests that most de novo dup(21q) chromosomes in patients with Down syndrome are isochromosomes and not translocations. Am J Hum Genet *47*, 968-972.

Antonarakis, S.E., Avramopoulos, D., Blouin, J.L., Talbot, C.C., Jr., and Schinzel, A.A. (1993). Mitotic errors in somatic cells cause trisomy 21 in about 4.5% of cases and are not associated with advanced maternal age. Nat Genet *3*, 146-150.

Antonarakis, S.E., Lyle, R., Dermitzakis, E.T., Reymond, A., and Deutsch, S. (2004). Chromosome 21 and down syndrome: from genomics to pathophysiology. Nat Rev Genet *5*, 725-738.

Antonarakis, S.E., Petersen, M.B., McInnis, M.G., Adelsberger, P.A., Schinzel, A.A., Binkert, F., Pangalos, C., Raoul, O., Slaugenhaupt, S.A., Hafez, M.*, et al.* (1992). The meiotic stage of nondisjunction in trisomy 21: determination by using DNA polymorphisms. Am J Hum Genet *50*, 544-550.

Arinobu, Y., Mizuno, S., Chong, Y., Shigematsu, H., Iino, T., Iwasaki, H., Graf, T., Mayfield, R., Chan, S., Kastner, P.*, et al.* (2007). Reciprocal activation of GATA-1 and PU.1 marks initial specification of hematopoietic stem cells into myeloerythroid and myelolymphoid lineages. Cell Stem Cell *1*, 416-427.

Arron, J.R., Winslow, M.M., Polleri, A., Chang, C.P., Wu, H., Gao, X., Neilson, J.R., Chen, L., Heit, J.J., Kim, S.K.*, et al.* (2006). NFAT dysregulation by increased dosage of DSCR1 and DYRK1A on chromosome 21. Nature *441*, 595-600.

Azuara, V., Perry, P., Sauer, S., Spivakov, M., Jorgensen, H.F., John, R.M., Gouti, M., Casanova, M., Warnes, G., Merkenschlager, M.*, et al.* (2006). Chromatin signatures of pluripotent cell lines. Nat Cell Biol *8*, 532-538.

Baird, P.A., and Sadovnick, A.D. (1989). Life tables for Down syndrome. Hum Genet *82*, 291-292.

Balkany, T.J., Downs, M.P., Jafek, B.W., and Krajicek, M.J. (1979). Hearing loss in Down's syndrome. A treatable handicap more common than generally recognized. Clin Pediatr (Phila) *18*, 116-118.

Baxter, E.J., Scott, L.M., Campbell, P.J., East, C., Fourouclas, N., Swanton, S., Vassiliou, G.S., Bench, A.J., Boyd, E.M., Curtin, N.*, et al.* (2005). Acquired mutation of the tyrosine kinase JAK2 in human myeloproliferative disorders. Lancet *365*, 1054-1061.

Baxter, L.L., Moran, T.H., Richtsmeier, J.T., Troncoso, J., and Reeves, R.H. (2000). Discovery and genetic localization of Down syndrome cerebellar phenotypes using the Ts65Dn mouse. Hum Mol Genet *9*, 195-202.

Bercovich, D., Ganmore, I., Scott, L.M., Wainreb, G., Birger, Y., Elimelech, A., Shochat, C., Cazzaniga, G., Biondi, A., Basso, G.*, et al.* (2008). Mutations of JAK2 in acute lymphoblastic leukaemias associated with Down's syndrome. Lancet *372*, 1484-1492.

Bernstein, B.E., Mikkelsen, T.S., Xie, X., Kamal, M., Huebert, D.J., Cuff, J., Fry, B., Meissner, A., Wernig, M., Plath, K.*, et al.* (2006). A bivalent chromatin structure marks key developmental genes in embryonic stem cells. Cell *125*, 315-326.

Boker, L.K., Blumstein, T., Sadetzki, S., Luxenburg, O., Litvak, I., Akstein, E., and Modan, B. (2001). Incidence of leukemia and other cancers in Down syndrome subjects in Israel. Int J Cancer *93*, 741-744.

Borzillo, G.V., Ashmun, R.A., and Sherr, C.J. (1990). Macrophage lineage switching of murine early pre-B lymphoid cells expressing transduced fms genes. Mol Cell Biol *10*, 2703-2714.

Bouilloux, F., Juban, G., Cohet, N., Buet, D., Guyot, B., Vainchenker, W., Louache, F., and Morle, F. (2008). EKLF restricts megakaryocytic differentiation at the benefit of erythrocytic differentiation. Blood *112*, 576-584.

Bourquin, J.P., Subramanian, A., Langebrake, C., Reinhardt, D., Bernard, O., Ballerini, P., Baruchel, A., Cave, H., Dastugue, N., Hasle, H.*, et al.* (2006). Identification of distinct molecular phenotypes in acute megakaryoblastic leukemia by gene expression profiling. Proc Natl Acad Sci U S A *103*, 3339-3344.

Bovicelli, L., Orsini, L.F., Rizzo, N., Montacuti, V., and Bacchetta, M. (1982). Reproduction in Down syndrome. Obstet Gynecol *59*, 13S-17S.

Boyer, L.A., Plath, K., Zeitlinger, J., Brambrink, T., Medeiros, L.A., Lee, T.I., Levine, S.S., Wernig, M., Tajonar, A., Ray, M.K.*, et al.* (2006). Polycomb complexes repress developmental regulators in murine embryonic stem cells. Nature *441*, 349-353.

Brown, A.S., Feingold, E., Broman, K.W., and Sherman, S.L. (2000). Genome-wide variation in recombination in female meiosis: a risk factor for non-disjunction of chromosome 21. Hum Mol Genet *9*, 515-523.

Broxmeyer, H.E., Srour, E.F., Hangoc, G., Cooper, S., Anderson, S.A., and Bodine, D.M. (2003). High-efficiency recovery of functional hematopoietic progenitor and stem cells from human cord blood cryopreserved for 15 years. Proc Natl Acad Sci U S A *100*, 645-650.

Cabelof, D.C., Patel, H.V., Chen, Q., van Remmen, H., Matherly, L.H., Ge, Y., and Taub, J.W. (2009). Mutational spectrum at GATA1 provides insights into mutagenesis and leukemogenesis in down syndrome. Blood.

Cai, Z., de Bruijn, M., Ma, X., Dortland, B., Luteijn, T., Downing, R.J., and Dzierzak, E. (2000). Haploinsufficiency of AML1 affects the temporal and spatial generation of hematopoietic stem cells in the mouse embryo. Immunity *13*, 423-431.

Calligaris, R., Bottardi, S., Cogoi, S., Apezteguia, I., and Santoro, C. (1995). Alternative translation initiation site usage results in two functionally distinct forms of the GATA-1 transcription factor. Proc Natl Acad Sci U S A *92*, 11598-11602.

Candotti, F., Oakes, S.A., Johnston, J.A., Giliani, S., Schumacher, R.F., Mella, P., Fiorini, M., Ugazio, A.G., Badolato, R., Notarangelo, L.D.*, et al.* (1997). Structural and functional basis for JAK3-deficient severe combined immunodeficiency. Blood *90*, 3996-4003.

Cantor, A.B., and Orkin, S.H. (2002). Transcriptional regulation of erythropoiesis: an affair involving multiple partners. Oncogene *21*, 3368-3376.

Canzonetta, C., Mulligan, C., Deutsch, S., Ruf, S., O'Doherty, A., Lyle, R., Borel, C., Lin-Marq, N., Delom, F., Groet, J.*, et al.* (2008). DYRK1A-dosage imbalance perturbs NRSF/REST levels, deregulating pluripotency and embryonic stem cell fate in Down syndrome. Am J Hum Genet *83*, 388-400.

Carmichael, C.L., Majewski, I.J., Alexander, W.S., Metcalf, D., Hilton, D.J., Hewitt, C.A., and Scott, H.S. (2009). Hematopoietic defects in the Ts1Cje mouse model of Down syndrome. Blood *113*, 1929-1937.

Changelian, P.S., Flanagan, M.E., Ball, D.J., Kent, C.R., Magnuson, K.S., Martin, W.H., Rizzuti, B.J., Sawyer, P.S., Perry, B.D., Brissette, W.H.*, et al.* (2003). Prevention of organ allograft rejection by a specific Janus kinase 3 inhibitor. Science *302*, 875-878.

Chen, C.Z., Li, L., Lodish, H.F., and Bartel, D.P. (2004). MicroRNAs modulate hematopoietic lineage differentiation. Science *303*, 83-86.

Chen, L., and Daley, G.Q. (2008). Molecular basis of pluripotency. Hum Mol Genet *17*, R23-27.

Chen, M.J., Yokomizo, T., Zeigler, B.M., Dzierzak, E., and Speck, N.A. (2009). Runx1 is required for the endothelial to haematopoietic cell transition but not thereafter. Nature *457*, 887-891.

Cherry, S.R., Biniszkiewicz, D., van Parijs, L., Baltimore, D., and Jaenisch, R. (2000). Retroviral expression in embryonic stem cells and hematopoietic stem cells. Mol Cell Biol *20*, 7419-7426.

Choi, K., Kennedy, M., Kazarov, A., Papadimitriou, J.C., and Keller, G. (1998). A common precursor for hematopoietic and endothelial cells. Development *125*, 725-732.

Chou, S.T., Opalinska, J.B., Yao, Y., Fernandes, M.A., Kalota, A., Brooks, J.S., Choi, J.K., Gewirtz, A.M., Danet-Desnoyers, G.A., Nemiroff, R.L.*, et al.* (2008). Trisomy 21 enhances human fetal erythro-megakaryocytic development. Blood *112*, 4503-4506.

Chrast, R., Scott, H.S., Papasavvas, M.P., Rossier, C., Antonarakis, E.S., Barras, C., Davisson, M.T., Schmidt, C., Estivill, X., Dierssen, M.*, et al.* (2000). The mouse brain transcriptome by SAGE: differences in gene expression between P30 brains of the partial trisomy 16 mouse model of Down syndrome (Ts65Dn) and normals. Genome Res *10*, 2006-2021.

Cox, D.R., Smith, S.A., Epstein, L.B., and Epstein, C.J. (1984). Mouse trisomy 16 as an animal model of human trisomy 21 (Down syndrome): production of viable trisomy 16 diploid mouse chimeras. Dev Biol *101*, 416-424.

Crider, K.S., Olney R.S., and Cragan J.D. (2008). Trisomies 13 and 18: Population Prevalences, Characteristics, and Prenatal Diagnosis, Metropolitan Atlanta, 1994–2003. Am Journ of Med Genetics Part A *146A*: 820–826

Crispino, J.D., Lodish, M.B., MacKay, J.P., and Orkin, S.H. (1999). Use of altered specificity mutants to probe a specific protein-protein interaction in differentiation: the GATA-1:FOG complex. Mol Cell *3*, 219-228.

Cuthbert, A.P., Trott, D.A., Ekong, R.M., Jezzard, S., England, N.L., Themis, M., Todd, C.M., and Newbold, R.F. (1995). Construction and characterization of a highly stable human: rodent monochromosomal hybrid panel for genetic complementation and genome mapping studies. Cytogenet Cell Genet *71*, 68-76.

Daley, G.Q. (2003). From embryos to embryoid bodies: generating blood from embryonic stem cells. Ann N Y Acad Sci *996*, 122-131.

Datta, A., and Jinks-Robertson, S. (1995). Association of increased spontaneous mutation rates with high levels of transcription in yeast. Science *268*, 1616-1619.

Davisson, M.T., Schmidt, C., and Akeson, E.C. (1990). Segmental trisomy of murine chromosome 16: a new model system for studying Down syndrome. Prog Clin Biol Res *360*, 263-280.

de Bruijn, M.F., Speck, N.A., Peeters, M.C., and Dzierzak, E. (2000). Definitive hematopoietic stem cells first develop within the major arterial regions of the mouse embryo. EMBO J *19*, 2465-2474.

Delabar, J.M., Theophile, D., Rahmani, Z., Chettouh, Z., Blouin, J.L., Prieur, M., Noel, B., and Sinet, P.M. (1993). Molecular mapping of twenty-four features of Down syndrome on chromosome 21. Eur J Hum Genet *1*, 114-124.

Dierssen, M., Fillat, C., Crnic, L., Arbones, M., Florez, J., and Estivill, X. (2001). Murine models for Down syndrome. Physiol Behav *73*, 859-871.

Doetschman, T.C., Eistetter, H., Katz, M., Schmidt, W., and Kemler, R. (1985). The in vitro development of blastocyst-derived embryonic stem cell lines: formation of visceral yolk sac, blood islands and myocardium. J Embryol Exp Morphol *87*, 27-45.

Down, J.L. (1995). Observations on an ethnic classification of idiots. 1866. Ment Retard *33*, 54-56.

Dowton, S.B., Beardsley, D., Jamison, D., Blattner, S., and Li, F.P. (1985). Studies of a familial platelet disorder. Blood *65*, 557-563.

Dzierzak, E., and Speck, N.A. (2008). Of lineage and legacy: the development of mammalian hematopoietic stem cells. Nat Immunol *9*, 129-136.

Elagib, K.E., Racke, F.K., Mogass, M., Khetawat, R., Delehanty, L.L., and Goldfarb, A.N. (2003). RUNX1 and GATA-1 coexpression and cooperation in megakaryocytic differentiation. Blood *101*, 4333-4341.

Epstein, C.J. (2001). Down Syndrome (Trisomy 21) In The metabolic and molecular bases of inherited disease, 8th edition (New York, McGraw-Hill.)

Epstein, C.J., Hofmeister, B.G., Yee, D., Smith, S.A., Philip, R., Cox, D.R., and Epstein, L.B. (1985). Stem cell deficiencies and thymic abnormalities in fetal mouse trisomy 16. J Exp Med *162*, 695-712.

Era, T., Takagi, T., Takahashi, T., Bories, J.C., and Nakano, T. (2000). Characterization of hematopoietic lineage-specific gene expression by ES cell in vitro differentiation induction system. Blood *95*, 870-878.

Eto, K., Leavitt, A.L., Nakano, T., and Shattil, S.J. (2003). Development and analysis of megakaryocytes from murine embryonic stem cells. Methods Enzymol *365*, 142-158.

Eto, K., Murphy, R., Kerrigan, S.W., Bertoni, A., Stuhlmann, H., Nakano, T., Leavitt, A.D., and Shattil, S.J. (2002). Megakaryocytes derived from embryonic stem cells implicate CalDAG-GEFI in integrin signaling. Proc Natl Acad Sci U S A *99*, 12819-12824.

Evans, M.J., and Kaufman, M.H. (1981). Establishment in culture of pluripotential cells from mouse embryos. Nature *292*, 154-156.

Ferkowicz, M.J., Starr, M., Xie, X., Li, W., Johnson, S.A., Shelley, W.C., Morrison, P.R., and Yoder, M.C. (2003). CD41 expression defines the onset of primitive and definitive hematopoiesis in the murine embryo. Development *130*, 4393-4403.

Ferreira, R., Ohneda, K., Yamamoto, M., and Philipsen, S. (2005). GATA1 function, a paradigm for transcription factors in hematopoiesis. Mol Cell Biol *25*, 1215-1227.

Ferrer, I., and Gullotta, F. (1990). Down's syndrome and Alzheimer's disease: dendritic spine counts in the hippocampus. Acta Neuropathol (Berl) *79*, 680-685.

Fisher, A.G. (2002). Cellular identity and lineage choice. Nat Rev Immunol *2*, 977-982.

Flex, E., Petrangeli, V., Stella, L., Chiaretti, S., Hornakova, T., Knoops, L., Ariola, C., Fodale, V., Clappier, E., Paoloni, F.*, et al.* (2008). Somatically acquired JAK1 mutations in adult acute lymphoblastic leukemia. J Exp Med *205*, 751-758.

Forestier, E., Izraeli, S., Beverloo, B., Haas, O., Pession, A., Michalova, K., Stark, B., Harrison, C.J., Teigler-Schlegel, A., and Johansson, B. (2008). Cytogenetic features of acute lymphoblastic and myeloid leukemias in pediatric patients with Down syndrome: an iBFM-SG study. Blood *111*, 1575-1583.

Fournier, R.E., and Ruddle, F.H. (1977). Microcell-mediated transfer of murine chromosomes into mouse, Chinese hamster, and human somatic cells. Proc Natl Acad Sci U S A *74*, 319-323.

Fuentes, J.J., Pritchard, M.A., Planas, A.M., Bosch, A., Ferrer, I., and Estivill, X. (1995). A new human gene from the Down syndrome critical region encodes a proline-rich protein highly expressed in fetal brain and heart. Hum Mol Genet *4*, 1935-1944.

Fujita, Y., Nishimura, M., Taniwaki, M., Abe, T., and Okuda, T. (2001). Identification of an alternatively spliced form of the mouse AML1/RUNX1 gene transcript AML1c and its expression in early hematopoietic development. Biochem Biophys Res Commun *281*, 1248-1255.

Fujiwara, Y., Browne, C.P., Cunniff, K., Goff, S.C., and Orkin, S.H. (1996). Arrested development of embryonic red cell precursors in mouse embryos lacking transcription factor GATA-1. Proc Natl Acad Sci U S A *93*, 12355-12358.

Gaines, P., Geiger, J.N., Knudsen, G., Seshasayee, D., and Wojchowski, D.M. (2000). GATA-1- and FOG-dependent activation of megakaryocytic alpha IIB gene expression. J Biol Chem *275*, 34114-34121.

Galante, M., Jani, H., Vanes, L., Daniel, H., Fisher, E.M., Tybulewicz, V.L., Bliss, T.V., and Morice, E. (2009). Impairments in motor coordination without major changes in cerebellar plasticity in the Tc1 mouse model of Down syndrome. Hum Mol Genet *18*, 1449-1463.

Gamis, A.S., and Hilden, J.M. (2002). Transient myeloproliferative disorder, a disorder with too few data and many unanswered questions: does it contain an important piece of the puzzle to understanding hematopoiesis and acute myelogenous leukemia? J Pediatr Hematol Oncol *24*, 2-5.

Garzon, R., Pichiorri, F., Palumbo, T., Iuliano, R., Cimmino, A., Aqeilan, R., Volinia, S., Bhatt, D., Alder, H., Marcucci, G.*, et al.* (2006). MicroRNA fingerprints during human megakaryocytopoiesis. Proc Natl Acad Sci U S A *103*, 5078-5083.

Glasson, E.J., Sullivan, S.G., Hussain, R., Petterson, B.A., Montgomery, P.D. and Bittles, A.H. (2002). The changing survival profile of people with Down's syndrome: implications for genetic counselling. Clin Genet., *62*, 390–393.

Ge, Y., LaFiura, K.M., Dombkowski, A.A., Chen, Q., Payton, S.G., Buck, S.A., Salagrama, S., Diakiw, A.E., Matherly, L.H., and Taub, J.W. (2008). The role of the proto-oncogene ETS2 in acute megakaryocytic leukemia biology and therapy. Leukemia *22*, 521-529.

Gilliland, D.G., and Tallman, M.S. (2002). Focus on acute leukemias. Cancer Cell *1*, 417-420.

Goldacre, M.J., Wotton, C.J., Seagroatt, V., and Yeates, D. (2004). Cancers and immune related diseases associated with Down's syndrome: a record linkage study. Arch Dis Child *89*, 1014-1017.

Granholm, A.C., Sanders, L.A., and Crnic, L.S. (2000). Loss of cholinergic phenotype in basal forebrain coincides with cognitive decline in a mouse model of Down's syndrome. Exp Neurol *161*, 647-663.

Grasso, M., Giovannucci Uzielli, M.L., Pierluigi, M., Tavellini, F., Perroni, L., and Dagna Bricarelli, F. (1989). Isochromosome not translocation in trisomy 21q21q. Hum Genet *84*, 63-65.

Groet, J., Ives, J.H., Jones, T.A., Danton, M., Flomen, R.H., Sheer, D., Hrascan, R., Pavelic, K., and Nizetic, D. (2000). Narrowing of the region of allelic loss in 21q11-21 in squamous non-small cell lung carcinoma and cloning of a novel ubiquitin-specific protease gene from the deleted segment. Genes Chromosomes Cancer *27*, 153-161.

Groet, J., McElwaine, S., Spinelli, M., Rinaldi, A., Burtscher, I., Mulligan, C., Mensah, A., Cavani, S., Dagna-Bricarelli, F., Basso, G*., et al.* (2003). Acquired mutations in GATA1 in neonates with Down's syndrome with transient myeloid disorder. Lancet *361*, 1617-1620.

Groet, J., Mulligan, C., Spinelli, M., Serra, A., McElwaine, S., Cotter, F.E., Dagna-Bricarelli, F., Saglio, G., Basso, G., and Nizetic, D. (2005). Independent clones at separable stages of differentiation, bearing different GATA1 mutations, in the same TMD patient with Down syndrome. Blood *106*, 1887-1888.

Habets, G.G., Scholtes, E.H., Zuydgeest, D., van der Kammen, R.A., Stam, J.C., Berns, A., and Collard, J.G. (1994). Identification of an invasion-inducing gene, Tiam-1, that encodes a protein with homology to GDP-GTP exchangers for Rho-like proteins. Cell *77*, 537-549.

Hammerle, B., Vera-Samper, E., Speicher, S., Arencibia, R., Martinez, S., and Tejedor, F.J. (2002). Mnb/Dyrk1A is transiently expressed and asymmetrically segregated in neural progenitor cells at the transition to neurogenic divisions. Dev Biol *246*, 259-273.

Hasle, H., Clemmensen, I.H., and Mikkelsen, M. (2000). Risks of leukaemia and solid tumours in individuals with Down's syndrome. Lancet *355*, 165-169.

Hassold, T., Abruzzo, M., Adkins, K., Griffin, D., Merrill, M., Millie, E., Saker, D., Shen, J. and Zaragoza, M. (1996). Human aneuploidy: incidence, origin, and etiology. Environ Mol Mutagen *28*, 167–175.

Hassold, T., and Hunt, P. (2001). To err (meiotically) is human: the genesis of human aneuploidy. Nat Rev Genet *2*, 280-291.

Hassold, T.J., and Jacobs, P.A. (1984). Trisomy in man. Annu Rev Genet *18*, 69-97.

Helgason, C.D., Sauvageau, G., Lawrence, H.J., Largman, C., and Humphries, R.K. (1996). Overexpression of HOXB4 enhances the hematopoietic potential of embryonic stem cells differentiated in vitro. Blood *87*, 2740-2749.

Henry, E., Walker, D., Wiedmeier, S.E., and Christensen, R.D. (2007). Hematological abnormalities during the first week of life among neonates with Down syndrome: data from a multihospital healthcare system. Am J Med Genet A *143*, 42-50.

Hermon, C., Alberman, E., Beral, V., and Swerdlow, A.J. (2001). Mortality and cancer incidence in persons with Down's syndrome, their parents and siblings. Ann Hum Genet *65*, 167-176.

Hernandez, D., Mee, P.J., Martin, J.E., Tybulewicz, V.L., and Fisher, E.M. (1999). Transchromosomal mouse embryonic stem cell lines and chimeric mice that contain freely segregating segments of human chromosome 21. Hum Mol Genet *8*, 923-933.

Hill, D.A., Gridley, G., Cnattingius, S., Mellemkjaer, L., Linet, M., Adami, H.O., Olsen, J.H., Nyren, O., and Fraumeni, J.F., Jr. (2003). Mortality and cancer incidence among individuals with Down syndrome. Arch Intern Med *163*, 705-711.

Hirose, Y., Kudo, K., Kiyoi, H., Hayashi, Y., Naoe, T., and Kojima, S. (2003). Comprehensive analysis of gene alterations in acute megakaryoblastic leukemia of Down's syndrome. Leukemia *17*, 2250-2252.

Hitzler, J.K. (2007). Acute megakaryoblastic leukemia in Down syndrome. Pediatr Blood Cancer *49*, 1066-1069.

Hitzler, J.K., Cheung, J., Li, Y., Scherer, S.W., and Zipursky, A. (2003). GATA1 mutations in transient leukemia and acute megakaryoblastic leukemia of Down syndrome. Blood *101*, 4301-4304.

Hitzler, J.K., and Zipursky, A. (2005). Origins of leukaemia in children with Down syndrome. Nat Rev Cancer *5*, 11-20.

Ho, C.Y., Otterud, B., Legare, R.D., Varvil, T., Saxena, R., DeHart, D.B., Kohler, S.E., Aster, J.C., Dowton, S.B., Li, F.P., *et al.* (1996). Linkage of a familial platelet disorder with a propensity to develop myeloid malignancies to human chromosome 21q22.1-22.2. Blood *87*, 5218-5224.

Hoffmann, G.R., Dellarco, V.L., and Voytek, P.E. (1986). A review of the symposium on aneuploidy: etiology and mechanism. Environ Mutagen *8*, 643-651.

Hollanda, L.M., Lima, C.S., Cunha, A.F., Albuquerque, D.M., Vassallo, J., Ozelo, M.C., Joazeiro, P.P., Saad, S.T., and Costa, F.F. (2006). An inherited mutation leading to production of only the short isoform of GATA-1 is associated with impaired erythropoiesis. Nat Genet *38*, 807-812.

Holtzman, D.M., Santucci, D., Kilbridge, J., Chua-Couzens, J., Fontana, D.J., Daniels, S.E., Johnson, R.M., Chen, K., Sun, Y., Carlson, E., *et al.* (1996). Developmental abnormalities and age-related neurodegeneration in a mouse model of Down syndrome. Proc Natl Acad Sci U S A *93*, 13333-13338.

Houbaviy, H.B., Murray, M.F., and Sharp, P.A. (2003). Embryonic stem cell-specific MicroRNAs. Dev Cell *5*, 351-358.

Huang, H., Yu, M., Akie, T.E., Moran, T.B., Woo, A.J., Tu, N., Waldon, Z., Lin, Y.Y., Steen, H., and Cantor, A.B. (2009a). Differentiation-dependent Interactions between RUNX-1 and FLI-1 During Megakaryocyte Development. Mol Cell Biol.

Huang, Z., Dore, L.C., Li, Z., Orkin, S.H., Feng, G., Lin, S., and Crispino, J.D. (2009b). GATA-2 reinforces megakaryocyte development in the absence of GATA-1. Mol Cell Biol.

Hulten, M.A., Patel, S.D., Tankimanova, M., Westgren, M., Papadogiannakis, N., Jonsson, A.M., and Iwarsson, E. (2008). On the origin of trisomy 21 Down syndrome. Mol Cytogenet *1*, 21.

Huret, J.L., and Leonard, C. (1997). Chromosome 21 and platelets: a gene dosage effect? Clin Genet *51*, 140-141.

Ichikawa, M., Asai, T., Chiba, S., Kurokawa, M., and Ogawa, S. (2004a). Runx1/AML-1 ranks as a master regulator of adult hematopoiesis. Cell Cycle *3*, 722-724.

Ichikawa, M., Asai, T., Saito, T., Seo, S., Yamazaki, I., Yamagata, T., Mitani, K., Chiba, S., Ogawa, S., Kurokawa, M.*, et al.* (2004b). AML-1 is required for megakaryocytic maturation and lymphocytic differentiation, but not for maintenance of hematopoietic stem cells in adult hematopoiesis. Nat Med *10*, 299-304.

Ito, E., Kasai, M., Hayashi, Y., Toki, T., Arai, K., Yokoyama, S., Kato, K., Tachibana, N., Yamamoto, M., and Yokoyama, M. (1995). Expression of erythroid-specific genes in acute megakaryoblastic leukaemia and transient myeloproliferative disorder in Down's syndrome. Br J Haematol *90*, 607-614.

Ives, J.H., Dagna-Bricarelli, F., Basso, G., Antonarakis, S.E., Jee, R., Cotter, F., and Nizetic, D. (1998). Increased levels of a chromosome 21-encoded tumour invasion and metastasis factor (TIAM1) mRNA in bone marrow of Down syndrome children during the acute phase of AML(M7). Genes Chromosomes Cancer *23*, 61-66.

Izraeli, S. (2008). Trisomy 21 tilts the balance. Blood *112*, 4361-4362.

Jackers, P., Szalai, G., Moussa, O., and Watson, D.K. (2004). Ets-dependent regulation of target gene expression during megakaryopoiesis. J Biol Chem *279*, 52183-52190.

Jacobs, P.A. (1992). The chromosome complement of human gametes. Oxf Rev Reprod Biol *14*, 47-72.

Jacobs, P.A., Baikie, A.G., Court Brown, W.M., and Strong, J.A. (1959). The somatic chromosomes in mongolism. Lancet *1*, 710.

Jaffredo, T., Gautier, R., Eichmann, A., and Dieterlen-Lievre, F. (1998). Intraaortic hemopoietic cells are derived from endothelial cells during ontogeny. Development *125*, 4575-4583.

Jaffredo, T., Nottingham, W., Liddiard, K., Bollerot, K., Pouget, C., and de Bruijn, M. (2005). From hemangioblast to hematopoietic stem cell: an endothelial connection? Exp Hematol *33*, 1029-1040.

Jezierski, A., Swedani, A., and Wang, L. (2007). Development of hematopoietic and endothelial cells from human embryonic stem cells: lessons from the studies using mouse as a model. ScientificWorldJournal *7*, 1950-1964.

Kadri, Z., Shimizu, R., Ohneda, O., Maouche-Chretien, L., Gisselbrecht, S., Yamamoto, M., Romeo, P.H., Leboulch, P., and Chretien, S. (2009). Direct binding of pRb/E2F-2 to GATA-1 regulates maturation and terminal cell division during erythropoiesis. PLoS Biol *7*, e1000123.

Kearney, L., Gonzalez De Castro, D., Yeung, J., Procter, J., Horsley, S.W., Eguchi-Ishimae, M., Bateman, C.M., Anderson, K., Chaplin, T., Young, B.D.*, et al.* (2009). Specific JAK2 mutation (JAK2R683) and multiple gene deletions in Down syndrome acute lymphoblastic leukemia. Blood *113*, 646-648.

Keller, G., Kennedy, M., Papayannopoulou, T., and Wiles, M.V. (1993). Hematopoietic commitment during embryonic stem cell differentiation in culture. Mol Cell Biol *13*, 473-486.

Kelly, L.M., and Gilliland, D.G. (2002). Genetics of myeloid leukemias. Annu Rev Genomics Hum Genet *3*, 179-198.

Kirsammer, G., Jilani, S., Liu, H., Davis, E., Gurbuxani, S., Le Beau, M.M., and Crispino, J.D. (2007). Highly penetrant myeloproliferative disease in the Ts65Dn mouse model of Down syndrome. Blood *111*(2), 767-75.

Kitajima, K., Masuhara, M., Era, T., Enver, T., and Nakano, T. (2002). GATA-2 and GATA-2/ER display opposing activities in the development and differentiation of blood progenitors. EMBO J *21*, 3060-3069.

Kitajima, K., Tanaka, M., Zheng, J., Sakai-Ogawa, E., and Nakano, T. (2003). In vitro differentiation of mouse embryonic stem cells to hematopoietic cells on an OP9 stromal cell monolayer. Methods Enzymol *365*, 72-83.

Kiyoi, H., Yamaji, S., Kojima, S., and Naoe, T. (2007). JAK3 mutations occur in acute megakaryoblastic leukemia both in Down syndrome children and non-Down syndrome adults. Leukemia *21*, 574-576.

Kohno, T., Kawanishi, M., Matsuda, S., Ichikawa, H., Takada, M., Ohki, M., Yamamoto, T., and Yokota, J. (1998). Homozygous deletion and frequent allelic loss of the 21q11.1-q21.1 region including the ANA gene in human lung carcinoma. Genes Chromosomes Cancer *21*, 236-243.

Korbel, J.O., Tirosh-Wagner, T., Urban, A.E., Chen, X.N., Kasowski, M., Dai, L., Grubert, F., Erdman, C., Gao, M.C., Lange, K.*, et al.* (2009). The genetic architecture of Down syndrome phenotypes revealed by high-resolution analysis of human segmental trisomies. Proc Natl Acad Sci U S A *106*, 12031-12036.

Korenberg, J.R., Chen, X.N., Schipper, R., Sun, Z., Gonsky, R., Gerwehr, S., Carpenter, N., Daumer, C., Dignan, P., Disteche, C.*, et al.* (1994). Down syndrome phenotypes: the consequences of chromosomal imbalance. Proc Natl Acad Sci U S A *91*, 4997-5001.

Kuhl, C., Atzberger, A., Iborra, F., Nieswandt, B., Porcher, C., and Vyas, P. (2005). GATA1-mediated megakaryocyte differentiation and growth control can be uncoupled and mapped to different domains in GATA1. Mol Cell Biol *25*, 8592-8606.

Kyba, M., Perlingeiro, R.C., and Daley, G.Q. (2002). HoxB4 confers definitive lymphoid-myeloid engraftment potential on embryonic stem cell and yolk sac hematopoietic progenitors. Cell *109*, 29-37.

Kyttala, S., Habermann, I., Minami, T., Ehninger, G., and Kiani, A. (2009). Regulation of Down Syndrome Critical Region 1 expression by Nuclear Factor of Activated T cells in megakaryocytes. Br J Haematol *144*, 395-408.

Lai, K.S., Jin, Y., Graham, D.K., Witthuhn, B.A., Ihle, J.N., and Liu, E.T. (1995). A kinase-deficient splice variant of the human JAK3 is expressed in hematopoietic and epithelial cancer cells. J Biol Chem *270*, 25028-25036.

Lamb, N.E., Freeman, S.B., Savage-Austin, A., Pettay, D., Taft, L., Hersey, J., Gu, Y., Shen, J., Saker, D., May, K.M.*, et al.* (1996). Susceptible chiasmate configurations of chromosome 21 predispose to non-disjunction in both maternal meiosis I and meiosis II. Nat Genet *14*, 400-405.

Lamb, N.E., Yu, K., Shaffer, J., Feingold, E., and Sherman, S.L. (2005). Association between maternal age and meiotic recombination for trisomy 21. Am J Hum Genet *76*, 91-99.

Lancrin, C., Sroczynska, P., Stephenson, C., Allen, T., Kouskoff, V., and Lacaud, G. (2009). The haemangioblast generates haematopoietic cells through a haemogenic endothelium stage. Nature *457*, 892-895.

Lange, B.J., Kobrinsky, N., Barnard, D.R., Arthur, D.C., Buckley, J.D., Howells, W.B., Gold, S., Sanders, J., Neudorf, S., Smith, F.O.*, et al.* (1998). Distinctive demography, biology, and outcome of acute myeloid leukemia and myelodysplastic syndrome in children with Down syndrome: Children's Cancer Group Studies 2861 and 2891. Blood *91*, 608-615.

Langebrake, C., Creutzig, U., and Reinhardt, D. (2005). Immunophenotype of Down syndrome acute myeloid leukemia and transient myeloproliferative disease differs significantly from other diseases with morphologically identical or similar blasts. Klin Padiatr *217*, 126-134.

Lee, T.I., Jenner, R.G., Boyer, L.A., Guenther, M.G., Levine, S.S., Kumar, R.M., Chevalier, B., Johnstone, S.E., Cole, M.F., Isono, K.*, et al.* (2006). Control of developmental regulators by Polycomb in human embryonic stem cells. Cell *125*, 301-313.

Legare, R.D., Lu, D., Gallagher, M., Ho, C., Tan, X., Barker, G., Shimizu, K., Ohki, M., Lenny, N., Hiebert, S.*, et al.* (1997). CBFA2, frequently rearranged in leukemia, is not responsible for a familial leukemia syndrome. Leukemia *11*, 2111-2119.

Lejeune, J., Turpin, R., and Gautier, M. (1959). Mongolism; a chromosomal disease (trisomy). Bull Acad Natl Med *143*, 256-265.

Lemarchandel, V., Ghysdael, J., Mignotte, V., Rahuel, C., and Romeo, P.H. (1993). GATA and Ets cis-acting sequences mediate megakaryocyte-specific expression. Mol Cell Biol *13*, 668-676.

Lensch, M.W., and Daley, G.Q. (2006). Scientific and clinical opportunities for modeling blood disorders with embryonic stem cells. Blood *107*, 2605-2612.

Lessard, J., Faubert, A., and Sauvageau, G. (2004). Genetic programs regulating HSC specification, maintenance and expansion. Oncogene *23*, 7199-7209.

Levine, R.L., Wadleigh, M., Cools, J., Ebert, B.L., Wernig, G., Huntly, B.J., Boggon, T.J., Wlodarska, I., Clark, J.J., Moore, S.*, et al.* (2005). Activating mutation in the tyrosine kinase JAK2 in polycythemia vera, essential thrombocythemia, and myeloid metaplasia with myelofibrosis. Cancer Cell *7*, 387-397.

Li, Z., Godinho, F.J., Klusmann, J.H., Garriga-Canut, M., Yu, C., and Orkin, S.H. (2005). Developmental stage-selective effect of somatically mutated leukemogenic transcription factor GATA1. Nat Genet *37*, 613-619.

Lightfoot, J., Hitzler, J.K., Zipursky, A., Albert, M., and Macgregor, P.F. (2004). Distinct gene signatures of transient and acute megakaryoblastic leukemia in Down syndrome. Leukemia *18*, 1617-1623.

Ling, K.W., Ottersbach, K., van Hamburg, J.P., Oziemlak, A., Tsai, F.Y., Orkin, S.H., Ploemacher, R., Hendriks, R.W., and Dzierzak, E. (2004). GATA-2 plays two functionally distinct roles during the ontogeny of hematopoietic stem cells. J Exp Med *200*, 871-882.

Loughran, S.J., Kruse, E.A., Hacking, D.F., de Graaf, C.A., Hyland, C.D., Willson, T.A., Henley, K.J., Ellis, S., Voss, A.K., Metcalf, D.*, et al.* (2008). The transcription factor Erg is essential for definitive hematopoiesis and the function of adult hematopoietic stem cells. Nat Immunol *9*, 810-819.

Lugus, J.J., Chung, Y.S., Mills, J.C., Kim, S.I., Grass, J., Kyba, M., Doherty, J.M., Bresnick, E.H., and Choi, K. (2007). GATA2 functions at multiple steps in hemangioblast development and differentiation. Development *134*, 393-405.

Lux, C.T., Yoshimoto, M., McGrath, K., Conway, S.J., Palis, J., and Yoder, M.C. (2008). All primitive and definitive hematopoietic progenitor cells emerging before E10 in the mouse embryo are products of the yolk sac. Blood *111*, 3435-3438.

Lyle, R., Bena, F., Gagos, S., Gehrig, C., Lopez, G., Schinzel, A., Lespinasse, J., Bottani, A., Dahoun, S., Taine, L.*, et al.* (2009). Genotype-phenotype correlations in

Down syndrome identified by array CGH in 30 cases of partial trisomy and partial monosomy chromosome 21. Eur J Hum Genet *17*, 454-466.

Ma, Z., Morris, S.W., Valentine, V., Li, M., Herbrick, J.A., Cui, X., Bouman, D., Li, Y., Mehta, P.K., Nizetic, D*., et al.* (2001). Fusion of two novel genes, RBM15 and MKL1, in the t(1;22)(p13;q13) of acute megakaryoblastic leukemia. Nat Genet *28*, 220-221.

Malinge, S., Ben-Abdelali, R., Settegrana, C., Radford-Weiss, I., Debre, M., Beldjord, K., Macintyre, E.A., Villeval, J.L., Vainchenker, W., Berger, R*., et al.* (2007). Novel activating JAK2 mutation in a patient with Down syndrome and B-cell precursor acute lymphoblastic leukemia. Blood *109*, 2202-2204.

Malinge, S., Izraeli, S., and Crispino, J.D. (2009). Insights into the manifestations, outcomes, and mechanisms of leukemogenesis in Down syndrome. Blood *113*, 2619-2628.

Malinge, S., Ragu, C., Della-Valle, V., Pisani, D., Constantinescu, S.N., Perez, C., Villeval, J.L., Reinhardt, D., Landman-Parker, J., Michaux, L*., et al.* (2008). Activating mutations in human acute megakaryoblastic leukemia. Blood *112*, 4220-4226.

Malkin, D., Brown, E.J., and Zipursky, A. (2000). The role of p53 in megakaryocyte differentiation and the megakaryocytic leukemias of Down syndrome. Cancer Genet Cytogenet *116*, 1-5.

Mann, D.M. (1988). The pathological association between Down syndrome and Alzheimer disease. Mech Ageing Dev *43*, 99-136.

Martin, D.I., and Orkin, S.H. (1990). Transcriptional activation and DNA binding by the erythroid factor GF-1/NF-E1/Eryf 1. Genes Dev *4*, 1886-1898.

Martin, D.I., Zon, L.I., Mutter, G., and Orkin, S.H. (1990). Expression of an erythroid transcription factor in megakaryocytic and mast cell lineages. Nature *344*, 444-447.

Martin, G.R. (1981). Isolation of a pluripotent cell line from early mouse embryos cultured in medium conditioned by teratocarcinoma stem cells. Proc Natl Acad Sci U S A *78*, 7634-7638.

McElwaine, S., Mulligan, C., Groet, J., Spinelli, M., Rinaldi, A., Denyer, G., Mensah, A., Cavani, S., Baldo, C., Dagna-Bricarelli, F*., et al.* (2004). Microarray transcript profiling distinguishes the transient from the acute type of megakaryoblastic leukaemia (M7) in Down's syndrome, revealing PRAME as a specific discriminating marker. Br J Haematol *125*, 729-742.

Mella, P., Schumacher, R.F., Cranston, T., de Saint Basile, G., Savoldi, G., and Notarangelo, L.D. (2001). Eleven novel JAK3 mutations in patients with severe combined immunodeficiency-including the first patients with mutations in the kinase domain. Hum Mutat *18*, 355-356.

Mensah, A., Mulligan, C., Linehan, J., Ruf, S., O'Doherty, A., Grygalewicz, B., Shipley, J., Groet, J., Tybulewicz, V., Fisher, E., *et al.* (2007). An additional human chromosome 21 causes suppression of neural fate of pluripotent mouse embryonic stem cells in a teratoma model. BMC Dev Biol *7*, 131.

Mikkelsen, M. (1977). Down syndrome: cytogenetical epidemiology. Hereditas *86*, 45-50.

Mikkola, H.K., Fujiwara, Y., Schlaeger, T.M., Traver, D., and Orkin, S.H. (2003). Expression of CD41 marks the initiation of definitive hematopoiesis in the mouse embryo. Blood *101*, 508-516.

Mikkola, H.K., and Orkin, S.H. (2006). The journey of developing hematopoietic stem cells. Development *133*, 3733-3744.

Minegishi, N., Suzuki, N., Yokomizo, T., Pan, X., Fujimoto, T., Takahashi, S., Hara, T., Miyajima, A., Nishikawa, S., and Yamamoto, M. (2003). Expression and domain-specific function of GATA-2 during differentiation of the hematopoietic precursor cells in midgestation mouse embryos. Blood *102*, 896-905.

Mitsui, K., Tokuzawa, Y., Itoh, H., Segawa, K., Murakami, M., Takahashi, K., Maruyama, M., Maeda, M., and Yamanaka, S. (2003). The homeoprotein Nanog is required for maintenance of pluripotency in mouse epiblast and ES cells. Cell *113*, 631-642.

Moore, C.S. (2006). Postnatal lethality and cardiac anomalies in the Ts65Dn Down syndrome mouse model. Mamm Genome *17*, 1005-1012

Moore, M.A., Shieh, J.H., and Lee, G. (2006). Hematopoietic cells. Methods Enzymol *418*, 208-242.

Morice, E., Andreae, L.C., Cooke, S.F., Vanes, L., Fisher, E.M., Tybulewicz, V.L., and Bliss, T.V. (2008). Preservation of long-term memory and synaptic plasticity despite short-term impairments in the Tc1 mouse model of Down syndrome. Learn Mem *15*, 492-500.

Morita, S., Kojima, T., and Kitamura, T. (2000). Plat-E: an efficient and stable system for transient packaging of retroviruses. Gene Ther *7*, 1063-1066.

Morris, J.K. and Alberman E. (2009). Trends in Down's syndrome live births and antenatal diagnoses in England and Wales from 1989 to 2008: analysis of data from the National Down Syndrome Cytogenetic Register. BMJ Oct 26;339:b3794. doi: 10.1136/bmj.b3794.

Muntean, A.G., and Crispino, J.D. (2005). Differential requirements for the activation domain and FOG-interaction surface of GATA-1 in megakaryocyte gene expression and development. Blood *106*, 1223-1231.

Muntean, A.G., Ge, Y., Taub, J.W., and Crispino, J.D. (2006). Transcription factor GATA-1 and Down syndrome leukemogenesis. Leuk Lymphoma *47*, 986-997.

Muntean, A.G., Pang, L., Poncz, M., Dowdy, S.F., Blobel, G.A., and Crispino, J.D. (2007). Cyclin D-Cdk4 is regulated by GATA-1 and required for megakaryocyte growth and polyploidization. Blood *109*, 5199-5207.

Murphy, M., and Epstein, L.B. (1992). Down syndrome (DS) peripheral blood contains phenotypically mature CD3+TCR alpha, beta+ cells but abnormal proportions of TCR alpha, beta+, TCR gamma, delta+, and CD4+ CD45RA+ cells: evidence for an inefficient release of mature T cells by the DS thymus. Clin Immunol Immunopathol *62*, 245-251.

Nakano, T., Kodama, H., and Honjo, T. (1994). Generation of lymphohematopoietic cells from embryonic stem cells in culture. Science *265*, 1098-1101.

Nichols, J., Zevnik, B., Anastassiadis, K., Niwa, H., Klewe-Nebenius, D., Chambers, I., Scholer, H., and Smith, A. (1998). Formation of pluripotent stem cells in the mammalian embryo depends on the POU transcription factor Oct4. Cell *95*, 379-391.

Norton, A., Fisher, C., Liu, H., Wen, Q., Mundschau, G., Fuster, J.L., Hasle, H., Zeller, B., Webb, D.K., O'Marcaigh, A.*, et al.* (2007). Analysis of JAK3, JAK2, and C-MPL mutations in transient myeloproliferative disorder and myeloid leukemia of Down syndrome blasts in children with Down syndrome. Blood *110*, 1077-1079.

Nottingham, W.T., Jarratt, A., Burgess, M., Speck, C.L., Cheng, J.F., Prabhakar, S., Rubin, E.M., Li, P.S., Sloane-Stanley, J., Kong, A.S.J.*, et al.* (2007). Runx1-mediated hematopoietic stem-cell emergence is controlled by a Gata/Ets/SCL-regulated enhancer. Blood *110*, 4188-4197.

O'Doherty, A., Ruf, S., Mulligan, C., Hildreth, V., Errington, M.L., Cooke, S., Sesay, A., Modino, S., Vanes, L., Hernandez, D.*, et al.* (2005). An aneuploid mouse strain carrying human chromosome 21 with Down syndrome phenotypes. Science *309*, 2033-2037.

O'Shea, J.J., Husa, M., Li, D., Hofmann, S.R., Watford, W., Roberts, J.L., Buckley, R.H., Changelian, P., and Candotti, F. (2004). Jak3 and the pathogenesis of severe combined immunodeficiency. Mol Immunol *41*, 727-737.

Ogawa, M., Nishikawa, S., Yoshinaga, K., Hayashi, S., Kunisada, T., Nakao, J., Kina, T., Sudo, T., and Kodama, H. (1993). Expression and function of c-Kit in fetal hemopoietic progenitor cells: transition from the early c-Kit-independent to the late c-Kit-dependent wave of hemopoiesis in the murine embryo. Development *117*, 1089-1098.

Ohgaki, K., Iida, A., Kasumi, F., Sakamoto, G., Akimoto, M., Nakamura, Y., and Emi, M. (1998). Mapping of a new target region of allelic loss to a 6-cM interval at 21q21 in primary breast cancers. Genes Chromosomes Cancer *23*, 244-247.

Okuda, T., van Deursen, J., Hiebert, S.W., Grosveld, G., and Downing, J.R. (1996). AML1, the target of multiple chromosomal translocations in human leukemia, is essential for normal fetal liver hematopoiesis. Cell *84*, 321-330.

Olsen, A.L., Stachura, D.L., and Weiss, M.J. (2006). Designer blood: creating hematopoietic lineages from embryonic stem cells. Blood *107*, 1265-1275.

Olson, L.E., Roper, R.J., Baxter, L.L., Carlson, E.J., Epstein, C.J., and Reeves, R.H. (2004). Down syndrome mouse models Ts65Dn, Ts1Cje, and Ms1Cje/Ts65Dn exhibit variable severity of cerebellar phenotypes. Dev Dyn *230*, 581-589.

Orkin, S.H. (2003). Priming the hematopoietic pump. Immunity *19*, 633-634.

Orkin, S.H., and Zon, L.I. (2008). Hematopoiesis: an evolving paradigm for stem cell biology. Cell *132*, 631-644.

Orlovskaya, I., Schraufstatter, I., Loring, J., and Khaldoyanidi, S. (2008). Hematopoietic differentiation of embryonic stem cells. Methods *45*, 159-167.

Osato, M., Asou, N., Abdalla, E., Hoshino, K., Yamasaki, H., Okubo, T., Suzushima, H., Takatsuki, K., Kanno, T., Shigesada, K.*, et al.* (1999). Biallelic and heterozygous point mutations in the runt domain of the AML1/PEBP2alphaB gene associated with myeloblastic leukemias. Blood *93*, 1817-1824.

Oster, J., Mikkelsen, M., and Nielsen, A. (1975). Mortality and life-table in Down's syndrome. Acta Paediatr Scand *64*, 322-326.

Ottersbach, K., and Dzierzak, E. (2005). The murine placenta contains hematopoietic stem cells within the vascular labyrinth region. Dev Cell *8*, 377-387.

Pang, L., Xue, H.H., Szalai, G., Wang, X., Wang, Y., Watson, D.K., Leonard, W.J., Blobel, G.A., and Poncz, M. (2006). Maturation stage-specific regulation of megakaryopoiesis by pointed-domain Ets proteins. Blood *108*, 2198-2206.

Park, C., Ma, Y.D., and Choi, K. (2005). Evidence for the hemangioblast. Exp Hematol *33*, 965-970.

Paz-Miguel, J.E., Flores, R., Sanchez-Velasco, P., Ocejo-Vinyals, G., Escribano de Diego, J., Lopez de Rego, J., and Leyva-Cobian, F. (1999). Reactive oxygen intermediates during programmed cell death induced in the thymus of the Ts(1716)65Dn mouse, a murine model for human Down's syndrome. J Immunol *163*, 5399-5410.

Penrose, L. (1933). The relative effects of paternal and maternal age in mongolism. J Genet *27*, 219-224.

Peters, D.G., Klucher, K.M., Perlingeiro, R.C., Dessain, S.K., Koh, E.Y., and Daley, G.Q. (2001). Autocrine and paracrine effects of an ES-cell derived, BCR/ABL-

transformed hematopoietic cell line that induces leukemia in mice. Oncogene *20*, 2636-2646.

Petersen, M.B., Adelsberger, P.A., Schinzel, A.A., Binkert, F., Hinkel, G.K., and Antonarakis, S.E. (1991). Down syndrome due to de novo Robertsonian translocation t(14q;21q): DNA polymorphism analysis suggests that the origin of the extra 21q is maternal. Am J Hum Genet *49*, 529-536.

Philip, R., Berger, A.C., McManus, N.H., Warner, N.H., Peacock, M.A., and Epstein, L.B. (1986). Abnormalities of the in vitro cellular and humoral responses to tetanus and influenza antigens with concomitant numerical alterations in lymphocyte subsets in Down syndrome (trisomy 21). J Immunol *136*, 1661-1667.

Pimanda, J.E., Ottersbach, K., Knezevic, K., Kinston, S., Chan, W.Y., Wilson, N.K., Landry, J.R., Wood, A.D., Kolb-Kokocinski, A., Green, A.R.*, et al.* (2007). Gata2, Fli1, and Scl form a recursively wired gene-regulatory circuit during early hematopoietic development. Proc Natl Acad Sci U S A *104*, 17692-17697.

Prandini, P., Deutsch, S., Lyle, R., Gagnebin, M., Delucinge Vivier, C., Delorenzi, M., Gehrig, C., Descombes, P., Sherman, S., Dagna Bricarelli, F.*, et al.* (2007). Natural gene-expression variation in Down syndrome modulates the outcome of gene-dosage imbalance. Am J Hum Genet *81*, 252-263.

Preudhomme, C., Renneville, A., Bourdon, V., Philippe, N., Roche-Lestienne, C., Boissel, N., Dhedin, N., Andre, J.M., Cornillet-Lefebvre, P., Baruchel, A.*, et al.* (2009). High frequency of RUNX1 biallelic alteration in acute myeloid leukemia secondary to familial platelet disorder. Blood *113*, 5583-5587.

Preudhomme, C., Warot-Loze, D., Roumier, C., Grardel-Duflos, N., Garand, R., Lai, J.L., Dastugue, N., Macintyre, E., Denis, C., Bauters, F.*, et al.* (2000). High incidence of biallelic point mutations in the Runt domain of the AML1/PEBP2 alpha B gene in Mo acute myeloid leukemia and in myeloid malignancies with acquired trisomy 21. Blood *96*, 2862-2869.

Pui, C.H., Raimondi, S.C., Borowitz, M.J., Land, V.J., Behm, F.G., Pullen, D.J., Hancock, M.L., Shuster, J.J., Steuber, C.P., Crist, W.M.*, et al.* (1993). Immunophenotypes and karyotypes of leukemic cells in children with Down syndrome and acute lymphoblastic leukemia. J Clin Oncol *11*, 1361-1367.

Purton, L.E., and Scadden, D.T. (2007). Limiting factors in murine hematopoietic stem cell assays. Cell Stem Cell *1*, 263-270.

Rahmani, Z., Blouin, J.L., Creau-Goldberg, N., Watkins, P.C., Mattei, J.F., Poissonnier, M., Prieur, M., Chettouh, Z., Nicole, A., Aurias, A.*, et al.* (1989). Critical role of the D21S55 region on chromosome 21 in the pathogenesis of Down syndrome. Proc Natl Acad Sci U S A *86*, 5958-5962.

Rainis, L., Toki, T., Pimanda, J.E., Rosenthal, E., Machol, K., Strehl, S., Gottgens, B., Ito, E., and Izraeli, S. (2005). The proto-oncogene ERG in megakaryoblastic leukemias. Cancer Res *65*, 7596-7602.

Ravid, K., Lu, J., Zimmet, J.M., and Jones, M.R. (2002). Roads to polyploidy: the megakaryocyte example. J Cell Physiol *190*, 7-20.

Ravindranath, Y. (2005). Down syndrome and leukemia: new insights into the epidemiology, pathogenesis, and treatment. Pediatr Blood Cancer *44*, 1-7.

Redon, R., Ishikawa, S., Fitch, K.R., Feuk, L., Perry, G.H., Andrews, T.D., Fiegler, H., Shapero, M.H., Carson, A.R., Chen, W.*, et al.* (2006). Global variation in copy number in the human genome. Nature *444*, 444-454.

Reeves, R.H., Irving, N.G., Moran, T.H., Wohn, A., Kitt, C., Sisodia, S.S., Schmidt, C., Bronson, R.T., and Davisson, M.T. (1995). A mouse model for Down syndrome exhibits learning and behaviour deficits. Nat Genet *11*, 177-184.

Rex, A.P., and Preus, M. (1982). A diagnostic index for Down syndrome. J Pediatr *100*, 903-906.

Rhodes, K.E., Gekas, C., Wang, Y., Lux, C.T., Francis, C.S., Chan, D.N., Conway, S., Orkin, S.H., Yoder, M.C., and Mikkola, H.K. (2008). The emergence of hematopoietic stem cells is initiated in the placental vasculature in the absence of circulation. Cell Stem Cell *2*, 252-263.

Richtsmeier, J.T., Baxter, L.L., and Reeves, R.H. (2000). Parallels of craniofacial maldevelopment in Down syndrome and Ts65Dn mice. Dev Dyn *217*, 137-145.

Roizen, N.J., and Patterson, D. (2003). Down's syndrome. Lancet *361*, 1281-1289.

Romeo, P.H., Prandini, M.H., Joulin, V., Mignotte, V., Prenant, M., Vainchenker, W., Marguerie, G., and Uzan, G. (1990). Megakaryocytic and erythrocytic lineages share specific transcription factors. Nature *344*, 447-449.

Ronan, A., Fagan, K., Christie, L., Conroy, J., Nowak, N.J., and Turner, G. (2007). Familial 4.3 Mb duplication of 21q22 sheds new light on the Down syndrome critical region. J Med Genet *44*, 448-451.

Rosenbauer, F., and Tenen, D.G. (2007). Transcription factors in myeloid development: balancing differentiation with transformation. Nat Rev Immunol *7*, 105-117.

Sago, H., Carlson, E.J., Smith, D.J., Kilbridge, J., Rubin, E.M., Mobley, W.C., Epstein, C.J., and Huang, T.T. (1998). Ts1Cje, a partial trisomy 16 mouse model for Down syndrome, exhibits learning and behavioral abnormalities. Proc Natl Acad Sci U S A *95*, 6256-6261.

Sago, H., Carlson, E.J., Smith, D.J., Rubin, E.M., Crnic, L.S., Huang, T.T., and Epstein, C.J. (2000). Genetic dissection of region associated with behavioral abnormalities in mouse models for Down syndrome. Pediatr Res *48*, 606-613.

Sakai, E., Kitajima, K., Sato, A., and Nakano, T. (2009). Increase of hematopoietic progenitor and suppression of endothelial gene expression by Runx1 expression during in vitro ES differentiation. Exp Hematol *37*, 334-345.

Salek-Ardakani, S., Smooha, G., de Boer, J., Sebire, N.J., Morrow, M., Rainis, L., Lee, S., Williams, O., Izraeli, S., and Brady, H.J. (2009). ERG is a megakaryocytic oncogene. Cancer Res *69*, 4665-4673.

Sanchez-Font, M.F., Bosch-Comas, A., Gonzalez-Duarte, R., and Marfany, G. (2003). Overexpression of FABP7 in Down syndrome fetal brains is associated with PKNOX1 gene-dosage imbalance. Nucleic Acids Res *31*, 2769-2777.

Satge, D., Sasco, A.J., and Lacour, B. (2003). Are solid tumours different in children with Down's syndrome? Int J Cancer *106*, 297-298.

Sato, T., Toki, T., Kanezaki, R., Xu, G., Terui, K., Kanegane, H., Miura, M., Adachi, S., Migita, M., Morinaga, S.*, et al.* (2008). Functional analysis of JAK3 mutations in transient myeloproliferative disorder and acute megakaryoblastic leukaemia accompanying Down syndrome. Br J Haematol *141*, 681-688.

Savage, A.R., Petersen, M.B., Pettay, D., Taft, L., Allran, K., Freeman, S.B., Karadima, G., Avramopoulos, D., Torfs, C., Mikkelsen, M.*, et al.* (1998). Elucidating the mechanisms of paternal non-disjunction of chromosome 21 in humans. Hum Mol Genet *7*, 1221-1227.

Scholl, T., Stein, Z., and Hansen, H. (1982). Leukemia and other cancers, anomalies and infections as causes of death in Down's syndrome in the United States during 1976. Dev Med Child Neurol *24*, 817-829.

Schuringa, J.J., Wu, K., Morrone, G., and Moore, M.A. (2004). Enforced activation of STAT5A facilitates the generation of embryonic stem-derived hematopoietic stem cells that contribute to hematopoiesis in vivo. Stem Cells *22*, 1191-1204.

Scott, L.M., Tong, W., Levine, R.L., Scott, M.A., Beer, P.A., Stratton, M.R., Futreal, P.A., Erber, W.N., McMullin, M.F., Harrison, C.N.*, et al.* (2007). JAK2 exon 12 mutations in polycythemia vera and idiopathic erythrocytosis. N Engl J Med *356*, 459-468.

Shaffer, L.G., Jackson-Cook, C.K., Stasiowski, B.A., Spence, J.E., and Brown, J.A. (1992). Parental origin determination in thirty de novo Robertsonian translocations. Am J Med Genet *43*, 957-963.

Shaikh, T.H., Gai, X., Perin, J.C., Glessner, J.T., Xie, H., Murphy, K., O'Hara, R., Casalunovo, T., Conlin, L.K., D'Arcy, M.*, et al.* (2009). High-resolution mapping and analysis of copy number variations in the human genome: A data resource for clinical and research applications. Genome Res. *9* (9),1682-90.

Sherman, S.L., Freeman, S.B., Allen, E.G., and Lamb, N.E. (2005). Risk factors for nondisjunction of trisomy 21. Cytogenet Genome Res *111*, 273-280.

Sherman, S.L., Petersen, M.B., Freeman, S.B., Hersey, J., Pettay, D., Taft, L., Frantzen, M., Mikkelsen, M., and Hassold, T.J. (1994). Non-disjunction of chromosome 21 in maternal meiosis I: evidence for a maternal age-dependent mechanism involving reduced recombination. Hum Mol Genet *3*, 1529-1535.

Sherman, S.L., Takaesu, N., Freeman, S.B., Grantham, M., Phillips, C., Blackston, R.D., Jacobs, P.A., Cockwell, A.E., Freeman, V., Uchida, I.*, et al.* (1991). Trisomy 21: association between reduced recombination and nondisjunction. Am J Hum Genet *49*, 608-620.

Shi, S.R., Datar, R., Liu, C., Wu, L., Zhang, Z., Cote, R.J., and Taylor, C.R. (2004). DNA extraction from archival formalin-fixed, paraffin-embedded tissues: heat-induced retrieval in alkaline solution. Histochem Cell Biol *122*, 211-218.

Shivdasani, R.A., Fujiwara, Y., McDevitt, M.A., and Orkin, S.H. (1997). A lineage-selective knockout establishes the critical role of transcription factor GATA-1 in megakaryocyte growth and platelet development. EMBO J *16*, 3965-3973.

Simon, M.C., Pevny, L., Wiles, M.V., Keller, G., Costantini, F., and Orkin, S.H. (1992). Rescue of erythroid development in gene targeted GATA-1- mouse embryonic stem cells. Nat Genet *1*, 92-98.

Smith, D.J., Stevens, M.E., Sudanagunta, S.P., Bronson, R.T., Makhinson, M., Watabe, A.M., O'Dell, T.J., Fung, J., Weier, H.U., Cheng, J.F.*, et al.* (1997). Functional screening of 2 Mb of human chromosome 21q22.2 in transgenic mice implicates minibrain in learning defects associated with Down syndrome. Nat Genet *16*, 28-36.

Song, W.J., Sullivan, M.G., Legare, R.D., Hutchings, S., Tan, X., Kufrin, D., Ratajczak, J., Resende, I.C., Haworth, C., Hock, R.*, et al.* (1999). Haploinsufficiency of CBFA2 causes familial thrombocytopenia with propensity to develop acute myelogenous leukaemia. Nat Genet *23*, 166-175.

Stankiewicz, M.J., and Crispino, J.D. (2009). ETS2 and ERG promote megakaryopoiesis and synergize with alterations in GATA-1 to immortalize hematopoietic progenitor cells. Blood *113*, 3337-3347.

Suh, M.R., Lee, Y., Kim, J.Y., Kim, S.K., Moon, S.H., Lee, J.Y., Cha, K.Y., Chung, H.M., Yoon, H.S., Moon, S.Y.*, et al.* (2004). Human embryonic stem cells express a unique set of microRNAs. Dev Biol *270*, 488-498.

Sultan, M., Piccini, I., Balzereit, D., Herwig, R., Saran, N.G., Lehrach, H., Reeves, R.H., and Yaspo, M.L. (2007). Gene expression variation in Down's syndrome mice allows prioritization of candidate genes. Genome Biol *8*, R91.

Sussan, T.E., Yang, A., Li, F., Ostrowski, M.C., and Reeves, R.H. (2008). Trisomy represses Apc(Min)-mediated tumours in mouse models of Down's syndrome. Nature *451*, 73-75.

Taub, J.W., Huang, X., Matherly, L.H., Stout, M.L., Buck, S.A., Massey, G.V., Becton, D.L., Chang, M.N., Weinstein, H.J., and Ravindranath, Y. (1999). Expression of chromosome 21-localized genes in acute myeloid leukemia: differences between Down syndrome and non-Down syndrome blast cells and relationship to in vitro sensitivity to cytosine arabinoside and daunorubicin. Blood *94*, 1393-1400.

Taub, J.W., Mundschau, G., Ge, Y., Poulik, J.M., Qureshi, F., Jensen, T., James, S.J., Matherly, L.H., Wechsler, J., and Crispino, J.D. (2004). Prenatal origin of GATA1 mutations may be an initiating step in the development of megakaryocytic leukemia in Down syndrome. Blood *104*, 1588-1589.

Tchernia, G., Lejeune, F., Boccara, J.F., Denavit, M.F., Dommergues, J.P., and Bernaudin, F. (1996). Erythroblastic and/or megakaryoblastic leukemia in Down syndrome: treatment with low-dose arabinosyl cytosine. J Pediatr Hematol Oncol *18*, 59-62.

Teller, J.K., Russo, C., DeBusk, L.M., Angelini, G., Zaccheo, D., Dagna-Bricarelli, F., Scartezzini, P., Bertolini, S., Mann, D.M., Tabaton, M.*, et al.* (1996). Presence of soluble amyloid beta-peptide precedes amyloid plaque formation in Down's syndrome. Nat Med *2*, 93-95.

Templado, C., Bosch, M., and Benet, J. (2005). Frequency and distribution of chromosome abnormalities in human spermatozoa. Cytogenet Genome Res *111*, 199-205.

Teyssier-Le Discorde, M., Prost, S., Nandrot, E., and Kirszenbaum, M. (1999). Spatial and temporal mapping of c-kit and its ligand, stem cell factor expression during human embryonic haemopoiesis. Br J Haematol *107*, 247-253.

Thaline, H.C., Pueschel, S.M. (1982). Cytogenetics in Down syndrome. In: Down Syndrome Advances in Biomedicine and the Behavioural Sciences R. S. M. Pueschel, J.E., Ware Press ed., p.133.

Toki, T., Katsuoka, F., Kanezaki, R., Xu, G., Kurotaki, H., Sun, J., Kamio, T., Watanabe, S., Tandai, S., Terui, K.*, et al.* (2005). Transgenic expression of BACH1 transcription factor results in megakaryocytic impairment. Blood *105*, 3100-3108.

Tomizuka, K., Yoshida, H., Uejima, H., Kugoh, H., Sato, K., Ohguma, A., Hayasaka, M., Hanaoka, K., Oshimura, M., and Ishida, I. (1997). Functional expression and germline transmission of a human chromosome fragment in chimaeric mice. Nat Genet *16*, 133-143.

Tsai, F.Y., Keller, G., Kuo, F.C., Weiss, M., Chen, J., Rosenblatt, M., Alt, F.W., and Orkin, S.H. (1994). An early haematopoietic defect in mice lacking the transcription factor GATA-2. Nature *371*, 221-226.

Tsai, F.Y., and Orkin, S.H. (1997). Transcription factor GATA-2 is required for proliferation/survival of early hematopoietic cells and mast cell formation, but not for erythroid and myeloid terminal differentiation. Blood *89*, 3636-3643.

Tunstall-Pedoe, O., Roy, A., Karadimitris, A., de la Fuente, J., Fisk, N.M., Bennett, P., Norton, A., Vyas, P., and Roberts, I. (2008). Abnormalities in the myeloid progenitor compartment in Down syndrome fetal liver precede acquisition of GATA1 mutations. Blood *112*, 4507-4511.

Ugazio, A.G., Maccario, R., Notarangelo, L.D., and Burgio, G.R. (1990). Immunology of Down syndrome: a review. Am J Med Genet Suppl *7*, 204-212.

Vainchenker, W., Dusa, A., and Constantinescu, S.N. (2008). JAKs in pathology: role of Janus kinases in hematopoietic malignancies and immunodeficiencies. Semin Cell Dev Biol *19*, 385-393.

Vyas, P., Ault, K., Jackson, C.W., Orkin, S.H., and Shivdasani, R.A. (1999). Consequences of GATA-1 deficiency in megakaryocytes and platelets. Blood *93*, 2867-2875.

Walters, D.K., Mercher, T., Gu, T.L., O'Hare, T., Tyner, J.W., Loriaux, M., Goss, V.L., Lee, K.A., Eide, C.A., Wong, M.J.*, et al.* (2006). Activating alleles of JAK3 in acute megakaryoblastic leukemia. Cancer Cell *10*, 65-75.

Wang, J., Rao, S., Chu, J., Shen, X., Levasseur, D.N., Theunissen, T.W., and Orkin, S.H. (2006). A protein interaction network for pluripotency of embryonic stem cells. Nature *444*, 364-368.

Wang, Q., Stacy, T., Binder, M., Marin-Padilla, M., Sharpe, A.H., and Speck, N.A. (1996). Disruption of the Cbfa2 gene causes necrosis and hemorrhaging in the central nervous system and blocks definitive hematopoiesis. Proc Natl Acad Sci U S A *93*, 3444-3449.

Wang, Y., Mulligan, C., Denyer, G., Delom, F., Dagna-Bricarelli, F., Tybulewicz, V.L., Fisher, E.M., Griffiths, W.J., Nizetic, D., and Groet, J. (2009). Quantitative proteomics characterization of a mouse embryonic stem cell model of Down syndrome. Mol Cell Proteomics *8*, 585-595.

Ward, O.C. (1999). John Langdon Down: the man and the message. Downs Syndr Res Pract *6*, 19-24.

Wechsler, J., Greene, M., McDevitt, M.A., Anastasi, J., Karp, J.E., Le Beau, M.M., and Crispino, J.D. (2002). Acquired mutations in GATA1 in the megakaryoblastic leukemia of Down syndrome. Nat Genet *32*, 148-152.

Weisel, K.C., Gao, Y., Shieh, J.H., and Moore, M.A. (2006). Stromal cell lines from the aorta-gonado-mesonephros region are potent supporters of murine and human hematopoiesis. Exp Hematol *34*, 1505-1516.

Weissman, I.L., Anderson, D.J., and Gage, F. (2001). Stem and progenitor cells: origins, phenotypes, lineage commitments, and transdifferentiations. Annu Rev Cell Dev Biol *17*, 387-403.

Whyatt, D., Lindeboom, F., Karis, A., Ferreira, R., Milot, E., Hendriks, R., de Bruijn, M., Langeveld, A., Gribnau, J., Grosveld, F*., et al.* (2000). An intrinsic but cell-nonautonomous defect in GATA-1-overexpressing mouse erythroid cells. Nature *406*, 519-524.

Whyatt, D.J., Karis, A., Harkes, I.C., Verkerk, A., Gillemans, N., Elefanty, A.G., Vairo, G., Ploemacher, R., Grosveld, F., and Philipsen, S. (1997). The level of the tissue-specific factor GATA-1 affects the cell-cycle machinery. Genes Funct *1*, 11-24.

Wiles, M.V., and Keller, G. (1991). Multiple hematopoietic lineages develop from embryonic stem (ES) cells in culture. Development *111*, 259-267.

Williams, R.S., and Matthysse, S. (1986). Age-related changes in Down syndrome brain and the cellular pathology of Alzheimer disease. Prog Brain Res *70*, 49-67.

Wilson, A., Murphy, M.J., Oskarsson, T., Kaloulis, K., Bettess, M.D., Oser, G.M., Pasche, A.C., Knabenhans, C., Macdonald, H.R., and Trumpp, A. (2004). c-Myc controls the balance between hematopoietic stem cell self-renewal and differentiation. Genes Dev *18*, 2747-2763.

Wilson, M.D., Barbosa-Morais, N.L., Schmidt, D., Conboy, C.M., Vanes, L., Tybulewicz, V.L., Fisher, E.M., Tavare, S., and Odom, D.T. (2008). Species-specific transcription in mice carrying human chromosome 21. Science *322*, 434-438.

Wiseman, F.K., Alford, K.A., Tybulewicz, V.L., and Fisher, E.M. (2009). Down syndrome--recent progress and future prospects. Hum Mol Genet *18*, R75-83.

Wisniewski, K.E., Dalton, A.J., McLachlan, C., Wen, G.Y., and Wisniewski, H.M. (1985). Alzheimer's disease in Down's syndrome: clinicopathologic studies. Neurology *35*, 957-961.

Wolf, D., and Goff, S.P. (2009). Embryonic stem cells use ZFP809 to silence retroviral DNAs. Nature *458*, 1201-1204.

Yamamoto, N., Uzawa, K., Yakushiji, T., Shibahara, T., Noma, H., and Tanzawa, H. (2001). Analysis of the ANA gene as a candidate for the chromosome 21q oral cancer susceptibility locus. Br J Cancer *84*, 754-759.

Yamamoto, T., Isomura, M., Xu, Y., Liang, J., Yagasaki, H., Kamachi, Y., Kudo, K., Kiyoi, H., Naoe, T., and Kojma, S. (2006). PTPN11, RAS and FLT3 mutations in childhood acute lymphoblastic leukemia. Leuk Res *30*, 1085-1089.

Yanagida, M., Osato, M., Yamashita, N., Liqun, H., Jacob, B., Wu, F., Cao, X., Nakamura, T., Yokomizo, T., Takahashi, S*., et al.* (2005). Increased dosage of Runx1/AML1 acts as a positive modulator of myeloid leukemogenesis in BXH2 mice. Oncogene *24*, 4477-4485.

Yang, Q., Rasmussen, S.A., and Friedman, J.M. (2002). Mortality associated with Down's syndrome in the USA from 1983 to 1997: a population-based study. Lancet *359*, 1019-1025.

Yang, S., Delgado, R., King, S.R., Woffendin, C., Barker, C.S., Yang, Z.Y., Xu, L., Nolan, G.P., and Nabel, G.J. (1999). Generation of retroviral vector for clinical studies using transient transfection. Hum Gene Ther *10*, 123-132.

Zhang, W.J., Park, C., Arentson, E., and Choi, K. (2005). Modulation of hematopoietic and endothelial cell differentiation from mouse embryonic stem cells by different culture conditions. Blood *105*, 111-114.

Zipursky, A. (2003). Transient leukaemia--a benign form of leukaemia in newborn infants with trisomy 21. Br J Haematol *120*, 930-938.

Zipursky, A., Poon, A., and Doyle, J. (1992). Leukemia in Down syndrome: a review. Pediatr Hematol Oncol *9*, 139-149.

Zon, L.I., Yamaguchi, Y., Yee, K., Albee, E.A., Kimura, A., Bennett, J.C., Orkin, S.H., and Ackerman, S.J. (1993). Expression of mRNA for the GATA-binding proteins in human eosinophils and basophils: potential role in gene transcription. Blood *81*, 3234-3241.

Zwaan, C.M., Kaspers, G.J., Pieters, R., Ramakers-Van Woerden, N.L., den Boer, M.L., Wunsche, R., Rottier, M.M., Hahlen, K., van Wering, E.R., Janka-Schaub, G.E.*, et al.* (2000). Cellular drug resistance profiles in childhood acute myeloid leukemia: differences between FAB types and comparison with acute lymphoblastic leukemia. Blood *96*, 2879-2886.
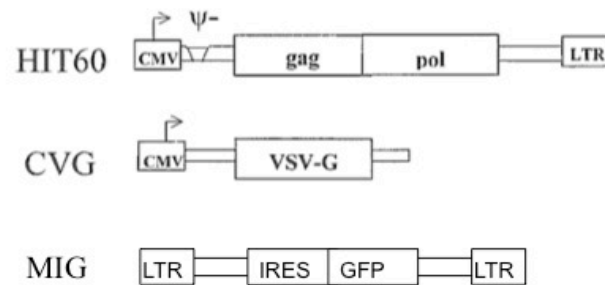
6. Appendix

6.1. Vectors, plasmids and oligos

The GATA-1s-MSCV construct was generated by cloning FLAG-tagged GATA-1s into the BglII and XhoI site of the MSCV-PURO (mouse stem cell virus) retroviral vector (Clontech). Map of the vector is provided below.
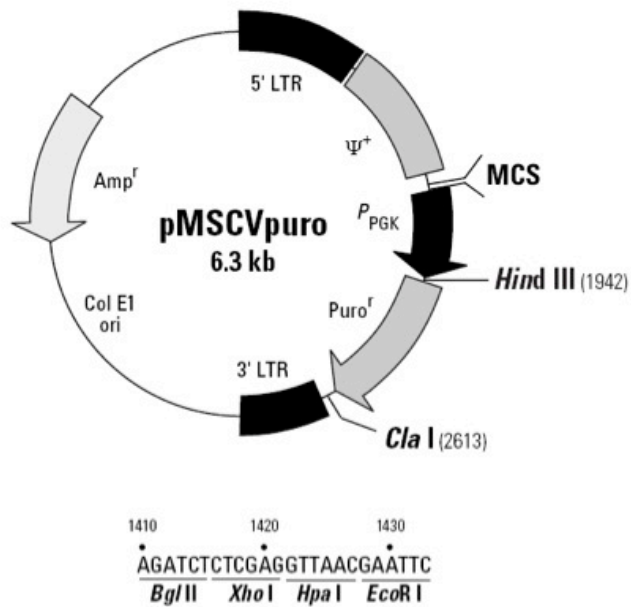
A schematic view of the constructs used for the optimization of the transduction protocol is provided below.

Plasmids HIT60 and CVG encode the viral components gag-pol and env, respectively. They were employed in the triple transfection approach in combination with the retroviral vector MSCV-IRES-GFP (MIG). MIG was derived from the MSCV backbone by replacing the puromycin resistance cassette with a green fluorescent protein (GFP) tag.

Target sequences for the hRUNX-1 oligos used in the RNAi experiments were as follows:

RUNX-1/1 GACAUCGGCAGAAACUAGA

RUNX-1/2 CACCGCAAGUCGCCACCUA

RUNX-1/3 CAAAUUGAAAUGACGGUAU

RUNX-1/4 GGCGAUAGGUCUCACGCAA

Sequence for the control (non-targeting) RNAi was:

UAAUGUAUUGGAACGCAUATT

6.2. List of units and abbreviations

μg	Microgram
μl	Microlitre
μM	Micromolar
μm	Micron
ACHE	Acetylcholinesterase
AD	Alzheimer disease
ALL	acute lymphocytic leukaemia
AMKL	acute megakaryocytic leukaemia
AML	acute myeloid leukaemia
AGM	aorta-gonad-mesonephros
APC	Allophycocyanin
AV	Atrioventricular
APC	adenomatous polyposis coli
BAC	bacterial artificial chromosome
BACH-1	basic leucine zipper transcription factor 1
BM	bone marrow
bp	base pair
CBS	cystathionine β-synthase
cDNA	Complementary DNA
CFU	colony forming unit
CFU-E	colony forming unit erythroid
CFU-GM	colony forming unit granulocyte-macrophage
CFU-GEMM	colony forming unit granulocyte-erythrocyte-monocyte-megakaryocyte
CFU-MK	colony forming unit megakaryocytes
CLP	common lymphoid progenitor
CMP	common myeloid progenitor
CNS	central nervous system
Ct	cycle threshold
DAB	3,3 diaminobenzidine
del	Deletion
DEPC	diethyl pyrocarbonate
DMEM	Dulbecco's modified Eagle's medium
dNTPS	deoxynucleotides
DNA	deoxyribonucleic acid
DS	Down syndrome
DSCR	Down syndrome critical region
DSCR1	Down syndrome critical region 1
DTT	Dithiothreitol
dup	Duplication
DYRK1A	dual-specificity tyrosine phosphorylation-regulated kinase 1A
E	embryonic day
EB	embryoid body
ECM	extracellular matrix
ENU	N-ethyl-N-nitrosurea
EPO	Erythropoietin
EpoR	erythropoietin receptor
eQTL	Expression Quantitative Trait Locus
ES cell	embryonic stem cell
EST	expressed sequence tag

EtOH	Ethanol
FACS	fluorescence-activated cell sorter
FISH	fluorescent in situ hybridization
FAM	5-carboxyfluorescein
FCS	foetal calf serum
FFPE	Formalin fixed paraffin embedded
FITC	fluorescein isothiocyanate
FWD	Forward
FL	foetal liver
FLK-1	foetal liver kinase 1
G	Gram
G418	Geneticin
GAPDH	Glyceraldehyde-3-phosphate dehydrogenase
GATA-1	GATA-binding protein 1
GATA-2	GATA-binding protein 2
GFP	green fluorescent protein
GMP	granulocyte-macrophage progenitor
H&E	Haematoxylin and Eosin
HF	Hydrops foetalis
Hr	Hour
HRP	Horse radish peroxydase
HSA	human chromosome
HSC	Haematopoietic stem cell
HPC	Haematopoietic progenitor cell
ICM	inner cell mass
IL	Interleukin
JAK	Januse kinase
KDa	Kilodalton
LIF	leukaemia inhibitory factor
LOH	loss of heterozygosity
LTP	long-term potentiation
M	Molar
M-CSF	macrophage colony-stimulating factor
Mb	mega base pair
MDS	myelodysplastic syndrome
MEP	megakaryocyte-erythroid progenitor
Mg	Milligram
Min(s)	minute(s)
MK	Megakaryocyte
mM	Millimolar
mm^2	millimetre square
MMU	mouse chromosome
mRNA	messenger RNA
MSCV	murine stem cell virus
NaOAC	sodium acetate
Neo	neomycin
ng	Nanogram
nM	Nanomolar
NSCLC	non-small cell lung carcinoma
ºC	Degrees Celsius
OCT-4	Octamer-binding transcription factor 4
pp^2	square pixel
PB	peripheral blood

PBS	phosphate-buffered saline
PCR	polymerase chain reaction
PEG	polyethylene glycol
PI	propidium iodide
Q-PCR	quantitative PCR
rER	rough endoplasmic reticulum
REST	RE1-silencing transcription factor
REV	Reverse
RNA	ribonucleic acid
RT	room temperature
RT-PCR	reverse transcription-polymerase chain reaction
SDS	sequence detection system
sec(s)	second(s)
s.e.m.	standard error of the mean
SOD1	superoxide dismutase 1
T	Translocation
t21	trisomy 21
TC	tissue culture
TF	transcription factor
TL	transient leukaemia
TIAM1	T-cell lymphoma invasion and metastasis-1
TIE-2	endothelium-specific receptor tyrosine kinase 2
TK	Tyrosine kinase
Tm	melting temperature
TMD	transient myeloproliferative disorder
tRNA	transfer RNA
TPO	Thrombopoietin
TSG	tumour suppressor gene
U	Unit
UV	Ultraviolet
vWF	von Willebrand Factor
WB	western blotting
YAC	yeast artificial chromosome
XMMCT	irradiation microcell-mediated chromosome transfer

6.3. Publications

231

The two first-author publications reported in this appendix were produced between June 2006 and the time of submission of this thesis and were obtained from work carried out toward the completion of my PhD at Queen Mary, University of London.

Loss-of-function *JAK3* mutations in TMD and AMKL of Down syndrome

Serena De Vita,[1] Claire Mulligan,[1] Suzanne McElwaine,[1] Franca Dagna-Bricarelli,[2] Monica Spinelli,[3] Giuseppe Basso,[3] Dean Nizetic[1] and Jürgen Groet[1]

[1]Centre for Haematology, Institute of Cell and Molecular Science, Barts & The London, Queen Mary's School of Medicine, University of London, London, UK, [2]Human Genetics Institute, Galliera Hospital, Genoa, Italy, and [3]Italian National Association for Paediatric Haemato-Oncology (AIEOP), Department of Paediatrics, Faculty of Medicine, University of Padua, Padua, Italy

Summary

Acquired mutations activating Janus kinase 3 (jak3) have been reported in Down syndrome (DS) and non-DS patients with acute megakaryoblastic leukaemia (AMKL). This highlighted jak3-activation as an important event in the pathogenesis of AMKL, and predicted inhibitors of jak3 as conceptual therapeutics for AMKL. Of 16 DS-transient myeloproliferative disorder (TMD)/AMKL patients tested, seven showed *JAK3* mutations. Three mutations deleted the kinase (JH1) domain, abolishing the main function of jak3. Another patient displayed a mutation identical to a previously reported inherited loss-of-function causing severe combined immunodeficiency. Our data suggest that both gain-, and loss-of function mutations of jak3 can be acquired in DS-TMD/AMKL.

Keywords: myeloproliferative disorder, tyrosine kinase, Janus kinase 3, Down syndrome, acute megakaryoblastic leukaemia.

Megakaryoblastic leukaemia occurring in Down Syndrome (DS) children appears in two forms: a self-regressing, pre-leukaemic hyperproliferative state known as transient myeloproliferative disorder (TMD) affecting 10% of DS neonates, and the progressive and potentially lethal acute megakaryoblastic leukaemia (AMKL), which develops in 20–30% of TMD patients 1–3 years later (Hitzler & Zipursky, 2005; Muntean *et al*, 2006). As such, this disease represents an interesting system for understanding the pathogenesis and progression of myeloid leukaemias in general. A combination of trisomy 21 and acquired mutations in *GATA1*, eliminating its full length product, have been reported to co-exist in the proliferating cells of all patients with this type of leukaemia (Wechsler *et al*, 2002; Groet *et al*, 2003). Factors that predispose 10% of DS to this disease, factors that predispose a third of the TMD patients to AMKL, and additional molecular events that are necessary for progression from TMD to AMKL remain largely unknown (McElwaine *et al*, 2004; Hitzler & Zipursky, 2005; Muntean *et al*, 2006).

Walters *et al* (2006) reported three acquired mutations in AMKL (DS and non-DS), each rendering Janus kinase3 (jak3) constitutionally active. Each of these activating mutations was capable of oncogenically transforming cells, as well as conferring features of AMKL to mice. Recently, Kiyoi *et al* (2007) found two additional AMKL patients (a DS and a non-DS) with mutations in the same domain of jak3 (JH2/ pseudokinase domain), shown to harbour activating mutations. They also reported a single DS-TMD patient with a mutation in the JH7 domain, the functional consequences of which were not examined. Although representing a limited number of patients, taken together, these data propose jak3-activation as an important event in the pathogenesis of AMKL, compatible with acting as one of the possible 'second hits' leading to progression from TMD to AMKL. Selective chemical inhibitors of jak3, already in clinical use as immunosuppressives (Changelian *et al*, 2003), have therefore been proposed as a therapeutic concept for AMKL (Walters *et al*, 2006).

Methods

Patients and samples

The project was approved by the ethical committee of the North East London Strategic Health Authority. Samples were

surplus clinical, or archived clinical material collected by the tissue bank of the Italian National Association for Paediatric Haematology-Oncology (AIEOP) and the Italian National Down's Syndrome Association, (CEPIM), (samples kept by the team of Galliera Genetic Bank, http://ggb.galliera.it/). Informed written consent was obtained by the tissue banks for all subjects. Other details about the samples used, including methods for genomic DNA extraction, RNA extraction and cDNA synthesis were previously published (Groet *et al*, 2003; McElwaine *et al*, 2004; Groet *et al*, 2005).

Polymerase chain reaction amplification, sequencing and sequence analysis

Amplification of the exons of *JAK3* we performed by polymerase chain reaction (PCR) with 5–10 ng of genomic (g)DNA using 15 pairs of primers as indicated in Table SIA. Reverse transcription (RT)-PCR was performed with 1 μl of random primed cDNA using five pairs of overlapping primers, spanning the *JAK3* coding sequence (Table SIB). PCR conditions were: 7·5 min at 95°C; 35 cycles of 0·5 min at 95°C, 0·5 min at 58°C and 1 min at 72°C; followed by 9 min at 72°C. Cycle sequencing was performed with an ABI BigDye terminator V3·1 using an ABI3130XL automated sequencer (Applied Biosystems, Foster City, CA, USA). Selected PCR products were cloned using the TA cloning kit (Invitrogen, Carlsbad, CA, USA) according to manufacturer's recommendations, and their sequence was verified as above.

Results

The sequence of *JAK3* was analysed in presentation samples of eight DS-TMD and eight DS-AMKL patients. Patient details and results are summarised in Table I. gDNA was available for three TMD patients and two AMKL patients. In these samples, all exons of *JAK3* sequenced and were all wild-type (Table I). The remaining patient presentation samples ($n = 11$) were available as cDNA. In these, we found a high proportion (7/11) with mutations in the *JAK3* transcript (Table I). Interestingly, three patients (TMD3, TMD11 and AMKL4) showed a large (592 bp) deletion (see Fig 1), eliminating the most C-terminal 192 amino acids (exons 20-24). This includes the JH1 kinase domain, which is essential for the kinase function of jak3. Mutations resulting in a premature stop-codon in exon 21 were shown to completely abolish phosphorylation in a patient with severe combined immunodeficiency (SCID) (Mella *et al*, 2001) and even smaller deletions in the JH1 domain abolish the kinase activity of the protein (Lai *et al*, 1995). Another mutation in patient TMD3 (P151R) was also reported among the loss-of-function inherited mutations in patients with SCID (reviewed in O'Shea *et al*, 2004). We were unable to ascertain if the two mutations in TMD3 (C-terminal deletion and P151R) result in a compound heterozygote, or are independent mutation on the same chromosome. Patient AMKL5 showed an A573V substitution, directly adjacent to the A572V substitution reported to be an activating (gain-of-function) mutation (Walters *et al*, 2006). Two patients (TMD8 and

Patients	Material	Blast (%)	*GATA1* mutations	*JAK3* mutations
TMD1	gDNA	85	270-271ins7bp	WT
TMD2	gDNA	50	259dup34bp, 305dup4bp, 307ins8bp	WT
TMD3	cDNA	60	161C>T, STOP	P151R, 2851-3442del592
TMD6	cDNA	ND	splice Δ-exon2	P434R
TMD8	cDNA	50	344-345ins2bp	splice Δexon2-5, Δexon3-5
TMD10	cDNA	98	245-266del22bp	WT
TMD11	cDNA	78	263delG	2851-3442del592
TMD15	gDNA	20	259dup34bp	WT
AMKL1	cDNA	50	270-271ins7bp	splice Δexon3-5, Δexon3, 5
AMKL1 (rem)	cDNA	0	WT	WT
AMKL4	cDNA	40	splice Δ-exon2	2851-3442del592
AMKL5	cDNA	95	251delT	A573V
AMKL7	cDNA	60	splice Δ-exon2	WT
AMKL8	cDNA	>50	197G>T, STOP	WT
AMKL11	cDNA	50	262-263ins7bp	WT
AMKL13	gDNA	78	298-299ins5bp	WT
AMKL14	gDNA	80	285-286ins19bp	WT

Table I. Patient details and results. Presentation samples from Down syndrome patients with TMD or AMKL used in this study. The blast percentages are indicated, together with the mutations previously found in *GATA1* (for a more detailed description of these, see Groet *et al*, 2003; McElwaine *et al*, 2004; Groet *et al*, 2005). The *JAK3* mutations detected in this study are indicated in the last column.

TMD, transient myeloproliferative disorder; AMKL, acute megakaryoblastic leukaemia; rem, remission; cDNA, complementary DNA; gDNA, genomic DNA; ND, not determined; WT, wild type; ins, insertion; dup, duplication; del, deletion; Δ-exon, exons missing in the alternative splicing form.
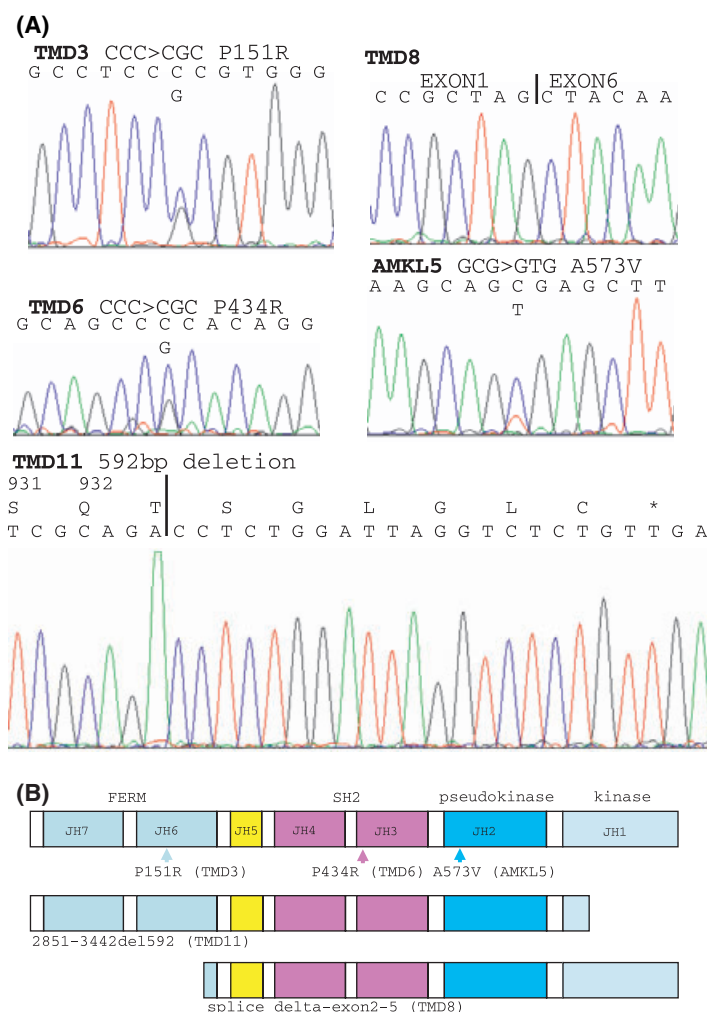
Fig 1. (A) Sequence data chromatograms from *JAK3* mutations in Down syndrome patients with transient myeloproliferative disorder (TMD) and acute megakaryoblastic leukaemia (AMKL). Patients TMD3, TMD6 and AMKL5 showed substitutions in presentation sample cDNA. In TMD8, alternative splicing removes exons 2-5 from the transcript, possibly removing 234 N-terminal amino acids. In TMD11 a 592 bp deletion removes the 192 most C-terminal amino acids. For both TMD8 and TMD11 the chromatograms are shown of the cloned RT-PCR products (RT-PCR analysis of the presentation samples shows wild-type *JAK3* sequence in addition to the mutation). (B) Predicted consequences of the mutations on the structural organisation of the jak3 protein.

AMKL1) showed alternatively spliced forms of *JAK3*, eliminating a large portion of the FERM region from the protein. The predicted start codon, for the alternatively spliced cDNAs is at amino acid position 235 in exon 6 of jak3. A remission sample of AMKL1 did not show the alternatively spliced products, indicating that this change was specific for the leukaemic clone (Table I). The large deletion and the splicing variants were confirmed by cloning and sequencing the RT-PCR products (Fig 1A shows the chromatograms of the cloned RT-PCR products for patients TMD8 and TMD11). One out of one clone showed the alternative splicing in TMD8, and one out of four clones showed the deletion in patient TMD11. In chromatograms from sequences of whole presentation samples' cDNA (not shown) the peaks of the alternatively spliced, and of the deleted product, were approximately half the height of the wild-type sequence, reflecting the

proportion of blasts in the total population. Patient TMD6 contained a P434R substitution in the SH2 domain. The function of this domain is not completely understood and binding partners have not yet been identified. All the patients had constitutional trisomy 21, and all had acquired mutations in *GATA1* (Table I, see also Groet *et al*, 2003; McElwaine *et al*, 2004; Groet *et al*, 2005).

Discussion

The Jak family is one of ten families of non-receptor tyrosine kinases. All mammals have four members of this family: jak1, jak2, jak3 and tyk2. These proteins have a C-terminal kinase domain, a catalytically inactive pseudo-kinase domain, and they bind cytokine receptors through amino-terminal FERM domains. Upon binding of cytokines to their receptors, jaks are

activated and phosphorylate downstream targets, such as members of the STAT family (Yamaoka *et al*, 2004). Loss-of-function of jak3 is the basis of autosomal SCID. Upon revision of the literature (O'Shea *et al*, 2004), we noted that, among the mutations found in SCID patients, at least one (V722I) was subsequently found to be an activating mutation (Walters *et al*, 2006). Therefore, in SCID too, the observed mutations can, in rare cases, be a gain-of-function, although by far the majority is expected to confer a loss of function. The gain-of-function mutations reported by Walters *et al* (2006) had a transforming and oncogenic effect *in vitro* and *in vivo*, and prompted the proposal of a recently developed selective small molecule inhibitor of jak3 as a therapeutic for AMKL (Changelian *et al*, 2003; Walters *et al*, 2006). Our data reveal a more complex spectrum of mutations (gain-, as well as loss-of-function), suggesting that a simple inhibition of jak3 may not be the theoretically viable approach for all DS-AMKL patients.

The apparent difference in mutation frequency between genomic DNA (0/5) and cDNA (7/11) can be explained by the fact that with the current assay set-up, only the substitutions would have been detected in genomic DNA. The number of substitutions in genomic DNA compared with cDNA was not statistically significant (0/5 and 3/11 respectively).

Taken together, our data allow several conclusions. Firstly, both gain- and loss-of-function mutations in jak3 can be seen in leukaemic samples of both DS-TMD and DS-AMKL patients. Secondly, mutations are not the 'second hit' responsible for progression of DS-TMD to DS-AMKL, as a similar spectrum of mutations is found in both groups of patients. Lastly, since 3/3 DS-TMD patients for which the relevant data were available (TMD3, TMD6 and TMD11) are all in spontaneous complete remission (for >11, >11 and >4 years respectively), past the age typical for progression to AMKL, we can conclude that their mutations were not a predictive factor as to the progression from TMD to AMKL. Our data provides additional facts, which are helpful in further elucidation of the structural and pathological consequences of alternative forms of this exciting protein.

Acknowledgements

References

Changelian, P.S., Flanagan, M.E., Ball, D.J., Kent, C.R., Magnuson, K.S., Martin, W.H., Rizzuti, B.J., Sawyer, P.S., Perry, B.D., Brissette, W.H., McCurdy, S.P., Kudlacz, E.M., Conklyn, M.J., Elliott, E.A., Koslov, E.R., Fisher, M.B., Strelevitz, T.J., Yoon, K, Whipple, D.A., Sun, J., Munchhof, M.J., Doty, J.L., Casavant, J.M., Blumenkopf, T.A., Hines, M., Brown, M.F., Lillie, B.M., Subramanyam, C., Shang-Poa, C., Milici, A.J., Beckius, G.E., Moyer, J.D., Su, C., Woodworth, T.G., Gaweco, A.S., Beals, C.R., Littman, B.H., Fisher, D.A., Smith, J.F., Zagouras, P., Magna, H.A., Saltarelli, M.J., Johnson, K.S., Nelms, L.F., Des Etages, S.G., Hayes, L.S., Kawabata, T.T., Finco-Kent, D., Baker, D.L., Larson, M., Si, M.S., Paniagua, R., Higgins, J., Holm, B., Reitz, B., Zhou, Y.J., Morris, R.E., O'Shea, J.J. & Borie, D.C. (2003) Prevention of organ allograft rejection by a specific Janus kinase 3 inhibitor. *Science*, **302**, 875–878.

Groet, J., McElwaine, S., Spinelli, M., Rinaldi, A., Burtscher, I., Mulligan, C., Mensah, A., Cavani, S., Dagna-Bricarelli, F., Basso, G., Cotter, F.E. & Nizetic, D. (2003) Acquired mutations in GATA1 in neonates with down's syndrome with transient myeloid disorder. *Lancet*, **361**, 1617–1620.

Groet, J., Mulligan, C., Spinelli, M., Serra, A., McElwaine, S., Cotter, F.E., Dagna-Bricarelli, F., Saglio, G., Basso, G. & Nizetic, D. (2005) Independent clones at separable stages of differentiation, bearing different GATA1 mutations, in the same TMD patient with Down syndrome. *Blood*, **106**, 1887–1888.

Hitzler, J.K. & Zipursky, A. (2005) Origins of leukaemia in children with Down syndrome. *Nature Reviews Cancer*, **5**, 11–20.

Kiyoi, H., Yamaji, S., Kojima, S., Naoe, T. (2007) JAK3 mutations occur in acute megakaryoblastic leukemia both in Down syndrome children and non-Down syndrome adults. *Leukemia*, **21**, 574–576.

Lai, K.S., Jin, Y., Graham, D.K., Witthuhn, B.A., Ihle, J.N., Liu, E.T. (1995) A kinase-deficient splice variant of the human JAK3 is expressed in hematopoietic and epithelial cancer cells. *Journal of Biological Chemistry*, **270**, 25028–25036.

McElwaine, S., Mulligan, C., Groet, J., Spinelli, M., Rinaldi, A., Denyer, G., Mensah, A., Cavani, S., Baldo, C., Dagna-Bricarelli, F., Hann, I., Basso, G., Cotter, F.E. & Nizetic, D. (2004) Microarray transcript profiling distinguishes the transient from the acute type of mega-karyoblastic leukaemia (M7) in Down's syndrome, revealing PRAME as a specific discriminating marker. *British Journal of Haematology*, **125**, 729–742.

Mella, P., Schumacher, R.F., Cranston, T., de Saint Basile, G., Savoldi, G. & Notarangelo, L.D. (2001) Eleven novel JAK3 mutations in patients with severe combined immunodeficiency-including the first patients with mutations in the kinase domain. *Human Mutation*, **18**, 355–356.

Muntean, A.G., Ge, Y., Taub, J.W. & Crispino, J.D. (2006) Transcription factor GATA-1 and Down syndrome leukemogenesis. *Leukemia & Lymphoma*, **47**, 986–997.

O'Shea, J.J., Husa, M., Li, D., Hofmann, S.R., Watford, W., Roberts, J.L., Buckley, R.H., Changelian, P. & Candotti, F. (2004) Jak3 and the pathogenesis of severe combined immunodeficiency. *Molecular Immunology*, **41**, 727–737.

Walters, D.K., Mercher, T., Gu, T.L., O'Hare, T., Tyner, J.W., Loriaux, M., Goss, V.L., Lee, K.A., Eide, C.A., Wong, M.J., Stoffregen, E.P., McGreevey, L., Nardone, J., Moore, S.A., Crispino, J., Boggon, T.J., Heinrich, M.C., Deininger, M.W., Polakiewicz, R.D., Gilliland, D.G. & Druker, B.J. (2006) Activating alleles of JAK3 in acute mega-karyoblastic leukemia. *Cancer Cell*, **10**, 65–75.

Wechsler, J., Greene, M., McDevitt, M.A., Anastasi, J., Karp, J.E., Le Beau, M.M. & Crispino, J.D. (2002) Acquired mutations in GATA1

in the megakaryoblastic leukemia of Down syndrome. *Nature Genetics*, **32,** 148–152.

Yamaoka, K., Saharinen, P., Pesu, M., Holt, III, V.E., Silvennoinen, O. & O'Shea, J.J. (2004) The Janus kinases (Jaks). *Genome Biology*, **5,** 253.

Supplementary material

The following supplementary material is available for this article:

Table SI (A) Shown are primer pairs used for PCR amplification from genomic DNA and subsequent sequencing.

(B) Indicates the primer pairs used in the PCR amplification of cDNA and subsequent sequencing.

This material is available as part of the online article from: http://www.blackwell-synergy.com/doi/abs/10.1111/j.1365-2141. 2007.06546.x

Please note: Blackwell Publishing are not responsible for the content or functionality of any supplementary materials supplied by the authors. Any queries (other than missing material) should be directed to the corresponding author for the article.

Thus, with regard to their known anticoagulant activities in the regulation of blood coagulation, the PZ polymorphism PZ_{R255H} and the ZPI polymorphisms ZPI_{K25R} and ZPI_{S40G} appear to be functionally identical to their respective WT counterparts. Although it is conceivable that PZ and ZPI possess additional anticoagulant properties that have not yet been discovered, our results are consistent with genetic studies, which have not identified these polymorphisms as significant risk factors for venous thrombosis (Rice et al, 2001; Van de Water et al, 2004; Corral et al, 2006).

Matthew Ndonwi
Lan Lu
Yizheng Tu
Michelle Phillips
George Broze Jr
Division of Hematology, Jewish Hospital, Washington University, Saint Louis, MO, USA.
E-mail: gbroze@im.wustl.edu

References

Corral, J., González-Conejero, R., Soria, J.M., González-Porras, J.R., Pérez-Ceballos, E., Lecumberri, R., Roldán, V., Souto, J.C., Miñano, A., Hernández-Espinosa, D., Alberca, I., Fontcuberta, J. & Vicente, V. (2006) A nonsense polymorphism in the protein Z-dependent protease inhibitor increases the risk for venous thrombosis. *Blood*, **108**, 177–183.

Han, X., Fiehler, R. & Broze, Jr, G. (1998) Isolation of protein Z-dependent plasma protease inhibitor. *Proceedings of the National Academy of Sciences of the United States of America*, **95**, 9250–9255.

Han, X., Fiehler, R. & Broze, Jr, G. (2000) Characterization of the protein Z-dependent plasma protease inhibitor. *Blood*, **96**, 3049–3055.

Kemkes-Matthes, B., Matthes, K.J., Souri, M., Koseki-Kuno, S. & Ichinose, A. (2004) R255h amino acid substitution of protein Z identified in patients with factor V Leiden mutation. *British Journal of Haematology*, **128**, 248–252.

Rice, G.I., Futers, T.S. & Grant, P.J. (2001) Identification of novel polymorphisms within the protein Z gene, haplotype distribution and linkage analysis. *Thrombosis and Haemostasis*, **85**, 1123–1124.

Tabatabai, A., Fiehler, R. & Broze, Jr, G. (2001) Protein Z circulates in plasma in a complex with protein Z-dependent protease inhibitor. *Thrombosis and Haemostasis*, **85**, 655–660.

Van de Water, N., Tan, T., Ashton, F., O'Grady, A., Day, T., Browett, P., Ockelford, P. & Harper, P. (2004) Mutations within the protein Z-dependent protease inhibitor gene are associated with venous thromboembolic disease: a new form of thrombophilia. *British Journal of Haematology*, **127**, 190–194.

Megakaryocyte hyperproliferation without *GATA1* mutation in foetal liver of a case of Down syndrome with hydrops foetalis

A higher incidence of lymphocytic and myeloid leukaemias is observed in children with Down syndrome (DS). The highest difference in relative incidence (500×) is seen for megakaryoblastic leukaemia, which appears in two forms: a self-regressing, pre-leukaemic hyperproliferative state known as transient myeloproliferative disorder (TMD), affecting 10% of DS neonates, and frank acute megakaryoblastic leukaemia (AMKL) which develops in 20–30% of TMD patients over a period of 2–4 years (Hitzler & Zipursky, 2005; Muntean et al, 2006). Trisomy 21 and *in utero* acquired mutations in *GATA1* are observed in all cases of DS-TMD and DS-AMKL, and co-exist in the proliferating myeloid cells (Wechsler et al, 2002; Groet et al, 2003). Factors that predispose 10% of DS to this disease, and additional events that are necessary for progression from TMD to AMKL, remain largely unknown (McElwaine et al, 2004; Hitzler & Zipursky, 2005). *GATA1* mutations in DS-TMD can be detected in genomic DNA from foetal livers at 18–23 weeks of gestational age (Taub et al, 2004). To date, acquired *GATA1* mutations have never been reported in neonatal TMD blasts that did not also carry a trisomy 21 (either as constitutional DS, or in individuals mosaic for trisomy 21). The role of trisomy 21 remains to be fully clarified. It appears to provide a cell-autonomous proliferative advantage for the *GATA1* mutant clones, but its possible contribution to the increased risk of occurrence of *GATA1* mutations has not been ruled out. We present an intriguing case of a perinatal hydrops foetalis (HF) in DS, with hyperproliferation of megakaryocytes in both foetal liver and spleen, without a detectable *GATA1* mutation.

The case was identified after screening the archival autopsy collection of specimens at the Dept. of Pathology, University of Split Medical School, for DS. All archived material was consented for use in research, and the project was covered by ethical approval from the North East London Health

Authority. Records showed that this female premature was delivered at 29 gestational weeks, with slight dysmorphic facial features resembling DS, and lived for less than 1 h before succumbing to severe generalised HF. Standard karyotype analysis revealed the karyotype as trisomy 21 (47XX + 21). Histopathological analysis of liver and spleen biopsies has shown numerous clusters of large, multinucleated, cells with megakaryocyte morphology in the sinusoids. Both tissues also contained a greater than normal amount of haemosiderin pigment, and a mild degree of fibrosis. There were no obvious abnormalities in morphology or number of any other cell type in liver, spleen or bone marrow (not shown). The type of

infiltrating cells was confirmed by performing an immunohistochemical analysis of archived, paraffin-embedded tissues from the liver and spleen biopsy specimens. As a control, archived foetal liver biopsy of a therapeutically terminated DS matched for sex and gestational age was used. Morphological and immunohistochemical analysis of liver sections showed numerous and widespread islands of apparent hyperproliferation of large cells, containing large cytoplasm and large, in many cases multiple nuclei (Fig 1Aa,c,e). Cells showed strongly positive staining with CD41 (Fig 1Ac,e). No such islands were visible in the gestational age-matched DS foetal liver, analysed as a comparison control (Fig 1Ab,d). Similar,
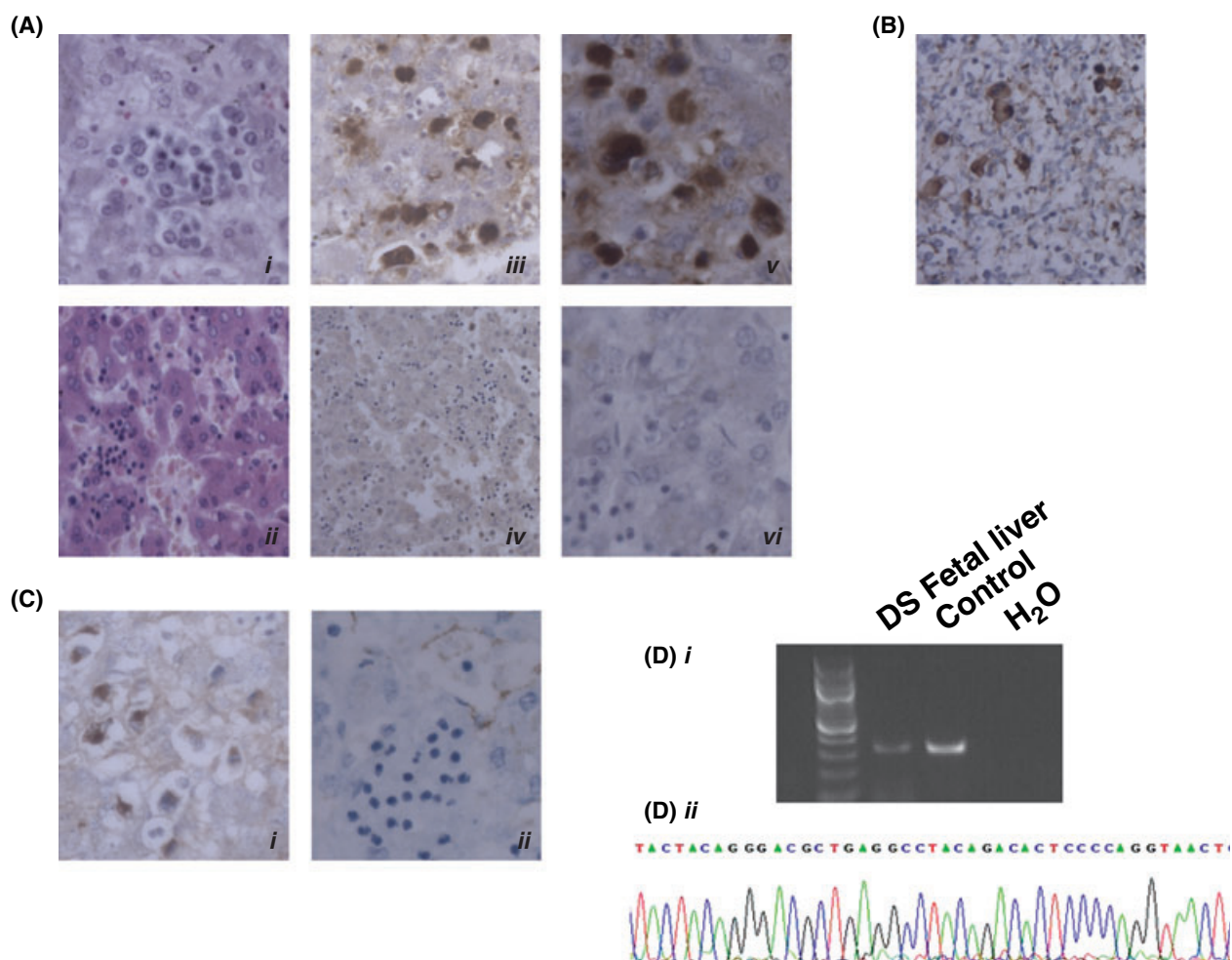

Fig 1. (A) Morphological features of the megakaryocytic hyperproliferation in the liver of the Down syndrome case prematurely born with hydrops foetalis. a,b: 400× magnification of the haemotoxylin-eosin staining of the liver specimen from the case (a); and a gestational age matched DS control foetal liver (b). c,d,e: Immunohistochemical analysis of CD41 expression (200×) in the liver of the case (c), the DS control (d) the case in greater detail (400×) (e). f: Negative control for the staining, omitting the primary antibody (liver specimen of the case at 400×). (B) Immunohistochemical analysis of CD41 expression of the spleen of the case (200×). (C) Further analysis of the hyperproliferative cells in the liver of the case for the expression of von Willebrand factor (200×) (a) and CD34 (200×) (b). Methods: After deparaffinization, 5 μm thick sections were incubated with polyclonal goat anti-CD41 (Santa Cruz, Heidelberg, Germany) (1:500 dilution), polyclonal rabbit anti-von Willebrand (Dako, Ely, UK) (1:400 dilution) and monoclonal mouse anti CD34 (Dako, Glostrup, Denmark A/S) (1:50 dilution). Immunoreactivity was developed with the Vectastain Elite ABC Kit (Vector Laboratories, Peterborough, UK). Slides not incubated with the primary antibody served as negative controls. Sections were analyzed with the Leica Application Suite software on a Leica Q5501W Microscope (Leica LTD, Heidelberg, Germany). (D) (i) Gel electrophoresis of PCR products obtained from the liver DNA with primers spanning GATA1 exon 2. (ii) Chromatogram showing part of the wild type sequence of the PCR product from (i).

though less numerous accumulations of hyperproliferating large CD41+ cells were observed in the spleen (Fig 1B). The cells from foetal liver were then analysed for the presence of Von Willebrand factor (VWF) and CD34. The large hyperproliferative cells in the case liver were found to be VWF+ (Fig 1Ca) and CD34− (Fig 1Cb). The overall picture distinguishes this case from typical DS-TMD, the vast majority of cases of which show a proliferation of immature megakaryoblasts, rarely multinucleated, which are VWF− and CD34+.

Genomic DNA was then extracted from the case's liver specimen after deparaffinization using a standard phenol–chlorophorm precipitation. Amplification of *GATA1* exon 2 (the site of all acquired DS-TMD mutations) and sequencing of both DNA strands was performed as described (Groet *et al*, 2005). The amplified product of *GATA1* exon2 was the correct length, with a completely wild type sequence that showed no signs of mutation (Fig 1D).

In summary, this is the first report of a case of HF in DS with an apparent hyperproliferation of megakaryocytes in the liver and spleen, without evidence of an acquired *GATA1* mutation. Though insufficient sensitivity to detect a low percentage cryptic *GATA1* mutation due to technical limitations remains theoretically a caveat, and conclusions based on a single case are clearly limited anyway, the possibility of a similar phenotype in a significant fraction of DS cannot be excluded at this stage. Our preliminary results on RNA from 13 random DS foetal livers (unpublished data, histological samples unavailable) identified at least two with unusually high levels of CD41 transcript, compared to matched euploid controls, while only wild type *GATA1* sequence was obtained in reverse transcription polymerase chain reaction (RT-PCR) products from all cases. HF occurs in only 7% of TMD (Gassas *et al*, 2005), and in 14% of all DS (Smrcek *et al*, 2001). In the latter study, of 79 DS subjects, 11 cases of HF were detected, and seven of those (64%) did not have TMD determined by the umbilical blood cell count. This study was performed before *GATA1* mutations in DS had been discovered.

Taken together, these data maintain the possibility that hyperproliferation of megakaryocyte-like cells could occur in DS foetal liver, without an overt TMD, in the absence of *GATA1* mutation. This hyperproliferation could be distinct from TMD, in that the cells appeared more mature. Nevertheless, it is an intriguing possibility that unknown events different from *GATA1* mutation may initiate this hyperproliferation, and that augmented megakaryopoiesis in a fraction of DS foetuses may increase the risk of acquisition of *GATA1* mutations, subsequently providing the mutated clone with a proliferative advantage over all others, causing TMD. Human chromosome 21 harbours several genes with important physiological roles in haematopoietic, particularly megakaryocytic differentiation (Rainis *et al*, 2005) (*BACH1*, *ERG*), and also a known co-operative function with *GATA1* (*RUNX1*). These (and/or other genes or other genetic elements, such as microRNAs) could play a role in altering the rate of erythroid/megakaryocytic differentiation, thereby increasing the risk of occurrence of *GATA1* mutations. Further studies are clearly needed to put these hypotheses to the test.

Acknowledgements

Serena De Vita[1]
Anny Devoy[1]
Juergen Groet[1]
Božo Krušlin[2]
Ivana Kuzmić-Prusac[3]
Dean Nižetić[1]

[1]*Institute of Cell and Molecular Science, Barts and The London, Queen Mary's School of Medicine and Dentistry, London, UK,*
[2]*Croatian Institute for Brain Research, Zagreb, Croatia, and*
[3]*Department of Pathology, University of Split Medical School, Split, Croatia.*
E-mail: d.nizetic@qmul.ac.uk

References

Gassas, A., Doyle, J.J., Weitzman, S., Freedman, M.H., Hitzler, J.K., Sharathkumar, A. & Dror, Y. (2005) A basic classification and a comprehensive examination of pediatric myeloproliferative syndromes. *Journal of Pediatric Hematology/Oncology*, **27**, 192–196.

Groet, J., McElwaine, S., Spinelli, M., Rinaldi, A., Burtscher, I., Mulligan, C., Mensah, A., Cavani, S., Dagna-Bricarelli, F., Basso, G., Cotter, F.E. & Nizetic, D. (2003) Acquired mutations in GATA1 in neonates with Down's syndrome with transient myeloid disorder. *Lancet*, **361**, 1617–1620.

Groet, J., Mulligan, C., Spinelli, M., Serra, A., McElwaine, S., Cotter, F.E., Dagna-Bricarelli, F., Saglio, G., Basso, G. & Nizetic, D. (2005) Independent clones at separable stages of differentiation, bearing different GATA1 mutations, in the same TMD patient with Down syndrome. *Blood*, **106**, 1887–1888.

Hitzler, J.K. & Zipursky, A. (2005) Origins of leukaemia in children with Down syndrome. *Nature Review Cancer*, **5**, 11–20.

McElwaine, S., Mulligan, C., Groet, J., Spinelli, M., Rinaldi, A., Denyer, G., Mensah, A., Cavani, S., Baldo, C., Dagna-Bricarelli, F., Hann, I., Basso, G., Cotter, F.E. & Nizetic, D. (2004) Microarray transcript profiling distinguishes the transient from the acute type of megakaryoblastic leukaemia (M7) in Down's syndrome, revealing PRAME as a specific discriminating marker. *British Journal Haematology*, **125**, 729–742.

Muntean, A.G., Ge, Y., Taub, J.W. & Crispino, J.D. (2006) Transcription factor GATA-1 and Down syndrome leukemogenesis. *Leukaemia & Lymphoma*, **47**, 986–997.

Rainis, L., Toki, T., Pimanda, J.E., Rosenthal, E., Machol, K., Strehl, S., Gottgens, B., Ito, E. & Izraeli, S. (2005) The proto-oncogene ERG in megakaryoblastic leukemias. *Cancer Research*, **65**, 7596–7602.

Smrcek, J.M., Baschat, A.A., Germer, U., Gloeckner-Hofmann, K. & Gembruch, U. (2001) Fetal hydrops and hepatosplenomegaly in the second half of pregnancy: a sign of myeloproliferative disorder in

fetuses with trisomy 21. *Ultrasound in Obstetrics and Gynecology*, **17**, 403–409.

Taub, J.W., Mundschau, G., Ge, Y., Poulik, J.M., Qureshi, F., Jensen, T., James, S.J., Matherly, L.H., Wechsler, J. & Crispino, J.D. (2004) Prenatal origin of GATA1 mutations may be an initiating step in the development of megakaryocytic leukemia in Down syndrome. *Blood*, **104**, 1588–1589.

Wechsler, J., Greene, M., McDevitt, M.A., Anastasi, J., Karp, J.E., Le Beau, M.M. & Crispino, J.D. (2002) Acquired mutations in GATA1 in the megakaryoblastic leukemia of Down syndrome. *Nature Genetics*, **32**, 148–152.